University of Alberta

Ion Transport Pharmacology in Heart Disease and Type-2 Diabetes.

by

Daniel Soliman

A thesis submitted to the Faculty of Graduate Studies and Research
in partial fulfillment of the requirements for the degree of

Doctor of Philosophy

Department of Pharmacology

Daniel Soliman

Spring 2011
Edmonton, Alberta

✠

To My Lord, for His love

To my father, for your strength

To my mother, for your kindness

To my sister and brother, for your true friendship.

Acknowledgements

The work presented in this thesis could not have been possible without the assistance of many important individuals.

I would like to first thank my supervisor and mentor Dr. Peter Light for taking me on as a graduate student in his laboratory. I am grateful for his expertise throughout my thesis research. Working with Peter was an invaluable experience and one that has given me the foundation to commence a meaningful career in medical research.

I would also like to thank Dr. Kevin Hamming for his friendship during my PhD studies. His experience was very instrumental throughout my PhD research and I look forward to future collaborations and a long-lasting friendship. Coffee time!

Thanks to Dr. Gavin Searle and Dr. Nicola Webster for their patience and for teaching me the ways of the laboratory.

Thanks to David Liknes, Dr. Mobeen Raja, Dr. Mohammed Fatehi, Dr. Wei Wang, Veronica Lang, Beth Hunter, Laura Matemisz, Shaheen Rahman, Omid Niazi, Nancy Smith, Jelena Kolic, Catherine Hajmrle, Dr. Marina Casimir, Aliya Spigelman, Chantal St. Aubin, Xianshuo Lu and Lynn Jones for their camaraderie, contributions, and technical assistance throughout my studies.

I would also like to thank the members of my supervisory committee, Dr. Alexander Clanachan and Dr. Larry Fliegel for their positive contributions, guidance and encouragement during my studies.

I also would like to acknowledge Dr. Jason Dyck, Jamie Boisvenue, and Amy Barr for supplying the viruses and neonatal myocyte preparations used for experiments in this thesis.

I also thank the Department of Pharmacology and the funding agencies that have supported my PhD studies: Alberta Innovates Health Solutions, the Faculty of Medicine and Dentistry, and the Faculty of Graduate Studies and Research.

Finally, I would like to express my gratitude again to my family and also to my friends who have endured my PhD experience with me and for giving me the motivation and support I needed to complete my degree.

Abstract

The cardiac sodium-calcium exchanger (NCX) is an important membrane protein which regulates cellular calcium necessary for the optimal contractile function of the heart. NCX has become a focal point in ischemic heart disease (IHD) research as evidence strongly suggests that reactive oxygen species (ROS) produced during IHD aids in causing NCX to malfunction resulting in an intracellular calcium overload in cardiac muscle leading to cardiac contractile abnormalities. Therefore, I hypothesized that NCX function is mediated by ROS increasing NCX1 activity during cardiac ischemia-reperfusion. To research this hypothesis, I investigated cellular mechanisms which may play a role in NCX dysfunction and also examined methods to correct NCX function. My studies were conducted with the use of patch clamping studies, fluorescence imaging, and whole heart studies in experimental models of IHD.

I found that reactive oxygen species directly and irreversibly modify NCX protein, increasing its activity thereby worsening the calcium overload that is deleterious to cardiac function. I also elucidated the molecular means by which NCX protein modification occurs, as ROS target a region of NCX involved in calcium binding which augments the ability of NCX to transport calcium. I also explored pharmacological means by which to decrease NCX function to relieve the calcium overload and reduce the damage to the heart. I discovered that ranolazine (Ranexa™), which is indicated for the treatment of angina pectoris in the United States inhibits NCX activity directly, thereby further reducing the calcium overload-induced injury to the heart.

Furthermore, many IHD patients are also co-morbid for type-2 diabetes. These patients are prescribed sulfonylurea (SU) agents which act at the ATP-sensitive K^+ channel (K_{ATP}). One agent such as glibenclamide is known to have cardiotoxic side effects. Therefore, SUs which are devoid of any cardiac side effects would be more beneficial. Interestingly, patients possessing the newly discovered genetic variant E23K-S1369A K_{ATP} channel have improved blood glucose levels with the use of the SU gliclazide. Therefore, I determined the functional mechanism by which gliclazide has increased inhibition at the K_{ATP} channel, observing that gliclazide is more potent than glibenclamide in the variant K_{ATP} channels. These findings have implications for type-2 diabetes therapy, in which 20% of the type-2 diabetic population carries the K_{ATP} channel variant. Furthermore, these findings highlight the cardiac effects of SUs and the potential use of gliclazide in the treatment of cardiac arrhythmias.

In summary, the findings presented in this thesis have implications on treatment strategies in the clinical setting, as a NCX inhibitor can be beneficial in ischemic heart disease, and also in heart failure, cardiac arrhythmias and possibly type-2 diabetes. Moreover, a pharmacogenomic approach in treating type-2 diabetes may also similarly provide a positive outcome when considering co-morbid cardiac complications such as atrial fibrillation and heart failure.

Table of Contents

List of Abbreviations

ADP	Adenosine diphosphate
AF	Atrial fibrillation
ASR	Alternative splice region
ATP	Adenosine triphosphate
Ca^{2+}	Calcium ion
Ca^{2+}_i	Intracellular Calcium ion
CAD	Coronary artery disease
CBD	Calcium binding domain
CICR	Calcium-induced calcium release
DEND	Developmental and epileptic neonatal diabetes
EGTA	Ethylene-glycol-tetra-acetic acid
Fe-DTT	Iron-dithiothreitol
FM	Forward-mode
GDP	Guanosine diphosphate
GTP	Guanosine triphosphate
H^+	Hydrogen Ion (proton)
HDL	High density lipoprotein
HEPES	4-(2-hydroxyethyl)-1-piperazineethanesulfonic acid
HF	Heart failure
HI	Hyperinsulinemia
IHD	Ischemic heart disease
I_{Na}	Sodium current

I_{NCX}	Sodium-Calcium exchanger current
IR	Ischemia-reperfusion
K^+	Potasssium ion
K_{ATP}	ATP-sensitive potassium channel
KCO	Potassium channel opener
K_d	Dissociation constant
K_{IR}	Inwardly-rectifying potassium channel family
K_m	Affinity constant
LDL	Low density lipoprotein
LPC	Lysophosphatidylcholine
MgADP	Magnesium ADP
MgATP	Magnesium ATP
MgGDP	Magnesium guanosine diphosphate
MgGTP	Magnesium guanosine triphosphate
MODY	Maturity onset diabetes of the young
Na^+	Sodium ion
Na^+_i	Intracellular Sodium ion
NBC	Sodium-bicarbonate co-transporter
NBF	Nucleotide binding fold
NCX	Sodium-Calcium exchanger
ND	Neonatal diabetes
NHE1	Sodium-Hydrogen exchanger type-1
NKA	Sodium-Potassium ATPase

NO	Nitric oxide
NRVMs	Neonatal rat ventricular myocytes
$ONOO^-$	Peroxynitrite
RM	Reverse-mode
ROS	Reactive oxygen species
SERCA2A	Sacroplasmic reticulum Calcium ATPase type-2A
SNP	Single nucelotide polymorphism
SR	Sacroplasmic reticulum
SSH	Salt-sensitive hypertension
SU	Sulfonylurea
SUR	Sulfonyluea receptor
TEA	tetraethylammonium
TG	Thapsigargin
TI	Transient inward
TMD	Transmembrane domain
TTX	Tetrodotoxin
VGCC	Voltage-gated calcium channels
V_{max}	Maximum reaction velocity
XIP	Exchanger inhibitory peptide

Chapter 1

General Introduction

In the 21st century, the prevalence of a sedentary lifestyle is well-understood to be an independent risk factor for the development of coronary artery disease (CAD) [1-3], which is directly correlative with ischemic heart disease (IHD) [4,5]. Even recent scientific evidence links physical activity time directly to intimal media thickness in the common carotid artery, which may be indicative of an early atherosclerotic process in individuals possessing other disease risk factors such as smoking, body weight and age [6].

In addition to physical activity, dietary intake is also an important variable when considering IHD risk. Nutritional factors, specifically the content, composition and amount of dietary fat, cholesterol, and carbohydrates can influence plasma lipid and lipoprotein levels. These factors can subsequently elevate the risk and progression of IHD [7,8]. For instance, an elevated intake of long-chain saturated fatty acids increases low-density lipoprotein (LDL), high-density lipoprotein (HDL) and plasma triglyceride levels, which are independent risk factors for IHD [10,11]. These risk factors can have a direct impact on cardiac function during IHD, as increased intracellular acyl-CoA levels in the heart have been shown to increase intracellular Ca^{2+} through stimulation of the Na-Ca^{2+} exchanger (NCX1) [12].

However, not only do dietary factors and a sedentary lifestyle correlate with IHD, they also increase the risk for type-2 diabetes development [13,14]. Furthermore, genetic polymorphisms can also predispose individuals to type-2 diabetes in combination with dietary and lifestyle influences. For example, the recently discovered E23K variant of the ATP-sensitive K^+ channel approximated

to be in 20% of the type-2 diabetic population is modulated by increased cytoplasmic acyl-CoAs, which increases K_{ATP} channel activity [15-17]. Furthermore, NCX1 can also be modulated in a similar manner by acyl-CoAs, increasing the rate of intracellular Ca^{2+} clearance and reducing insulin secretion [18]. Therefore, dietary factors can have a direct impact on the function of ion channels and exchangers which govern insulin secretion.

Furthermore, not only do fats, in the form of acyl-CoA, affect ion channels and exchangers, other metabolic intermediates such as reactive oxygen species (ROS) may also play a role in modulating ion transport mechanisms. Dietary, lifestyle and genetic factors can impact ion transport mechanisms highlighting the need for pharmacological interventions in order to effectively treat type-2 diabetes and IHD. Therefore, it is the objective of this thesis to detail how (1) ROS can influence NCX1 during IHD, (2) the pharmacological properties of ranolazine, a cardioprotective agent which inhibits NCX1 activity, and (3) the molecular means by which a recently elucidated variant of the K_{ATP} channel E23K-S1369A increases the risk of type-2 diabetes while increasing the potency of gliclazide, a sulfonylurea agent used to treat type-2 diabetes. The work contained in this thesis will provide insight as to how pharmacological approaches to treat IHD can in fact be beneficial in type-2 diabetes treatment and vice versa, and may also be effective in other disease scenarios such as heart failure, hypertension, stroke, multiple sclerosis and Alzheimer's disease.

Section I – Sodium-Calcium Exchanger Studies

Ionic Dysregulation during Cardiac Ischemia-Reperfusion

Sustained high levels of plasma LDL herald the development of atherosclerosis and CAD which highly correlates with acute coronary syndromes. The accumulation and oxidation of LDL within the arterial intima engages a complex series of inflammatory reactions which ultimately lead to the formation of unstable atherosclerotic plaques [19]. These plaques can rupture, causing intracoronary thrombosis [20], that occludes the coronary circulation resulting in myocardial ischemia [21,22]. Myocardial ischemia has drastic consequences on cardiac metabolism as disruptions in oxygen and nutrient supply impair mitochondrial oxidative phosphorylation, which is critical in maintaining myocardial ATP levels. Furthermore, due to the inhibition of oxidative phosphorylation, glycolysis becomes the sole method of ATP production [23]. However, glycolytic ATP production is not enough to replenish ATP stores, and also contributes to metabolic perturbations that occur during ischemia. Glycolysis produces 4 molecules of ATP per molecule glucose. However, 2 molecules of ATP are hydrolyzed in glycolytic reactions producing H^+ ions, which under normoxic conditions would be utilized in the tri-carboxylic acid (TCA) cycle. Yet, as glucose oxidation and glycolysis are uncoupled during ischemia preventing TCA cycle activity, H^+ ions accumulate and cause intracellular acidosis [23]. Together, the intracellular H^+ accumulation and depletion of ATP result in alterations to cardiac ionic homeostasis. Reduced ATP levels slow or halt the activity of the Na^+-K^+ ATPase (NKA), which is responsible for maintaining

the Na^+ and K^+ gradients necessary for action potential generation [24]. Therefore, as intracellular Na^+ is unable to be extruded, the resting membrane potential of cardiac myocytes during ischemia becomes depolarized, especially in addition to Na^+ influx pathways that become active during ischemia [25]. Late Na^+ current (I_{Na}) contributes to intracellular Na^+ loading as hypoxic conditions and ischemic metabolites decrease the rate of inactivation of the Na^+ channel and is suggested to be a considerable source of intracellular Na^+ accumulation [26-30]. Furthermore, a high intracellular H^+ concentration stimulates the exchange for extracellular Na^+ through the function of Na^+-H^+ exchanger (NHE1) and the Na^+-HCO_3^- co-transporter (NBC) [30-32]. Therefore, as intracellular Na^+ accumulates, the Na^+-Ca^{2+} exchanger (NCX1) is stimulated and initiates Ca^{2+} influx. NCX1 governs the electrogenic, anti port transport of Na^+ and Ca^{2+} across the membrane in a 3:1 ratio [24,33,34]. As intracellular Ca^{2+} increases, electrical, contractile and cellular dysfunction occur in the form of atrial and ventricular fibrillation, myocardial stunning, reactive oxygen species generation, protease and phospholipase activation, sarcolemmal swelling and cytoskeletal damage [25,35-37]. These processes can cumulatively cause cardiac myocyte apoptosis and necrosis leading to myocardial infarct formation and irreversible injury to the heart.

In this regard, NCX1 has become a highlight of cardiac ischemia research as it is mainly responsible for Ca^{2+} mishandling during cardiac ischemia and also during cardiac reperfusion, in which restoration of coronary perfusion can paradoxically contribute to cardiac injury [38-44]. In recent years, much effort has

focused on elucidating the physiological function of NCX1 and its regulation by intracellular signalling pathways as well as substrates, due to its pathophysiological contribution in cardiac ischemia-reperfusion (IR). Furthermore, NCX1 inhibitors have been developed to aid in alleviating intracellular Ca^{2+} accumulation during cardiac IR and show promise in becoming clinical therapeutic agents to treat IHD, as well as other related ailments such as hypertension and heart failure. Before inferences and conclusions can be made as to the importance of NCX1 in this thesis, it is necessary to delve into the molecular, electrophysiological and pharmacological aspects of NCX1 in order to garner an understanding of NCX1 function.

Molecular and Structural Aspects of the Sodium-Calcium Exchanger

Na^{+}-Ca^{2+} anti port exchange was initially described in the heart and also in the squid axon [45,46]. Years later, NCX1 was cloned from a canine cardiac cDNA library [47]. NCX1 is encoded by the gene SLC8A1 on chromosome 2p22-23 and was recently cloned from right atrial tissue to obtain the human isoform of NCX1 [18]. The initial cloning of NCX1 lead to the discovery of a superfamily of NCX isoforms, named NCX1, NCX2 and NCX3, respectively. NCX1 exhibits ubiquitous tissue expression, particularly in the heart, brain, vasculature, and endocrine pancreas, while NCX2 and NCX3 are expressed exclusively in the brain and skeletal muscle [48,49]. NCX1 consists of 970 amino acids with a molecular weight of 110kD. It was originally understood by hydropathy plot analysis that NCX1 resided in the plasma membrane with 12 transmembrane segments and 1 large intracellular loop domain [47]. However, cysteine

susceptibility analysis and epitope tagging studies revealed that NCX1 more likely has 1 large cytosolic domain and 9 transmembrane segments, with 2 re-entrant loops (Figure 1-1) [34,50,51]. It is suggested that the re-entrant repeat segments, named α-1 and α-2 respectively, form the ion-conduction pore, in a manner analogous to ion channels [52]. This is further highlighted by helix-packing models that place the α-1 and α-2 segments in close proximity to one another [53,54], which suggests that NCX1 functions as a monomer. The large intracellular domain comprises the majority of the exchange molecule and contains regulatory regions critical to NCX1 function. The 4 regions important to NCX1 function are the exchanger-inhibitory-peptide (XIP) region, calcium binding domains (CBD) 1 and 2 and the alternative splice region (ASR). The aptly-named XIP region, a 20 amino acid segment that begins the large intracellular domain of NCX1, was shown by Li et al. to have regulatory properties, as a peptide with the identical sequence inhibits exchanger function [55]. More evidence also suggests that the XIP region may functionally interact and be physically associated with the ASR as ablation of the ASR negates the effect of XIP on the XIP region [56]. Downstream of the XIP region are the calcium binding domains CBD1 and CBD2. Ca^{2+} binding to CBD1 has been shown to activate the exchanger and binds Ca^{2+} with high affinity (K_d ~ 140-400 nM) [57-60]. CBD1 binds 4 Ca^{2+} ions as a result of the polydendate coordination by 2 groups of conserved acidic aspartate residues in CBD1, the first of two Calx-β domains composed of 7 anti-parallel β strands [58]. CBD1 is also the primary Ca^{2+} sensor of NCX1, as mutations of acidic residues in CBD1 strongly reduced

the affinity to intracellular Ca^{2+}, thereby altering exchanger function [60]. The second Calx-β domain (CBD2) exhibits unique tissue specific properties as it houses the ASR (Figure 1-1A). The ASR dictates the expression of up to 5 exons, mutually exclusive exons A or B, and a combination of exons C, D, E and F thereafter. With respect to Ca^{2+} binding, exon A and B possess a conserved EEYEK motif which is necessary for Ca^{2+} binding, in a similar manner to CBD1 when considering residue acidity. However, only 2 Ca^{2+} ions associate with CBD2 [60,61]. Moreover, exon A is essentially present in NCX1 splice variants expressed in tissues such as the heart, brain, and skeletal muscle in which rapid and substantial fluxes of Ca^{2+} are required for proper maintenance of Ca^{2+} dynamics and signalling pathways [54]. Conversely, in tissues which have generalized requirements for Ca^{2+} dynamics, such as vascular smooth muscle and in the insulin secreting β-cells of the endocrine pancreas, the B exon is expressed [18,48]. Furthermore, exon A and B feature a differential response to changes in intracellular Ca^{2+} concentrations. High cytoplasmic Ca^{2+} present during the peak of the Ca^{2+}-induced Ca^{2+} release (CICR) in cardiac systole or during pre-synaptic neurotransmitter release in the CNS for instance, would require increased exchanger capacity to extrude intracellular Ca^{2+} to reset the Ca^{2+} gradient required for a proceeding systole or neurotransmitter release. This is observed experimentally, as the Ca^{2+} efflux, forward-mode (FM) of NCX1 differs between splice variants. NCX1.3, possessing exons B and D, exhibits a slight inactivation process, while NCX1.1, having the ACDEF exon complement displays no inactivation process [18]. Furthermore, the roles of the exons C, D, E and F

require further study in order to elucidate their individual roles in exchanger function. Collectively, the aforementioned structural and molecular elements of NCX1 have been examined using electrophysiological and biophysical approaches. As NCX1 electrophysiology forms the basis of this dissertation, the biophysical and electrophysiological aspects of NCX1 function are discussed in the following section.

Electrophysiological and Biophysical Elements of the Sodium-Calcium Exchanger

Hilgemann et al. were the first to describe the use of the inside-out patch clamp technique to measure outward NCX1 current from guinea pig cardiac myocytes [62,63]. Together with the molecular cloning of NCX1, a reliable and accurate determination of NCX1 activity could be attained through the transient expression of recombinant NCX1 isoforms and splice variants in surrogate cell lines, such as *Xenopus* oocytes and the human embryonic kidney (HEK293) cell line [64-66]. The operation of NCX1 is fully reversible, in that, the direction of ion movement depends entirely upon the Na^+ and Ca^{2+} electrochemical gradients, the number of Na^+ and Ca^{2+} ions that bind and are transported, and membrane potential [52]. Therefore, NCX1 can work in forward-mode (FM), transporting Na^+ into the cell, while extruding Ca^{2+}, and reverse-mode (RM), which is the transport of Ca^{2+} into the cytosol, while extruding intracellular Na^+. Furthermore, the electrogenicity of NCX1 function is a result of the stoichiometry of NCX1 exchange which is 3 Na^+ ions per 1 Ca^{2+} ion, equalling a +1 charge disparity, allowing the electrophysiological measurement of NCX1 activity (Figure 1-2).

Yet, much debate exists regarding the exact Na^+-Ca^{2+} stoichiometry of NCX1, as a result of varying methodologies in recording NCX1 currents. In particular, an examination of NCX1 current from guinea-pig cardiac myocytes revealed a 4:1 Na^+:Ca^{2+} ratio [67-69], however, a majority of studies support a 3:1 stoichiometry. The stoichiometric ratios do in fact have implications on NCX1 activity in regards to its rate of transport, as a 4:1 ratio would essentially half the transport rate [34]. Measured transport rates of NCX1 range from 75 turnovers per second to 5000 turnovers per second, as the methods and techniques used to determine turnover rates vary between studies. Furthermore, transport rates also give insight into the exchanger density and membrane localization, especially in cardiac myocytes. Some reports estimate NCX1 density in the cardiac sarcolemma to be between 250 and ~1200 exchanger proteins per square micron [70,71]. In regards to cardiac sarcolemma localization, a recent study finds that NCX1 is present in the surface sarcolemma, the inter-calated discs and T-tubules at the level of the Z-disk.. Labeling of NCX1 in the T-tubules was in close proximity to the ryanodine receptor, in a similar manner to the L-type voltage-gated Ca^{2+} channel (VGCC) [72], and therefore may in fact be directly involved in modulating CICR.

The majority of the biophysical findings of NCX1 were made through inside-out patch clamp studies in cells transiently expressing recombinant NCX1 protein. One of the most important observations was the rapid decline of NCX1 current, termed Na^+ dependent inactivation, originally reported by Hilgemann et al. [63]. Subsequently termed I_1-inactivation, Na^+-dependent inactivation is the

rapid decline of NCX1 activity into a steady-state level in the presence of high intracellular Na^+. This phenomenon is exclusive to the RM-NCX1, as high concentrations of intracellular Na^+ are used to activate the exchanger experimentally. Furthermore, the earlier-described XIP region was found to be a regulator of I_1-inactivation. Mutagenesis of the XIP region produced two mutants which exhibit opposing effects on Na^+-dependent inactivation. A phenylalanine-to-glutamate change at position 223 (F223E) and lysine-to-glutamine substitution at position 229 (K229Q) dramatically altered NCX1 function. The F223E mutant substantially enhanced I_1-inactivation, while the K229Q mutant completely abrogated I_1-inactivation [63,73]. Therefore, not only is XIP an intrinsic regulator of RM-NCX1 activity, it also has biophysical implications on exchanger function and also is amenable to regulation by membrane-associated lipids, such as, phosphoinositol-4,5-bisphosphate (PIP_2). Exogenously applied PIP_2 strongly activates RM-NCX1 currents, also explaining the ATP stimulatory effects on NCX1 exchange, while PIP_2 depletion potently reduces NCX1 activity, and may also play a role in determining membrane expression [63,74-76]. Another observation made was the Ca^{2+}-dependent (I_2) regulation of NCX1 exchange. I_2 regulation is the enhancement of NCX1 activity by non-transported cytoplasmic Ca^{2+}, again a phenomenon of outward, RM-NCX1 currents. When comparing NCX1 splice variants containing either exons A and D (NCX1.4) or exons B and D (NCX1.3), it was found that A-containing splice variants exhibit Ca^{2+}-dependent alleviation of Na^+-dependent inactivation, whereas B-containing variants of NCX1 do not [61]. This finding adds credence to the notion that the

XIP region and the CBD2 contained within the ASR are functionally associated. Another regulator of Na^+-dependent inactivation is intracellular pH. Low intracellular pH has been shown to accelerate I_1-inactivation inhibiting outward NCX1 exchange, while an alkaline pH reduces Na^+-dependent inactivation, promoting NCX1 activity [77,78]. Yet, the specific region that is responsible for this phenomenon remains unclear [52].

NCX1 is also regulated by a recently elucidated integral membrane protein termed phospholemman. A member of the 'FXYD' family of transport regulators, phospholemman, when phosphorylated at serine-68 by protein kinase A, binds to residues 218-371 and 508-764 of the NCX1 intracellular domain, inhibiting NCX1 function [79,80]. In contrast, phospholemman has been demonstrated to have a stimulatory effect on NKA [81]. Considering that NCX1 and NKA are localized in macro-molecular complexes in the cardiac sarcolemma [82-84], the functional coordination of these transporters may be physiologically relevant [52]. Furthermore, although NCX1 possesses available serine residues for phosphorylation by protein kinases, NCX1 phosphorylation is a debated topic. Heterologous expression studies provide direct evidence of NCX1 phosphorylation, however adrenergically-mediated activation of NCX1 can be attributed to indirect effects on the exchanger. Therefore it is inferred that NCX1 activity can be regulated by protein kinases indirectly, such as by phospholemman [34,52].

The biophysical and electrophysiological aspects of NCX1 function are quite relevant in order place NCX1 in physiological context, as a participant in

myocardial Ca^{2+} handling during the cardiac action potential. As NCX1 is a key contributor to intracellular Ca^{2+} overload during cardiac IR, the physiological and pathophysiological aspects of NCX1 will be explored.

Physiology and Pathophysiology of NCX1 in the Myocardium

NCX1 plays a predominant role in regulating trans-sarcolemmal Ca^{2+} flux in the myocardium (for reviews see [34,39,85,86]). The cardiac-specific NCX1 splice variant, NCX1.1, containing the exon complement ACDEF, possesses specialized Ca^{2+} transport properties, to manage the beat-to-beat Ca^{2+} dynamics of the contracting myocardium. Upon stimulation by a cardiac action potential during systole, Ca^{2+} influx is initiated by the L-type VGCCs. Localized in the T-tubules, L-type VGCCs are proximal to ryanodine receptors in the sarcoplasmic reticulum (SR) membrane, which upon L-type Ca^{2+} entry, commences the release of Ca^{2+} from the SR, forming the basis of CICR. At this stage, intracellular Ca^{2+} concentrations are above micromolar levels. In order to reset the Ca^{2+} gradient for a subsequent systole and also to relax the myocardium, intracellular Ca^{2+} levels must be lowered to sub-micromolar levels between 100-150 nM. NCX1.1 is a primary mechanism by which intracellular Ca^{2+} levels are restored for a proceeding contraction. Functioning in FM, NCX1.1 facilitates the removal of one Ca^{2+} ion for the transport of three Na^{+} ions into the cell. However, not only does NCX1.1 remove intracellular Ca^{2+}, it is thought that during the upstroke of the cardiac action potential, the cardiac membrane is depolarized, and as NCX1.1 is electrogenic, a depolarized membrane potential would force NCX1.1 to transiently operate in RM, possibly modulating the gain of Ca^{2+} influx for CICR.

NCX1.1 is understood to play a major role in intracellular Ca^{2+} extrusion during diastole, removing approximately 30% of total intracellular Ca^{2+} and is the predominant transsarcolemmal Ca^{2+} transporter. Other Ca^{2+} transporters, namely the sarcoplasmic reticulum Ca^{2+}-ATPase (SERCA2a) removes the majority of intracellular Ca^{2+} especially in rat, in which it contributes to ~90% of total intracellular Ca^{2+} removal. The sarcolemmal Ca^{2+}-ATPase and the mitochondrial Ca^{2+} uniporter participate in regulating intracellular Ca^{2+} only in a minor capacity [34,87].

As NCX1.1 is a central player in cardiac Ca^{2+} homeostasis, it is of no co-incidence that NCX1.1 is involved in intracellular Ca^{2+} overload during cardiac IR. Na^{+}-dependent Ca^{2+} loading mediated by RM-NCX1.1 exchange was described almost two decades ago [24,33]. Furthermore, as cardiac-specific knockout studies of NCX1 have been shown to be protective [88], NCX1.1 has become a novel target for pharmacological therapy in alleviating cardiac IR injury. Moreover, as ischemia produces metabolic changes that result in alterations to ionic homeostasis, recent research has focused on the interaction of intracellular metabolic substrates with ion channels and exchangers. In particular, fatty acyl-CoA molecules accumulate due to the inhibition of fatty acid β-oxidation during ischemia [89]. It has been discovered that saturated fatty acyl-CoAs increase the activity of RM-NCX1.1, thereby increasing Ca^{2+} influx during IR [12]. Moreover, many studies have shown that reactive oxygen species (ROS), a by-product of myocardial metabolism, are produced in significant amounts during IR [90-92]. ROS have been implicated in myocardial cellular and

mechanical dysfunction in IR by having negative effects on cardiac membrane proteins, particularly ion channels and exchangers. L-type Ca^{2+} channels and inward rectifying K^+ channels exhibit suppressed activity in response to ROS [93,94]. Peak Na^+ currents were unaffected by ROS, whereas K_{ATP} channels were stimulated directly by modulating ATP binding sites or indirectly due to decreased ATP levels by mitochondrial inhibition [93,95,96]. Tani originally suggested that ROS may modulate the function of NCX1.1 during IR citing a study by Reeves et al [24]. In that study, NCX1.1 activity in sarcolemmal vesicles was altered with redox agents, hydroxyl and superoxide radicals [97]. Moreover, Reeves accounts the alterations in NCX1.1 function by redox reagents as the interchange of disulfide bridges by cysteine thiol residues, which decreased the K_m of Ca^{2+} binding, increasing NCX1.1 activity [97]. Furthermore, Goldhaber suggested that NCX1.1 activity may be increased directly by ROS, particularly in RM, adding credence to the idea that NCX1.1 contributes to the Ca^{2+} overload in IR [98]. Further investigations exhibited that NCX1.1 over-expression in rabbit cardiac myocytes predisposed them to ROS-mediated injury versus normal cardiomyocytes, and that ROS activated RM-NCX1.1 during IR [40,99,100]

Hypothesis I

The functional and molecular aspects of ROS-modification of NCX1.1 activity remain to be fully elucidated. It has been suggested that ROS-mediated effects on NCX1.1 are direct in nature, modifying the protein itself [98]. Therefore, it is the aim of this project to study the nature of ROS-induced alterations of NCX1 activity and to characterize these effects. **I hypothesize that**

ROS directly and irreversibly modifies NCX1.1, augmenting reverse mode activity, thereby contributing to the intracellular Ca^{2+} overload that occurs during cardiac IR. I will test this hypothesis by using patch clamp methods, specifically the inside-out excised technique in tSA201 cells transiently over-expressing recombinant NCX1.1 protein. Our protocol employs the application of H_2O_2, a stable ROS intermediate to the intracellular side of excised patches and measuring NCX1 current (I_{NCX}). Based on the outcome of these experiments, other experimental approaches will be utilized to further investigate and reaffirm the hypothesis that ROS modifies NCX1 current. For instance, we intend to investigate how NCX1 modification can be corrected to rectify cellular dysfunction by using pharmacological approaches. These approaches include determining the effect of NCX1 inhibitors on ROS modified NCX1 currents and also whether NCX1 splice variants have differing responses to ROS, particularly NCX1.3, NCX1.4 and NCX1.11. Results from this project will have ramifications on (1) our current understanding of cardiac IR and (2) other related disease states such as hypertension, heart failure and cerebral IR.

Sodium-Calcium Exchanger Pharmacology

With the notion that ROS may directly augment RM-NCX1.1, further impacting Ca^{2+} overload-mediated cardiac dysfunction, an understanding of NCX1 pharmacology is necessary to approach a solution to reduce the morbidity associated with cardiac IR injury. NCX1 inhibition was first investigated in 1991 with the use of the XIP [55]. The amino acid sequence of XIP, RRLLFYKYVYKRYRAGKQRG, corresponding to amino acids 219-238 of the

N-terminal segment of the large intracellular loop of NCX1, when applied to the cytoplasmic face of the exchanger potently inhibits NCX1 activity (IC_{50} = 0.15 – 1.5 μM) [34,55,101]. However, the clinical use of XIP is hindered by the inability of XIP to cross the sarcolemmal membrane and is also encumbered by peptide degradation. Therefore, chemical NCX1 inhibitors are in development. KB-R7943, a benzyloxyphenyl derivative, was the first rationally screened NCX1 inhibitor shown to be effective in models of Na^+-dependent $^{45}Ca^{2+}$ uptake (Figure 1-3) [102]. Since its development, KB-R7943 has been shown to be effective in reducing intracellular Ca^{2+} overload, improving cardiac contractile function in models of cardiac IR and arrhythmias [103-106]. However, KB-R7943 lacks specificity for NCX1, as it inhibits other ion channels and membrane proteins such as L-type VGCCs, inwardly-rectifying K^+ channels, the neuronal nicotinic acetylcholine receptor, N-methyl-D-aspartate receptor and the noradrenaline transporter [107-109]. Shortly after KB-R7943 development, SEA0400 was discovered be a more potent and selective inhibitor of NCX1 in models of IR [110-115]. KB-R7943 and SEA0400 were independently screened, although sharing a common benzyloxyphenyl structure, which suggests that the benzyloxyphenyl moiety may be necessary for NCX1 inhibition [108]. Both KB-R7943 and SEA0400 have been suggested to target the α-2 repeat re-entrant domain of NCX1, the location in which transposition of Na^+ and Ca^{2+} is understood to occur, as mutation of specific residues in the α-2 region prevents NCX1 inhibition [116,117]. Although being more potent than KB-R7943, SEA0400 still lacks the necessary specificity to be employed clinically, as both

agents have been shown to alter Ca^{2+} transients in NCX1 KO heart tubes [118]. Therefore, NCX1 inhibitor development continues in an effort to discover NCX1 specific agents. The compounds SN-6 and YM-244769 were successfully screened for NCX1 inhibition, and also possess therapeutic potential for protection during cerebral and cardiac IR (Figure 1-3), however more study is required to ascertain the specificity of these agents [107,119-121]. Although all NCX1 inhibitors discovered have the important feature of RM selectivity, the non-specificity of NCX1 inhibitors and their effects on myocardial ion currents precludes any clinical application of these pharmacological mediators for cardiac syndromes. Therefore, other approaches to reduce intracellular Ca^{2+} loading during cardiac IR are being investigated.

Intracellular Na^+ Accumulation and Late Na^+ Current.

As intracellular Na^+ accumulation precedes RM-NCX1 mediated Ca^{2+} overload, reducing intracellular Na^+ influx during ischemia would also alleviate intracellular Ca^{2+} loading (Figure 1-4). NHE1, like NCX1 is a promising pharmacological target for cardiac IR. In experimental models NHE1 showed promise in ameliorating Ca^{2+} mishandling during in models of cardiac IR, which have translated into the clinical application of the NHE1 inhibitor cariporide (see reviews [122-124]). Another significant source of intracellular Na^+ during cardiac IR is the late I_{Na}. Physiologically, cardiac I_{Na} is responsible for the upstroke of the cardiac action potential, which depolarizes the myocardium, allowing for voltage-gated activation of the L-type VGCCs, necessary to induce systole [125]. Normally, I_{Na} rapidly inactivates and becomes inactivated for a specific time

period, until the myocardium repolarizes to resting membrane potential. This feature of the Na^+ channel is important to prevent the generation of early-after depolarizations (EADs), which can trigger re-entrant arrhythmias. Mutations in Na^+ channels which reduce the inactivation process can lead to long-QT interval syndromes, action potential duration prolongation, and the development of EADs, from which arrhythmias such as Torsade de Pointes and ventricular fibrillation develop [126,127].

A similar reduction in Na^+ channel inactivation occurs during cardiac ischemia. Ischemic metabolites such as L-palmitoyl carnitine, lysophosphatidylcholine (LPC) and ROS can activate late I_{Na} [128-130]. Stress signalling mechanisms such as CaMKII and AMPK can also stimulate late I_{Na} [131]. Cumulatively, NHE1-mediated exchange of metabolically derived H^+ for Na^+ and the inactivity of NKA due to depleted ATP levels, increases intracellular Na^+ levels to 12-15mM, three times higher than the physiological ~5mM concentration [26,27]. High intracellular Na^+ and elevated intracellular Ca^{2+} levels, along with a depolarized membrane potential can result in the "flipping" of NCX1 into calcium-influx mode, which is responsible for the Ca^{2+} overload and cardiac IR injury as a result. Therefore, late I_{Na} can also be a pharmacological target for the treatment of cardiac IR. Agents such as R56865 showed promise as pharmacological modulators of late I_{Na}, however studies have shown that the R56865 mediated cardioprotection is independent of late I_{Na}. [132-134]. Interestingly, a trimetazidine-lidocaine analogue, ranolazine (Ranexa™),, was recently shown to inhibit late I_{Na}. Developed by Gilead Pharmaceuticals (Palo

Alto, CA, USA), ranolazine was originally thought to be an anti-ischemic agent for angina pectoris via its inhibitory action on fatty-acid metabolism and stimulation of glucose oxidation [135-137]. Yet, as a cardiac-directed agent, it was plausible that ranolazine may have effects on the electrophysiology of cardiac myocytes, that is to say it may be a pharmacological modulator of ion currents and exchangers. It was found that ranolazine blocks late I_{Na} with an IC_{50} of 6 μM (Figure 1-3) [138,139]. Ranolazine, recently approved for use in angina pectoris treatment, is currently thought to produce its anti-ischemic effects via the selective inhibition of late I_{Na} current [138-141]. By preventing the accumulation of intracellular Na^+, ranolazine has the indirect effect of reducing Ca^{2+} influx via RM-NCX1.1, which causes the intracellular Ca^{2+} overload responsible for the electrical and mechanical dysfunction in cardiac IR [142-146]. The ischemic protection offered by ranolazine has been investigated in various experimental models in which late I_{Na} is activated. Ranolazine was effective in (1) reducing diastolic intracellular Ca^{2+} levels and restoring left-ventricular function IR induced late I_{Na} [144], (2) reducing oxidative stress-mediated increases in intracellular Na^+ and Ca^{2+} in ventricular myocytes [143], (3) improving diastolic recovery after cardioplegia [147], and (4) restoring intracellular Ca^{2+} homeostasis after ATX-II induction of late I_{Na} [148].

Working-mode heart perfusion models have been extensively used to investigate the functional aspects of ranolazine-mediated cardiac protection. ATX-II, a sea anemone toxin that induces late I_{Na}, was employed in some of these models to mimic the ionic dysregulation of IR in a normoxic state [144].

However, the ionic dysregulation caused by ATX-II does not precisely represent the alterations to myocardial ion homeostasis. Another method with which to increase intracellular Na^+ is the use of NKA inhibitors such as ouabain. Ouabain prevents the extrusion of intracellular Na^+ thereby reducing FM-NCX1.1 function and promoting RM-NCX1.1, which is required to increase intracellular Ca^{2+} [149-151]. Intracellular Na^+ levels rise after each contraction, as approximately 0.5 mM/min Na^+ enters the cytosol per minute and due to NKA inhibition, which normally removes Na^+ at a rate of 4 mM/min [27], it is inferred that intracellular Na^+ increases progressively with each contraction gradually causing Ca^{2+} influx through RM-NCX1.1 exchange.

The initial study of ranolazine on myocardial ion exchangers did not accurately assess the effect of ranolazine on RM-NCX1.1 exchange. The activity of NCX1.1 investigated depicts an inward current, which corresponds to the physiological FM-NCX1.1 activity [138]. Ranolazine's weak potency on FM-NCX1.1 function is advantageous, as it would not alter calcium efflux physiologically. However, the effects of ranolazine on RM-NCX1.1 function have not been studied to date. As RM-NCX1.1 activity is downstream of late I_{Na} and intracellular Na^+ overload, it is highly plausible that the cardioprotective effectiveness of ranolazine may be via a direct inhibition of RM-NCX1.1.

Hypothesis II

The effects of ranolazine on models of ATX-II mediated Ca^{2+} overload may not be fully attributable to late I_{Na} block and further study of ranolazine's action on RM-NCX1 current is required. **Therefore, I hypothesize that the**

protective benefit afforded by ranolazine in cardiac IR occurs through the inhibition of reverse-mode NCX1, in addition to late I_{Na} block. This hypothesis will be studied through the use of working mode perfusions of isolated rat hearts, fluorescent calcium imaging of evoked RM-NCX1.1 activity in neonatal rat cardiac myocytes and the electrophysiological study of recombinant I_{Na} and I_{NCX}. Outcomes from this investigation will have important considerations for ranolazine. As NCX1 inhibitors, KB-R7943 and SEA0400, do not possess the required clinical specificity for NCX1.1, ranolazine may be a novel NCX1.1 inhibitor. Therefore ranolazine may provide the therapeutic benefit necessary to improve myocardial outcomes in cardiac syndromes such as IR, heart failure and arrhythmias.

Section II – ATP-Sensitive Potassium (K_{ATP}) Channel Studies

K_{ATP} – Dependent Regulation of NCX1 Activity

Reverse-mode NCX1-mediated Ca^{2+} overload during cardiac IR is the result of imbalances in the ionic milieu, such as intracellular acidosis and Na^+ accumulation (Figure 1-4). Furthermore, the prolonged depolarized state of the cardiac membrane potential in IR favors RM-NCX1 activity, causing the influx of Ca^{2+} into cardiac myocytes. Another factor is the increased extracellular K^+ accumulation, as a result of NKA uncoupling, AP firing cessation and ischemia. This would also act to depolarize the membrane potential, in addition to increasing intracellular Na^+ and Ca^{2+} levels [152]. Furthermore, the ventricular myocyte membrane potential is governed by the Nernst equation ($E_m=RT/zF\cdot\ln[X_o/X_i]$) and stabilized by inwardly-rectifying K^+ channels, such as

IK1 and K_{ATP}, due to the membrane potential being clamped near E_K. Therefore, it is possible to pharmacologically modulate the activity of these K^+ channels to hyperpolarize the membrane potential, thereby reducing the NCX1-mediated Ca^{2+} influx [153]. K_{ATP} channel openers such as pinacidil and P-1075, specific to the cardiac K_{ATP} channel through their targeting of the SUR2A subunit, have been shown to reduce intracellular Ca^{2+} loading. However, closing cardiac K_{ATP} channels with HMR-1098 is detrimental to cardiac function, worsening recovery from IR [154,155]. Also of note is that the co-application of both the NCX1 inhibitor KB-R7943 and the KCO P-1075 did not provide further benefit than KB-R7943 or P-1075 application alone, indicating a link between increased K_{ATP} channel activity and a reduction in NCX1 function. Furthermore, it has been suggested that using KCOs or a low extracellular K^+ concentration to clamp the myocardial membrane potential in a hyperpolarized state could be substantially cardioprotective by increasing the threshold for electrical excitability [154].

Interestingly, many IHD patients are also patients or at high-risk to develop type-2 diabetes [156-158]. The majority of type-2 diabetic patients are treated with sulfonylurea (SU) agents which target the SUR1 subunit β-cell specific K_{ATP} channel, inhibiting its activity, leading to insulin secretion to reduce hyperglycemia. One of the first-line therapeutic agents for type-2 diabetes, glibenclamide, is noticeably associated with cardiac toxicity [159]. This is due to glibenclamide's lack of discrimination between cardiac SUR2A and β-cell SUR1, having an IC_{50} of ~4 nM and ~28 nM at cloned β-cell and cardiac K_{ATP} channels, respectively [160]. Studies have shown that glibenclamide is associated with an

increase in infarct size, reduced left-ventricular function and an abolishment of ischemic preconditioning effects that occur due to acute ischemic events such as "first effort angina" [161-163]. However, glibenclamide's benefit as an insulin secretagogue is usually considered over its cardiotoxic potential.

Although glibenclamide's cardiotoxic effects are documented, other compounding factors arise in the SU treatment paradigm for type-2 diabetes that are genetic in nature. A recent study by Reyes et al. highlights that the common E23K variant in the $K_{IR}6.2$ subunit of the K_{ATP} channel is overrepresented in a heart failure cohort [164]. Although, it is unknown whether patients in the cohort were type-2 diabetics, glibenclamide potency in E23K-K_{ATP} channels has been exhibited to be reduced [165]. Therefore, it is possible that glibenclamide dosing is increased in patients expressing the E23K-K_{ATP} variant, leading to increased cases of cardiac toxicity and morbidity in IHD, due to inappropriate closure of cardiac K_{ATP} channels. Therefore, as interplay between type-2 diabetes treatment and extra-pancreatic effects of SU therapy may exist, it is necessary to further investigate the genetic etiology of type-2 diabetes to determine if a pharmacogenomic approach to treating type-2 diabetes is warranted that may also reduce the incidence of cardiac SU toxicity.

Implications of Genetics in Type-2 Diabetes Mellitus.

Non-insulin-dependent diabetes mellitus (NIDDM), referred to as type-2 diabetes, is an endocrine disease of continuing concern in the early 21st century. The main clinical feature of type-2 diabetes is generally accepted to be hyperglycemia, due to a reduction in insulin sensitivity and insulin secretion.

Highly prevalent in Western societies, and growing rapidly in developing societies, type-2 diabetes affects more than 171 million individuals worldwide, and is expected to climb to 366 million in 2030 [166,167]. Not only do environmental factors contribute to the development of type-2 diabetes, genotypic components play a significant role in the susceptibility of the diabetic phenotype [168]. Mutations in glucokinase, hepatic nuclear factors 1α and 4α, insulin promoter factor-1 result in marked reductions in insulin secretion and also manifest extra-pancreatic phenotypes. Furthermore mutations in the insulin receptor, peroxisome proliferator-activated receptor-γ and AKT2 reduce insulin's action at its peripheral receptors [169,170]. While these mutations result in the rare case of the monogenic maturity onset diabetes of the young (MODY), finding common genetic mutations or polymorphisms which directly equate to the susceptibility of type-2 diabetes has proven to be inconclusive, until the discovery of a proline-12-alanine polymorphism in PPARγ, which adequately demonstrated altering type-2 diabetes susceptibility, by reducing peripheral insulin sensitivity [171].

Recent clinical studies highlight that the genes which encode the K_{ATP} channel can be a novel locus for genetic susceptibility to type-2 diabetes. The pancreatic K_{ATP} channel is encoded by genes *KCNJ11* and *ABCC8*, from which the K^+-conducting pore ($K_{IR}6.2$) subunit and the sulfonylurea-sensitive receptor-1 (SUR1) protein subunits are derived, respectively. Monogenic mutations in either $K_{IR}6.2$ or SUR1 can cause differing degrees of neonatal diabetes ranging from the less severe MODY to DEND syndrome the latter characterized by drastic

developmental delays and epilepsy, likely as a result of the widespread expression of K_{ATP} in the CNS (see reviews [172,173]). Mutations causing neonatal diabetes or hyperinsulinemia result in significant alterations in K_{ATP} channel function. For instance, the R201H mutation in $K_{IR}6.2$ exhibits reduced ATP sensitivity. This change in ATP sensitivity is due to the replacement of positively charged arginine with the neutral residue histidine reducing the interaction with the negatively charged α-phosphate of the ATP molecule for K_{ATP} channel inhibition [174]. An example of an activating mutation which precipitates hyperinsulinemia is R1394H; located within the 2nd nucleotide binding domain of SUR1, the mutation reduced MgADP binding, essential for ADP-dependent relief of K_{ATP} channel inhibition. This mutation effectively keeps the K_{ATP} closed resulting in the persistent secretion of insulin [175].

Monogenic mutations which result in neonatal diabetes (ND) or hyperinsulinemia (HI) have direct and drastic implications on K_{ATP} channel function. Therefore, polymorphic mutations are also expected to alter K_{ATP} channel function, albeit in a subtle manner, only increasing susceptibility to type-2 diabetes development. Screening for type-2 diabetes susceptibility yielded single-nucleotide polymorphisms (SNPs) in which mis-sense mutations in the coding region for the K_{ATP} channel subunit, $K_{IR}6.2$, were found. These included E10K, E23K, L270V, and I337V. Initially, it was thought that these mutations were not associated with Caucasian cases of type-2 diabetes. However, further study found that the E23K SNP was linked to type-2 diabetes susceptibility in a large-scale association cohort [16,176-178]. Furthermore, functional studies of the

E23K-K_{ATP} channel found that it exhibited a slight reduction in ATP sensitivity, which in conjunction with dietary and physical activity factors, can precipitate the type-2 diabetic phenotype [179,180]. Moreover, investigation of euglycemic E23K patients also found that these individuals displayed a ~40% drop in insulin secretion, that was however compensated by an up-regulation of hepatic insulin sensitivity [181]. However, the risk of type-2 diabetes development does increase as E23K patients develop peripheral insulin resistance.

Furthermore, detailed mapping of the 11p15.1 chromosomal locus containing neighbouring *KCNJ11* and *ABCC8* genes revealed that SNP rs757110, a serine to alanine mis-sense mutation at position 1369 (S1369A) in SUR1, showed near-perfect linkage disequilibirum with E23K [182]. Therefore, individuals who carried the K risk allele of the E23K SNP in all likelihood carried the A allele of the S1369A SNP, forming the E23K-S1369A haplotype. However, the genetic evidence was not sufficient to determine which allele at 1369 is the causal variant [182].

Therefore, as monogenic and polygenic mutations to the K_{ATP} channel can cause the diabetic phenotype in varying degrees, it is important to delve into the physiological role of K_{ATP} channels in regulating insulin secretion and to explore the molecular and structural aspects of the K_{ATP} channel and their translation into function. Furthermore, as K_{ATP} channels are the target for pharmacotherapy of type-2 diabetes K_{ATP} channel pharmacology will also be reviewed.

Physiological Regulation of Insulin Secretion: The Role of the K_{ATP} Channel

Ashcroft et al. first reported the glucose-dependent closure of single K^+ channels, and hypothesized that glucose itself induced the closure of "G-channels." [183]. Shortly thereafter, it was discovered that the glucose sensitive "G-channel" was in fact the K_{ATP} channel, in which K^+ conductance was inhibited by the intracellular application of ATP and stimulated by ADP [184-186]. The ATP-sensing ability of the K_{ATP} channel allows it to control the electrical properties of the insulin-secreting pancreatic β-cell coupling metabolism to insulin release (Figure 1-5). Furthermore, K_{ATP} channels are the major regulators of β-cell resting membrane potential as K_{ATP} channels are open at resting potential while their closure signals β-cell depolarization [187]. During a fasting or pre-prandial state in which plasma glucose levels are less than 6 mM, the ATP:ADP ratio is relatively low, and as ADP stimulates K_{ATP} channel opening, K^+ efflux from the β-cell maintains a hyperpolarized membrane potential, measured to be approximately -70 mV [173]. Post-prandially, plasma concentrations of glucose rise to between 7 mM and 10 mM [188,189]. Glucose is a major fuel for high energy phosphate production and is converted to ATP through the metabolic processes of glycolysis, glucose oxidation, the TCA cycle and oxidative phosphorylation [15,190]. Therefore, as ADP is converted to ATP, the ATP:ADP ratio increases, which leads to inhibition of K^+ efflux via K_{ATP} channels. This causes a depolarization of the β-cell membrane to a threshold potential of -50 mV, permitting the activation of voltage-gated L-type Ca^{2+} channels, as Ca^{2+} influx is necessary to stimulate the Ca^{2+}-dependent vesicle

fusion to the membrane, thereby releasing insulin from β-cells [191,192]. This stimulatory pathway is not a single event; as plasma glucose concentrations remain elevated. Furthermore, insulin is secreted in an oscillatory manner, as L-type Ca^{2+} channels inactivate slowly, the bursting reflects a balance between the depolarizing P/Q Ca^{2+} currents and repolarizing K^+ currents from K_{ATP}, delayed-rectifying and Ca^{2+}-activated K^+ currents in human β-cells [193]. The burst is terminated when the L-type Ca^{2+} current becomes refractory allowing the outward K^+ currents to collectively repolarize the membrane potential. Moreover, as recently elucidated mutations (discussed above) at the K_{ATP} channel genes *KCNJ11* and *ABCC8* result in neonatal diabetes or hyperinsulinemia has made the role of the K_{ATP} in regulating insulin secretion paramount. To further understand the function of the K_{ATP} channel, the molecular and structural aspects of the K_{ATP} channel and its subunits $K_{IR}6.2$ and SUR1 will be examined.

Molecular and Structural Aspects of K_{ATP}: $K_{IR}6.2$ & SUR1.

The K_{ATP} channel consists of the $K_{IR}6.2$ conducting pore subunit and the regulatory sulfonylurea subunit, assembled as a heterooctomeric complex, with SUR1 subunits interacting with $K_{IR}6.2$ subunits in a 4:4 stoichiometric ratio, respectively (Figure 1-6) (see reviews [173,194-196]). Part of the K_{IR} family of channels ($K_{IR}1.x$-$K_{IR}6.x$), $K_{IR}6.2$ is a weak inwardly-rectifying K^+ channel, expressed in the heart, the CNS, and endocrine pancreas, in the insulin-secreting β-cells and also in the glucagon-secreting α-cells. Smaller than stereotypical voltage-gated K^+ channels, membrane topology of $K_{IR}6.2$ reveals 2 transmembrane helices, termed M1 and M2 respectively, as well as a re-entrant

loop, which houses the K^+ selectivity filter GYG motif. K^+ conduction through $K_{IR}6.2$ is regulated by cytosolic ATP, by its binding at the N- and C-terminal domains preceding or following the M1 and M2 domains, respectively [197,198]. SUR1, the regulatory subunit of the K_{ATP}, is expressed almost exclusively in the CNS and pancreas. The study of SUR1 regulation of K_{ATP} channels was expedited through the cloning of the β-cell specific sulfonylurea receptor in 1995 [199]. SUR1 is part of a family of SU receptors in which SUR2A and SUR2B are also members. In depth, SUR1 is 140kD membrane protein, contains 3 transmembrane domains (TMD), with TMD0 containing 5 spanning segments, and TMD1 and TMD2 containing 6 membrane spanning segments, respectively. The intracellular loop between TMD1 and TMD2 houses the first nucleotide binding fold (NBF1) and while the large C-terminal tail of SUR1 houses the second nucleotide binding fold (NBF2). NBF1 and NBF2 are critical in the MgATP-dependent regulation of K_{ATP} channels. They contain conserved Walker A and Walker B motifs that are characteristic of ATP binding cassette proteins, possessing the GlyXXGlyXGlyLysSerThr- (X being another amino acid) and –YYYYAsp- (Y being any hydrophobic amino acid) motifs, respectively. Forming a functional dimer, NBF1 and NBF2 catalyze the hydrolysis of MgATP, which modulates the gating of the K_{ATP} channel. MgATP bound in the pre-hydrolytic state works to inhibit K_{ATP} activity, while the conversion of MgATP to MgADP and MgADP bound in the post-hydrolytic state relieves the inhibition of the K_{ATP} channel by ATP at $K_{IR}6.2$ (Figure 1-7) [200,201]. This highlights the ATP:ADP ratio as the determinant of K_{ATP} activity and not ATP levels. Moreover, mutations proximal

to the NBFs can result in hyperinsulemia or neonatal diabetes due to alterations in the rate of MgATP hydrolysis. For instance, mutations G1382S, ΔF1388, R1394H and G1479R are located within NBF2 and cause hyperinsulinemia by negating relief of inhibition by MgADP [175]. Furthermore, SUR1 was discovered to be the site of pharmacological modulation of K_{ATP} channel activity, through the finding that therapeutic agents for the treatment of type-2 diabetes act at SUR1 [202,203].

K_{ATP} Channel Pharmacology: Sulfonylureas.

During World War II, Dr. Marcel Janbon, a French pharmacologist, attempting to isolate a treatment for typhoid fever tested a drug named 'sulfonylurea' on animals and found that the animals' blood sugar levels decreased drastically [204]. Shortly afterwards in 1958, four oral hypoglycemics (tolbutamide, chlorpropamide, acetohexamide and tolazamide) were available for the treatment of type-2 diabetes [205]. SUs are grouped in generations: first, second and third generation. First generation SUs include, tolbutamide and chlorpropamide; second generation SUs include gliclazide and glibenclamide, and an example of a third generation SU is glimepiride [206,207]. Glinides, another subclass of agents acting at SUR1 include repaglinide and metiglinide [208]. All oral-hypoglycemic agents that act at the K_{ATP} channel can also be classified according to their site of action at the SUR1 subunit. Two drug binding pockets have been elucidated and designated A and B-sites, respectively. SUs or glinides can act at either site, or even both sites simultaneously. For example, gliclazide is an A-site drug, glibenclamide an AB-site agent, and repaglinide a B-site ligand.

The A-site at SUR lies within the transmembrane helices 14 and 15 and is proximal to NBF2, while the B-site lies at the cytoplasmic loop between TMD0 and TMD1 and the N-terminal domain of $K_{IR}6.2$ [209,210]. Confirming these binding pockets are mutational studies which removed effect of A-site ligands at SUR1 with the S1237Y mutation, while removal of the first 33 amino acids in $K_{IR}6.2$ removes B-site drug action [211-214]. How SUs transduce their inhibitory actions on K_{ATP} is currently unclear, however it is suggested that SUs may interfere with MgATPase activity of SUR1, especially A-site ligands, or through affecting gating of K^+ conduction at $K_{IR}6.2$ [211,215,216]. Furthermore, not only do SUs exert their inhibitory effects at SUR1, they also have inhibitory effects at the cardiac SUR2A receptor. This accounts for the cardiotoxic effects of some SUs with similar SUR1 and SUR2A affinities [160,162].

Pharmacogenomic Approaches for Neonatal Diabetes & Hyperinsulinism: A View to Type-2 Diabetes Treatment.

In regards to the monogenic mutations of the K_{ATP} channel which precipitate either ND or HI, only recently has a pharmacological approach been undertaken. Previously, exogenous insulin therapy or a pancreatecomy could only treat or cure ND or HI, respectively [172]. Since the K_{ATP} subunits $K_{IR}6.2$ and SUR1 have been found to be the locus of the majority of the monogenic mutations causing ND or HI, agents that modulate K_{ATP} activity have been examined as to their likely benefit. For instance, SU therapy has been successful in ND patients, due to the ability of SUs to bypass nucleotide dependent channel gating at $K_{IR}6.2$, such as the case for $K_{IR}6.2$ mutations Q52R, I82V and V59M [217,218]. In

regards to SUR1 mutations, although affecting MgATP binding, the I1424V and H1023Y mutations, retain their sensitivity to tolbutamide [217,219]. In regards to HI, KCOs are mostly effective in patients, who possess the less common $K_{IR}6.2$ loss-of-function mutations, as mutations in SUR1 causing HI more often result in protein-membrane trafficking deficits as well as the formation of non-functional channels. However, KCOs are effective in HI cases which are independent of K_{ATP} channels. For example, mutations in glutamate dehydrogenase and short-chain L-3-hydroxyacyl-CoA dehydrogenase respond well to diazoxide [172]. Therefore, it is plausible that certain SUs or KCOs may have an increased efficacy due to the alteration in the protein structure-function relationship the mutation precipitated. Therefore, linking the genetic and molecular aspects of K_{ATP} channel function to pharmacological methods to treat ND and HI may present an opportunity in managing type-2 diabetes in individuals which possess polymorphisms altering K_{ATP} channel function.

Hypothesis III

Interestingly, a recent study of ~1300 Chinese patients found that gliclaizide was more effective at lowering blood glucose levels in patients possessing the S1369A variant [220]. Another finding important to consider is that a neighbouring mutation, R1380L causes neonatal diabetes [221]. Therefore, understanding that the E23K-S1369A $K_{IR}6.2$-SUR1 variants are strongly associated highlighted the need to perform functional studies. This is necessary in order to ascertain the molecular mechanism which increases risk of type-2 diabetes development and modifies SU effectiveness of the E23K-S1369A K_{ATP}

channel haplotype. **I hypothesized that the E23K-S1369A K_{ATP} channel variant alters ATP-sensitivity and affects sulfonylurea potency, thereby altering K_{ATP} channel function in increasing the risk for type-2 diabetes**. We utilized electrophysiological techniques to study the functional properties of the E23K-S1369A haplotype. Findings from this study will provide insight into the molecular function of SUR1 and may impact treatment strategies in type-2 diabetic patients.

Summary of Hypotheses and Aims for this Thesis.

General Rationale

Ionic homeostasis is crucial for the physiological function of the myocardium and the insulin-secreting β-cells of the pancreas. Perturbance of ionic homeostasis, such as ROS-mediated intracellular Ca^{2+} accumulation via NCX1 in cardiac IR or the inability of K_{ATP} channels to close appropriately in response to glucose metabolism leads to IHD and type-2 diabetes, respectively. However, as NCX1 and the K_{ATP} channel play central roles in precipitating disease, a pharmacological approach may be taken to treat IHD and type-2 diabetes.

Hypothesis I – Chapter 2

ROS directly and irreversibly modifies NCX1.1, augmenting RM activity, thereby contributing to the intracellular Ca^{2+} overload that occurs during cardiac IR.

Hypothesis II – Chapter 3

The protective benefit afforded by ranolazine in cardiac IR occurs through the inhibition of RM-NCX1, in addition to late I_{Na} block.

Hypothesis III – Chapter 4

The E23K-S1369A K_{ATP} channel variant alters ATP-sensitivity and affects sulfonylurea potency, thereby altering K_{ATP} channel function in increasing the risk for type-2 diabetes.

Specific Aims

1. To elucidate the effect of ROS on recombinant NCX1 currents from NCX1 splice variants and the biophysical manner in which NCX1 currents are modified.
2. To determine whether NCX1 pharmacology is altered by ROS-modification of NCX1 protein.
3. To differentiate the effects of lidocaine and ranolazine in a ouabain-induced cardiac dysfunction model in an *ex vivo* working heart configuration.
4. To investigate the effect that ranolazine and lidocaine have on an *in vitro* assessment of RM-NCX1.1 activity.
5. To determine the pharmacological properties of ranolazine on RM-NCX1.1 current in comparison to NCX1 inhibitors.
6. To examine the MgATP and MgADP sensitivity on the haplotype E23K-S1369A human K_{ATP} channel.
7. To ascertain the functional and molecular mechanism which increases gliclazide potency in the haplotypic K_{ATP} channel versus other SUs.

Figure 1-1

Alternative Splicing of NCX1. (A) Diagrammatic Representation of human NCX1 Membrane Topology displaying the α-1 and α-2 re-entrant loops, the XIP region, calcium binding domains 1 and 2 (CBD1, CBD2), and the alternative splice region (ASR). Residues phenylalanine-223 (F223) and lysine-229 (K229) are critical for the Na^+-dependent, I_1-inactivation processs. **(B)** A diagram of the alternative splice region, depicting the mutually exclusive exons A and B, and cassette exons C, D, E, and F. Exon D is required in all NCX1 splice variants. **(C)** The amino acid sequences of NCX1 splice variants, NCX1.1, 1.3, 1.4, 1.7 and 1.11. The highlighted residues represent the conserved acid cluster required for Ca^{2+} binding.

A.

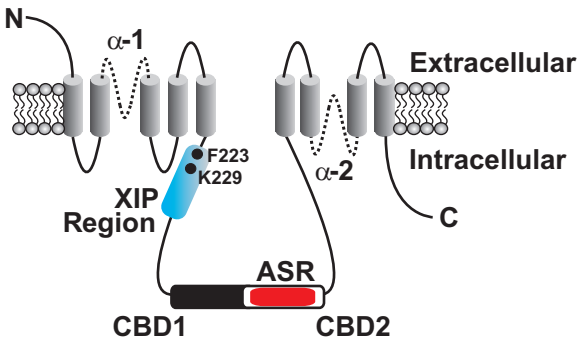

B.

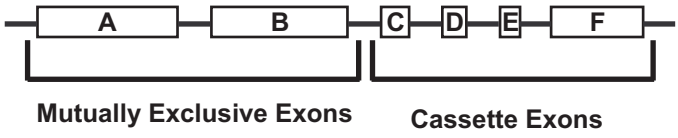

C.

		EXON A or B	EXON C	EXON D	EXON E	EXON F	
NCX1.1	604	KTISVKVIDD**EEYE**KNKTFFLEIGEPRLVEMSEKK	ALLLNEL	GGFTIT	GKYLF	GQPVFRKVHAREHPILSTVITIA	679
NCX1.3	604	KIITIRIFDR**EEYE**KECSFSLVLEEPKWIRRGMK-	-------	GGFTIT	-----	----------	643
NCX1.4	604	KTISVKVIDD**EEYE**KNKTFFLEIGEPRLVEMSEKK	-------	GGFTIT	-----	----------	644
NCX1.7	604	KIITIRIFDR**EEYE**KECSFSLVLEEPKWIRRGMK-	-------	GGFTIT	-----	GQPVFRKVHAREHPILSTVITIA	678
NCX1.11	604	KIITIRIFDR**EEYE**KECSFSLVLEEPKWIRRGMK-	ALLLNEL	GGFTIT	GKYLF	GQPVFRKVHAREHPILSTVITIA	666

Figure 1-2

Representative Recordings of human NCX1.1 and NCX1.3 current in Forward and Reverse Mode. (Ai & ii) Diagrammatic representation of NCX1 FM and RM currents, depicting a 3:1 ratio of Na^+:Ca^{2+} anti-transport. **(B-C)** Sample traces of human NCX1.1 and NCX1.3 currents in the inside-out excised patch clamp configuration recorded from transient expression in tsA201 cells. **(i)** Forward-mode. **(ii)** Reverse-mode.

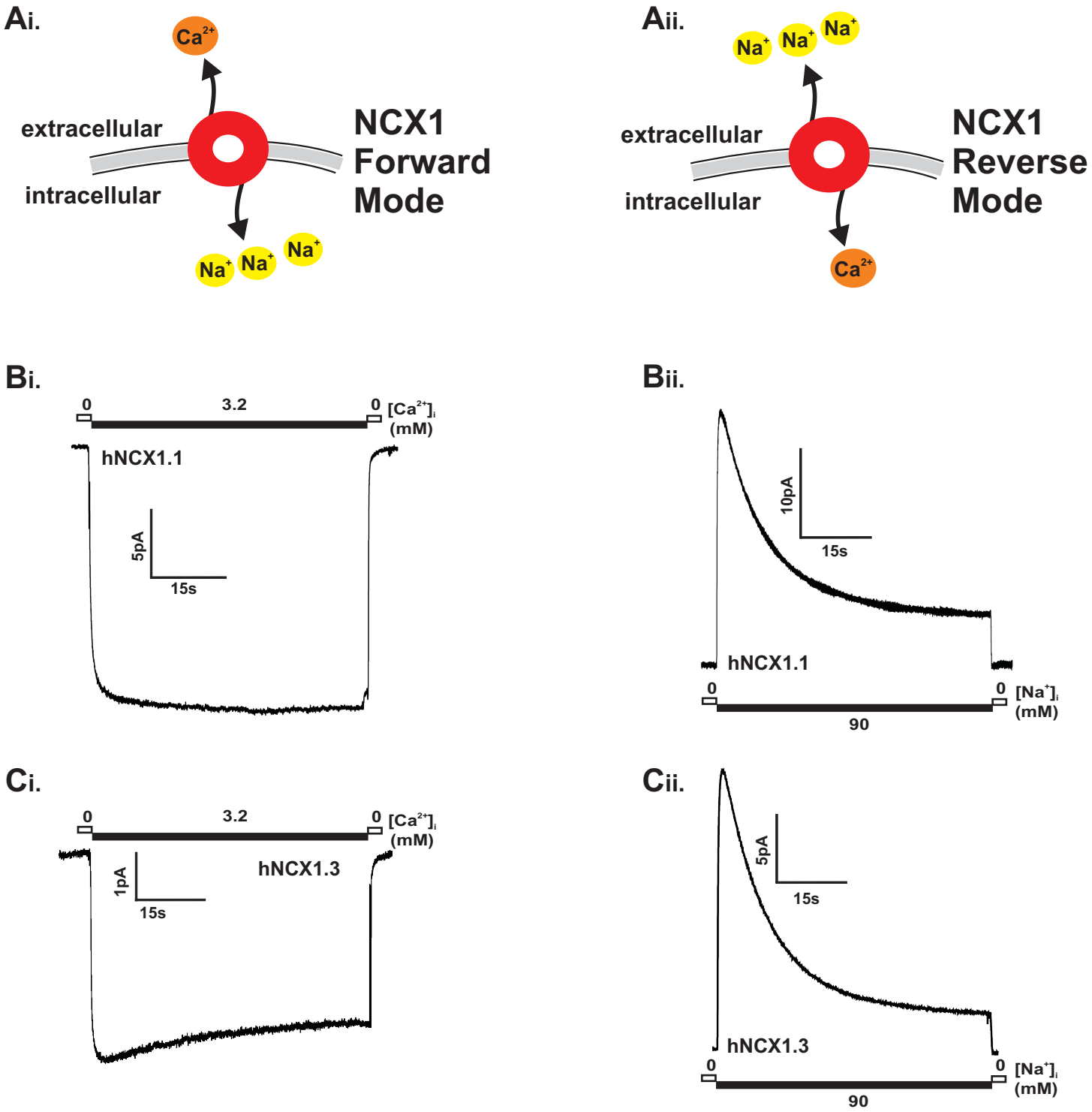
Ai.
Ca2+
extracellular
intracellular
NCX1
Forward
Mode
Na+
Na+
Na+
Aii.
Na+
Na+
Na+
extracellular
intracellular
NCX1
Reverse
Mode
Ca2+
Bi.
0
3.2
0
[Ca2+]i
(mM)
hNCX1.1
5pA
15s
Bii.
10pA
15s
hNCX1.1
0
0
[Na+]i
(mM)
90
Ci.
0
3.2
0
[Ca2+]i
(mM)
1pA
15s
hNCX1.3
Cii.
5pA
15s
hNCX1.3
0
0
[Na+]i
(mM)
90

Figure 1-3

Chemical Structures of NCX1 and Late I_{Na} Inhibitors. (A) NCX1 Inhibitors. KB-R7943 was derived into SN-6, while SEA0400 was further developed into YM-281956. KB-R7943 and SEA0400 were discovered in separate drug screening platforms. Dotted box depicts the benzyloxyphenyl moiety that is common to rationally screened NCX1 inhibitors. **(B)** Late I_{Na} inhibitors. Ranolazine contains the structural component of lidocaine, which is thought to bestow its selective late I_{Na} inhibition.

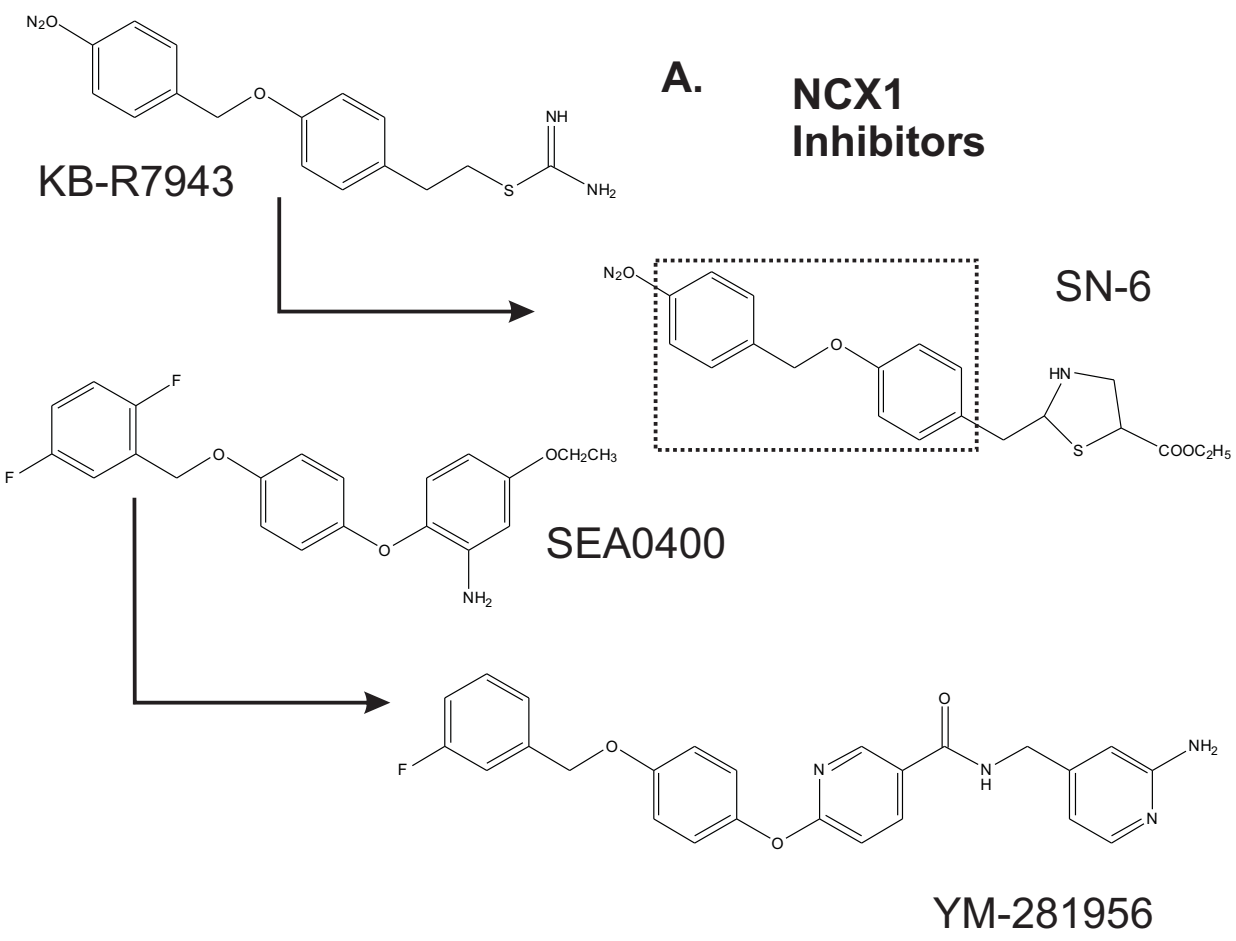
A.
NCX1 Inhibitors
KB-R7943
SN-6
SEA0400
YM-281956

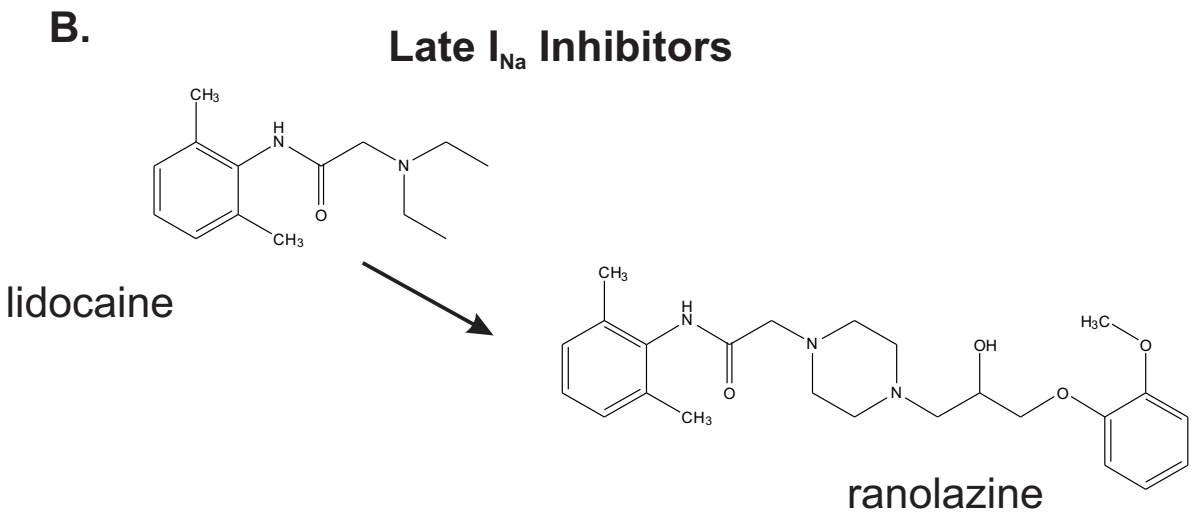
B.
Late I_{Na} Inhibitors
lidocaine
ranolazine

Figure 1-4

Ionic Dysfunction during Myocardial Ischemia-Reperfusion. During cardiac IR, a reliance on glycolysis reduces ATP production, as only a net of 2 molecules of ATP are generated per molecule glucose and increases H^+ production. Low intracellular ATP levels inhibits the Na^+-K^+-ATPase (NKA) preventing intracellular Na^+ extrusion. Intracellular H^+ acidosis is relieved through the Na^+-H^+ exchanger (NHE1), as H^+ are exchanged for Na^+. Late I_{Na} ($Na_v1.5$) also develops during IR and further contributes to intracellular Na^+ accumulation. The high intracellular Na^+ concentrations in combination with a depolarized membrane potential causes the Na^+-Ca^{2+} exchanger (NCX1.1) to function in RM, resulting in Ca^{2+} influx. Ca^{2+} overload ensues and is responsible for the myocardial dysfunction in the form of arrhythmias and stunning, and also myocyte apoptosis and necrosis. For this purpose, pharmacological interventions have been investigated in order to reduce cardiac IR injury. K_{ATP} channel openers repolarize the membrane potential reducing RM-NCX1 activity, while cariporide, inhibiting NHE1 and lidocaine and ranolazine, acting at $Na_v1.5$ aid to decrease intracellular Na^+ accumulation. KB-R7943 and SEA0400 can selectively inhibit the RM-NCX1.1, ameliorating intracellular Ca^{2+} overload.

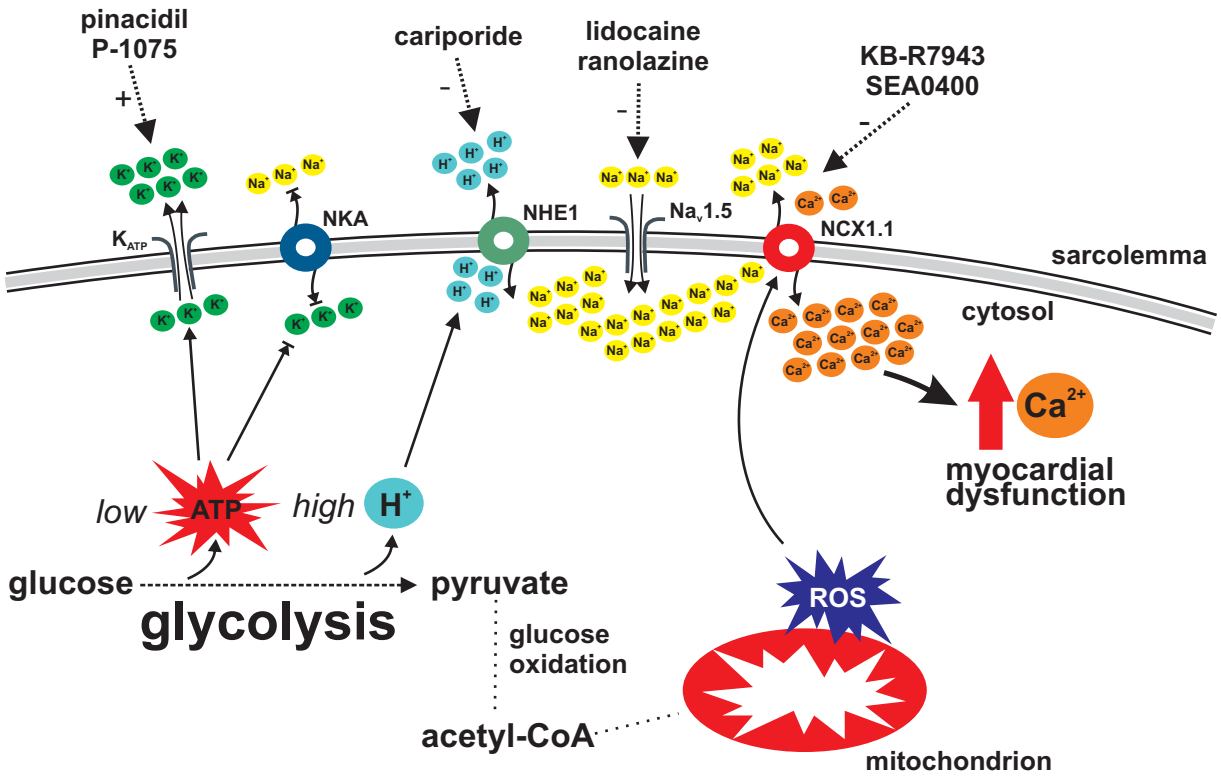
pinacidil
P-1075
+
cariporide
–
lidocaine
ranolazine
–
KB-R7943
SEA0400
–
NKA
NHE1
Na$_v$1.5
NCX1.1
K$_{ATP}$
sarcolemma
cytosol
Ca^{2+}
myocardial
dysfunction
low
ATP
high
H$^+$
glucose
pyruvate
glycolysis
glucose
oxidation
acetyl-CoA
ROS
mitochondrion

Figure 1-5

Diagrammatic Representation of Glucose-Stimulated Insulin Secretion from Pancreatic β-cells. (A) Low ATP:ADP ratio lends to K^+ efflux via K_{ATP} channels, which keeps the β-cell membrane potential at rest at approximately -70mV. This prevents Ca^{2+} through L-type VGCCs and insulin vesicle release. **(B)** High ATP:ADP ratio, from glucose metabolism initiates the closure of K_{ATP} channels, which depolarizes the β-cell membrane potential, causing the opening of L-type voltage gated Ca^{2+} channels (VGCC). The influx of Ca^{2+} is required for Ca^{2+}-dependent vesicle fusion of insulin granules. NCX1.3 regulates intracellular Ca^{2+} levels through Ca^{2+} extrusion. NKA maintains the necessary K^+ and Na^+ gradients. SUs, used for type-2 diabetes therapy, direct the closure of the K_{ATP} channel causing insulin secretion.

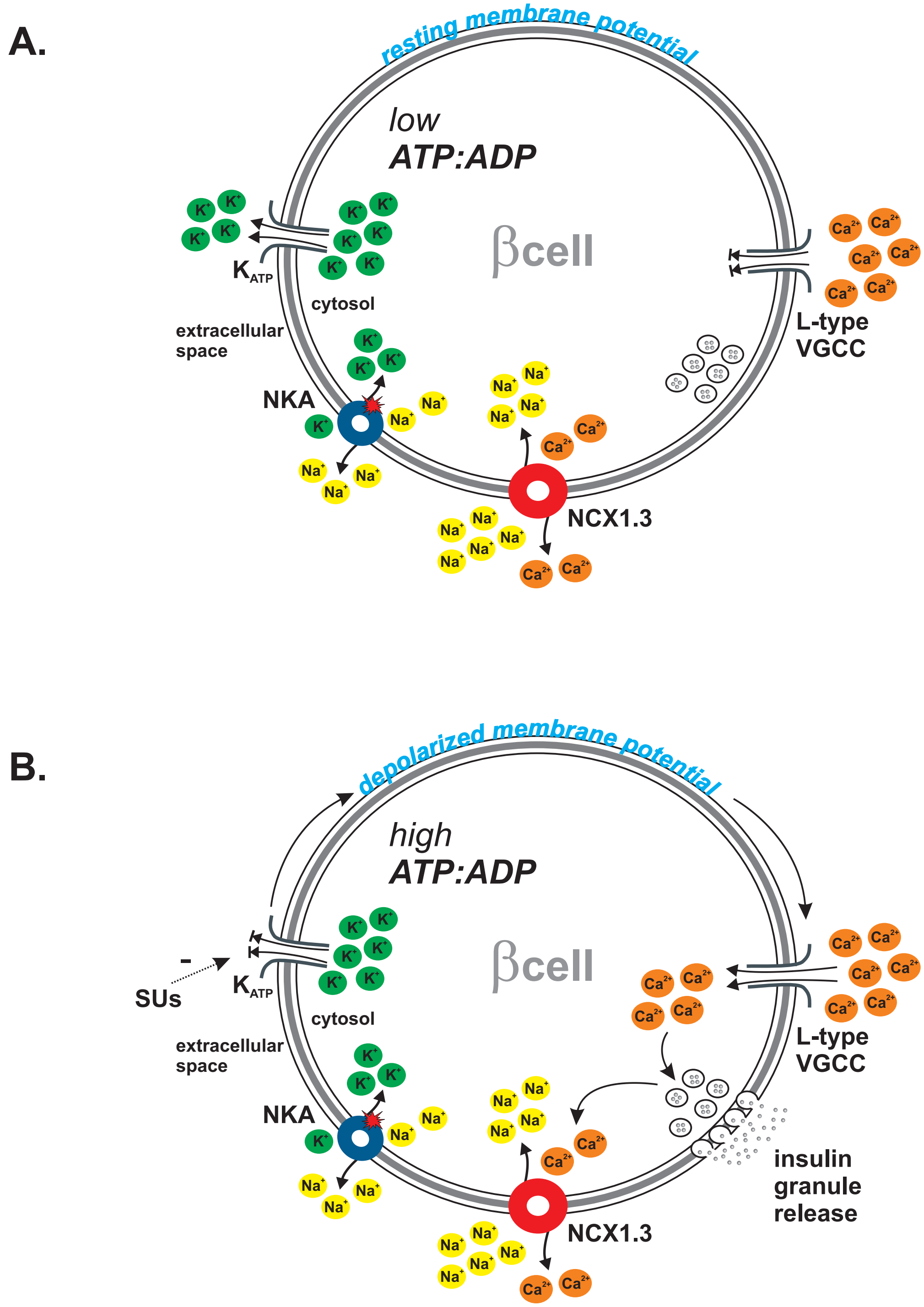
A.
resting membrane potential
low
ATP:ADP
βcell
K+
K_{ATP}
cytosol
extracellular space
NKA
Na+
Ca2+
NCX1.3
L-type VGCC
B.
depolarized membrane potential
high
ATP:ADP
βcell
-
SUs
K_{ATP}
cytosol
extracellular space
NKA
NCX1.3
L-type VGCC
insulin granule release

Figure 1-6

K_{ATP} channel K_{IR}6.2 and SUR1 subunits, Mutations and Pharmacology. The K_{ATP} channel is composed of the K^+-conducting pore subunit K_{IR}6.2 and the ATP-binding cassette protein, SUR1 in a 4:4 ratio to form a functional K_{ATP} channel. SUR1 contains nucleotide binding folds (NBFs 1 and 2) which confer its intrinsic MgATPase activity. Mutation R1380L precipitates neonatal diabetes, while S1369A is strongly associated with the K_{IR}6.2 variant E23K, which significantly increases risk for type-2 diabetes development. R201H mutation in K_{IR}6.2 also causes neonatal diabetes. SUR1 subunit is the site of action of sulfonylureas used in the treatment of type-2 diabetes. SUs can bind at the A-site (gliclazide), the B-site (repaglinide) or simultaneously occupying both sites (AB-site, glibenclamide). S1237Y removes gliclazide efficacy.

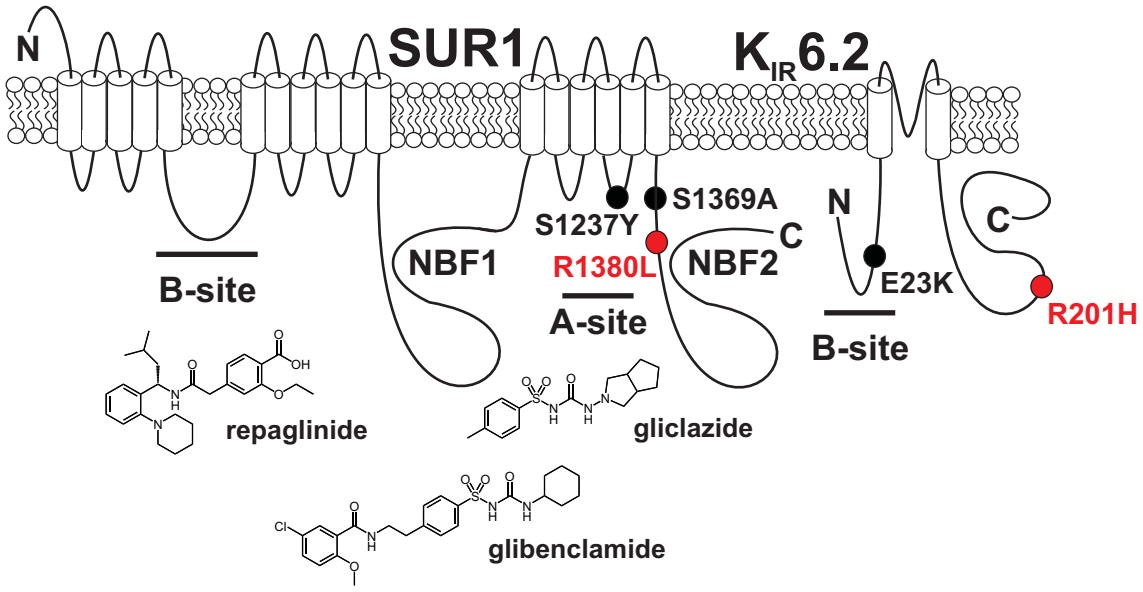
N
SUR1
K IR 6.2
S1369A
S1237Y
C
N
C
NBF1
R1380L
NBF2
E23K
R201H
B-site
A-site
B-site
repaglinide
gliclazide
glibenclamide

Figure 1-7

Intrinsic MgATP Hydrolysis at the SUR1 subunit of the K_{ATP} channel. MgATP is hydrolyzed to MgADP and P_i within the nucleotide binding folds, NBF1 and NBF2 within SUR1. MgADP in the post-hydrolytic state of MgATP hydrolysis removes free ATP mediated inhibition of the K_{ATP} channel at the $K_{IR}6.2$ subunit.

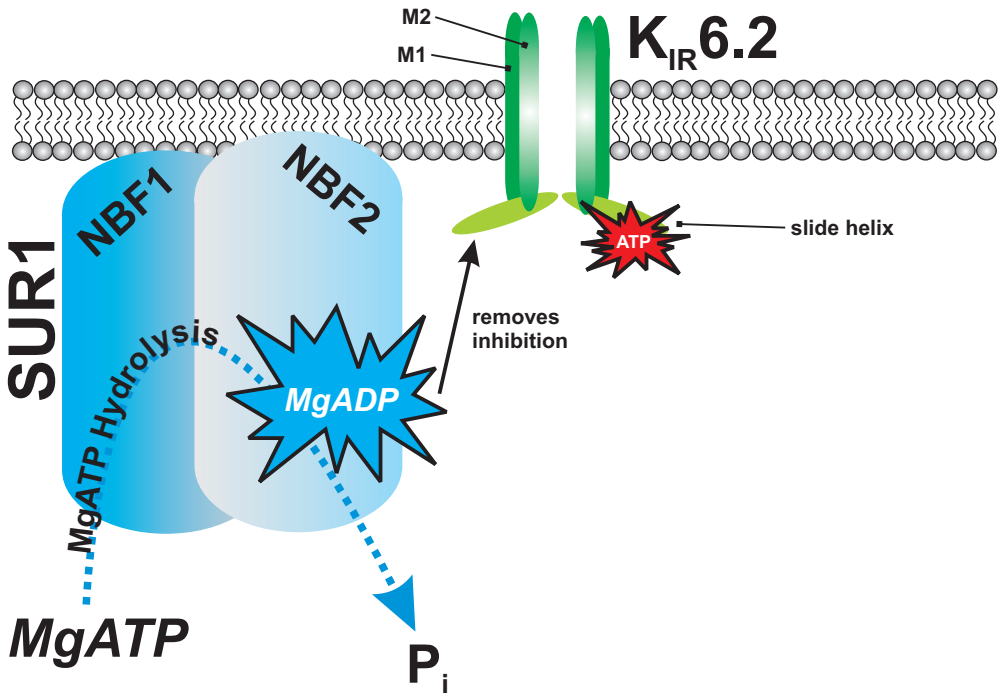
M2
M1
$K_{IR}6.2$
SUR1
NBF1
NBF2
slide helix
ATP
removes
inhibition
MgADP
MgATP Hydrolysis
MgATP
P_i

References

1. Mansfield E, McPherson R, Koski KG. Diet and waist-to-hip ratio: important predictors of lipoprotein levels in sedentary and active young men with no evidence of cardiovascular disease. J.Am.Diet.Assoc. 1999 Nov;99(11):1373-1379.

2. Fletcher GF, Balady G, Blair SN, Blumenthal J, Caspersen C, Chaitman B, et al. Statement on exercise: benefits and recommendations for physical activity programs for all Americans. A statement for health professionals by the Committee on Exercise and Cardiac Rehabilitation of the Council on Clinical Cardiology, American Heart Association. Circulation 1996 Aug 15;94(4):857-862.

3. Powell KE, Thompson PD, Caspersen CJ, Kendrick JS. Physical activity and the incidence of coronary heart disease. Annu.Rev.Public Health 1987;8:253-287.

4. Fuster V, Badimon L, Badimon JJ, Chesebro JH. The pathogenesis of coronary artery disease and the acute coronary syndromes (1). N.Engl.J.Med. 1992 Jan 23;326(4):242-250.

5. Misra MK, Sarwat M, Bhakuni P, Tuteja R, Tuteja N. Oxidative stress and ischemic myocardial syndromes. Med.Sci.Monit. 2009 Oct;15(10):RA209-219.

6. Kozakova M, Palombo C, Morizzo C, Nolan JJ, Konrad T, Balkau B, et al. Effect of sedentary behaviour and vigorous physical activity on segment-specific carotid wall thickness and its progression in a healthy population. Eur.Heart J. 2010 Apr 17.

7. Watts GF, Jackson P, Burke V, Lewis B. Dietary fatty acids and progression of coronary artery disease in men. Am.J.Clin.Nutr. 1996 Aug;64(2):202-209.

8. Grundy SM, Denke MA. Dietary influences on serum lipids and lipoproteins. J.Lipid Res. 1990 Jul;31(7):1149-1172.

9. Fried SK, Rao SP. Sugars, hypertriglyceridemia, and cardiovascular disease. Am.J.Clin.Nutr. 2003 Oct;78(4):873S-880S.

10. Sacks FM, Katan M. Randomized clinical trials on the effects of dietary fat and carbohydrate on plasma lipoproteins and cardiovascular disease. Am.J.Med. 2002 Dec 30;113 Suppl 9B:13S-24S.

11. Mensink RP, Katan MB. Effect of dietary fatty acids on serum lipids and lipoproteins. A meta-analysis of 27 trials. Arterioscler.Thromb. 1992 Aug;12(8):911-919.

12. Riedel MJ, Baczko I, Searle GJ, Webster N, Fercho M, Jones L, et al. Metabolic regulation of sodium-calcium exchange by intracellular acyl CoAs. EMBO J. 2006 Oct 4;25(19):4605-4614.

13. Peters AL. Patient and treatment perspectives: Revisiting the link between type 2 diabetes, weight gain, and cardiovascular risk. Cleve.Clin.J.Med. 2009 Dec;76 Suppl 5:S20-7.

14. Horton ES. Effects of lifestyle changes to reduce risks of diabetes and associated cardiovascular risks: results from large scale efficacy trials. Obesity (Silver Spring) 2009 Dec;17 Suppl 3:S43-8.

15. Riedel MJ, Steckley DC, Light PE. Current status of the E23K Kir6.2 polymorphism: implications for type-2 diabetes. Hum.Genet. 2005 Feb;116(3):133-145.

16. Gloyn AL, Weedon MN, Owen KR, Turner MJ, Knight BA, Hitman G, et al. Large-scale association studies of variants in genes encoding the pancreatic beta-cell KATP channel subunits Kir6.2 (KCNJ11) and SUR1 (ABCC8) confirm that the KCNJ11 E23K variant is associated with type 2 diabetes. Diabetes 2003 Feb;52(2):568-572.

17. Riedel MJ, Boora P, Steckley D, de Vries G, Light PE. Kir6.2 polymorphisms sensitize beta-cell ATP-sensitive potassium channels to activation by acyl CoAs: a possible cellular mechanism for increased susceptibility to type 2 diabetes? Diabetes 2003 Oct;52(10):2630-2635.

18. Hamming KS, Riedel MJ, Soliman D, Matemisz LC, Webster NJ, Searle GJ, et al. Splice variant-dependent regulation of beta-cell sodium-calcium exchange by acyl-coenzyme As. Mol.Endocrinol. 2008 Oct;22(10):2293-2306.

19. Bui QT, Prempeh M, Wilensky RL. Atherosclerotic plaque development. Int.J.Biochem.Cell Biol. 2009 Nov;41(11):2109-2113.

20. Gutstein DE, Fuster V. Pathophysiology and clinical significance of atherosclerotic plaque rupture. Cardiovasc.Res. 1999 Feb;41(2):323-333.

21. Asano G, Takashi E, Ishiwata T, Onda M, Yokoyama M, Naito Z, et al. Pathogenesis and protection of ischemia and reperfusion injury in myocardium. J.Nippon Med.Sch. 2003 Oct;70(5):384-392.

22. Katz AM. Effects of ischemia on the contractile processes of heart muscle. Am.J.Cardiol. 1973 Sep 20;32(4):456-460.

23. Clanachan AS. Contribution of protons to post-ischemic Na(+) and Ca(2+) overload and left ventricular mechanical dysfunction. J.Cardiovasc.Electrophysiol. 2006 May;17 Suppl 1:S141-S148.

24. Tani M, Neely JR. Role of intracellular Na+ in Ca2+ overload and depressed recovery of ventricular function of reperfused ischemic rat hearts. Possible involvement of H+-Na+ and Na+-Ca2+ exchange. Circ.Res. 1989 Oct;65(4):1045-1056.

25. Barry WH. Mechanisms of myocardial cell injury during ischemia and reperfusion. J.Card.Surg. 1987 Sep;2(3):375-383.

26. Noble D, Noble PJ. Late sodium current in the pathophysiology of cardiovascular disease: consequences of sodium-calcium overload. Heart 2006 Jul;92 Suppl 4:iv1-iv5.

27. Bers DM, Barry WH, Despa S. Intracellular Na+ regulation in cardiac myocytes. Cardiovasc.Res. 2003 Mar 15;57(4):897-912.

28. Saint DA. The role of the persistent Na(+) current during cardiac ischemia and hypoxia. J.Cardiovasc.Electrophysiol. 2006 May;17 Suppl 1:S96-S103.

29. Eigel BN, Hadley RW. Antisense inhibition of Na+/Ca2+ exchange during anoxia/reoxygenation in ventricular myocytes. Am.J.Physiol.Heart Circ.Physiol. 2001 Nov;281(5):H2184-90.

30. Eigel BN, Hadley RW. Contribution of the Na(+) channel and Na(+)/H(+) exchanger to the anoxic rise of [Na(+)] in ventricular myocytes. Am.J.Physiol. 1999 Nov;277(5 Pt 2):H1817-22.

31. Allen DG, Xiao XH. Role of the cardiac Na+/H+ exchanger during ischemia and reperfusion. Cardiovasc.Res. 2003 Mar 15;57(4):934-941.

32. Fliegel L. Regulation of the Na(+)/H(+) exchanger in the healthy and diseased myocardium. Expert Opin.Ther.Targets 2009 Jan;13(1):55-68.

33. Tani M. Mechanisms of Ca2+ overload in reperfused ischemic myocardium. Annu.Rev.Physiol. 1990;52:543-559.

34. Hryshko LV. The Cardiac Na+-Ca2+ Exchanger. In: Page E, Fozzard HA, Solaro RJ, editors. Handbook of Physiology, Section 2: The Cardiovascular System, Volume I: The Heart New York, New York, USA: Oxford University Press; 2002. p. 388.

35. Orrenius S, Zhivotovsky B, Nicotera P. Regulation of cell death: the calcium-apoptosis link. Nat.Rev.Mol.Cell Biol. 2003 Jul;4(7):552-565.

36. Akar JG, Akar FG. Regulation of ion channels and arrhythmias in the ischemic heart. J.Electrocardiol. 2007 Nov-Dec;40(6 Suppl):S37-41.

37. Schmitt J, Duray G, Gersh BJ, Hohnloser SH. Atrial fibrillation in acute myocardial infarction: a systematic review of the incidence, clinical features and prognostic implications. Eur.Heart J. 2009 May;30(9):1038-1045.

38. Akabas MH. Na+/Ca2+ exchange inhibitors: potential drugs to mitigate the severity of ischemic injury. Mol.Pharmacol. 2004 Jul;66(1):8-10.

39. Blaustein MP, Lederer WJ. Sodium/calcium exchange: its physiological implications. Physiol.Rev. 1999 Jul;79(3):763-854.

40. Zeitz O, Maass AE, Van Nguyen P, Hensmann G, Kogler H, Moller K, et al. Hydroxyl radical-induced acute diastolic dysfunction is due to calcium overload via reverse-mode Na(+)-Ca(2+) exchange. Circ.Res. 2002 May 17;90(9):988-995.

41. Lee C, Dhalla NS, Hryshko LV. Therapeutic potential of novel Na+-Ca2+ exchange inhibitors in attenuating ischemia-reperfusion injury. Can.J.Cardiol. 2005 May 1;21(6):509-516.

42. Schafer C, Ladilov Y, Inserte J, Schafer M, Haffner S, Garcia-Dorado D, et al. Role of the reverse mode of the Na+/Ca2+ exchanger in reoxygenation-induced cardiomyocyte injury. Cardiovasc.Res. 2001 Aug 1;51(2):241-250.

43. Dhalla NS, Temash RM, Netticadan T, Sandhu MS. Calcium overload in ischemia/reperfusion injury. In: Sperelakis N, Kurachi Y, Terzic A, Cohen MV, editors. Heart Physiology and Pathophysiology. San Diego: Academic Press; 2001. p. 949-965.

44. Hayashi H. Pathogenesis and the role of Ca2+ overload during myocardial ischemia/reperfusion. Nagoya J.Med.Sci. 2000 Nov;63(3-4):91-98.

45. Reuter H, Seitz N. The dependence of calcium efflux from cardiac muscle on temperature and external ion composition. J.Physiol. 1968 Mar;195(2):451-470.

46. Baker PF, Blaustein MP, Hodgkin AL, Steinhardt RA. The influence of calcium on sodium efflux in squid axons. J.Physiol. 1969 Feb;200(2):431-458.

47. Nicoll DA, Longoni S, Philipson KD. Molecular cloning and functional expression of the cardiac sarcolemmal Na(+)-Ca2+ exchanger. Science 1990 Oct 26;250(4980):562-565.

48. Quednau BD, Nicoll DA, Philipson KD. Tissue specificity and alternative splicing of the Na+/Ca2+ exchanger isoforms NCX1, NCX2, and NCX3 in rat. Am.J.Physiol. 1997 Apr;272(4 Pt 1):C1250-61.

49. Quednau BD, Nicoll DA, Philipson KD. The sodium/calcium exchanger family-SLC8. Pflugers Arch. 2004 Feb;447(5):543-548.

50. Nicoll DA, Ottolia M, Lu L, Lu Y, Philipson KD. A new topological model of the cardiac sarcolemmal Na+-Ca2+ exchanger. J.Biol.Chem. 1999 Jan 8;274(2):910-917.

51. Iwamoto T, Nakamura TY, Pan Y, Uehara A, Imanaga I, Shigekawa M. Unique topology of the internal repeats in the cardiac Na+/Ca2+ exchanger. FEBS Lett. 1999 Mar 12;446(2-3):264-268.

52. Lytton J. Na+/Ca2+ exchangers: three mammalian gene families control Ca2+ transport. Biochem.J. 2007 Sep 15;406(3):365-382.

53. Ren X, Nicoll DA, Philipson KD. Helix packing of the cardiac Na+-Ca2+ exchanger: proximity of transmembrane segments 1, 2, and 6. J.Biol.Chem. 2006 Aug 11;281(32):22808-22814.

54. Qiu Z, Nicoll DA, Philipson KD. Helix packing of functionally important regions of the cardiac Na(+)-Ca(2+) exchanger. J.Biol.Chem. 2001 Jan 5;276(1):194-199.

55. Li Z, Nicoll DA, Collins A, Hilgemann DW, Filoteo AG, Penniston JT, et al. Identification of a peptide inhibitor of the cardiac sarcolemmal Na(+)-Ca2+ exchanger. J.Biol.Chem. 1991 Jan 15;266(2):1014-1020.

56. Maack C, Ganesan A, Sidor A, O'Rourke B. Cardiac sodium-calcium exchanger is regulated by allosteric calcium and exchanger inhibitory peptide at distinct sites. Circ.Res. 2005 Jan 7;96(1):91-99.

57. Nicoll DA, Sawaya MR, Kwon S, Cascio D, Philipson KD, Abramson J. The crystal structure of the primary Ca2+ sensor of the Na+/Ca2+ exchanger reveals a novel Ca2+ binding motif. J.Biol.Chem. 2006 Aug 4;281(31):21577-21581.

58. Ottolia M, Nicoll DA, Philipson KD. Roles of two Ca2+-binding domains in regulation of the cardiac Na+-Ca2+ exchanger. J.Biol.Chem. 2009 Nov 20;284(47):32735-32741.

59. Levitsky DO, Nicoll DA, Philipson KD. Identification of the high affinity Ca(2+)-binding domain of the cardiac Na(+)-Ca2+ exchanger. J.Biol.Chem. 1994 Sep 9;269(36):22847-22852.

60. Hilge M, Aelen J, Vuister GW. Ca2+ regulation in the Na+/Ca2+ exchanger involves two markedly different Ca2+ sensors. Mol.Cell 2006 Apr 7;22(1):15-25.

61. Dunn J, Elias CL, Le HD, Omelchenko A, Hryshko LV, Lytton J. The molecular determinants of ionic regulatory differences between brain and kidney Na+/Ca2+ exchanger (NCX1) isoforms. J.Biol.Chem. 2002 Sep 13;277(37):33957-33962.

62. Hilgemann DW. Giant excised cardiac sarcolemmal membrane patches: sodium and sodium-calcium exchange currents. Pflugers Arch. 1989 Nov;415(2):247-249.

63. Hilgemann DW. Regulation and deregulation of cardiac Na(+)-Ca2+ exchange in giant excised sarcolemmal membrane patches. Nature 1990 Mar 15;344(6263):242-245.

64. Dong H, Light PE, French RJ, Lytton J. Electrophysiological characterization and ionic stoichiometry of the rat brain K(+)-dependent NA(+)/CA(2+) exchanger, NCKX2. J.Biol.Chem. 2001 Jul 13;276(28):25919-25928.

65. Lytton J, Dong H. Rat heart NCX1.1 stoichiometry measured in a transfected cell system. Ann.N.Y.Acad.Sci. 2002 Nov;976:137-141.

66. Matsuoka S, Nicoll DA, Reilly RF, Hilgemann DW, Philipson KD. Initial localization of regulatory regions of the cardiac sarcolemmal Na(+)-Ca2+ exchanger. Proc.Natl.Acad.Sci.U.S.A. 1993 May 1;90(9):3870-3874.

67. Dong H, Dunn J, Lytton J. Stoichiometry of the Cardiac Na+/Ca2+ exchanger NCX1.1 measured in transfected HEK cells. Biophys.J. 2002 Apr;82(4):1943-1952.

68. Dong H, Dunn J, Lytton J. Electrophysiological studies of the cloned rat cardiac NCX1.1 in transfected HEK cells: a focus on the stoichiometry. Ann.N.Y.Acad.Sci. 2002 Nov;976:159-165.

69. Fujioka Y, Komeda M, Matsuoka S. Stoichiometry of Na+-Ca2+ exchange in inside-out patches excised from guinea-pig ventricular myocytes. J.Physiol. 2000 Mar 1;523 Pt 2:339-351.

70. Niggli E, Lederer WJ. Molecular operations of the sodium-calcium exchanger revealed by conformation currents. Nature 1991 Feb 14;349(6310):621-624.

71. Powell T, Noma A, Shioya T, Kozlowski RZ. Turnover rate of the cardiac Na(+)-Ca2+ exchanger in guinea-pig ventricular myocytes. J.Physiol. 1993 Dec;472:45-53.

72. Thomas MJ, Sjaastad I, Andersen K, Helm PJ, Wasserstrom JA, Sejersted OM, et al. Localization and function of the Na+/Ca2+-exchanger in normal and detubulated rat cardiomyocytes. J.Mol.Cell.Cardiol. 2003 Nov;35(11):1325-1337.

73. Matsuoka S, Nicoll DA, He Z, Philipson KD. Regulation of cardiac Na(+)-Ca2+ exchanger by the endogenous XIP region. J.Gen.Physiol. 1997 Feb;109(2):273-286.

74. He Z, Feng S, Tong Q, Hilgemann DW, Philipson KD. Interaction of PIP(2) with the XIP region of the cardiac Na/Ca exchanger. Am.J.Physiol.Cell.Physiol. 2000 Apr;278(4):C661-6.

75. Yaradanakul A, Feng S, Shen C, Lariccia V, Lin MJ, Yang J, et al. Dual control of cardiac Na+ Ca2+ exchange by PIP(2): electrophysiological analysis of direct and indirect mechanisms. J.Physiol. 2007 Aug 1;582(Pt 3):991-1010.

76. Shen C, Lin MJ, Yaradanakul A, Lariccia V, Hill JA, Hilgemann DW. Dual control of cardiac Na+ Ca2+ exchange by PIP(2): analysis of the surface membrane fraction by extracellular cysteine PEGylation. J.Physiol. 2007 Aug 1;582(Pt 3):1011-1026.

77. Doering AE, Lederer WJ. The action of Na+ as a cofactor in the inhibition by cytoplasmic protons of the cardiac Na(+)-Ca2+ exchanger in the guinea-pig. J.Physiol. 1994 Oct 1;480 (Pt 1)(Pt 1):9-20.

78. Chernysh O, Condrescu M, Reeves JP. Sodium-dependent inactivation of sodium/calcium exchange in transfected Chinese hamster ovary cells. Am.J.Physiol.Cell.Physiol. 2008 Oct;295(4):C872-82.

79. Wang J, Zhang XQ, Ahlers BA, Carl LL, Song J, Rothblum LI, et al. Cytoplasmic tail of phospholemman interacts with the intracellular loop of the cardiac Na+/Ca2+ exchanger. J.Biol.Chem. 2006 Oct 20;281(42):32004-32014.

80. Cheung JY, Rothblum LI, Moorman JR, Tucker AL, Song J, Ahlers BA, et al. Regulation of cardiac Na+/Ca2+ exchanger by phospholemman. Ann.N.Y.Acad.Sci. 2007 Mar;1099:119-134.

81. Crambert G, Fuzesi M, Garty H, Karlish S, Geering K. Phospholemman (FXYD1) associates with Na,K-ATPase and regulates its transport properties. Proc.Natl.Acad.Sci.U.S.A. 2002 Aug 20;99(17):11476-11481.

82. Berry RG, Despa S, Fuller W, Bers DM, Shattock MJ. Differential distribution and regulation of mouse cardiac Na+/K+-ATPase alpha1 and alpha2 subunits in T-tubule and surface sarcolemmal membranes. Cardiovasc.Res. 2007 Jan 1;73(1):92-100.

83. Zhang XQ, Qureshi A, Song J, Carl LL, Tian Q, Stahl RC, et al. Phospholemman modulates Na+/Ca2+ exchange in adult rat cardiac myocytes. Am.J.Physiol.Heart Circ.Physiol. 2003 Jan;284(1):H225-33.

84. Swift F, Birkeland JA, Tovsrud N, Enger UH, Aronsen JM, Louch WE, et al. Altered Na+/Ca2+-exchanger activity due to downregulation of Na+/K+-ATPase alpha2-isoform in heart failure. Cardiovasc.Res. 2008 Apr 1;78(1):71-78.

85. Philipson KD, Nicoll DA, Ottolia M, Quednau BD, Reuter H, John S, et al. The Na+/Ca2+ exchange molecule: an overview. Ann.N.Y.Acad.Sci. 2002 Nov;976:1-10.

86. Bers DM. Regulation of cellular calcium in cardiac myocytes. In: Page E, Fozzard HA, Solaro RJ, editors. New York, New York, USA: Oxford University Press; 2002. p. 335.

87. Bers DM, Despa S. Cardiac myocytes Ca2+ and Na+ regulation in normal and failing hearts. J.Pharmacol.Sci. 2006;100(5):315-322.

88. Komuro I, Ohtsuka M. Forefront of Na+/Ca2+ exchanger studies: role of Na+/Ca2+ exchanger--lessons from knockout mice. J.Pharmacol.Sci. 2004 Sep;96(1):23-26.

89. Whitmer JT, Idell-Wenger JA, Rovetto MJ, Neely JR. Control of fatty acid metabolism in ischemic and hypoxic hearts. J.Biol.Chem. 1978 Jun 25;253(12):4305-4309.

90. Henry TD, Archer SL, Nelson D, Weir EK, From AH. Enhanced chemiluminescence as a measure of oxygen-derived free radical generation during ischemia and reperfusion. Circ.Res. 1990 Dec;67(6):1453-1461.

91. Ferrari R, Ceconi C, Curello S, Alfieri O, Visioli O. Myocardial damage during ischaemia and reperfusion. Eur.Heart J. 1993 Nov;14 Suppl G:25-30.

92. Zweier JL, Kuppusamy P, Thompson-Gorman S, Klunk D, Lutty GA. Measurement and characterization of free radical generation in reoxygenated human endothelial cells. Am.J.Physiol. 1994 Mar;266(3 Pt 1):C700-8.

93. Zima AV, Blatter LA. Redox regulation of cardiac calcium channels and transporters. Cardiovasc.Res. 2006 Jul 15;71(2):310-321.

94. Kourie JI. Interaction of reactive oxygen species with ion transport mechanisms. Am.J.Physiol. 1998 Jul;275(1 Pt 1):C1-24.

95. Tokube K, Kiyosue T, Arita M. Openings of cardiac KATP channel by oxygen free radicals produced by xanthine oxidase reaction. Am.J.Physiol. 1996 Aug;271(2 Pt 2):H478-89.

96. Tokube K, Kiyosue T, Arita M. Effects of hydroxyl radicals on KATP channels in guinea-pig ventricular myocytes. Pflugers Arch. 1998 Dec;437(1):155-157.

97. Reeves JP, Bailey CA, Hale CC. Redox modification of sodium-calcium exchange activity in cardiac sarcolemmal vesicles. J.Biol.Chem. 1986 Apr 15;261(11):4948-4955.

98. Goldhaber JI. Free radicals enhance Na+/Ca2+ exchange in ventricular myocytes. Am.J.Physiol. 1996 Sep;271(3 Pt 2):H823-33.

99. Wagner S, Seidler T, Picht E, Maier LS, Kazanski V, Teucher N, et al. Na(+)-Ca(2+) exchanger overexpression predisposes to reactive oxygen species-induced injury. Cardiovasc.Res. 2003 Nov 1;60(2):404-412.

100. Eigel BN, Gursahani H, Hadley RW. ROS are required for rapid reactivation of Na+/Ca2+ exchanger in hypoxic reoxygenated guinea pig ventricular myocytes. Am.J.Physiol.Heart Circ.Physiol. 2004 Mar;286(3):H955-63.

101. He Z, Petesch N, Voges K, Roben W, Philipson KD. Identification of important amino acid residues of the Na+-Ca2+ exchanger inhibitory peptide, XIP. J.Membr.Biol. 1997 Mar 15;156(2):149-156.

102. Iwamoto T, Watano T, Shigekawa M. A novel isothiourea derivative selectively inhibits the reverse mode of Na+/Ca2+ exchange in cells expressing NCX1. J.Biol.Chem. 1996 Sep 13;271(37):22391-22397.

103. Seki S, Taniguchi M, Takeda H, Nagai M, Taniguchi I, Mochizuki S. Inhibition by KB-r7943 of the reverse mode of the Na+/Ca2+ exchanger reduces Ca2+ overload in ischemic-reperfused rat hearts. Circ.J. 2002 Apr;66(4):390-396.

104. Watano T, Harada Y, Harada K, Nishimura N. Effect of Na+/Ca2+ exchange inhibitor, KB-R7943 on ouabain-induced arrhythmias in guinea-pigs. Br.J.Pharmacol. 1999 Aug;127(8):1846-1850.

105. Elias CL, Lukas A, Shurraw S, Scott J, Omelchenko A, Gross GJ, et al. Inhibition of Na+/Ca2+ exchange by KB-R7943: transport mode selectivity and antiarrhythmic consequences. Am.J.Physiol.Heart Circ.Physiol. 2001 Sep;281(3):H1334-45.

106. Matsumoto T, Miura T, Miki T, Genda S, Shimamoto K. Blockade of the Na+-Ca2+ exchanger is more efficient than blockade of the Na+-H+ exchanger for protection of the myocardium from lethal reperfusion injury. Cardiovasc.Drugs Ther. 2002 Jul;16(4):295-301.

107. Iwamoto T, Kita S. Development and application of Na+/Ca2+ exchange inhibitors. Mol.Cell.Biochem. 2004 Apr;259(1-2):157-161.

108. Iwamoto T. Forefront of Na+/Ca2+ exchanger studies: molecular pharmacology of Na+/Ca2+ exchange inhibitors. J.Pharmacol.Sci. 2004 Sep;96(1):27-32.

109. Watano T, Kimura J, Morita T, Nakanishi H. A novel antagonist, No. 7943, of the Na+/Ca2+ exchange current in guinea-pig cardiac ventricular cells. Br.J.Pharmacol. 1996 Oct;119(3):555-563.

110. Matsuda T, Arakawa N, Takuma K, Kishida Y, Kawasaki Y, Sakaue M, et al. SEA0400, a novel and selective inhibitor of the Na+-Ca2+ exchanger, attenuates reperfusion injury in the in vitro and in vivo cerebral ischemic models. J.Pharmacol.Exp.Ther. 2001 Jul;298(1):249-256.

111. Namekata I, Nakamura H, Shimada H, Tanaka H, Shigenobu K. Cardioprotection without cardiosuppression by SEA0400, a novel inhibitor of Na+-Ca2+ exchanger, during ischemia and reperfusion in guinea-pig myocardium. Life Sci. 2005 Jun 3;77(3):312-324.

112. Takahashi K, Takahashi T, Suzuki T, Onishi M, Tanaka Y, Hamano-Takahashi A, et al. Protective effects of SEA0400, a novel and selective inhibitor of the Na+/Ca2+ exchanger, on myocardial ischemia-reperfusion injuries. Eur.J.Pharmacol. 2003 Jan 1;458(1-2):155-162.

113. Magee WP, Deshmukh G, Deninno MP, Sutt JC, Chapman JG, Tracey WR. Differing cardioprotective efficacy of the Na+/Ca2+ exchanger inhibitors SEA0400 and KB-R7943. Am.J.Physiol.Heart Circ.Physiol. 2003 Mar;284(3):H903-10.

114. Yoshiyama M, Nakamura Y, Omura T, Hayashi T, Takagi Y, Hasegawa T, et al. Cardioprotective effect of SEA0400, a selective inhibitor of the Na(+)/Ca(2+) exchanger, on myocardial ischemia-reperfusion injury in rats. J.Pharmacol.Sci. 2004 Jun;95(2):196-202.

115. Feng NC, Satoh H, Urushida T, Katoh H, Terada H, Watanabe Y, et al. A selective inhibitor of Na+/Ca2+ exchanger, SEA0400, preserves cardiac function and high-energy phosphates against ischemia/reperfusion injury. J.Cardiovasc.Pharmacol. 2006 Feb;47(2):263-270.

116. Iwamoto T, Kita S, Uehara A, Inoue Y, Taniguchi Y, Imanaga I, et al. Structural domains influencing sensitivity to isothiourea derivative inhibitor KB-R7943 in cardiac Nna(+)/Ca(2+) exchanger. Mol.Pharmacol. 2001 Mar;59(3):524-531.

117. Iwamoto T, Kita S, Uehara A, Imanaga I, Matsuda T, Baba A, et al. Molecular determinants of Na+/Ca2+ exchange (NCX1) inhibition by SEA0400. J.Biol.Chem. 2004 Feb 27;279(9):7544-7553.

118. Reuter H, Henderson SA, Han T, Matsuda T, Baba A, Ross RS, et al. Knockout mice for pharmacological screening: testing the specificity of Na+-Ca2+ exchange inhibitors. Circ.Res. 2002 Jul 26;91(2):90-92.

119. Iwamoto T, Kita S. YM-244769, a novel Na+/Ca2+ exchange inhibitor that preferentially inhibits NCX3, efficiently protects against hypoxia/reoxygenation-induced SH-SY5Y neuronal cell damage. Mol.Pharmacol. 2006 Dec;70(6):2075-2083.

120. Iwamoto T, Inoue Y, Ito K, Sakaue T, Kita S, Katsuragi T. The exchanger inhibitory peptide region-dependent inhibition of Na+/Ca2+ exchange by SN-6 [2-[4-(4-nitrobenzyloxy)benzyl]thiazolidine-4-carboxylic acid ethyl ester], a novel benzyloxyphenyl derivative. Mol.Pharmacol. 2004 Jul;66(1):45-55.

121. Niu CF, Watanabe Y, Ono K, Iwamoto T, Yamashita K, Satoh H, et al. Characterization of SN-6, a novel Na+/Ca2+ exchange inhibitor in guinea pig cardiac ventricular myocytes. Eur.J.Pharmacol. 2007 Nov 14;573(1-3):161-169.

122. Karmazyn M. Pharmacology and clinical assessment of cariporide for the treatment coronary artery diseases. Expert Opin.Investig.Drugs 2000 May;9(5):1099-1108.

123. Karmazyn M, Sostaric JV, Gan XT. The myocardial Na+/H+ exchanger: a potential therapeutic target for the prevention of myocardial ischaemic and reperfusion injury and attenuation of postinfarction heart failure. Drugs 2001;61(3):375-389.

124. Doggrell SA, Hancox JC. Is timing everything? Therapeutic potential of modulators of cardiac Na(+) transporters. Expert Opin.Investig.Drugs 2003 Jul;12(7):1123-1142.

125. Rudy Y. The Cardiac Ventricular Action Potential. In: Page E, Fozzard HA, Solaro RJ, editors. Handbook of Physiology, Section 2: The Cardiovascular System, Volume I: The Heart New York, New York, USA: Oxford University Press; 2002. p. 531.

126. Saenen JB, Vrints CJ. Molecular aspects of the congenital and acquired Long QT Syndrome: clinical implications. J.Mol.Cell.Cardiol. 2008 Apr;44(4):633-646.

127. Fedida D, Orth PM, Hesketh JC, Ezrin AM. The role of late I and antiarrhythmic drugs in EAD formation and termination in Purkinje fibers. J.Cardiovasc.Electrophysiol. 2006 May;17 Suppl 1:S71-S78.

128. Wu J, Corr PB. Palmitoyl carnitine modifies sodium currents and induces transient inward current in ventricular myocytes. Am.J.Physiol. 1994 Mar;266(3 Pt 2):H1034-46.

129. Song Y, Shryock JC, Wagner S, Maier LS, Belardinelli L. Blocking late sodium current reduces hydrogen peroxide-induced arrhythmogenic activity and contractile dysfunction. J.Pharmacol.Exp.Ther. 2006 Jul;318(1):214-222.

130. Undrovinas AI, Fleidervish IA, Makielski JC. Inward sodium current at resting potentials in single cardiac myocytes induced by the ischemic metabolite lysophosphatidylcholine. Circ.Res. 1992 Nov;71(5):1231-1241.

131. Light PE, Wallace CH, Dyck JR. Constitutively active adenosine monophosphate-activated protein kinase regulates voltage-gated sodium channels in ventricular myocytes. Circulation 2003 Apr 22;107(15):1962-1965.

132. Le Grand B, Vie B, Talmant JM, Coraboeuf E, John GW. Alleviation of contractile dysfunction in ischemic hearts by slowly inactivating Na+ current blockers. Am.J.Physiol. 1995 Aug;269(2 Pt 2):H533-40.

133. Le Grand B, Coulombe A, John GW. Late sodium current inhibition in human isolated cardiomyocytes by R 56865. J.Cardiovasc.Pharmacol. 1998 May;31(5):800-804.

134. Hartmann M, Decking UK. R 56865 exerts cardioprotective properties independent of the intracellular Na(+)-overload in the guinea pig heart. Naunyn Schmiedebergs Arch.Pharmacol. 2003 Sep;368(3):160-165.

135. McCormack JG, Barr RL, Wolff AA, Lopaschuk GD. Ranolazine stimulates glucose oxidation in normoxic, ischemic, and reperfused ischemic rat hearts. Circulation 1996 Jan 1;93(1):135-142.

136. Wang P, Fraser H, Lloyd SG, McVeigh JJ, Belardinelli L, Chatham JC. A comparison between ranolazine and CVT-4325, a novel inhibitor of fatty acid oxidation, on cardiac metabolism and left ventricular function in rat isolated perfused heart during ischemia and reperfusion. J.Pharmacol.Exp.Ther. 2007 Apr;321(1):213-220.

137. Maier LS. A novel mechanism for the treatment of angina, arrhythmias, and diastolic dysfunction: inhibition of late I(Na) using ranolazine. J.Cardiovasc.Pharmacol. 2009 Oct;54(4):279-286.

138. Antzelevitch C, Belardinelli L, Zygmunt AC, Burashnikov A, Di Diego JM, Fish JM, et al. Electrophysiological effects of ranolazine, a novel antianginal agent with antiarrhythmic properties. Circulation 2004 Aug 24;110(8):904-910.

139. Antzelevitch C, Belardinelli L, Wu L, Fraser H, Zygmunt AC, Burashnikov A, et al. Electrophysiologic properties and antiarrhythmic actions of a novel antianginal agent. J.Cardiovasc.Pharmacol.Ther. 2004 Sep;9 Suppl 1:S65-83.

140. Hale SL, Shryock JC, Belardinelli L, Sweeney M, Kloner RA. Late sodium current inhibition as a new cardioprotective approach. J.Mol.Cell.Cardiol. 2008 Jun;44(6):954-967.

141. Hasenfuss G, Maier LS. Mechanism of action of the new anti-ischemia drug ranolazine. Clin.Res.Cardiol. 2008 Apr;97(4):222-226.

142. Stone PH. Ranolazine: new paradigm for management of myocardial ischemia, myocardial dysfunction, and arrhythmias. Cardiol.Clin. 2008 Nov;26(4):603-614.

143. Zhang XQ, Yamada S, Barry WH. Ranolazine inhibits an oxidative stress-induced increase in myocyte sodium and calcium loading during simulated-demand ischemia. J.Cardiovasc.Pharmacol. 2008 May;51(5):443-449.

144. Fraser H, Belardinelli L, Wang L, Light PE, McVeigh JJ, Clanachan AS. Ranolazine decreases diastolic calcium accumulation caused by ATX-II or ischemia in rat hearts. J.Mol.Cell.Cardiol. 2006 Dec;41(6):1031-1038.

145. Shryock JC, Belardinelli L. Inhibition of late sodium current to reduce electrical and mechanical dysfunction of ischaemic myocardium. Br.J.Pharmacol. 2008 Mar;153(6):1128-1132.

146. Saint DA. The cardiac persistent sodium current: an appealing therapeutic target? Br.J.Pharmacol. 2008 Mar;153(6):1133-1142.

147. Hwang H, Arcidi JM,Jr, Hale SL, Simkhovich BZ, Belardinelli L, Dhalla AK, et al. Ranolazine as a cardioplegia additive improves recovery of diastolic function in isolated rat hearts. Circulation 2009 Sep 15;120(11 Suppl):S16-21.

148. Wasserstrom JA, Sharma R, O'Toole MJ, Zheng J, Kelly JE, Shryock J, et al. Ranolazine antagonizes the effects of increased late sodium current on intracellular calcium cycling in rat isolated intact heart. J.Pharmacol.Exp.Ther. 2009 Nov;331(2):382-391.

149. Altamirano J, Li Y, DeSantiago J, Piacentino V,3rd, Houser SR, Bers DM. The inotropic effect of cardioactive glycosides in ventricular myocytes requires Na+-Ca2+ exchanger function. J.Physiol. 2006 Sep 15;575(Pt 3):845-854.

150. Nishio M, Ruch SW, Wasserstrom JA. Positive inotropic effects of ouabain in isolated cat ventricular myocytes in sodium-free conditions. Am.J.Physiol.Heart Circ.Physiol. 2002 Nov;283(5):H2045-53.

151. Reuter H, Henderson SA, Han T, Ross RS, Goldhaber JI, Philipson KD. The Na+-Ca2+ exchanger is essential for the action of cardiac glycosides. Circ.Res. 2002 Feb 22;90(3):305-308.

152. Cascio WE, Yang H, Johnson TA, Muller-Borer BJ, Lemasters JJ. Electrical properties and conduction in reperfused papillary muscle. Circ.Res. 2001 Oct 26;89(9):807-814.

153. Baczko I, Giles WR, Light PE. Resting membrane potential regulates Na(+)-Ca2+ exchange-mediated Ca2+ overload during hypoxia-reoxygenation in rat ventricular myocytes. J.Physiol. 2003 Aug 1;550(Pt 3):889-898.

154. Baczko I, Jones L, McGuigan CF, Manning Fox JE, Gandhi M, Giles WR, et al. Plasma membrane KATP channel-mediated cardioprotection involves posthypoxic reductions in calcium overload and contractile dysfunction: mechanistic insights into cardioplegia. FASEB J. 2005 Jun;19(8):980-982.

155. Baczko I, Giles WR, Light PE. Pharmacological activation of plasma-membrane KATP channels reduces reoxygenation-induced Ca(2+) overload in cardiac myocytes via modulation of the diastolic membrane potential. Br.J.Pharmacol. 2004 Mar;141(6):1059-1067.

156. Poulsen MK, Henriksen JE, Dahl J, Johansen A, Moller JE, Gerke O, et al. Myocardial ischemia, carotid, and peripheral arterial disease and their interrelationship in type 2 diabetes patients. J.Nucl.Cardiol. 2009 Nov-Dec;16(6):878-887.

157. Poulsen MK, Henriksen JE, Vach W, Dahl J, Moller JE, Johansen A, et al. Identification of asymptomatic type 2 diabetes mellitus patients with a low, intermediate and high risk of ischaemic heart disease: is there an algorithm? Diabetologia 2010 Apr;53(4):659-667.

158. Bartels DW, Davidson MH, Gong WC. Type 2 diabetes and cardiovascular disease: reducing the risk. J.Manag.Care.Pharm. 2007 Mar;13(2 Suppl A):S2-15; quiz S16-7.

159. McAlister FA, Eurich DT, Majumdar SR, Johnson JA. The risk of heart failure in patients with type 2 diabetes treated with oral agent monotherapy. Eur.J.Heart Fail. 2008 Jul;10(7):703-708.

160. Gribble FM, Tucker SJ, Seino S, Ashcroft FM. Tissue specificity of sulfonylureas: studies on cloned cardiac and beta-cell K(ATP) channels. Diabetes 1998 Sep;47(9):1412-1418.

161. Zunkler BJ. Human ether-a-go-go-related (HERG) gene and ATP-sensitive potassium channels as targets for adverse drug effects. Pharmacol.Ther. 2006 Oct;112(1):12-37.

162. Quast U, Stephan D, Bieger S, Russ U. The impact of ATP-sensitive K+ channel subtype selectivity of insulin secretagogues for the coronary vasculature and the myocardium. Diabetes 2004 Dec;53 Suppl 3:S156-64.

163. Yellon DM, Downey JM. Preconditioning the myocardium: from cellular physiology to clinical cardiology. Physiol.Rev. 2003 Oct;83(4):1113-1151.

164. Reyes S, Park S, Johnson BD, Terzic A, Olson TM. K(ATP) channel Kir6.2 E23K variant overrepresented in human heart failure is associated with impaired exercise stress response. Hum.Genet. 2009 Aug 14.

165. Sesti G, Laratta E, Cardellini M, Andreozzi F, Del Guerra S, Irace C, et al. The E23K variant of KCNJ11 encoding the pancreatic beta-cell adenosine 5'-triphosphate-sensitive potassium channel subunit Kir6.2 is associated with an increased risk of secondary failure to sulfonylurea in patients with type 2 diabetes. J.Clin.Endocrinol.Metab. 2006 Jun;91(6):2334-2339.

166. Wild S, Roglic G, Green A, Sicree R, King H. Global prevalence of diabetes: estimates for the year 2000 and projections for 2030. Diabetes Care 2004 May;27(5):1047-1053.

167. Setacci C, de Donato G, Setacci F, Chisci E. Diabetic patients: epidemiology and global impact. J.Cardiovasc.Surg.(Torino) 2009 Jun;50(3):263-273.

168. Staiger H, Machicao F, Fritsche A, Haring HU. Pathomechanisms of type 2 diabetes genes. Endocr.Rev. 2009 Oct;30(6):557-585.

169. Malecki MT. Genetics of type 2 diabetes mellitus. Diabetes Res.Clin.Pract. 2005 Jun;68 Suppl1:S10-21.

170. Gloyn AL. The search for type 2 diabetes genes. Ageing Res.Rev. 2003 Apr;2(2):111-127.

171. Rangwala SM, Lazar MA. Peroxisome proliferator-activated receptor gamma in diabetes and metabolism. Trends Pharmacol.Sci. 2004 Jun;25(6):331-336.

172. Ashcroft FM. ATP-sensitive potassium channelopathies: focus on insulin secretion. J.Clin.Invest. 2005 Aug;115(8):2047-2058.

173. Aguilar-Bryan L, Bryan J. Molecular biology of adenosine triphosphate-sensitive potassium channels. Endocr.Rev. 1999 Apr;20(2):101-135.

174. Gloyn AL, Pearson ER, Antcliff JF, Proks P, Bruining GJ, Slingerland AS, et al. Activating mutations in the gene encoding the ATP-sensitive potassium-channel subunit Kir6.2 and permanent neonatal diabetes. N.Engl.J.Med. 2004 Apr 29;350(18):1838-1849.

175. Shyng SL, Ferrigni T, Shepard JB, Nestorowicz A, Glaser B, Permutt MA, et al. Functional analyses of novel mutations in the sulfonylurea receptor 1 associated with persistent hyperinsulinemic hypoglycemia of infancy. Diabetes 1998 Jul;47(7):1145-1151.

176. Gloyn AL, Hashim Y, Ashcroft SJ, Ashfield R, Wiltshire S, Turner RC, et al. Association studies of variants in promoter and coding regions of beta-cell ATP-sensitive K-channel genes SUR1 and Kir6.2 with Type 2 diabetes mellitus (UKPDS 53). Diabet.Med. 2001 Mar;18(3):206-212.

177. Inoue H, Ferrer J, Warren-Perry M, Zhang Y, Millns H, Turner RC, et al. Sequence variants in the pancreatic islet beta-cell inwardly rectifying K+ channel Kir6.2 (Bir) gene: identification and lack of role in Caucasian patients with NIDDM. Diabetes 1997 Mar;46(3):502-507.

178. Hani EH, Boutin P, Durand E, Inoue H, Permutt MA, Velho G, et al. Missense mutations in the pancreatic islet beta cell inwardly rectifying K+ channel gene (KIR6.2/BIR): a meta-analysis suggests a role in the polygenic basis of Type II diabetes mellitus in Caucasians. Diabetologia 1998 Dec;41(12):1511-1515.

179. Schwanstecher C, Meyer U, Schwanstecher M. K(IR)6.2 polymorphism predisposes to type 2 diabetes by inducing overactivity of pancreatic beta-cell ATP-sensitive K(+) channels. Diabetes 2002 Mar;51(3):875-879.

180. Schwanstecher C, Neugebauer B, Schulz M, Schwanstecher M. The common single nucleotide polymorphism E23K in K(IR)6.2 sensitizes pancreatic beta-cell ATP-sensitive potassium channels toward activation through nucleoside diphosphates. Diabetes 2002 Dec;51 Suppl 3:S363-7.

181. Villareal DT, Koster JC, Robertson H, Akrouh A, Miyake K, Bell GI, et al. Kir6.2 variant E23K increases ATP-sensitive K+ channel activity and is associated with impaired insulin release and enhanced insulin sensitivity in adults with normal glucose tolerance. Diabetes 2009 Aug;58(8):1869-1878.

182. Florez JC, Burtt N, de Bakker PI, Almgren P, Tuomi T, Holmkvist J, et al. Haplotype structure and genotype-phenotype correlations of the sulfonylurea receptor and the islet ATP-sensitive potassium channel gene region. Diabetes 2004 May;53(5):1360-1368.

183. Ashcroft FM, Harrison DE, Ashcroft SJ. Glucose induces closure of single potassium channels in isolated rat pancreatic beta-cells. Nature 1984 Nov 29-Dec 5;312(5993):446-448.

184. Dunne MJ, Petersen OH. Intracellular ADP activates K+ channels that are inhibited by ATP in an insulin-secreting cell line. FEBS Lett. 1986 Nov 10;208(1):59-62.

185. Cook DL, Hales CN. Intracellular ATP directly blocks K+ channels in pancreatic B-cells. Nature 1984 Sep 20-26;311(5983):271-273.

186. Rorsman P, Trube G. Glucose dependent K+-channels in pancreatic beta-cells are regulated by intracellular ATP. Pflugers Arch. 1985 Dec;405(4):305-309.

187. Ashcroft FM, Rorsman P. Electrophysiology of the pancreatic beta-cell. Prog.Biophys.Mol.Biol. 1989;54(2):87-143.

188. Ashcroft FM, Rorsman P. ATP-sensitive K+ channels: a link between B-cell metabolism and insulin secretion. Biochem.Soc.Trans. 1990 Feb;18(1):109-111.

189. Kuzuya T, Nakagawa S, Satoh J, Kanazawa Y, Iwamoto Y, Kobayashi M, et al. Report of the Committee on the classification and diagnostic criteria of diabetes mellitus. Diabetes Res.Clin.Pract. 2002 Jan;55(1):65-85.

190. Nolan CJ, Madiraju MS, Delghingaro-Augusto V, Peyot ML, Prentki M. Fatty acid signaling in the beta-cell and insulin secretion. Diabetes 2006 Dec;55 Suppl 2:S16-23.

191. Barg S. Mechanisms of exocytosis in insulin-secreting B-cells and glucagon-secreting A-cells. Pharmacol.Toxicol. 2003 Jan;92(1):3-13.

192. Gratzl M, Ekerdt R, Dahl G. The role of Ca2+ as a trigger for membrane fusion. Horm.Metab.Res.Suppl. 1980;Suppl 10:144-149.

193. Braun M, Ramracheya R, Johnson PR, Rorsman P. Exocytotic properties of human pancreatic beta-cells. Ann.N.Y.Acad.Sci. 2009 Jan;1152:187-193.

194. Seino S, Miki T. Physiological and pathophysiological roles of ATP-sensitive K+ channels. Prog.Biophys.Mol.Biol. 2003 Feb;81(2):133-176.

195. Aguilar-Bryan L, Clement JP,4th, Gonzalez G, Kunjilwar K, Babenko A, Bryan J. Toward understanding the assembly and structure of KATP channels. Physiol.Rev. 1998 Jan;78(1):227-245.

196. Isomoto S, Kondo C, Kurachi Y. Inwardly rectifying potassium channels: their molecular heterogeneity and function. Jpn.J.Physiol. 1997 Feb;47(1):11-39.

197. Trapp S, Proks P, Tucker SJ, Ashcroft FM. Molecular analysis of ATP-sensitive K channel gating and implications for channel inhibition by ATP. J.Gen.Physiol. 1998 Sep;112(3):333-349.

198. Tucker SJ, Gribble FM, Proks P, Trapp S, Ryder TJ, Haug T, et al. Molecular determinants of KATP channel inhibition by ATP. EMBO J. 1998 Jun 15;17(12):3290-3296.

199. Aguilar-Bryan L, Nichols CG, Wechsler SW, Clement JP,4th, Boyd AE,3rd, Gonzalez G, et al. Cloning of the beta cell high-affinity sulfonylurea receptor: a regulator of insulin secretion. Science 1995 Apr 21;268(5209):423-426.

200. Zingman LV, Alekseev AE, Bienengraeber M, Hodgson D, Karger AB, Dzeja PP, et al. Signaling in channel/enzyme multimers: ATPase transitions in SUR module gate ATP-sensitive K+ conductance. Neuron 2001 Aug 2;31(2):233-245.

201. Nichols CG. KATP channels as molecular sensors of cellular metabolism. Nature 2006 Mar 23;440(7083):470-476.

202. Boyd AE,3rd, Aguilar-Bryan L, Nelson DA. Molecular mechanisms of action of glyburide on the beta cell. Am.J.Med. 1990 Aug 20;89(2A):3S-10S; discussion 51S-53S.

203. Aguilar-Bryan L, Nelson DA, Vu QA, Humphrey MB, Boyd AE,3rd. Photoaffinity labeling and partial purification of the beta cell sulfonylurea receptor using a novel, biologically active glyburide analog. J.Biol.Chem. 1990 May 15;265(14):8218-8224.

204. Patlak M. New weapons to combat an ancient disease: treating diabetes. FASEB J. 2002 Dec;16(14):1853.

205. Stowers JM. Oral treatment in diabetes. Clin.Endocrinol.Metab. 1972 Nov;1(3):721-750.

206. Feldman JM. Glyburide: a second-generation sulfonylurea hypoglycemic agent. History, chemistry, metabolism, pharmacokinetics, clinical use and adverse effects. Pharmacotherapy 1985 Mar-Apr;5(2):43-62.

207. Tal A. Oral hypoglycemic agents in the treatment of type II diabetes. Am.Fam.Physician 1993 Nov 1;48(6):1089-1095.

208. Dabrowski M, Wahl P, Holmes WE, Ashcroft FM. Effect of repaglinide on cloned beta cell, cardiac and smooth muscle types of ATP-sensitive potassium channels. Diabetologia 2001 Jun;44(6):747-756.

209. Winkler M, Stephan D, Bieger S, Kuhner P, Wolff F, Quast U. Testing the bipartite model of the sulfonylurea receptor binding site: binding of A-, B-, and A + B-site ligands. J.Pharmacol.Exp.Ther. 2007 Aug;322(2):701-708.

210. Bryan J, Crane A, Vila-Carriles WH, Babenko AP, Aguilar-Bryan L. Insulin secretagogues, sulfonylurea receptors and K(ATP) channels. Curr.Pharm.Des. 2005;11(21):2699-2716.

211. Vila-Carriles WH, Zhao G, Bryan J. Defining a binding pocket for sulfonylureas in ATP-sensitive potassium channels. FASEB J. 2007 Jan;21(1):18-25.

212. Hansen AM, Christensen IT, Hansen JB, Carr RD, Ashcroft FM, Wahl P. Differential interactions of nateglinide and repaglinide on the human beta-cell sulphonylurea receptor 1. Diabetes 2002 Sep;51(9):2789-2795.

213. Reimann F, Proks P, Ashcroft FM. Effects of mitiglinide (S 21403) on Kir6.2/SUR1, Kir6.2/SUR2A and Kir6.2/SUR2B types of ATP-sensitive potassium channel. Br.J.Pharmacol. 2001 Apr;132(7):1542-1548.

214. Ashfield R, Gribble FM, Ashcroft SJ, Ashcroft FM. Identification of the high-affinity tolbutamide site on the SUR1 subunit of the K(ATP) channel. Diabetes 1999 Jun;48(6):1341-1347.

215. Ueda K, Komine J, Matsuo M, Seino S, Amachi T. Cooperative binding of ATP and MgADP in the sulfonylurea receptor is modulated by glibenclamide. Proc.Natl.Acad.Sci.U.S.A. 1999 Feb 16;96(4):1268-1272.

216. Babenko AP, Gonzalez G, Bryan J. Pharmaco-topology of sulfonylurea receptors. Separate domains of the regulatory subunits of K(ATP) channel isoforms are required for selective interaction with K(+) channel openers. J.Biol.Chem. 2000 Jan 14;275(2):717-720.

217. Sattiraju S, Reyes S, Kane GC, Terzic A. K(ATP) channel pharmacogenomics: from bench to bedside. Clin.Pharmacol.Ther. 2008 Feb;83(2):354-357.

218. Koster JC, Remedi MS, Dao C, Nichols CG. ATP and sulfonylurea sensitivity of mutant ATP-sensitive K+ channels in neonatal diabetes: implications for pharmacogenomic therapy. Diabetes 2005 Sep;54(9):2645-2654.

219. Babenko AP, Polak M, Cave H, Busiah K, Czernichow P, Scharfmann R, et al. Activating mutations in the ABCC8 gene in neonatal diabetes mellitus. N.Engl.J.Med. 2006 Aug 3;355(5):456-466.

220. Feng Y, Mao G, Ren X, Xing H, Tang G, Li Q, et al. Ser1369Ala variant in sulfonylurea receptor gene ABCC8 is associated with antidiabetic efficacy of gliclazide in Chinese type 2 diabetic patients. Diabetes Care 2008 Oct;31(10):1939-1944.

221. de Wet H, Rees MG, Shimomura K, Aittoniemi J, Patch AM, Flanagan SE, et al. Increased ATPase activity produced by mutations at arginine-1380 in nucleotide-binding domain 2 of ABCC8 causes neonatal diabetes. Proc.Natl.Acad.Sci.U.S.A. 2007 Nov 27;104(48):18988-18992.

Chapter 2

Reactive Oxygen Species Directly Modify Sodium-Calcium Exchanger Activity in a Splice Variant-Dependent Manner.

A version of this chapter has been published under the following citation:

Soliman D., Hamming K.S.C., Matemisz L.C., Light P.E. (2009). Reactive Oxygen Species Directly Modify Sodium-Calcium Exchanger Activity in a Splice-Variant Dependent Manner. Journal of Molecular & Cellular Cardiology 47, 595-602.

Introduction

The sodium-calcium exchanger isoform 1 (NCX1) is an important membrane protein that regulates cellular calcium homeostasis in many tissues. NCX1 is encoded by the *SLC8A1* gene that contains an alternative splicing region allowing the expression of specific splice variants in different tissues [1,2]. NCX1.1 is the major splice variant in the heart where it plays a major role in regulating intracellular calcium, maintaining the necessary calcium gradient for contraction. NCX1.1 aids to accomplish intracellular calcium homeostasis by operating in FM (calcium-efflux mode), which is the electrogenic transport of 3-4 Na^+ ions into the cytosol for every Ca^{2+} ion that it extrudes [3,4]. However, NCX1 has become the focus of calcium mishandling in pathophysiological cardiac events. In cardiac IR, ionic disturbances such as Na^+ loading, favours sustained RM-NCX1.1 (Ca^{2+}-influx mode) activity, as excess intracellular Na^+ is extruded in exchange for Ca^{2+}, leading to increased intracellular Ca^{2+} (Ca^{2+}_i) levels [5,6]. This rise in Ca^{2+}_i contributes to reversible cellular dysfunction upon reperfusion, such as myocardial stunning and arrhythmias, or irreversible injury, such as apoptosis and necrosis which contribute to infarct formation [7,8].

Many studies have shown that reactive oxygen species (ROS) are produced in significant amounts during ischemia-reperfusion and contribute to myocardial injury [9-11]. ROS such as hydrogen peroxide (H_2O_2), hydroxyl radical ($OH\cdot$) and superoxide ($O_2^{-}\cdot$) are produced quite measurably in models of ischemia-reperfusion, with superoxide being produced primarily during ischemia, while hydrogen peroxide and hydroxyl radical being mainly produced during

reperfusion [12,13]. In addition to the numerous detrimental effects ROS can have on cellular processes, is evidence that ROS can increase RM-NCX1.1 function during cardiac ischemia-reperfusion. It has recently been shown that ROS contribute to Ca^{2+}_i loading in myocytes upon reoxygenation, via activation of RM-NCX1.1 [14]. Furthermore, over-expression of NCX1.1 worsens cardiac myocyte injury via a ROS-mediated mechanism [15], leading to the suggestion that ROS mediated effects on NCX1.1 are direct in nature, modifying the protein itself [16-18]. Moreover, others proposed that ROS activation of NCX1.1 activity may occur indirectly through a signalling pathway that involves activation of the sodium-hydrogen exchanger (NHE1), which is involved in Na^{+}_i loading during ischemia-reperfusion [19]. Although much evidence suggests that ROS augments NCX1.1 activity, the functional and mechanistic aspects of ROS modification of NCX1.1 activity remain to be elucidated.

Therefore, we hypothesized that ROS directly and irreversibly modifies NCX1.1 protein, increasing RM activity, thereby contributing to the intracellular Ca^{2+} overload in cardiac IR. We examined this hypothesis by utilizing the inside-out excised patch clamp technique with recombinant NCX1.1 protein. Our protocol employed the application of H_2O_2, a stable ROS intermediate, to the intracellular side of excised patches and measuring electrogenic NCX1.1 current. Furthermore, we investigated the effect of H_2O_2 on NCX1. In this study, we characterized the mechanism by which ROS alters NCX1 function and provided new insight into the regulation of calcium-influx NCX1.1 activity during

ischemia-reperfusion and on ROS-mediated molecular regulation of NCX1 protein.

Materials & Methods

Molecular Biology and Expression

The rat NCX1.1 adenovirus and the rat NCX1.4 cDNA were generously provided by Dr. J.Y Cheung (Pennsylvania State University, Hershey, PA) and Dr. J. Lytton (University of Calgary, Canada), respectively [20,21]. Human NCX1.1, 1.3, and 1.11 were generated as previously described [22]. Briefly, human NCX1.1 and 1.3 were obtained through RT-PCR of total human atrial and pancreatic islet RNA, respectively. Human NCX1.11 was generated by PCR fusion of overlapping NCX1.1 and NCX1.3 PCR products. The rat NCX1.1-F255E XIP region mutant was made previously [23], while the human NCX1.1-K264Q mutant was made using a Quikchange Site-Directed Mutagenesis Kit (Stratagene, La Jolla, CA) and its sequence verified by sequence analysis. The K264Q mutant corresponds to the K229Q substitution as previously described [24]. Adenoviral short-hairpin RNA for NCX1 (Ad-shRNA-NCX1) was generously provided by Dr. Grant Pierce (University of Manitoba, Canada) and was used as described by Hurtado *et al* [25].

Infection and transfection of NCX1 splice variants was conducted as previously described [23]. Briefly, rat NCX1.1 was expressed in cultured tsA201/HEK293 cells via adenoviral delivery at a concentration of ~30pfu/cell. All other NCX1 splice variants were co-transfected with a green fluorescent protein expression vector (Life Technologies, Gaithersburg, MD) into

tsA201/HEK293 cells using the calcium phosphate precipitation method. All macroscopic recordings of NCX1 currents were obtained 48-72 hours after infection/transfection.

Electrophysiology

A modification of the inside-out excised patch clamp technique was used to measure macroscopic RM- and FM-NCX1 currents as previously described [22,23]. Reverse-mode NCX1 currents were elicited by the application of 90 mM Na^+ to the intracellular side of the membrane patch, while FM currents were activated by 3.2 mM Ca^{2+}, for a period of 60s. Excised patches were held at 0 mV and NCX1 currents were measured using an Axopatch 200B amplifier and analyzed with Clampex 10.1 software (Axon Instruments, Foster City, CA). All experiments were performed at room temperature (22±1 ºC). For data presented in Figure 2-2F, a voltage ramp of 0 to +100 mV was applied to excised patches to assess any voltage-dependence of H_2O_2 modification on RM-NCX1.1 activity.

Rat Neonatal Cardiac Myocyte Ca^{2+} Imaging

Calcium imaging of neonatal rat cardiac myocytes was conducted as previously described [14,23]. Briefly, calcium green-1AM (Invitrogen, Burlington, ON) was loaded into myocytes for 30 min at room temperature, washed and then incubated for 30 min at 37 ºC. To assess intracellular Ca^{2+} flux, cells were superfused with a K^+-free solution for 5 min followed by a Na^+-free solution for 5 min. Experiments were conducted at 22 ± 1 ºC.

Experimental Compounds

30% v/v hydrogen peroxide (10M, Sigma Aldrich, Oakville, ON) was diluted to 100 μM prior to use. Periodically, titration with $KMnO_4$ was performed to confirm stock concentration. KB-R7943 (Tocris Bioscience, Ellisville, MO) was diluted from a 1 mM stock in DMSO for use in experiments. To control for any antioxidant effects of DMSO in the KB-R7943 experiments, its concentration was kept at 0.1 % v/v in all solutions.

Data Analysis & Statistical Methods

Peak and late NCX1 current amplitudes were measured and expressed as late:peak current ratios. The time constant of calcium-influx mode NCX1 current inactivation (Tau, τ) was obtained by fitting currents with a best-fit single exponential function. Statistical significance was assessed by using the unpaired and paired Student's t-test, and the ANOVA repeated-measures test with a Tukey's *post hoc* test, where appropriate. $P<0.05$ was considered to be statistically significant and data are displayed as mean ± standard error of the mean**.**

Results

H_2O_2 Increases Intracellular Calcium Levels in Intact Rat Neonatal Cardiomyocytes.

It was necessary to reproduce previous observations of H_2O_2-mediated increases in intracellular Ca^{2+} as a consequence of RM-NCX1 activity. For this, a previously published protocol to evoke RM-NCX1.1 activity from neonatal rat cardiac myocytes was utilized [14,23]. RT-PCR was used to determine the NCX1

splice variant profile in neonatal rat cardiac myocytes, finding that NCX1.1 is in fact the predominant splice variant in rat neonatal cardiac myocytes (Figure 2-1A). To provide evidence for H_2O_2-mediated increases in Ca^{2+}_i, a superfusion protocol was used to evoke NCX1.1 activity and changes in Ca^{2+}_i were then monitored using the Ca^{2+}-sensitive fluorescent dye Calcium Green-1AM (Figure 2-1B). Superfusion of extracellular K^+-free solution for 5 min uncouples the Na^+-K^+ ATPase pump, causing Na^+_i loading. Subsequent superfusion of extracellular Na^+-free solution for 5 min elicited Na^+ efflux and Ca^{2+} influx through RM-NCX1.1 activity leading to an increase in Ca^{2+}_i. This protocol was conducted in a paired-fashion; that is a control evocation of RM-NCX1.1 activity was conducted, after which a subsequent evocation for the experimental groups were completed. This allowed us to account for deviations in fluorescence signal within the same group of neonatal cardiac myocyte cells imaged. For the control group, this resulted in a non-significant 9.61 ± 3.78% decrease in fluorescence signal over the area attributed to RM-NCX1.1 activity (n=5 recordings, Figure 2-1D). When 100 μM H_2O_2 was added to the Na^+-free solution we observed an significant increase of 30.8 ± 5.9% versus control (n=6 recordings, $P<0.01$, Figure 2-1C,D). The H_2O_2 effects on Ca^{2+}_i may occur as a result of modification of a number of proteins involved in the influx, release, sequestration and efflux of Ca^{2+} via several different calcium-handling processes. With respect to NCX1.1, the evoked increase in Ca^{2+}_i was virtually abolished in neonatal cardiac myocytes where NCX1.1 expression was reduced by adenovirally-mediated delivery of NCX1 shRNA-NCX1 (73.9 ± 13.6% vs. control, n=6 recordings, $P<0.01$, Figure 2-

1C,D). These results indicate that: (1) H_2O_2 increases Ca^{2+}_i in isolated myocytes and, (2) H_2O_2 may increase calcium-influx mode NCX1.1 activity, however any direct effects of H_2O_2 on the NCX1.1 protein should be conclusively determined.

H_2O_2 Increases NCX1.1 Reverse-Mode Currents.

Therefore, in order to test whether H_2O_2 directly regulates NCX1.1 activity, the inside-out patch-clamp technique was used to measure recombinant rat NCX1.1 electrogenic currents. A 5 min application of 100μM H_2O_2 to the intracellular surface of excised membrane patches resulted in a significant increase (48.9 ± 11.3%, $P<0.001$, n=18 patches) in the steady-state or "late" component of RM-NCX1.1 current (late:peak current ratio, Figure 2-2A,E). The observed increase in NCX1.1 current was irreversible after 1 min of washout, as steady-state current was maintained at 45.9 ± 16.0% vs. control ($P<0.001$). To ensure that the results obtained were not a consequence of time, control solution was perfused along patches for 5 min. We found no significant effect on RM-NCX1.1 current (n=8 patches, Figure 2-2D).

The activity of the human NCX1.1 splice variant (94.9% sequence identity with rat NCX1.1), was similarly increased by H_2O_2 (late:peak ratio 50.3 ± 11.2% vs. control, $P<0.001$, n=11 patches, Figure 2-2B,E) and the H_2O_2 effect was also irreversible after washout (38.2 ± 7.9% vs. control, $P<0.001$). The magnitude of NCX1.1 activity is dependent on membrane potential and increases upon depolarization, as is the case during IR injury [26,27]. Therefore, the influence of membrane potential on the H_2O_2-induced changes of human RM-NCX1.1 current was studied. A 0 to +100 mV depolarizing voltage-ramp was applied to the late

portion of NCX1.1 current (~59 s after current activation), under control conditions, after 5 min 100 μM H_2O_2 application, and after 10 μM KB-R7943 inhibition, respectively. Thus, a KB-R7943 sensitive linear increase in RM-NCX1.1 current was observed during a depolarizing voltage-ramp which was further increased over the full 0 to +100 mV range after H_2O_2 application (Figure 2-2F). These results indicate that the H_2O_2-induced increase in RM-NCX1.1 current is independent of membrane potential.

As ROS are also implicated in dysfunctional calcium homeostasis in the vasculature [30], the major splice variant expressed in vascular smooth muscle, NCX1.3 [31], may also be modified by H_2O_2. In direct contrast to NCX1.1, H_2O_2 elicited a reduction of human RM-NCX1.3 current (43.2 ± 7.9% late:peak current ratio, $P<0.01$, n=15 patches, Figure 2-2C,E). This inhibitory effect was also irreversible.

The Effects of H_2O_2 on NCX1 Forward-Mode Currents.

As NCX1 predominantly operates in FM to extrude calcium, the effects of H_2O_2 on FM activity of NCX1 splice variants were also investigated. H_2O_2 did not significantly affect the non-inactivating FM currents of rat and human NCX1.1 (Figure 2-3A,B,D). In contrast, the inactivating FM current from human NCX1.3 exhibited a modest decrease in late:peak ratio after H_2O_2 application (11.4 ± 2.1% vs. control, $P<0.001$, n=10 patches, Figure 2-3C,D).

ROS Modification of NCX1 is Dependent on the Alternative Splicing Region.

The only difference between NCX1 splice variants is the exon composition of the alternative splicing region. Therefore, the contrasting effects

of H_2O_2 on NCX1.1 and NCX1.3 currents suggest that the alternative splicing region bestows the differing H_2O_2 sensitivities upon individual NCX1 splice variants. Figure 2-4 displays a membrane topology model of the NCX1 protein (4A), the alternatively spliced exon compositions (4B) and amino acid sequence (4C) of four NCX1 splice variants. Panel B illustrates the exon make-up and the presence of the A or B mutually exclusive exons in NCX1 splice variants. As the largest single exon sequence variation between NCX1.1 and NCX1.3 is the exon *A* to *B* switch, this sequence difference may account for the observed differences in H_2O_2 effects between these two splice variants. To test this notion, the effects of H_2O_2 were examined on NCX1.4 (NCX1.3 except for an exon *B* to *A* switch) and NCX1.11 (NCX1.1 except for an exon *A* to *B* switch).

NCX1.4 currents displayed an irreversible increase in RM activity upon H_2O_2 application (late:peak ratio 47.9 ± 10.4% increase vs. control, $P<0.001$, n=6 patches, Figure 2-5A,C,D). Conversely, the introduction of exon *B* into NCX1.1 in NCX1.11, resulted in an inhibitory effect of H_2O_2 on RM activity (late:peak ratio 14.9 ± 4.6% decrease vs. control, $P<0.05$, n=6 patches). Taken together, these results indicate that NCX1 splice variants containing exon *A* (NCX1.1 and NCX1.4) exhibit H_2O_2-mediated increases in RM current, while those containing exon *B* (NCX1.3 and 1.11) display decreased RM activity after H_2O_2 application. Thus, the mutually exclusive *A* and *B* exons confer the observed differential effects of H_2O_2 on NCX1splice variants.

The Effects of H_2O_2 are Dependent on NCX1 Current Inactivation.

One key observation is that H_2O_2 modulation of FM and RM-NCX1 currents is dependent on the presence of inactivation. For example, FM-NCX1.1 activity, which displays no inactivation, was the only splice variant mode unaffected by H_2O_2. In order to further explore the reliance of H_2O_2 on the calcium-influx mode NCX1 inactivation process, two mutations, F255E and K264Q, were separately introduced into NCX1.1. These mutations either accelerate or remove the RM inactivation process respectively, and are outside of the alternative splicing region, lying within the exchange inhibitory peptide region (XIP) [24]. Consequently, these mutations provide a convenient means to assess the effects of H_2O_2 on altered inactivation processes. NCX1.1-F255E RM currents exhibited a marked acceleration in the rate of inactivation as denoted by a reduction in the time constant (τ) of inactivation (1.2 ± 0.2 s vs. 12.1 ± 2.2 s for NCX1.1 control, $P<0.01$, n=10-11 patches). Even in the presence of a faster inactivation process, H_2O_2 increased τ to 2.1 ± 0.3 s ($P<0.01$, Figure 2-6A,B). In contrast, NCX1.1-K264Q RM currents displayed no inactivation and were insensitive to modulation by H_2O_2 (Figure 2-6C,D). These results further confirm that the modulatory effects of H_2O_2 are lost in the absence of any inactivation process.

ROS-Mediated Alterations in Reverse-Mode NCX1 Currents are Lipid Peroxidation-Independent and are Time-Dependent.

It is also possible that the effects of H_2O_2 are mediated by peroxidation of the lipid environment or by interactions with a lipophilic region of the NCX1.1

protein. Therefore, experiments were performed with the membrane permeable ROS, *t*-butyl hydroperoxide (100 μM), where no effects on RM-NCX1.1 currents were observed (Figure 2-7A).

After observing that RM-NCX1.1 activity was increased after a 5 min application of 100 μM H_2O_2, we examined whether the H_2O_2-mediated alterations to RM-NCX1.1 current is time-dependent. Therefore, we conducted experiments using a 2 min and 10 min application of 100 μM H_2O_2 and found that after a 2 min application of H_2O_2, NCX1.1 current was lessened by 41.9 ± 7.1% (P<0.01 vs. control, n=9 patches), while a 10 minute application of H_2O_2 enhanced late current by 33.0 ± 11.8% (P<0.05 vs. control, n=7 patches, Figure 2-7B,C,D). These findings allow us to infer that NCX1 modification by H_2O_2 is a time-dependent process, in which a finite period of time is required to irreversibly increase RM-NCX1.1 current.

H_2O_2 Decreases NCX1.1 Sensitivity to Pharmacological Inhibition.

NCX inhibitors, such as KB-R7943, selectively inhibit RM-NCX1.1 activity, and pharmacological inhibition of RM-NCX1.1 is considered a potential strategy to reduce cardiac IR injury [28]. NCX1 inhibitors display a marked preference for inhibition of the steady-state or late component of RM NCX1 current [29-31]. Since the H_2O_2 effect is dependent upon the presence of an inactivation process and modulates RM-NCX1.1 activity by decreasing the amount of inactivation (Figures 2-2 & 2-6), the possibility that pre-exposure of NCX1.1 to H_2O_2 may alter the exchanger's sensitivity to KB-R7943 was explored. Concentration-response curves for KB-R7943 RM inhibition were

obtained from NCX1.1 before and after exposure to H_2O_2. The IC_{50} of KB-R7943 increased by ~7-fold when pre-exposed to 100μM H_2O_2 (IC_{50} = 0.2 ± 0.1μM vs. 1.4 ± 0.4μM, Figure 2-7A,B,C, n=4-6 patches per concentration).

Discussion

The results obtained in this study collectively reveal novel insights into the mechanisms by which the ROS, H_2O_2, irreversibly modifies the biophysical properties of various NCX1 splice variants. Our first observation of NCX1 activity modification by ROS was the increase of evoked RM-NCX1.1 from neonatal rat cardiac myocytes after the application of 100μM H_2O_2 (Figure 2-1). Interestingly, others have employed the protocol to evoke RM-NCX1.1 in cardiac myocytes to exhibit changes in NCX1 regulation [14,23,32,33]. Previous examinations into intact cellular NCX1 function provided the impetus to examine whether ROS can increase RM-NCX1.1 activity. Although we are confident that suppression of NCX1 function by shRNA-NCX1 and by $NiCl_2$ highlights that the calcium signal displays NCX1 function solely, it is possible that other calcium sequestration and extrusion proteins may be involved. These include the sarco-endoplasmic reticulum calcium ATPase (SERCA) and the plasma membrane calcium ATPase (PMCA), which may contribute to the calcium signal in a temporal manner. Moreover, as any mechanistic and biophysical conclusions that can be made from the intact cellular assessment of RM-NCX1 function is limited, the inside-out patch clamping technique was used to directly measure recombinant NCX1 currents to further the investigation of the effects of ROS on NCX1 function.

One of the major findings in this study is the reliance of the H_2O_2 effect on the I_1, Na^+-dependent inactivation process. This observation is corroborated by a previous report utilizing the redox reagent, Fe-DTT, which slowed the inactivation of RM-NCX1.1 currents [18]. The I_1 dependence of H_2O_2-mediated effects on NCX1 currents is further supported by our observations in which H_2O_2 was unable to modify NCX1 currents if the I_1 inactivation process is absent, as in the case of FM-NCX1.1 and K264Q-NCX1.1 RM currents (Figure 2-3A,B,D; Figure 2-6B,D). In contrast, H_2O_2 decreases the amount of inactivation even when the rate of inactivation is dramatically increased in NCX1.1-F255E RM mode currents (Figure 2-6A,C). Taken together these results support the conclusion that modulation of RM-NCX1.1 activity by H_2O_2 requires the Na^+-dependent inactivation process. It is also interesting to note that FM-NCX1.3 currents, which exhibit a slight inactivation process, also showed changes in response to H_2O_2 application (Figure 2-3C,D), however, whether the inactivation process observed in FM-NCX1.3 currents is Na^+-dependent remains to be examined. Previous reports have shown that the inactivation process, either in forward- or RM, can be modulated by other metabolites such as acyl-coenzyme A esters [22,23]. These findings suggest that the inactivation process of NCX1 can be modulated by various cellular processes and may prove to be a common mechanistic means for its regulation in health and disease.

As the vast majority of NCX1 activity is in FM, which displays no inactivation (Figure 2-3), there is likely limited physiological relevance of the observed effects of H_2O_2 on the RM-NCX1.1 inactivation process. However, the

effects of ROS such as H_2O_2 on this inactivation process may contribute to elevated Ca^{2+}_i under pathophysiological conditions such as ischemia-reperfusion injury, where calcium influx via NCX1.1 activity plays a prominent role. During prolonged ischemic conditions, a number of ionic disturbances occur that favour sustained RM-NCX1 activity. For example, an accumulation of intracellular Na^+ ions from the exchange of excess protons from glycolysis by the Na^+-H^+ exchanger (NHE1) and from the late-component of voltage-gated Na^+ channel activity [34-36]. Additionally, the resting membrane potential of cardiac myocytes is depolarized during simulated ischemia [27]. Together, the Na^+ loading and membrane depolarization may shift the reversal potential for NCX1 such that prolonged calcium influx is favored during ischemia-reperfusion and the magnitude of the inactivation process becomes more important. Indeed, in this study, we show that ROS-induced increases in RM-NCX1.1 steady-state function continues in a depolarized state (Figure 2-2F). Furthermore, in this regard it has been recently shown that the RM inactivation process is enhanced if the cytosolic pH is lowered and that this inactivation is suggested to be protective during metabolic stress by limiting Ca^{2+} loading [37]. Therefore, any factors such as ROS generated during ischemia-reperfusion, which decrease the inactivation process, would likely facilitate myocardial calcium loading.

In addition to the ROS-mediated effects on NCX1 currents displaying I_1-inactivation dependence, the application of H_2O_2 was irreversible and also time-dependent. ROS such as H_2O_2 are capable of amino acid and lipid modifications that may contribute to the alterations in protein function. In regards to the lipid

environment, we investigated the effect that the membrane permeable ROS *t*-butyl hydroperoxide would have on RM-NCX1.1 currents, and found no significant alterations (Figure 2-7A). Therefore, lipid environment modifications by ROS do not play a significant role in regulating NCX1.1 activity. The irreversibility of H_2O_2 effects on NCX1 currents suggests that ROS may oxidize specific residues in the NCX1 protein. Oxidation of amino acid side chains produces a variety of derivatives that can modify protein-protein interactions. Backbone fragmentation, changes to aliphatic C-H bonds and changes to amino acid side chain residues can all result in irreversible modifications of protein function [38-40]. Moreover, H_2O_2 required several minutes to elicit its full irreversible effect (Figure 2-7B,C,D), further supporting the notion of direct modification of NCX1 protein. Examination of the amino acid sequence of exon *B* reveals cysteine, tryptophan, and methionine residues (Figure 2-4C) that may be amenable to H_2O_2 modification [39].

The differential effects of H_2O_2 on NCX1 splice variants provide insights into the molecular mechanisms by which H_2O_2 may act. In direct contrast to a stimulatory effect of H_2O_2 on RM-NCX1.1 currents, H_2O_2 inhibited RM-NCX1.3 currents, highlighting the alternative splicing region as a region of the protein that is susceptible to H_2O_2 modification. Our results reveal that it is the mutually exclusive exons *A* and *B* that bestow the differential sensitivities to H_2O_2 amongst the NCX1 splice variants (Figure 2-5). The dependence of the H_2O_2 effect on both the inactivation process and the *A*/*B* exons suggest that H_2O_2 may directly modify amino acid residues within exons *A* or *B* exons or other residues in the NCX1

protein, which interact with the alternative splicing region to regulate the inactivation process. Interestingly, the alternative splicing region lies within the second calcium binding domain (CBD2) in the NCX1 protein (Figure 2-4A) and has been shown to modulate the Na^+-dependent inactivation process [39,41]. Notably, mutations to charged amino acids in exon *A* within the CBD2 alters calcium binding and the inactivation process. Specifically, residue D613 is critical in the formation of the acidic cluster required for Ca^{2+}-binding, while K620 plays a role in preventing unfolding of CBD2 [21,41]. Mutating these residues to R613 and C620 (Figure 2-8C) has been shown to accelerate Na^+-dependent inactivation [21]. In fact, in a previous study conducted by our laboratory, we observed faster inactivation processes in the NCX1 splice variants that contain exon B, particularly NCX1.3 and 1.7 [22]. It is therefore plausible that H_2O_2 modifies exon A within CBD2, further stabilizing Ca^{2+} binding, leading to the relief of inactivation in NCX1.1. In contrast H_2O_2 modification of exon B within the CBD2 domain may destabilize Ca^{2+} binding accounting for the enhanced inactivation observed in NCX1.3 (Figure 2-8).

Moreover, the Na^+-dependent inactivation process is not only governed by CBD2, as the XIP region also plays a key role and may functionally interact with CBD2. Notably, the ablation of the entire alternative splicing region negates the effect of XIP on the RM inactivation process in NCX1.1 [42]. Indeed, the NCX1.1-F255E XIP region mutant, although possessing an accelerated inactivation process, is still sensitive to modulation by H_2O_2. Collectively, these findings and those published previously [22,23] indicate that there may be a

functional interaction between the alternative splicing region (specifically exon *A* or *B*) within CBD2 and the XIP region, and that this interaction accounts for the observed disparate effects of H_2O_2 between NCX1 splice variants.

Another interesting observation in this study is the decreased inhibition of the NCX1 inhibitor, KB-R7943, after H_2O_2 modification (Figure 2-7). As NCX1 inhibitors have potential for therapeutic exploitation, our results highlight the need to determine their potency under conditions of oxidative stress. The reduced effectiveness of KB-R7943 after H_2O_2 exposure could be explained by several reasons. Firstly, the reduced KB-R7943 potency on RM-NCX1.1 current is due to the decreased inactivation process and/or an increase in steady state current observed with H_2O_2 treatment. Since, NCX1 inhibitors preferentially inhibit the late or steady-state component of the NCX1.1 current [29-31], increased steady-state current would require higher drug concentrations to achieve the same level of block. Secondly, H_2O_2 may modify residues within the proposed inhibitor binding site residing within the α-2 membrane loop [31,43]. However, the lack of effect of the membrane permeable *t*-butyl hydroperoxide on NCX1.1 currents suggests that residues residing in the lipophilic membrane environment are resistant to ROS modification and may not account for the observed effects.

In conclusion, we reveal novel insights into the molecular mechanisms by which the ROS, H_2O_2, irreversibly modifies the activity of NCX1 splice variants expressed in the cardiovascular system. Our findings provide a greater understanding of the link between ROS and the dysfunctional calcium handling observed in cardiac ischemia-reperfusion and may have implications in related

disease states such as hypertension and heart failure, in which oxidative stress, calcium mishandling and NCX1 are involved.

Figure 2-1

The Effect of H_2O_2 on Intact Rat Neonatal Cardiac Myocytes. (A) RT-PCR amplification of the splice variant region of NCX1 from neonatal rat cardiac myocytes, shows NCX1.1 as the major splice variant present. **(B-C)** Calcium imaging of neonatal rat cardiac myocytes with evoked RM-NCX1.1 activity. The representative traces in (C) depict an increase in intracellular calcium, in part by the RM of NCX1.1 in response to 100μM H_2O_2 and an absence of NCX1.1 activity in myocytes treated with Ad-shRNA-NCX1. (**D**) Grouped data displaying that 100μM H_2O_2 increased evoked RM-NCX1.1 activity, while shRNA-NCX1 strongly negated NCX1 function. n=5-6 recordings per group of 6-8 cells, $^{**}P<0.01$ vs. control.

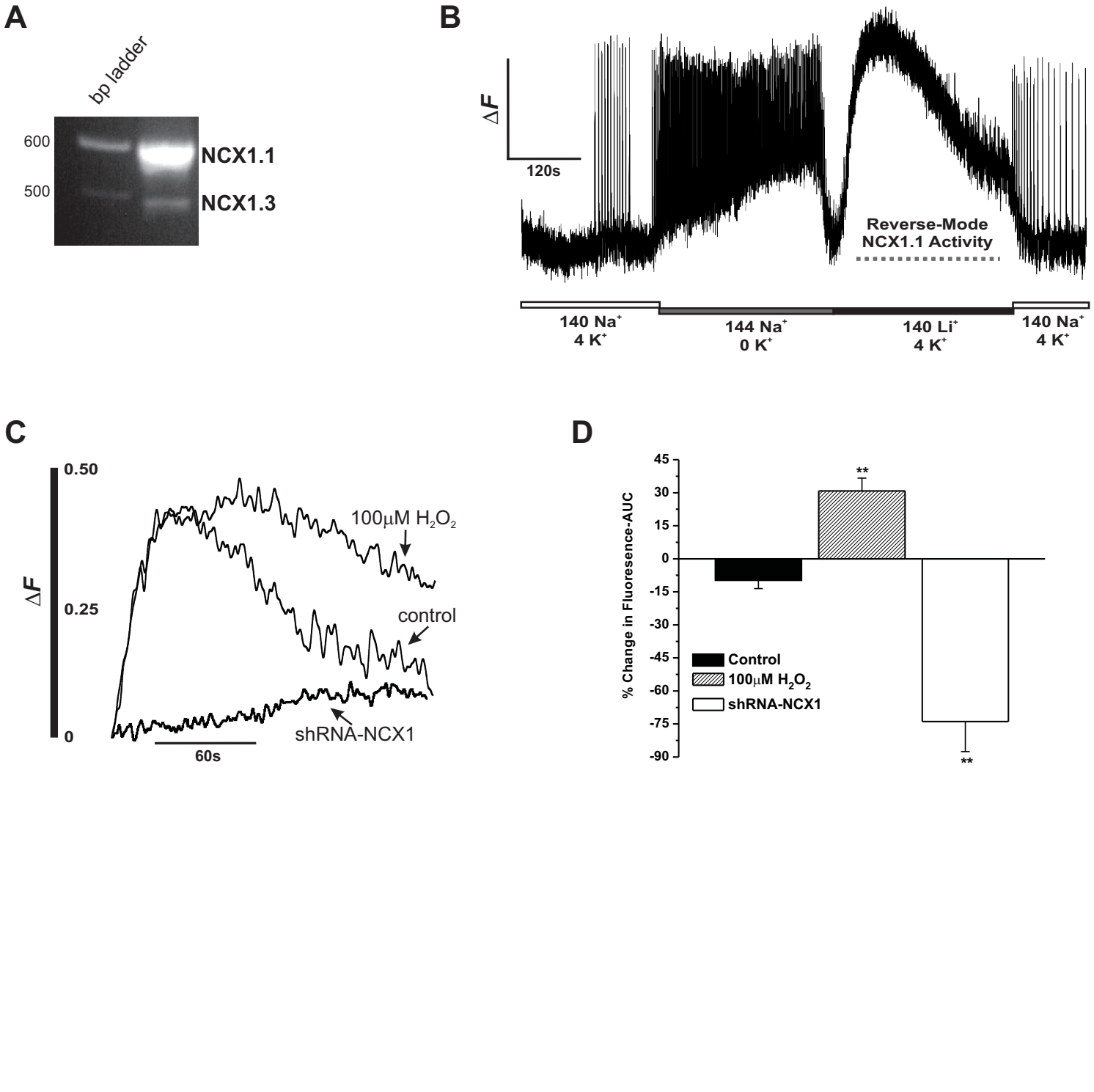
A
bp ladder
600
500
NCX1.1
NCX1.3
B
ΔF
120s
Reverse-Mode
NCX1.1 Activity
140 Na+
4 K+
144 Na+
0 K+
140 Li+
4 K+
140 Na+
4 K+
C
0.50
0.25
0
ΔF
100μM H2O2
control
shRNA-NCX1
60s
D
% Change in Fluoresence-AUC
45
30
15
0
-15
-30
-45
-60
-75
-90
**
**
Control
100μM H2O2
shRNA-NCX1

Figure 2-2

H_2O_2 Imparts Differential Effects upon Rat/Human NCX1.1 and NCX1.3 Reverse-mode Currents. (A-B) Representative traces illustrating the effects of H_2O_2 on RM rat and human NCX1.1 macroscopic currents respectively. **(C)** A representative RM current from human NCX1.3 which decreased following application of 100μM H_2O_2. **(D)** Sample recordings exhibiting that a 5 minute application of control solution has no influence on RM-NCX1.1 current magnitude. **(E)** Grouped data of RM late-to-peak current ratio (% vs. control). n=11-18 patches per condition, $^{**}P<0.01$, $^{***}P<0.001$ vs. control. **(F)** Averaged macroscopic ramp traces depicting a voltage-independent effect of H_2O_2 application on human RM-NCX1.1 currents, n=8 patches. rNCX – rat NCX, hNCX – human NCX.

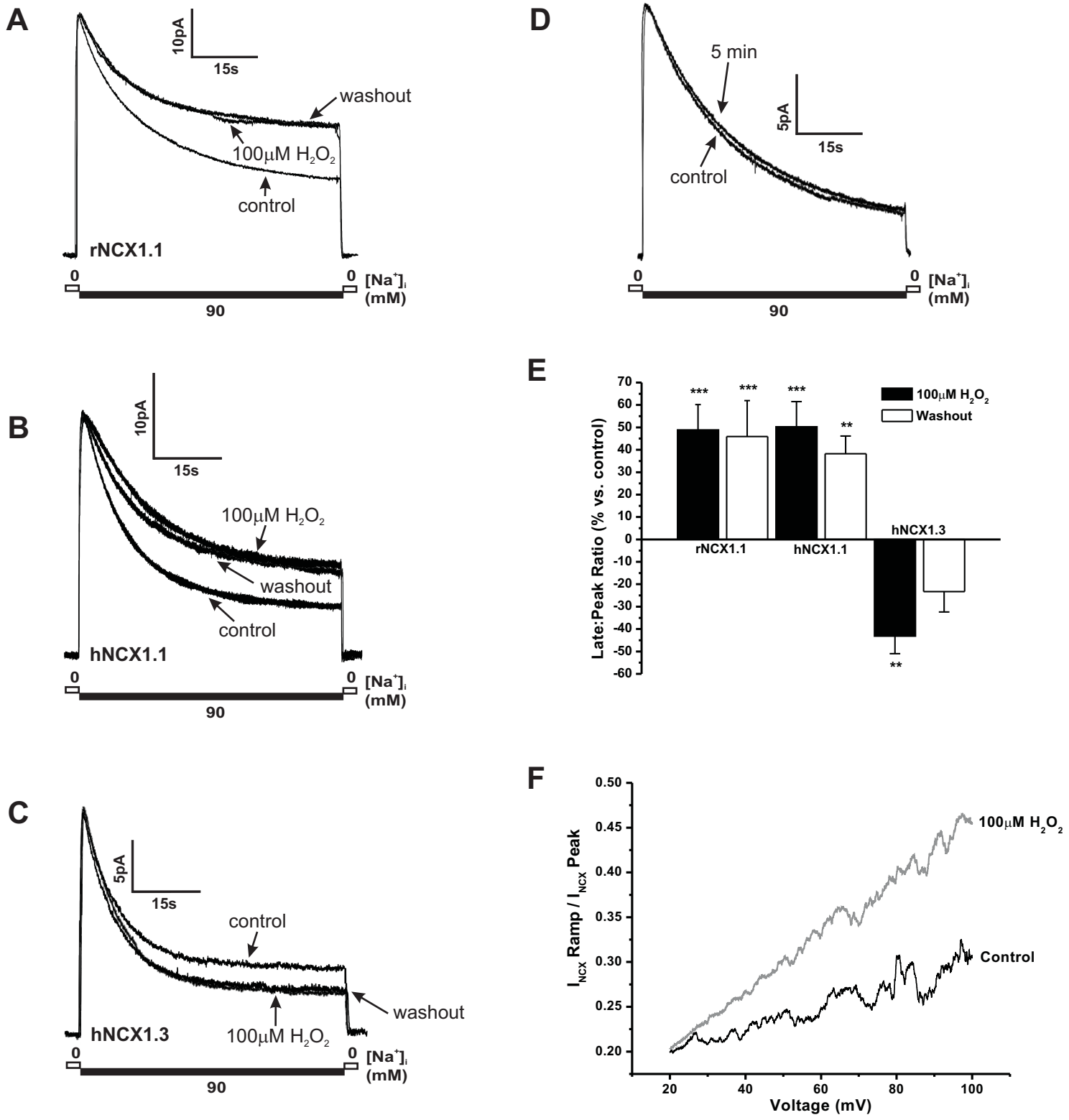
A
10pA
15s
washout
100μM H2O2
control
rNCX1.1
0
0
[Na+]i
(mM)
90
B
10pA
15s
100μM H2O2
washout
control
hNCX1.1
0
0
[Na+]i
(mM)
90
C
5pA
15s
control
washout
hNCX1.3
100μM H2O2
0
0
[Na+]i
(mM)
90
D
5 min
5pA
15s
control
0
0
[Na+]i
(mM)
90
E
Late:Peak Ratio (% vs. control)
100μM H2O2
Washout
***
***
***
**
hNCX1.3
rNCX1.1
hNCX1.1
**
F
INCX Ramp / INCX Peak
100μM H2O2
Control
Voltage (mV)

Figure 2-3

H_2O_2 Differentially Effects the Forward-mode Activity of Rat/Human NCX1.1 and NCX1.3. (A-B) Representative FM rat and human NCX1.1 currents showing no effect upon H_2O_2 application. **(C)** A sample trace of FM hNCX1.3 depicting a slight inhibition of current with 100μM H_2O_2 application. **(D)** Late-to-peak analysis of FM-NCX1.1 and NCX1.3 currents. n=6-10 patches per group, ***P<0.001 vs. control. rNCX – rat NCX, hNCX – human NCX.

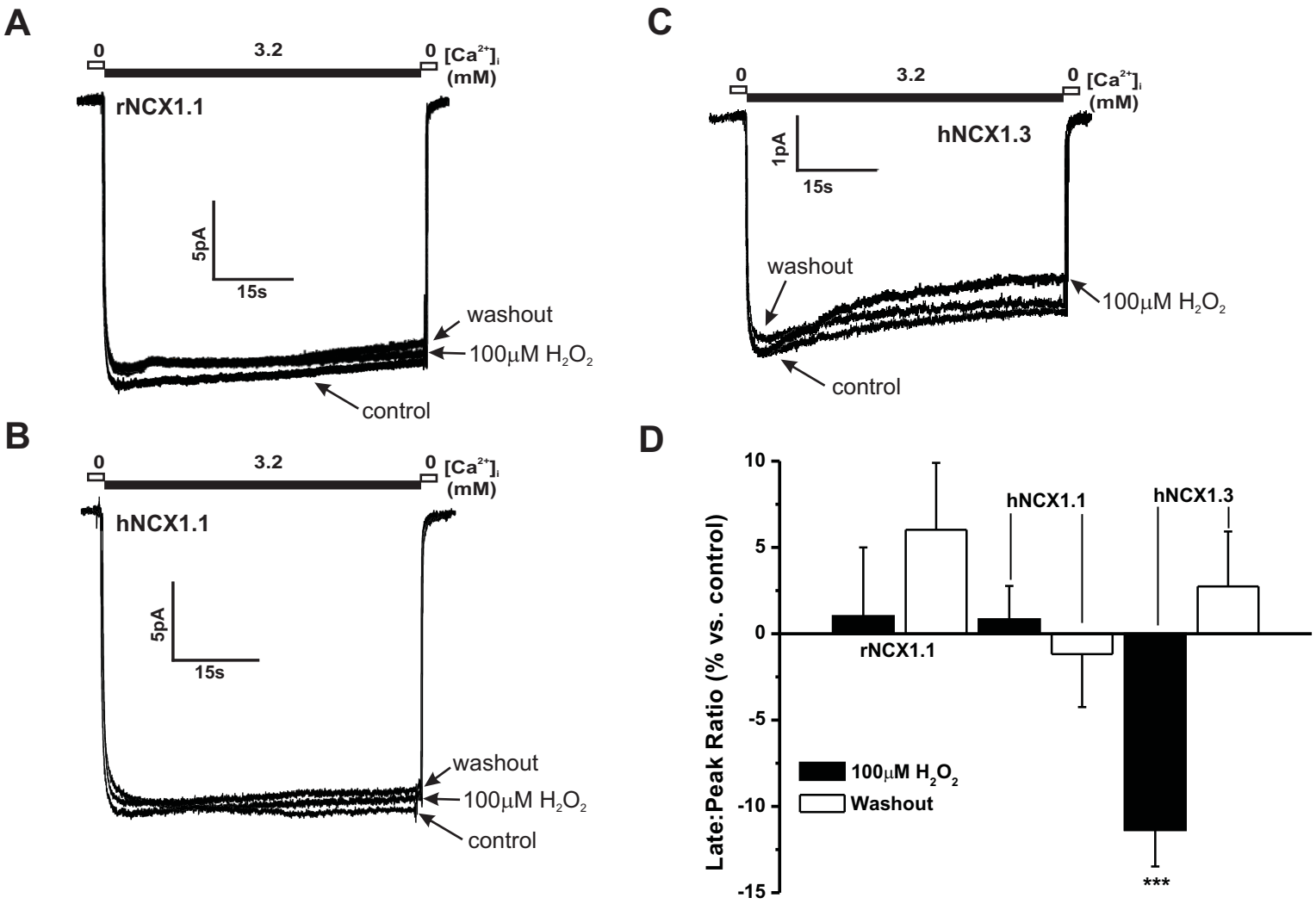
A
0
3.2
0 [Ca2+]i (mM)
rNCX1.1
5pA
15s
washout
100μM H2O2
control
B
0
3.2
0 [Ca2+]i (mM)
hNCX1.1
5pA
15s
washout
100μM H2O2
control
C
0
3.2
0 [Ca2+]i (mM)
hNCX1.3
1pA
15s
washout
100μM H2O2
control
D
Late:Peak Ratio (% vs. control)
10
5
0
-5
-10
-15
rNCX1.1
hNCX1.1
hNCX1.3
100μM H2O2
Washout
***

Figure 2-4

NCX1 Alternative Splicing. (A) Topological representation of NCX1 depicting the XIP region, the calcium binding domains, the alternative splicing region and the α-1 and α-2 repeat regions. **(B)** Detailed view of the exon composition of the different NCX1 splice variants examined in this study. **(C)** The amino acid sequences of the alternative splicing region for different human NCX1 splice variants. Bold letters represent amino acids amenable to ROS-mediated oxidation (Stadtman ER, Levine RL., 2003). Exon *A* is underlined. XIP-exchanger inhibitory peptide region, CBD-calcium binding domain, ASR-alternative splicing region.

A

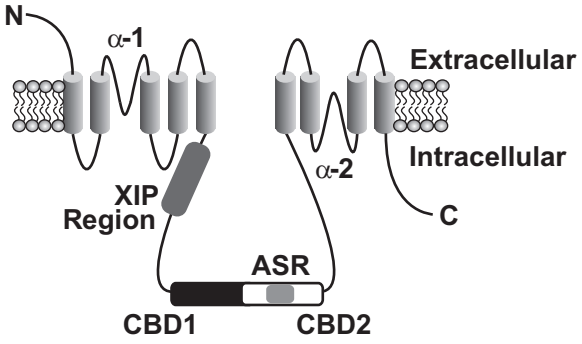

B

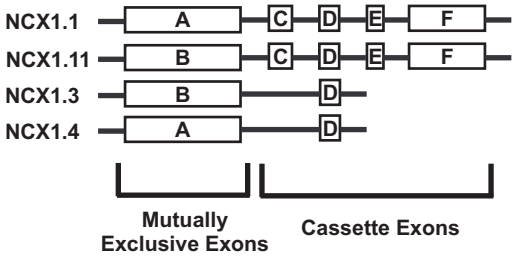

C

		EXON A or B	EXON C	EXON D	EXON E	EXON F	
NCX1.1	604	KTISVKVIDDEE**Y**EKNKTFFLEIGEPRLVE**M**SEKK	ALLLNEL	GGFTIT	GKYLF	GQPVFRKVHAREHPILSTVITIA	679
NCX1.11	604	KIITIRIFDREE**Y**EKE**C**SFSLVLEEPK**W**IRRG**M**K-	ALLLNEL	GGFTIT	GKYLF	GQPVFRKVHAREHPILSTVITIA	678
NCX1.3	604	KIITIRIFDREE**Y**EKE**C**SFSLVLEEPK**W**IRRG**M**K-	-------	GGFTIT	-----	----------	643
NCX1.4	604	KTISVKVIDDEE**Y**EKNKTFFLEIGEPRLVE**M**SEKK	-------	GGFTIT	-----	----------	644

Figure 2-5

The Effects of H_2O_2 on NCX1.4 and NCX1.11 Reverse-mode Currents. (A) Representative trace of a rat RM-NCX1.4 current showing an increase in current as a result of H_2O_2 application. **(B)** Representative trace of RM human NCX1.11 current displaying a decrease in late current after H_2O_2 treatment. **(C)** Grouped late:peak ratio data. n=6 patches per group, **P*<0.05, ****P*<0.001 vs. control. rNCX – rat NCX, hNCX – human NCX.

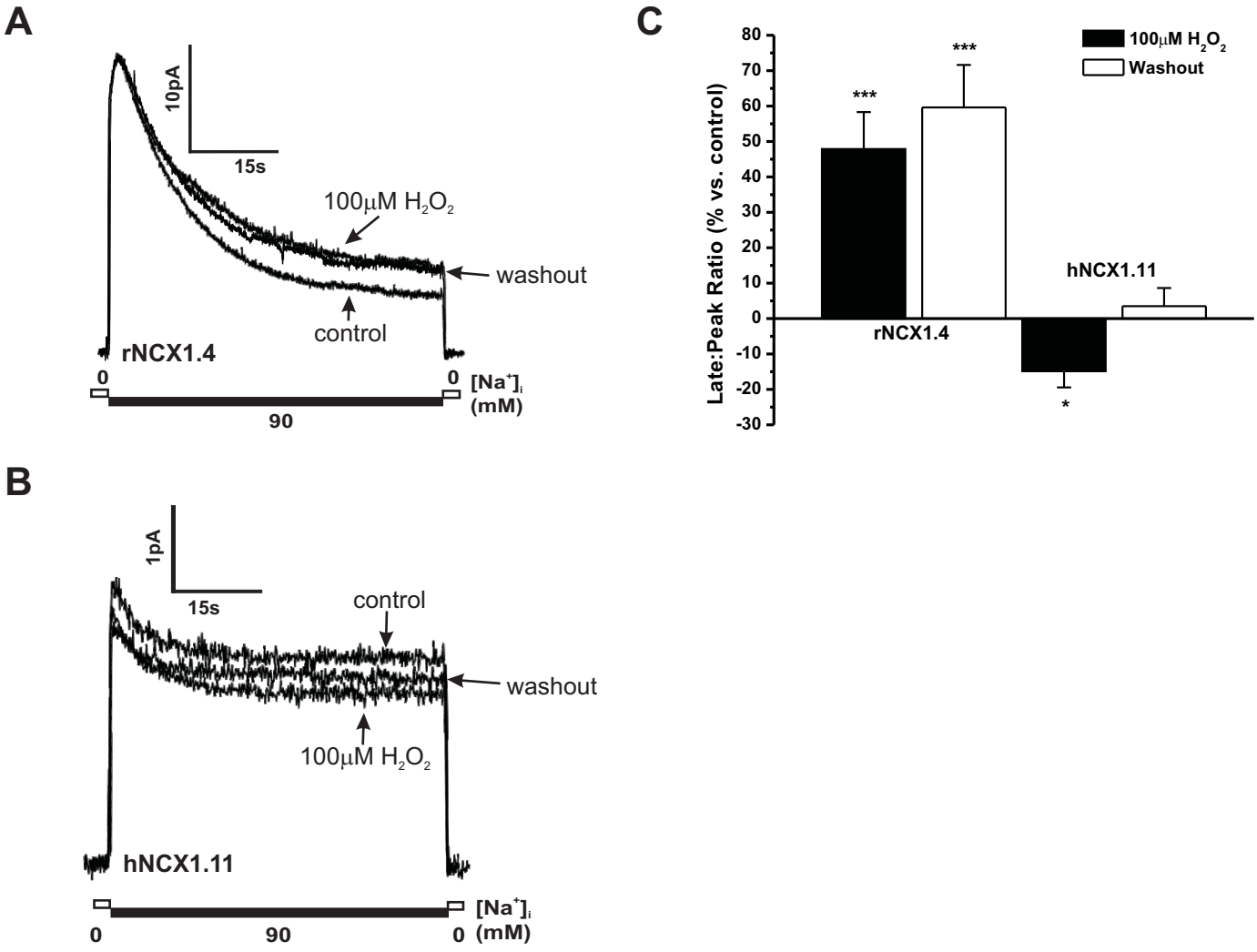
A
10pA
15s
100μM H2O2
washout
control
rNCX1.4
0
0
[Na+]i
(mM)
90
B
1pA
15s
control
washout
100μM H2O2
hNCX1.11
[Na+]i
0
90
0 (mM)
C
100μM H2O2
Washout
Late:Peak Ratio (% vs. control)
80
70
60
50
40
30
20
10
0
-10
-20
-30
***
***
rNCX1.4
hNCX1.11
*

Figure 2-6

H_2O_2 Modulation of NCX1.1 Currents Requires an Inactivation Process. (A) Representative trace of a rat NCX1.1-F255E RM current, displaying a pronounced inactivation that is slowed by H_2O_2 application. **(B)** Representative trace of a human NCX1.1-K264Q RM current exhibiting no inactivation process and is unaffected by H_2O_2. **(C)** Grouped rate of inactivation (τ) data for wild type human NCX1.1-F258 and the mutant rat NCX1.1-E255 currents. n=10-12 patches per group, $^{**}P<0.01$, $^{***}P<0.001$, vs. control. **(D)** Grouped analysis for late:peak current ratio for wild type human NCX1.1-K264 and the mutant human NCX1.1-Q264 currents. n=12-13 patches per group, $^{***}P<0.001$, vs. control.

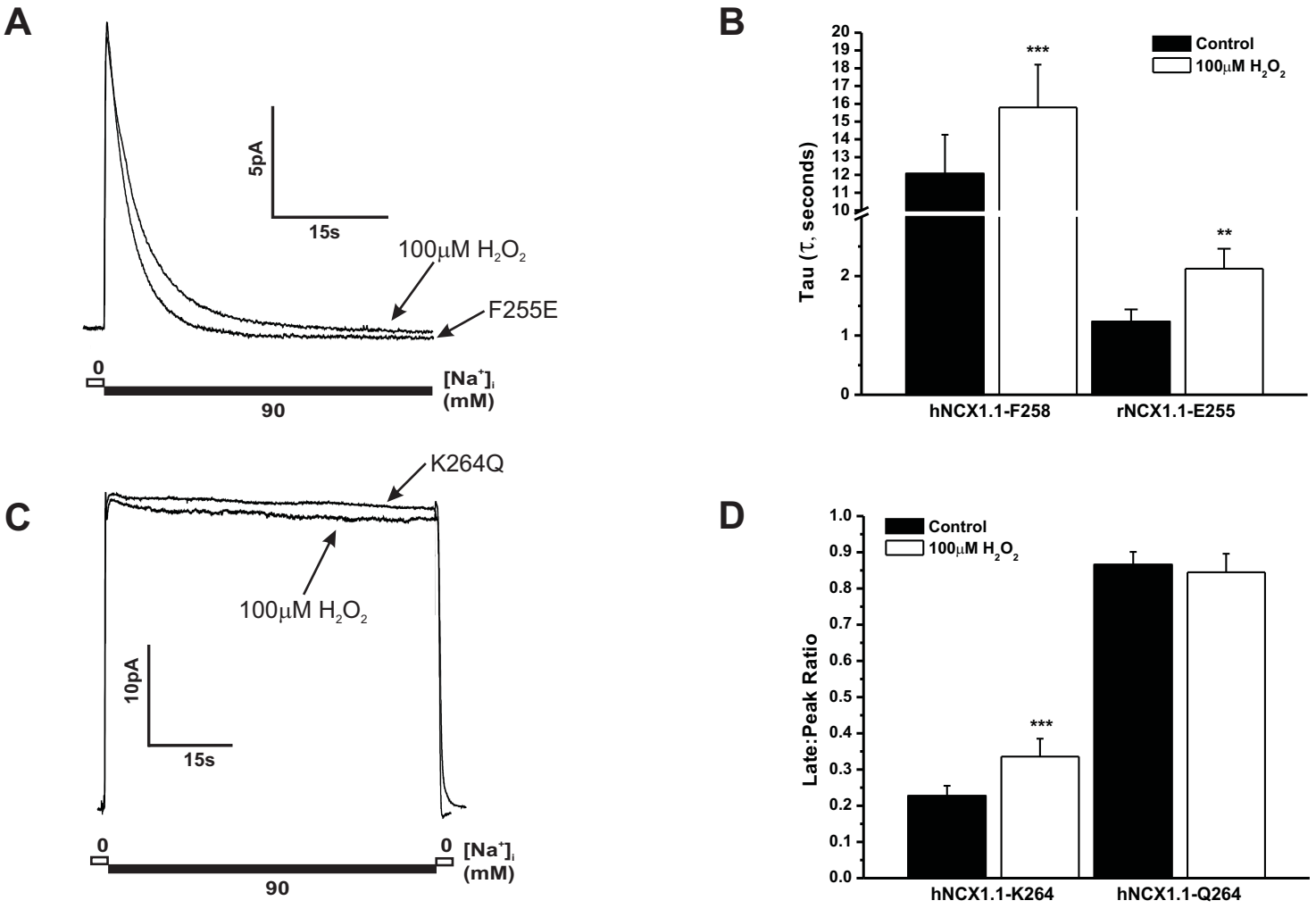
A
5pA
15s
100μM H2O2
F255E
0
[Na+]i
(mM)
90
B
Control
100μM H2O2
Tau (τ, seconds)
***
**
hNCX1.1-F258
rNCX1.1-E255
C
K264Q
100μM H2O2
10pA
15s
0
0
[Na+]i
(mM)
90
D
Control
100μM H2O2
Late:Peak Ratio
***
hNCX1.1-K264
hNCX1.1-Q264

Figure 2-7

ROS Modification of NCX1 Current is Lipid Peroxidation Independent and is Time-Dependent. (A) Representative trace of hNCX1.1 RM current that is unaffected by the application of 100μM *t*-butyl hydroperoxide. **(B-C)** Sample traces of hNCX1.1 RM currents showing the effects of a 2min and 10min 100μM H_2O_2 application, respectively. **(D)** Data analysis of late-to-peak ratios of hNCX1.1 currents after a 2min and 10min application of 100μM H_2O_2. n=7-9 patches per group, **P*<0.05, ***P*<0.01 vs. control.

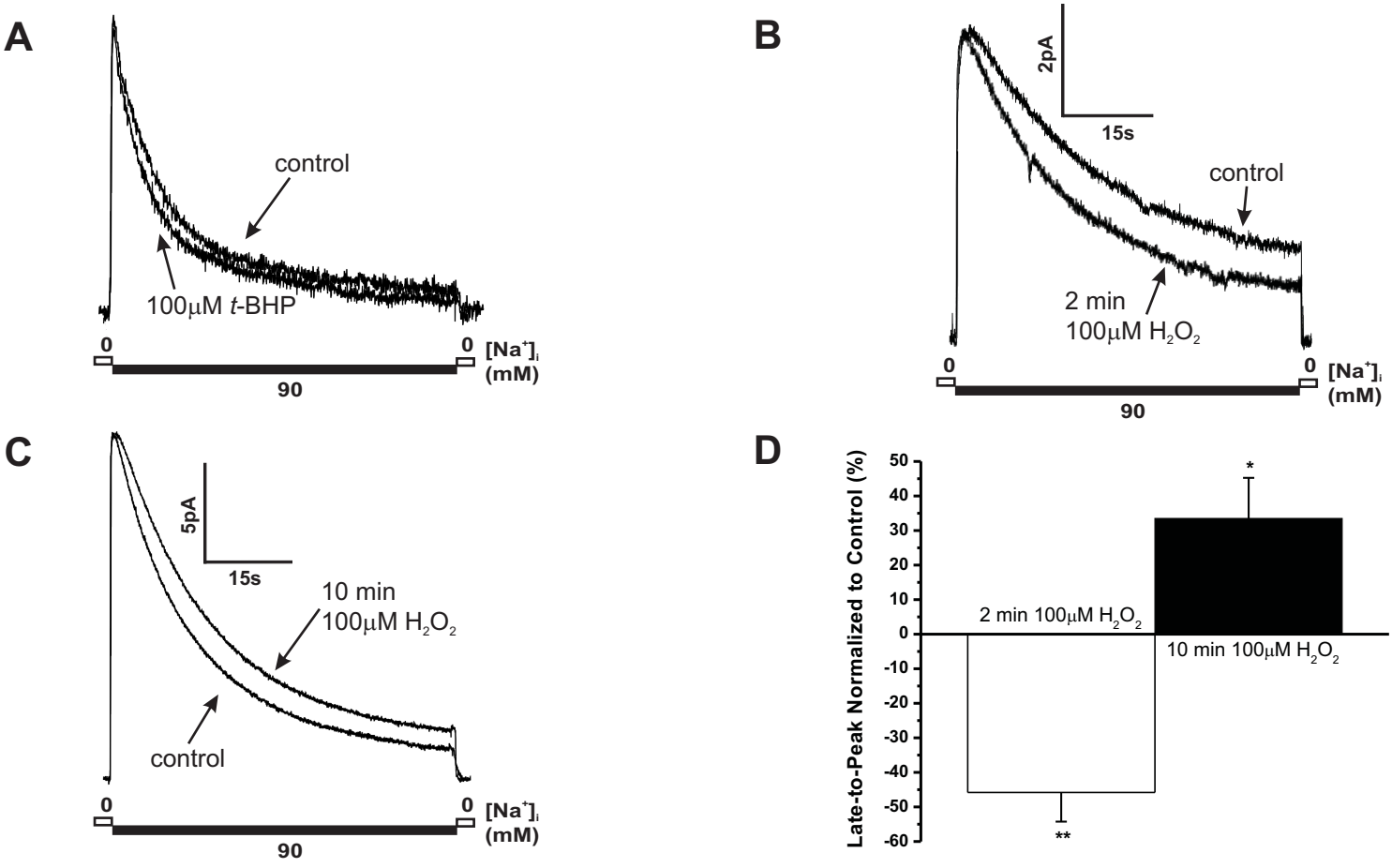
A
control
100μM t-BHP
0
0
[Na+]i
(mM)
90
B
2pA
15s
control
2 min
100μM H2O2
0
0
[Na+]i
(mM)
90
C
5pA
15s
10 min
100μM H2O2
control
0
0
[Na+]i
(mM)
90
D
Late-to-Peak Normalized to Control (%)
50
40
30
20
10
0
-10
-20
-30
-40
-50
-60
*
**
2 min 100μM H2O2
10 min 100μM H2O2

Figure 2-8

KB-R7943 Inhibition of NCX1.1 Activity is Reduced After Prior Exposure to H_2O_2. (A) Representative trace showing KB-R7943 (1μM) inhibition of human RM-NCX1.1 current. **(B)** Representative trace illustrating that pre-exposure to 100μM H_2O_2 reduces KB-R7943 inhibition. **(C)** Concentration-response curves showing a rightward-shift in KB-R7943 inhibition after 100μM H_2O_2 application. IC_{50} for KB-R7943: Control - 0.21 ± 0.1μM, H_2O_2 - IC_{50} – 1.37 ± 0.39μM, n=5-6 patches per group, **P*<0.05, ***P*<0.01, vs. control.

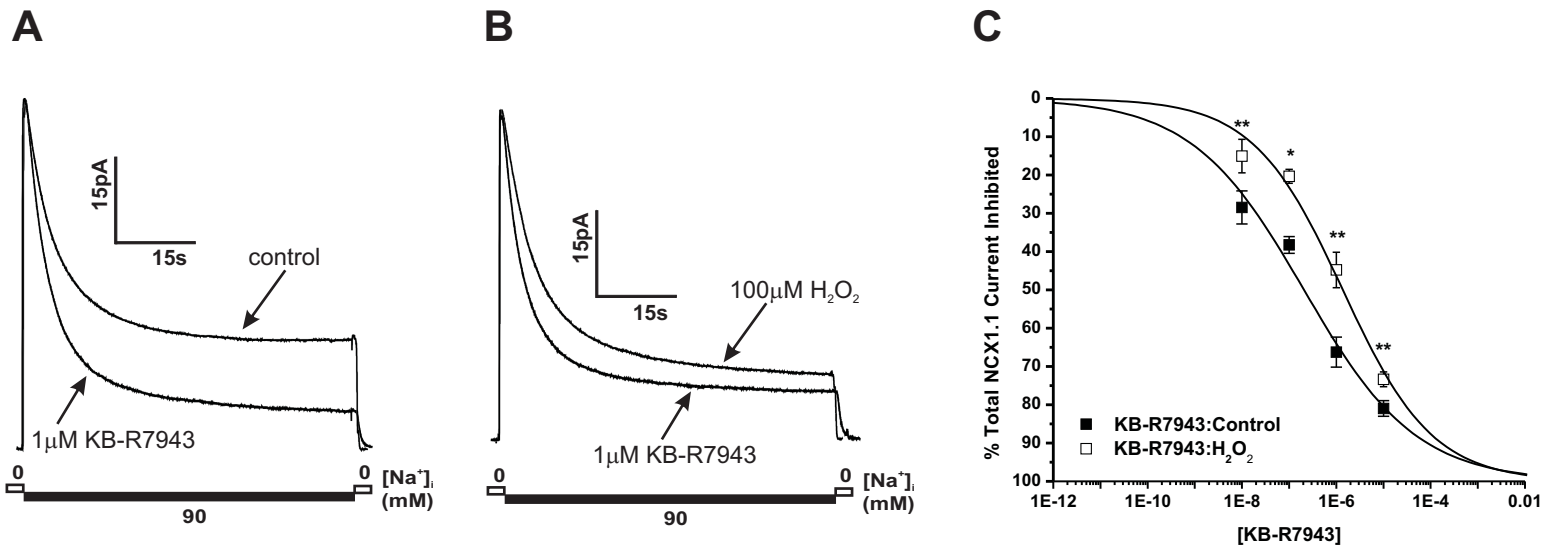
A
15pA
15s
control
1μM KB-R7943
0
0
90
[Na+]i
(mM)
B
15pA
15s
100μM H2O2
1μM KB-R7943
0
0
90
[Na+]i
(mM)
C
% Total NCX1.1 Current Inhibited
0
10
20
30
40
50
60
70
80
90
100
**
*
**
**
KB-R7943:Control
KB-R7943:H2O2
1E-12
1E-10
1E-8
1E-6
1E-4
0.01
[KB-R7943]

Figure 2-9

Protein Structures of the 2nd Intracellular Calcium Binding Domain of NCX1. Protein models were modified from Hilge et al., 2006., and accessed from the Protein Databank (accession code 2FWU). **(A)** Structure of the CBD2. Blue spheres represent Ca^{2+} ions. Exon A is highlighted in green. **(B)** Modelling of the exon *A* region contained in CBD2, with D613 and K620 labelled. D613 and K620 play a critical role in stabilizing calcium binding. **(C)** Exon *A* region depicted with R613 and C620 (present in exon *B*), showing alterations in the calcium binding locus of CBD2. R613 and C620 destabilize calcium binding in this region. Therefore, it is possible that the H_2O_2 induced changes in exon *A* further stabilizes the structure in **(B)** while destabilizing the structure in **(C)**, accounting for the splice variant specific effect of H_2O_2.

A

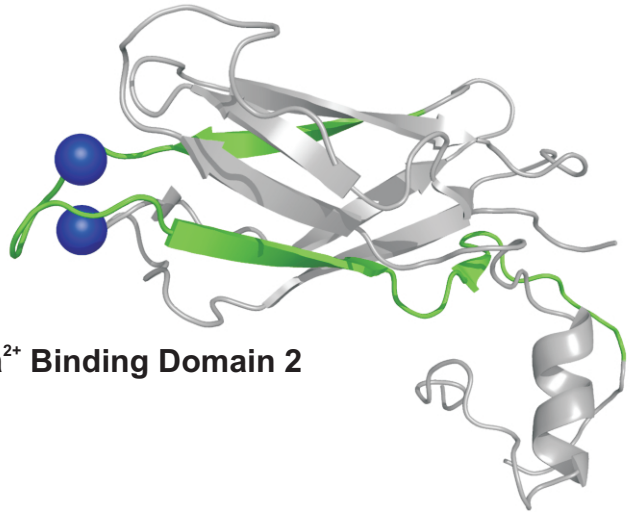

Ca^{2+} Binding Domain 2

B

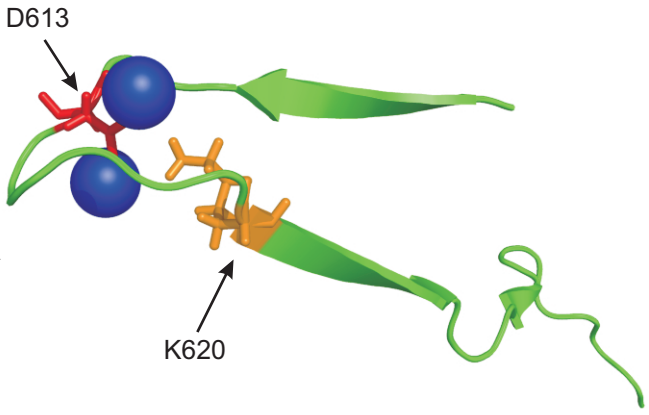

Exon A

C

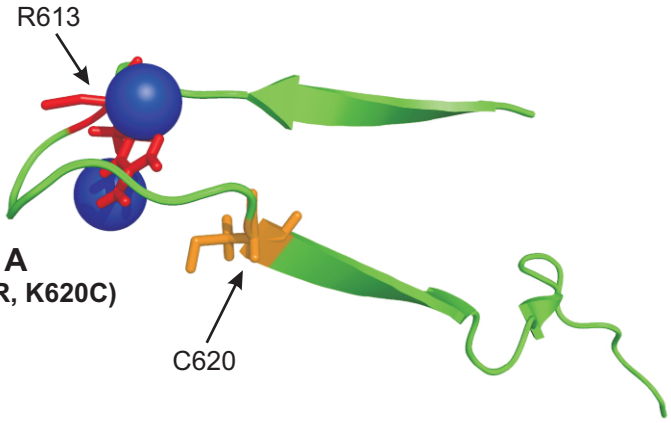

Exon A
(D613R, K620C)

References

1. Quednau BD, Nicoll DA, Philipson KD. Tissue specificity and alternative splicing of the Na+/Ca2+ exchanger isoforms NCX1, NCX2, and NCX3 in rat. Am.J.Physiol. 1997 Apr;272(4 Pt 1):C1250-61.

2. Quednau BD, Nicoll DA, Philipson KD. The sodium/calcium exchanger family-SLC8. Pflugers Arch. 2004 Feb;447(5):543-548.

3. Philipson KD, Nicoll DA, Ottolia M, Quednau BD, Reuter H, John S, et al. The Na+/Ca2+ exchange molecule: an overview. Ann.N.Y.Acad.Sci. 2002 Nov;976:1-10.

4. Blaustein MP, Lederer WJ. Sodium/calcium exchange: its physiological implications. Physiol.Rev. 1999 Jul;79(3):763-854.

5. Tani M, Neely JR. Role of intracellular Na+ in Ca2+ overload and depressed recovery of ventricular function of reperfused ischemic rat hearts. Possible involvement of H+-Na+ and Na+-Ca2+ exchange. Circ.Res. 1989 Oct;65(4):1045-1056.

6. Tani M. Mechanisms of Ca2+ overload in reperfused ischemic myocardium. Annu.Rev.Physiol. 1990;52:543-559.

7. Orrenius S, Zhivotovsky B, Nicotera P. Regulation of cell death: the calcium-apoptosis link. Nat.Rev.Mol.Cell Biol. 2003 Jul;4(7):552-565.

8. Piper HM, Meuter K, Schafer C. Cellular mechanisms of ischemia-reperfusion injury. Ann.Thorac.Surg. 2003 Feb;75(2):S644-8.

9. Henry TD, Archer SL, Nelson D, Weir EK, From AH. Enhanced chemiluminescence as a measure of oxygen-derived free radical generation during ischemia and reperfusion. Circ.Res. 1990 Dec;67(6):1453-1461.

10. Ferrari R, Ceconi C, Curello S, Alfieri O, Visioli O. Myocardial damage during ischaemia and reperfusion. Eur.Heart J. 1993 Nov;14 Suppl G:25-30.

11. Zweier JL, Kuppusamy P, Thompson-Gorman S, Klunk D, Lutty GA. Measurement and characterization of free radical generation in reoxygenated human endothelial cells. Am.J.Physiol. 1994 Mar;266(3 Pt 1):C700-8.

12. Vanden Hoek TL, Li C, Shao Z, Schumacker PT, Becker LB. Significant levels of oxidants are generated by isolated cardiomyocytes during ischemia prior to reperfusion. J.Mol.Cell.Cardiol. 1997 Sep;29(9):2571-2583.

13. Becker LB, vanden Hoek TL, Shao ZH, Li CQ, Schumacker PT. Generation of superoxide in cardiomyocytes during ischemia before reperfusion. Am.J.Physiol. 1999 Dec;277(6 Pt 2):H2240-6.

14. Eigel BN, Gursahani H, Hadley RW. ROS are required for rapid reactivation of Na+/Ca2+ exchanger in hypoxic reoxygenated guinea pig ventricular myocytes. Am.J.Physiol.Heart Circ.Physiol. 2004 Mar;286(3):H955-63.

15. Wagner S, Seidler T, Picht E, Maier LS, Kazanski V, Teucher N, et al. Na(+)-Ca(2+) exchanger overexpression predisposes to reactive oxygen species-induced injury. Cardiovasc.Res. 2003 Nov 1;60(2):404-412.

16. Goldhaber JI. Free radicals enhance Na+/Ca2+ exchange in ventricular myocytes. Am.J.Physiol. 1996 Sep;271(3 Pt 2):H823-33.

17. Goldhaber JI, Qayyum MS. Oxygen free radicals and excitation-contraction coupling. Antioxid.Redox Signal. 2000 Spring;2(1):55-64.

18. Santacruz-Toloza L, Ottolia M, Nicoll DA, Philipson KD. Functional analysis of a disulfide bond in the cardiac Na(+)-Ca(2+) exchanger. J.Biol.Chem. 2000 Jan 7;275(1):182-188.

19. Hinata M, Matsuoka I, Iwamoto T, Watanabe Y, Kimura J. Mechanism of Na+/Ca2+ exchanger activation by hydrogen peroxide in guinea-pig ventricular myocytes. J.Pharmacol.Sci. 2007 Mar;103(3):283-292.

20. Zhang XQ, Song J, Rothblum LI, Lun M, Wang X, Ding F, et al. Overexpression of Na+/Ca2+ exchanger alters contractility and SR Ca2+ content in adult rat myocytes. Am.J.Physiol.Heart Circ.Physiol. 2001 Nov;281(5):H2079-88.

21. Dunn J, Elias CL, Le HD, Omelchenko A, Hryshko LV, Lytton J. The molecular determinants of ionic regulatory differences between brain and kidney Na+/Ca2+ exchanger (NCX1) isoforms. J.Biol.Chem. 2002 Sep 13;277(37):33957-33962.

22. Hamming KS, Riedel MJ, Soliman D, Matemisz LC, Webster NJ, Searle GJ, et al. Splice variant-dependent regulation of beta-cell sodium-calcium exchange by acyl-coenzyme As. Mol.Endocrinol. 2008 Oct;22(10):2293-2306.

23. Riedel MJ, Baczko I, Searle GJ, Webster N, Fercho M, Jones L, et al. Metabolic regulation of sodium-calcium exchange by intracellular acyl CoAs. EMBO J. 2006 Oct 4;25(19):4605-4614.

24. Matsuoka S, Nicoll DA, He Z, Philipson KD. Regulation of cardiac Na(+)-Ca2+ exchanger by the endogenous XIP region. J.Gen.Physiol. 1997 Feb;109(2):273-286.

25. Hurtado C, Ander BP, Maddaford TG, Lukas A, Hryshko LV, Pierce GN. Adenovirally delivered shRNA strongly inhibits Na+-Ca2+ exchanger expression but does not prevent contraction of neonatal cardiomyocytes. J.Mol.Cell.Cardiol. 2005 Apr;38(4):647-654.

26. Schafer C, Ladilov Y, Inserte J, Schafer M, Haffner S, Garcia-Dorado D, et al. Role of the reverse mode of the Na+/Ca2+ exchanger in reoxygenation-induced cardiomyocyte injury. Cardiovasc.Res. 2001 Aug 1;51(2):241-250.

27. Baczko I, Giles WR, Light PE. Resting membrane potential regulates Na(+)-Ca2+ exchange-mediated Ca2+ overload during hypoxia-reoxygenation in rat ventricular myocytes. J.Physiol. 2003 Aug 1;550(Pt 3):889-898.

28. Lee C, Dhalla NS, Hryshko LV. Therapeutic potential of novel Na+-Ca2+ exchange inhibitors in attenuating ischemia-reperfusion injury. Can.J.Cardiol. 2005 May 1;21(6):509-516.

29. Elias CL, Lukas A, Shurraw S, Scott J, Omelchenko A, Gross GJ, et al. Inhibition of Na+/Ca2+ exchange by KB-R7943: transport mode selectivity and antiarrhythmic consequences. Am.J.Physiol.Heart Circ.Physiol. 2001 Sep;281(3):H1334-45.

30. Bouchard R, Omelchenko A, Le HD, Choptiany P, Matsuda T, Baba A, et al. Effects of SEA0400 on mutant NCX1.1 Na+-Ca2+ exchangers with altered ionic regulation. Mol.Pharmacol. 2004 Mar;65(3):802-810.

31. Iwamoto T, Kita S, Uehara A, Imanaga I, Matsuda T, Baba A, et al. Molecular determinants of Na+/Ca2+ exchange (NCX1) inhibition by SEA0400. J.Biol.Chem. 2004 Feb 27;279(9):7544-7553.

32. Eigel BN, Hadley RW. Antisense inhibition of Na+/Ca2+ exchange during anoxia/reoxygenation in ventricular myocytes. Am.J.Physiol.Heart Circ.Physiol. 2001 Nov;281(5):H2184-90.

33. Hurtado C, Prociuk M, Maddaford TG, Dibrov E, Mesaeli N, Hryshko LV, et al. Cells expressing unique Na+/Ca2+ exchange (NCX1) splice variants exhibit different susceptibilities to Ca2+ overload. Am.J.Physiol.Heart Circ.Physiol. 2006 May;290(5):H2155-62.

34. Zhang XQ, Yamada S, Barry WH. Ranolazine inhibits an oxidative stress-induced increase in myocyte sodium and calcium loading during simulated-demand ischemia. J.Cardiovasc.Pharmacol. 2008 May;51(5):443-449.

35. Imahashi K, Mraiche F, Steenbergen C, Murphy E, Fliegel L. Overexpression of the Na+/H+ exchanger and ischemia-reperfusion injury in the myocardium. Am.J.Physiol.Heart Circ.Physiol. 2007 May;292(5):H2237-47.

36. Eigel BN, Hadley RW. Contribution of the Na(+) channel and Na(+)/H(+) exchanger to the anoxic rise of [Na(+)] in ventricular myocytes. Am.J.Physiol. 1999 Nov;277(5 Pt 2):H1817-22.

37. Chernysh O, Condrescu M, Reeves JP. Sodium-dependent inactivation of sodium/calcium exchange in transfected Chinese hamster ovary cells. Am.J.Physiol.Cell.Physiol. 2008 Oct;295(4):C872-82.

38. Stadtman ER, Levine RL. Protein oxidation. Ann.N.Y.Acad.Sci. 2000;899:191-208.

39. Stadtman ER, Levine RL. Free radical-mediated oxidation of free amino acids and amino acid residues in proteins. Amino Acids 2003 Dec;25(3-4):207-218.

40. Davies MJ. The oxidative environment and protein damage. Biochim.Biophys.Acta 2005 Jan 17;1703(2):93-109.

41. Hilge M, Aelen J, Vuister GW. Ca2+ regulation in the Na+/Ca2+ exchanger involves two markedly different Ca2+ sensors. Mol.Cell 2006 Apr 7;22(1):15-25.

42. Maack C, Ganesan A, Sidor A, O'Rourke B. Cardiac sodium-calcium exchanger is regulated by allosteric calcium and exchanger inhibitory peptide at distinct sites. Circ.Res. 2005 Jan 7;96(1):91-99.

43. Iwamoto T, Kita S, Uehara A, Inoue Y, Taniguchi Y, Imanaga I, et al. Structural domains influencing sensitivity to isothiourea derivative inhibitor KB-R7943 in cardiac Nna(+)/Ca(2+) exchanger. Mol.Pharmacol. 2001 Mar;59(3):524-531.

Chapter 3

The Anti-Anginal Agent Ranolazine is a Potent Inhibitor of Cardiac Reverse-Mode Sodium-Calcium Exchange.

The ex vivo heart perfusions in Figure 3-1 and 3-2 were performed by Liango Wang (2010). The Na^+ channel data presented in Figure 3-3 were obtained by Wei Wang (2010).

Introduction

Cardiac ischemia-reperfusion (IR) injury is a complex phenomenon with many factors contributing to the type and magnitude of injury observed [1-3]. During IR injury, the onset of abnormal intracellular Ca^{2+} (Ca^{2+}_i) homeostasis and Ca^{2+}_i-overload mediated by increased reverse-mode (RM) activity of the Na^+-Ca^{2+} exchanger (NCX1.1) is the predominant Ca^{2+} entry pathway leading to LV mechanical dysfunction, myocyte hypercontracture and cell death [4,5]. Deleterious RM NCX1.1 activity is thought to occur as a downstream consequence of intracellular sodium (Na^+_i) loading via 1) increased sodium hydrogen exchanger activity [6,7] and 2) induction of a late current through voltage-gated sodium channels (late I_{Na}) [8,9]. Therefore, RM-NCX1.1, NHE1 and late I_{Na} represent potential therapeutic targets in the development of novel anti-ischemic agents (see reviews [10-12]).

The anti-ischemic agent ranolazine (Ranexa™) is a recently approved therapeutic agent for angina pectoris. At therapeutic plasma concentrations of 1-10 mM, ranolazine is thought to act via a selective inhibition of late I_{Na} with little or no effect on the physiological forward-mode (FM) activity of NCX1.1 [13,14]. Although the effects of ranolazine were not tested on the pathophysiological RM operation of NCX1.1, ranolazine has been shown to reduce diastolic Ca^{2+}_i levels and restore left ventricular function after induction of late I_{Na} with ATX-II [15-17]. Nevertheless, as RM NCX1.1 activity is the key downstream mediator of the ATX-II induced dysfunction, the possibility remains that ranolazine may be acting via direct inhibition of RM NCX1.1 activity. Therefore the primary aim of

this study was to directly investigate ranolazine's anti-ischemic mechanism of action.

To circumvent the involvement of late I_{Na}, the cardiac glycoside ouabain can be used to directly elevate intracellular Na^+_i by reducing the extrusion of Na^+_i via inhibition of the Na^+-K^+-ATPase (NKA). The resultant accumulation of Na^+_i leads to Ca^{2+} overload mediated by RM-NCX1.1 activity. Accordingly, we compared the effects of ranolazine with lidocaine, a known inhibitor of late I_{Na}, using 1) whole-heart models of ischemia-reperfusion and ouabain-induced intracellular Ca^{2+}_i overload, 2) a cellular model of Ca^{2+}_i overload independent of late I_{Na} inhibition, and 3) direct electrophysiological recording of electrogenic forward- and RM currents from recombinant cardiac NCX1.1.

Materials & Methods

Heart Perfusions and Measurements of Left Ventricular Function in Working Mode.

Rat heart isolation and working-mode perfusion were performed as detailed previously [17,18]. Adult male Sprague-Dawley rats weighing 300-400g were anesthetised with pentobarbital (150 mg/kg i.p.) in accordance to the University of Alberta Animal Policy and Welfare Committee and the Canadian Council on Animal Care guidelines. Each heart was promptly excised, the aorta cannulated and a non-working (Langendorff) perfusion was commenced within 30 seconds with Krebs-Henseleit solution. After 10 minutes, a working-mode perfusion was initiated as conducted previously [19], with a re-circulating perfusate (volume 100 mL, 37 ºC, pH 7.4, gassed with a 95% O_2-CO_2 mixture)

consisting of a modified Krebs-Henseleit solution containing the following (in mM): 118 NaCl, 4.7 KCl, 1.2 KH_2PO_4, 1.2 $MgSO_4$, 2.5 $CaCl_2$, 25 $NaHCO_3$, 11 glucose, 1.2 palmitate and 100 mU/L insulin. Palmitate was pre-bound to 3% bovine serum albumin. Heart perfusions were conducted at a constant workload (preload: 11.5 mmHg, afterload: 80 mmHg) and pacing at 5 Hz.

Measurements of left ventricular (LV) function parameters were observed using methods previously described [17,18]. Heart rate and systolic and diastolic aortic pressures (mmHg) were measured with a pressure transducer (AD Instruments, Colorado Springs, CO) attached to the aortic outflow line. Cardiac output (mL/min) and aortic flow (mL/min) were measured using ultrasonic flow probes (Transonic T206, Transonic Systems Inc., Ithica, NY) placed in the left atrial inflow line and the atrial outflow line, respectively. All parameters were digitally acquired using Chart 5.0 software (AD Instruments, Colorado Springs, CO). Left ventricular minute work (L/min · mmHg) was used as a continuous index of LV mechanical function and was calculated as cardiac output x LV developed pressure (aortic systolic pressure – preload pressure). Coronary flow (mL/min) was calculated as the difference between cardiac output and aortic flow and coronary vascular conductance (mL/min/mmHg) was measured as coronary flow divided by aortic diastolic perfusion pressure.

Measurement of Intracellular Ca^{2+}.

Measurement of intracellular Ca^{2+} was conducted as described previously [17,18]. Hearts were loaded with the fluorescent Ca^{2+} indicator indo-1AM (5 μM) and indo-1 fluorescence was measured at a ~0.3 cm^2 area of the LV-free wall of

the epicardial surface using a spectrofluorometer (Photon Technology International, London, ON) fitted with a bifurcated fiber optic cable containing both excitation emitter and emission detectors [20]. Fluorescent signals were sampled at 500 Hz and the ratio of indo-1 fluorescence emitted at 405 nm and 485 nm was calculated to give an index of beat-to-beat Ca^{2+}_i.

Experimental protocols for heart perfusions.

After the indo-1 loading procedure, normal aerobic perfusion of the hearts was conducted for 15 minute to obtain baseline diastolic Ca^{2+}_i, systolic Ca^{2+}_i, and LV function measurements. Following the 15 min baseline period, hearts were either: (1) subjected to an ischemia-reperfusion protocol which comprised of 20 min of global, no-flow ischemia (no-pacing), followed by 30 min of aerobic reperfusion (pacing at 5 Hz restarted within 2 min of reperfusion), in which 10 μM ranolazine or 10 μM lidocaine was added 5 min before ischemia was commenced or (2) administered ouabain (80 μM) for 30 min and ranolazine (10 μM) or lidocaine (10 μM) applied 10 min after ouabain application.

Na^+ Channel Electrophysiology

The dialyzed whole-cell patch-clamp technique was used to record Na^+ currents from tsA201 cells transiently expressing the human recombinant $Na_v1.5$ alpha-subunit as previously described [21]. Pipettes were backfilled with a solution containing either 5 mM Na^+ or 15 mM Na^+ and (in mM): 130 CsCl, 2.5 HEPES, 2 MgATP, 1 EGTA (pH was adjusted to 7.2 with CsOH), to examine the effect of intracellular Na^+ concentration on the development of late I_{Na}. After

membrane rupture, cells were held at -120 mV and stepped to 0 mV for 20 ms to evoke inward whole-cell Na^+ currents.

Measurement of Evoked Reverse-mode NCX1 Activity from Neonatal Rat Cardiac Myocytes using Ca^{2+}_i Fluorescence Imaging.

Neonatal rat cardiac myocytes were isolated and cultured as previously described [22]. After 48-72 hours isolation, neonatal myocytes were loaded with calcium green-1AM (2 uM) for 30 min at room temperature (22 ± 1 ºC) and for 30 min at 37 ºC, and subjected to the protocol below, as previously detailed [23,24]. Cells were excited with 488 nm light and fluorescent signals emitted at 520 nm measured using a photomultiplier detection system (PTI, Photon Technology International, London, ON). Data were analyzed using Felix32 (PTI) and Clampfit 10.1 software (Axon Instruments, Foster City, CA).

To assess Ca^{2+}_i influx via RM NCX1.1 activity, cells were superfused for 2 min with a solution containing (in mM): 140 NaCl, 4 KCl, 10 HEPES, 2.5 $CaCl_2$, 1 $MgCl_2$ and 10 dextrose. Cells were then superfused with a K^+-free solution (144 NaCl, 10 HEPES, 2.5 $CaCl_2$, 1 $MgCl_2$, and 10 dextrose) for 5 min, followed by a 5 min superfusion of Na^+-free solution (140 LiCl, 4 KCl , 10 HEPES, 2.5 $CaCl_2$, 1 $MgCl_2$, and 10 dextrose). 10μM tetrodotoxin (TTX) was added to both K^+-free and Na^+-free solutions to inhibit cardiac Na^+ channels ($Na_v1.5$) and 2 μM thapsigargin added to the Na^+-free solution to reduce Ca^{2+} sequestration by the sarco-endoplasmic reticulum Ca^{2+}-ATPase (SERCA2a). 5 μM KB-R7943, 10 μM ranolazine, 10 μM lidocaine or 5 mM $NiCl_2$ were applied during the Na^+-free perfusion period to assess the effects on RM NCX1 activity.

To silence NCX1 expression, neonatal cardiac myocytes were infected with an adenoviral vector encoding short hairpin RNA for NCX1 (AdshRNA-NCX1) 72 hours prior to experiments. The AdshRNA-NCX1 construct was generously provided by Dr. Grant Pierce, University of Manitoba [25].

Molecular Biology, Transfection & Electrophysiology of NCX1.1.

Human NCX1.1, rat NCX1.1-F255E and human NCX1.1-K264Q plasmids were generated and transfected as previously described [24,26,27]. Briefly, NCX1.1 variants were co-transfected with a green fluorescent protein vector (Life Technologies, Gaithersburg, MD) into tsA201 cells using the calcium phosphate precipitation method. All macroscopic recordings of NCX1 currents were obtained 48–72 h after transfection.

The inside-out excised patch-clamp technique was used to measure macroscopic RM and FM NCX1.1 currents as previously detailed [27]. RM NCX1.1 currents were elicited by the application of 90 mM Na^+ to the intracellular side of the membrane patch, while FM currents were activated by 3.2 mM Ca^{2+}, for a period of 60 s. Excised patches were held at 0 mV and NCX1.1 currents were measured using an Axopatch 200B amplifier and Clampex 10.1 software and analyzed with Clampex 10.1 software (Axon Instruments, Foster City, CA). All experiments were performed at room temperature (22±1 °C).

Experimental Compounds.

Ouabain, lidocaine, thapsigargin and $NiCl_2$ were purchased from Sigma Aldrich (Oakville, ON). KB-R7943 and ranolazine were purchased from Tocris Biosciences (Ellisville, MO). Tetrodotoxin was obtained from Alomone

Laboratories (Jerusalem, Israel). DMSO concentration did not exceed 0.25% v/v in heart perfusion experiments, 0.3% v/v in neonatal cardiac myocyte imaging and 0.1% v/v patch clamp experiments. DMSO was present in all control solutions as vehicle control.

Data Analysis and Statistical Methods.

Late NCX1.1 current amplitudes were measured and normalized to peak current. The time constant of RM NCX1.1 current inactivation (Tau, τ) was obtained by fitting currents with a best-fit single exponential function. The time constants of $Na_v1.5$ inactivation (Tau, τ) was best determined by fitting I_{Na} with a three-function exponential equation. Statistical significance was assessed by using the unpaired and paired Student's -test, and the one-way ANOVA test with a Tukey's post hoc analysis, where appropriate. $P<0.05$ was considered to be statistically significant and data are displayed as mean ± SEM.

Results

Ranolazine and Lidocaine Attenuate LV Mechanical Dysfunction and Intracellular Ca^{2+} Overload in Hearts Induced by Ischemia-reperfusion.

During baseline aerobic perfusion, indices of diastolic Ca^{2+}_i and LV work were within normal ranges (Figure 3-1). However, after 20 min of global ischemia, diastolic Ca^{2+}_i rose steadily in control hearts to 57.74 ± 5.75% vs. baseline (n=14). However, 10μM ranolazine and 10μM lidocaine reduced the observed increases in diastolic Ca^{2+}_i (35.78 ± 4.67% (n=8) and 25.84 ± 3.73% (n=5) vs. baseline, for ranolazine and lidocaine, respectively (Figure 3-1A). LV function at reperfusion was reduced significantly in control hearts, recovering to

18.37 ± 5.41% and 31.23 ± 6.13% (n=14) of aerobic baseline after 20 min ischemia and 30 min of reperfusion, respectively. Ranolazine protected hearts against LV dysfunction following 20 min global ischemia (53.85 ± 6.93% and 71.48 ± 4.74% of aerobic baseline function after 20 min ischemia and 30 min reperfusion, n=8, P<0.001 vs. vehicle). Similarly, lidocaine also significantly improved LV function after the ischemic period (73.44 ± 1.93% and 84.97 ± 3.68% after 20 min and 30 min reperfusion, respectively; n=5, P<0.001 vs. vehicle). Diastolic Ca^{2+}_i was significantly elevated in the control hearts after reperfusion (13.83 ± 2.34% (n=14) vs. aerobic baseline. However, ranolazine and lidocaine prevented the elevation in diastolic Ca^{2+}_i levels to near baseline values (3.07 ± 1.81% (n=8) and 1.50 ± 0.79% (n=5) vs. aerobic baseline for ranolazine and lidocaine, respectively, P<0.01 vs. vehicle, Figure 3-1A,B). Coronary flow and CVC were also restored with ranolazine and lidocaine treatments (Figure 3-1C,D).

Ranolazine and Lidocaine Protect Against Ouabain-induced Intracellular Ca^{2+} Overload and LV Mechanical Dysfunction.

In order to investigate further the underlying mechanisms for the protection afforded by ranolazine and lidocaine, the NKA inhibitor ouabain was used to induce intracellular Na^{+}_i and subsequent NCX1-mediated Ca^{2+}_i loading that is a characteristic feature of ischemia-reperfusion injury. Ouabain (80 μM) induced a significant elevation in diastolic Ca^{2+}_i to 32.81 ± 1.49% and 32.36 ± 1.67% vs. baseline levels after 15 and 30 min respectively (n=5, Figure 3-2A). Application of ranolazine or lidocaine reduced ouabain-induced diastolic Ca^{2+}_i

accumulation after 20 min (13.69 ± 3.05% (n=5) and 15.72 ± 1.95% (n=6), respectively, P<0.001 vs. vehicle). Parallel improvements in LV function were also observed with ranolazine and lidocaine. Ouabain alone depressed LV work to 57.48 ± 9.62 % of control levels after 30 min, whereas co-application of ouabain with either ranolazine or lidocaine decreased LV work by only 18.88 ± 4.67% (n=5, P<0.01 vs. vehicle) and 29.83 ± 4.54% (n=6, P<0.05 vs. vehicle), respectively (Figure 3-2B).

Elevating Na^+_i Alone Does Not Induce Late I_{Na}.

The possibility remains that elevating Na^+_i with ouabain may induce late I_{Na} that may account for the protective effects observed with ranolazine and lidocaine. Therefore, the effects of elevating Na^+_i on recombinant $Na_v1.5$ currents were investigated using the dialyzed whole-cell patch-clamp technique. A 3-exponential best-fit function was fitted to averaged $Na_v1.5$ currents elicited from cells dialyzed with pipette solutions containing either 5mM Na^+ or 15mM Na^+ (Figure 3-3A,B). Subsequent analysis revealed that τ values were not significantly different between 5mM and 15mM Na^+ groups (5mM Na^+: τ_1 16.17 ms, τ_2 3.45, τ_3 0 ms; 15mM Na^+: τ_1 13.67 ms, τ_2 3.52 ms, τ_3 0.84 ms). These results indicate that elevating Na^+_i alone does not directly influence late I_{Na}, suggesting that the protective effects of ranolazine are mediated through another mechanism.

Ranolazine Inhibits Evoked RM-NCX1.1 Activity in Intact Neonatal Rat Ventricular Myocytes.

Accordingly, we investigated the notion that ranolazine or lidocaine may directly inhibit RM NCX1 activity by employing a neonatal rat ventricular

myocyte (NRVM). RM-NCX1.1 activity was induced by superfusing NRVM monolayers with a K^+-free solution to uncouple the NKA and induce Na^+_i-loading. Subsequent superfusion with a Na^+-free solution was used to evoke RM NCX1.1 activity, as NCX1.1 will exchange Na^+_i for extracellular Ca^{2+}, resulting in Ca^{2+}_i loading via RM NCX1.1 activity. Ca^{2+}_i loading was quantified using fluorescence Ca^{2+}-imaging, using the Ca^{2+}-sensitive fluorophore calcium green-1AM. To verify RM NCX1.1 activity in this cellular model, 5mM $NiCl_2$ was applied during the Na^+-free superfusion period and was found to abolish the increases in Ca^{2+}_i (92.11±1.68% vs. control (n=3, $P<0.01$). A molecular knockdown approach was also utilized to evaluate RM NCX1.1 activity in this cellular model as follows. NRVMs were infected with an adenoviral vector encoding shRNA (AdshRNA-NCX1) for NCX1 72 hrs prior to experimentation. The Ca^{2+} signal evoked by the Na^+-free solution was reduced by 73.93 ± 13.59% in NRVMs infected with AdshRNA-NCX1 (n=6, $P<0.01$). These data confirm that the Ca^{2+} signal evoked during Na^+-free conditions is predominately mediated via RM NCX1.1 activity.

Using this validated cellular model of evoked RM NCX1 activity, the effects of ranalozine and lidocaine and the NCX1 inhibitor KB-R7943 were tested. 10 uM tetrodotoxin (TTX) was used in these experiments to eliminate any involvement of I_{Na}. Ranolazine (10 μM) decreased the Ca^{2+} signal by 23.62 ± 2.63% (n=9, $P<0.001$ vs. control). Interestingly, lidocaine (10 μM) was without effect (6.14 ± 8.00% decrease vs. control, n=5). KB-R7943 (5 μM) was similarly effective as ranolazine in decreasing the Ca^{2+} signal (20.68 ± 3.91%, n=8,

P<0.01). Therefore, it is highly plausible that the cardioprotective actions of ranolazine (but not lidocaine) observed in the whole heart studies may be mediated via a previously unreported direct inhibition of RM NCX1.1 activity.

Ranolazine potently inhibits reverse-mode recombinant human NCX1.1 currents.

Electrophysiological methods were undertaken to directly assess the effects of ranolazine on electrogenic FM and RM NCX1.1 currents. Human NCX1.1 (NCX1.1) was transiently expressed in tsA201 cells, and the inside-out excised patch clamp technique used to record electrogenic NCX1.1 FM and RM currents. Ranolazine application to the intracellular side of the patch produced a concentration-dependent inhibition of RM NCX1.1 current (IC_{50} = 27.7 ± 3.4 nM) for steady-state RM NCX1.1 current (n=4-6 patches per concentration, Figure 3-5A,B), although peak NCX1.1 current was not significantly inhibited. The inhibitory effects of ranolazine were readily reversible after 1 min of washout. Conversely, ranolazine (100 μM) failed to inhibit non-inactivating FM NCX1.1 currents (Figure 3-5C,D). In order to gain further insights into the mechanism of inhibition, the effects of ranolazine on the NCX1.1 K264Q and F255E mutants were assessed. Currents elicited from patches containing the NCX1.1-K264Q mutants do not exhibit Na^+-dependent inactivation that is characteristic of RM-NCX1.1 currents. Ranolazine application was unable to inhibit non-inactivating currents recorded from patches containing the NCX1.1-K264Q mutant exchangers (Figure 3-6A,B). Conversely, NCX1.1-F255E currents display an accelerated inactivation process that were slowed by application of 10 μM

ranolazine (τ =519 ± 42 ms in control currents, vs. 404 ± 29 ms (n=6, P<0.05, Figure 3-6C,D).

Discussion

Late I_{Na} inhibition has been suggested to be a useful approach to reduce myocardial dysfunction associated with Na^+_i and Ca^{2+}_i overload during IR (see reviews [28-30]). Indeed, our whole-heart studies confirm that ranolazine and lidocaine restore post-ischemic function and returned diastolic Ca^{2+}_i levels to near baseline values (Figure 3-1A,B). We also observed significant improvements in coronary flow and coronary vascular conductance (CVC) when ranolazine and lidocaine were applied during the IR protocol (Figure 3-1C,D). Previous studies have also demonstrated that ranolazine and lidocaine application during ischemia also attenuates ATP depletion, intracellular acidosis and the elevation of Na^+_i [31,32]. These data support the concept that ranolazine may provide ischemic cardioprotection via late I_{Na} inhibition by reducing Na^+ loading and subsequent Ca^{2+} loading via RM NCX1.1 activity.

Previously, the sea anemone toxin, ATX-II, which induces late I_{Na} by allosteric modification of Na^+ channel gating mechanism [33,34], was utilized to investigate cardiac dysfunction in working-mode rat heart perfusions under aerobic conditions. While ATX-II is well-understood to increase Na^+_i levels, other targets can modulate Na^+_i levels as well. For instance, NKA energetically transports 3 Na^+ ions out of the cell and 2 K^+ into the cell to maintain the necessary electrochemical gradient of depolarizing Na^+ and repolarizing K^+ [35,36]. Cardiotonic steroids such as ouabain are used clinically to increase

inotropy during heart failure [37,38] via inhibition of NKA activity. Therefore, inhibition of NKA-mediated Na^+_i efflux favours increased RM NCX1.1, leading to elevations in Ca^{2+}_i and increased contractility [39-41]. Therefore, high concentrations of ouabain can be used to induce Na^+ and Ca^{2+} overload independently of late I_{Na} induction. However, the effects of ranolazine and lidocaine have not been previously examined in an *ex vivo* model of ouabain-induced Ca^{2+}_i loading. Our results demonstrate that both ranolazine and lidocaine were effective in reducing ouabain-induced dysfunction and Ca^{2+}_i loading independently of late I_{Na} inhibition. While our patch-clamp data show that elevating Na^+_i does not directly influence late I_{Na} in recombinant human $Na_v1.5$ currents (Figure 3-5A,B), recent studies suggest that ouabain may induce late I_{Na} through a Ca^{2+}/calmodulin-dependent kinase II (CaMKII) mechanism [42,43]. Yet, it is unresolved whether the development of late I_{Na} occurs downstream of intracellular Ca^{2+} elevation. Therefore, it is still conceivable that the cardioprotective effects of ranolazine and lidocaine may be mediated by late I_{Na} inhibition in the *ex vivo* whole heart ouabain model. However, the possibility remains that the observed results may be accounted for via direct inhibition of RM-NCX1.1 activity which is the downstream mediator of Ca^{2+}_i loading resulting from the induction of late I_{Na}.

To investigate this possibility further, the cellular NRVM model was used to test the hypothesis that ranolazine and lidocaine inhibit RM-NCX1.1 activity directly. In this model, 10 μM ranolazine reduced the evoked RM-NCX1.1 activity by ~24%, while 10 μM lidocaine did not have a significant effect. It

should be noted that TTX was used in these experiments to inhibit both peak and late I_{Na}. Therefore, the observed effect of ranolazine is independent of any late I_{Na} inhibition. The NCX1 inhibitor KB-R7943 [44,45] (5 μM) also decreased evoked RM-NCX1.1 activity by ~21%. These data suggest that ranolazine, but not lidocaine, directly inhibits RM NCX1.1 activity, in addition to its action on late I_{Na}.

Previous studies have characterized the pharmacological profile of ranolazine with respect to cardiac ion channels and exchangers, such as peak and late I_{Na}, inwardly rectifying K^+ channels (I_{K1}), delayed rectifier K^+ channels (I_{Kr}), transient outward K^+ current (I_{to}), voltage gated L-type Ca^{2+} channels (I_{Ca}), and NCX1.1 [13,14]. At therapeutic concentrations of 1-10 μM, ranolazine inhibited late I_{Na} more potently than any other cardiac ion channel. Interestingly, ranolazine only weakly inhibited NCX1 currents (IC_{50} = 91 μM). Yet, these currents were elicited by FM-NCX1.1 exchange activity and the effects on RM NCX1.1 activity were not characterized. In direct contrast, our findings indicate that ranolazine is a potent inhibitor of RM NCX1.1 activity (IC_{50} = ~28 nM) although it was unable to inhibit of FM NCX1.1 activity even at 100 μM (Figure 3-5).

NCX1.1 inhibitors are thought to act via binding to exchangers undergoing the I_1-inactivation process characteristic of RM (but not FM) NCX1.1 currents [46,47]. To directly assess whether the inhibitory effect of ranolazine is similarly dependent on the I_1-inactivation process, we measured the effects of ranolazine on RM-NCX1.1 currents containing either the K264Q or F255E mutations that display altered I_1-inactivation properties [48]. Ranolazine did not

inhibit the non-inactivating the K264Q mutant currents, yet increased the rate of inactivation in the F255E mutant in which the inactivation process is accelerated. These results are very similar to those obtained with recently developed NCX1 inhibitors SEA0400 and KB-R7943 [46,47]. Taken together, our findings demonstrate that ranolazine is a potent RM-selective inhibitor of NCX1.1 activity and that the mechanism of action is similar to other known NCX1 inhibitors.

Ranolazine afforded protection against IR- and ouabain-induced dysfunction in the *ex vivo* model, however lidocaine also provided a similar benefit while providing no inhibition of RM-NCX1.1 evoked Ca^{2+} loading in the NRVM cellular model. While lidocaine and ranolazine have similar late I_{Na} inhibitory potencies, ranolazine targets only the Na^+ channel open-state, whereas lidocaine targets both the open- and inactivated-states of the Na^+ channel [15,49-51]. It is unknown whether this difference separates the effects of lidocaine and ranolazine, especially in regards to late I_{Na} inhibition. Furthermore, the effects of lidocaine and KB-R7943 have been previously examined in a ouabain-induced arrhythmia model in guinea pigs [52]. As Ca^{2+} accumulates in the cardiac myocyte through RM-NCX1.1 activity, a Ca^{2+} oscillation initiated by sarcoplasmic reticulum saturation causes a transient inward (TI) current. The TI current can activate Na^+ channels, forming proarrhythmic DADs. Therefore, it is plausible that lidocaine offers its protection against ouabain-induced dysfunction and also IR injury through protecting against TI generation. Furthermore, NCX1 inhibitors may work to reduce the intracellular Ca^{2+} accumulation upstream of TI development [52]. Moreover, from a structural perspective, the ranolazine

molecule is comprised of lidocaine and trimetazidine derivative moieties. Therefore it is not surprising that ranolazine is an effective late I_{Na} inhibitor. However, our data indicate that the addition of the trimetazidine-like structure bestows potent RM-NCX1.1 inhibitory activity upon the ranolazine molecule, as lidocaine was without effect in the NRVM model used in this study. However, trimetazidine itself does not inhibit RM-NCX1.1 activity [53].

NCX1.1 contribution to cardiac injury has been well studied due to the role NCX1.1 plays in mediating Ca^{2+}_i during IR. Moreover, RM-NCX1.1 is susceptible to modification by intracellular substrates and by signaling mechanisms during IR. Reactive oxygen species, such as H_2O_2, has been shown to alter NCX1.1 function by increasing the steady-state portion of RM-NCX1.1 current, thereby augmenting Ca^{2+} influx [24,54-56]. Fatty-acyl CoA molecules, in abundance during ischemia, have also been shown to modify steady-state RM-NCX1.1 current [26,27]. Lysophosphatidylcholine (LPC) also augments RM-NCX1.1 activity [57]. Therefore, not only is late I_{Na} induced by the above mechanisms [58-62], RM-NCX1.1 is also increased, which together, would work in tandem to greatly increase Ca^{2+}_i causing myocardial injury. Therefore, ranolazine provides a valuable approach in reducing Ca^{2+}-influx during cardiac pathologies such as IR and heart failure, as block of both late I_{Na} and RM-NCX1.1 activity may synergistically reduce the intracellular Na^+ and Ca^{2+} levels restoring myocardial mechanical function.

In summary, our data demonstrate for the first time that ranolazine is a potent inhibitor of RM-NCX1.1 activity that may contribute to the

cardioprotective efficacy of this clinically-used anti-ischemic agent. Taken together, our data confirm that 1) late I_{Na} is a key contributor to Na^{+}_{i} loading and subsequent increases in RM NCX1.1 activity and 2) the protective effect of lidocaine is likely mediated via peak and late I_{Na} inhibition alone, whereas the cardioprotective effectiveness of ranolazine likely involves RM NCX1.1 inhibition in addition to late (but not peak) I_{Na} inhibition. Additional investigations are required to further dissect the relative contributions RM NCX1.1 activity and late I_{Na} in other models of IR injury, and other cardiac complications such as AF and heart failure.

Figure 3-1

Effects of ranolazine and lidocaine on IR induced alterations in diastolic Ca^{2+}_i, LV work, coronary flow, and CVC. (A) Diastolic Ca^{2+}_i, (B) LV function, (C) coronary flow, and (D) CVC, were measured during aerobic perfusion (0 to 15 min), during global, no-flow ischemia (15 to 35 min), as well as during reperfusion (35 to 65 min). Hearts were treated with vehicle (DMSO, n=14), 10μM ranolazine (n=8), or 10μM lidocaine (n=5) that was applied 5 min before onset of ischemia. Coronary flow and CVC are displayed as % aerobic baseline at 5min. $^{###}P<0.001$, $^{##}P<0.01$, $^{#}P<0.05$, ranolazine vs. vehicle; ***P<0.001, **P<0.01, *P<0.05, lidocaine vs. vehicle; at the end of reperfusion (65min), one-way ANOVA, post-hoc Tukey analysis. Ranolazine results were reproduced from [17].

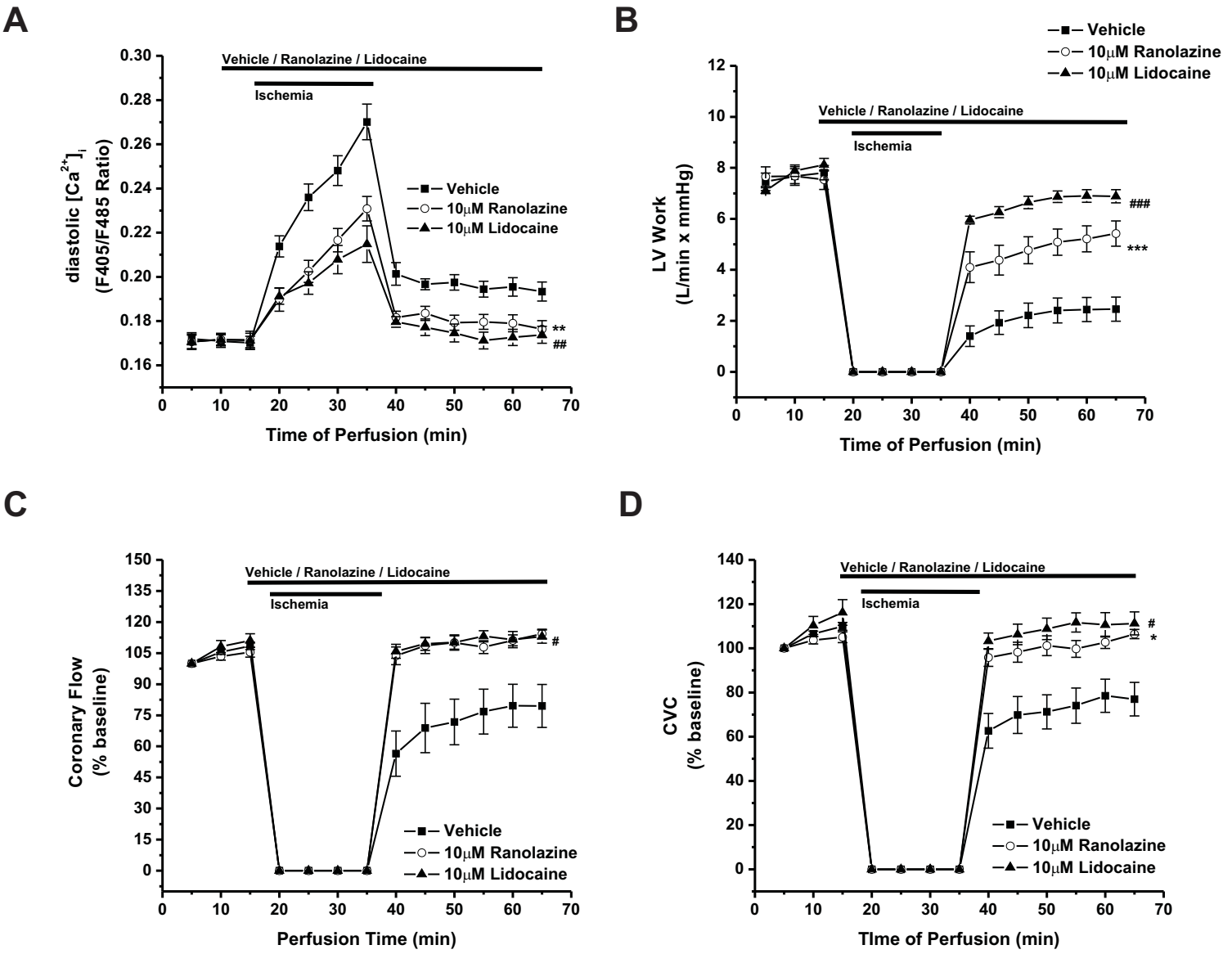
A
Vehicle / Ranolazine / Lidocaine
Ischemia
diastolic [Ca2+]i
(F405/F485 Ratio)
Vehicle
10μM Ranolazine
10μM Lidocaine
**
##
Time of Perfusion (min)
B
Vehicle
10μM Ranolazine
10μM Lidocaine
Vehicle / Ranolazine / Lidocaine
Ischemia
LV Work
(L/min x mmHg)
###
***
Time of Perfusion (min)
C
Vehicle / Ranolazine / Lidocaine
Ischemia
Coronary Flow
(% baseline)
#
Vehicle
10μM Ranolazine
10μM Lidocaine
Perfusion Time (min)
D
Vehicle / Ranolazine / Lidocaine
Ischemia
CVC
(% baseline)
#
*
Vehicle
10μM Ranolazine
10μM Lidocaine
TIme of Perfusion (min)

Figure 3-2

Effects of ranolazine and lidocaine on indices of diastolic Ca^{2+}_i and LV work during the application of 80μM ouabain. (A) Diastolic Ca^{2+}_i, and (B) LV work were observed during aerobic perfusion (0-15min) and 80μM ouabain application (15-45min). Vehicle (DMSO, n=5), 10μM ranolazine (n=5) or 10μM lidocaine (n=6) was added to the perfusion 10 min after ouabain was applied. $^{###}P<0.001$, $^{##}P<0.01$, $^{#}P<0.05$, ranolazine vs. vehicle; ***P<0.001, **P<0.01, *P<0.05, lidocaine vs. vehicle; at the end of perfusion protocol (45min), one-way ANOVA, post-hoc Tukey analysis.

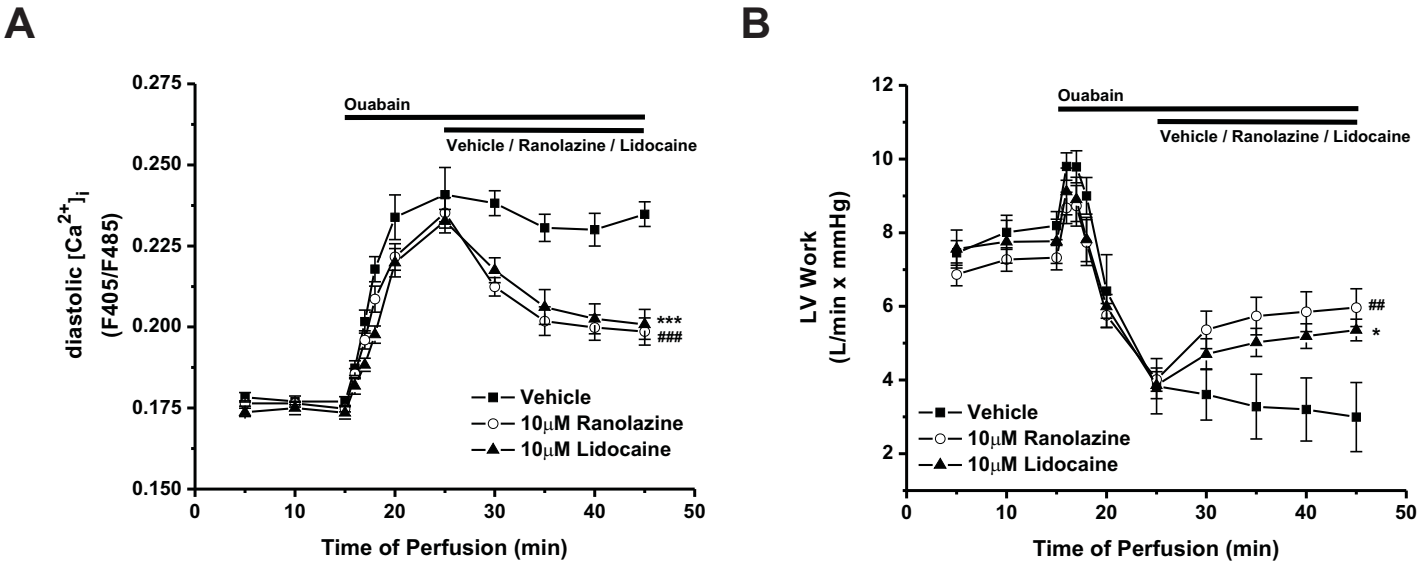
A
B
Ouabain
Vehicle / Ranolazine / Lidocaine
diastolic [Ca2+]i
(F405/F485)
Time of Perfusion (min)
Vehicle
10μM Ranolazine
10μM Lidocaine
***
###
LV Work
(L/min x mmHg)
##
*

Figure 3-3

Increased Na^+_i does not alter $Na_v1.5$ inactivation kinetics. (A) Representative human $Na_v1.5$ traces depicting the similarity of $Na_v1.5$ currents in the presence of 5mM Na^+_{pip} and 15mM Na^+_{pip}. Inset: Waveform protocol. (B) Grouped data showing 3-term exponential fits of $Na_v1.5$ τ (tau) are not different between 5mM Na^+_{pip} and 15mM Na^+_{pip}.

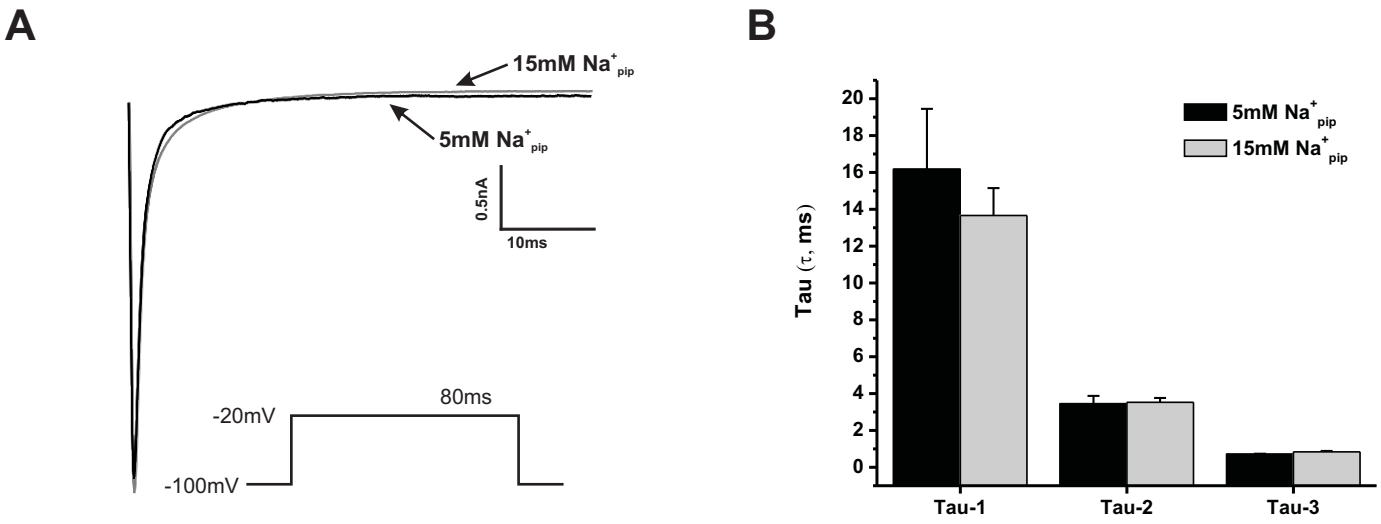
A
15mM Na+pip
5mM Na+pip
0.5nA
10ms
80ms
-20mV
-100mV
B
5mM Na+pip
15mM Na+pip
Tau (τ, ms)
20
18
16
14
12
10
8
6
4
2
0
Tau-1
Tau-2
Tau-3

Figure 3-4

Ranolazine reduces evoked RM-NCX1.1 activity in neonatal rat cardiac myocytes. (A) Sample traces of evoked RM-NCX1.1 activity Ca^{2+} imaging in the presence of 2μM TG, 5mM $NiCl_2$ or after NCRMs were treated with Ad-shRNA-NCX1 for 72 hours. (B) Grouped data exhibiting the reduction in decay rate expressed as τ (tau) in RM-NCX1.1 exchange with the addition of 2μM TG (n=9, *P<0.05 vs. control). (C) Representative Ca^{2+} imaging recordings of evoked RM-NCX1.1 exchange with the application of 10μM ranolazine, 10μM lidocaine and 5μM KB-R7943. (D) Analyzed ΔF-AUC data displaying that ranolazine and KB-R7943 reductions in RM-NCX1.1, in addition to 5mM Ni^{2+} (n=3) and shRNA-NCX1 (n=6) knockdown of RM-NCX1.1 function, while lidocaine did not have a significant effect. ***P<0.001, **P<0.01, experimental group vs. control.

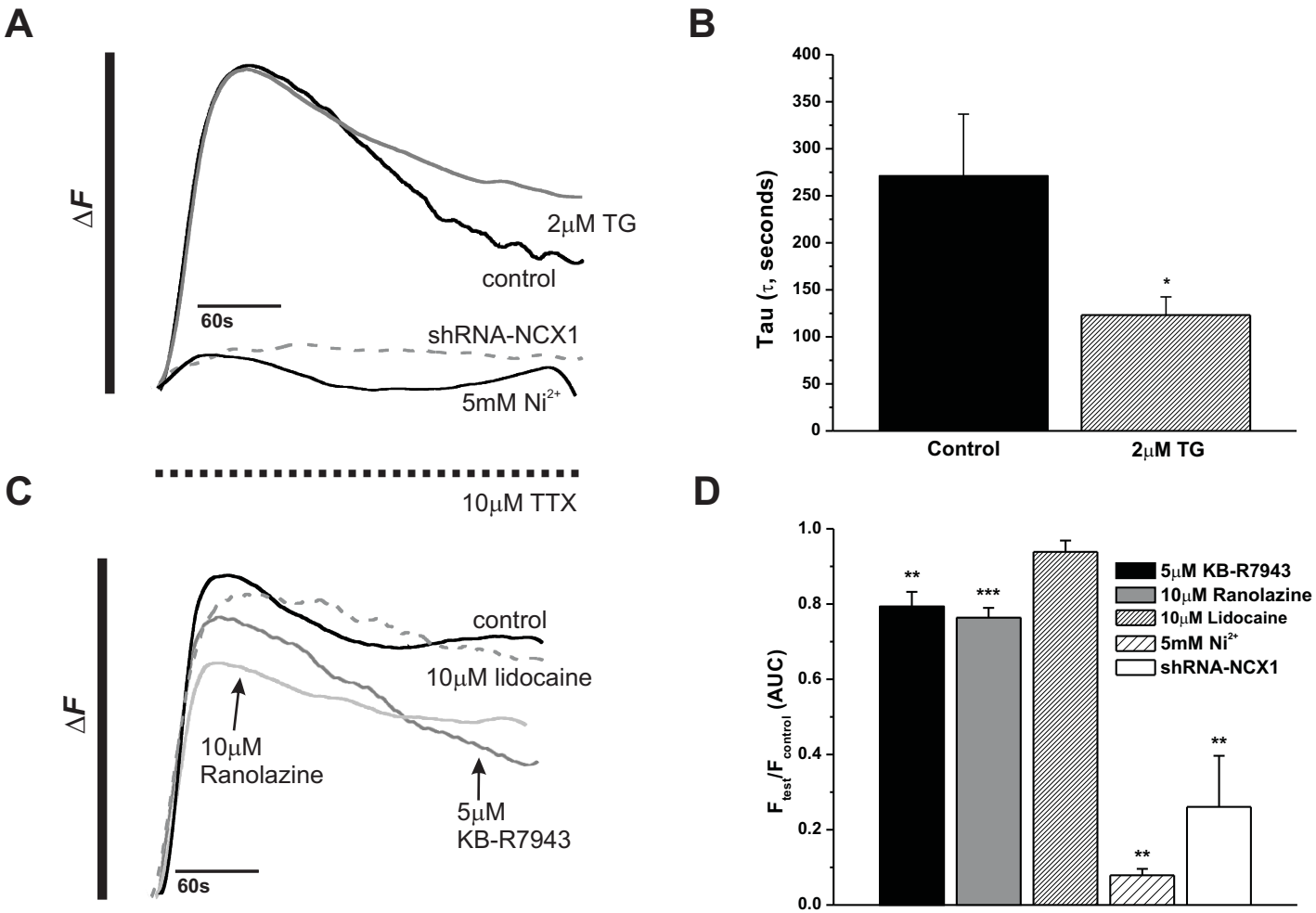
A
ΔF
2μM TG
control
60s
shRNA-NCX1
5mM Ni2+
B
Tau (τ, seconds)
400
350
300
250
200
150
100
50
0
*
Control
2μM TG
C
10μM TTX
control
10μM lidocaine
10μM
Ranolazine
5μM
KB-R7943
60s
D
F test/F control (AUC)
1.0
0.8
0.6
0.4
0.2
0.0
**
***
**
**
5μM KB-R7943
10μM Ranolazine
10μM Lidocaine
5mM Ni2+
shRNA-NCX1

Figure 3-5

Ranolazine concentration-dependently inhibits human RM NCX1.1 current from transiently expressing tsA201 cells. (A) Sample trace of RM-hNCX1.1 current exhibiting control hNCX1.1 current, inhibition with 10μM ranolazine and washout. (B) A concentration-response curve depicting that 1-10μM ranolazine, the reported therapeutic range, inhibits ~65-75% of late $I_{NCX1.1}$ current. Peak $I_{NCX1.1}$ current was unsusceptible to ranolazine inhibition. n=4-6 recordings per concentration. (C) Representative FM NCX1.1 current showing no effect with the application of 100μM ranolazine, n=6 recordings. (D) Grouped data exhibiting little effect of 100μM ranolazine on peak:peak ratio of FM hNCX1.1 current. ***P<0.001, **P<0.01, *P<0.05, ranolazine [M] vs. control.

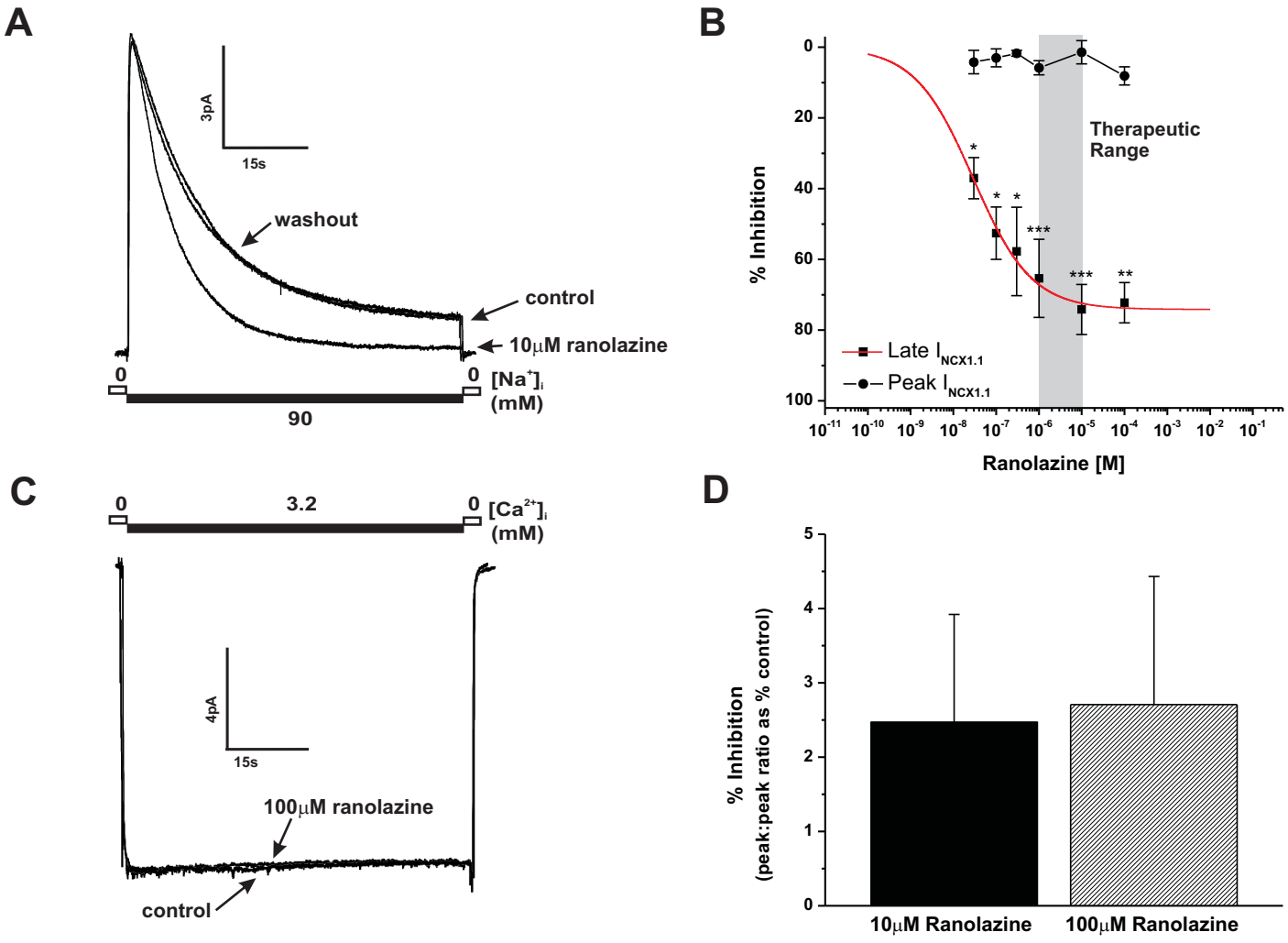
A
3pA
15s
washout
control
10μM ranolazine
0
0
[Na+]i
(mM)
90
B
% Inhibition
Therapeutic
Range
Late INCX1.1
Peak INCX1.1
Ranolazine [M]
C
0
3.2
0
[Ca2+]i
(mM)
4pA
15s
100μM ranolazine
control
D
% Inhibition
(peak:peak ratio as % control)
10μM Ranolazine
100μM Ranolazine

Figure 3-6

The effects of ranolazine on mutant NCX1.1 currents. (A) Sample recording of human NCX1.1 in the presence of 10μM ranolazine. (B) Analysis of relative peak current showing that ranolazine did not alter NCX1.1-K264Q currents, in which the I_1-dependent inactivation process is removed, in comparison to wild type (WT) hNCX1.1 current. n=4 patches. (C) Representative trace of rat NCX1.1-F255E current in which ranolazine reduced NCX1.1 current, even when the I_1-inactivation process is enhanced. (D) Grouped τ data displaying that 10μM ranolazine decreased time-to-inactivation. *P<0.05, ranolazine vs. control, n=6 recordings.

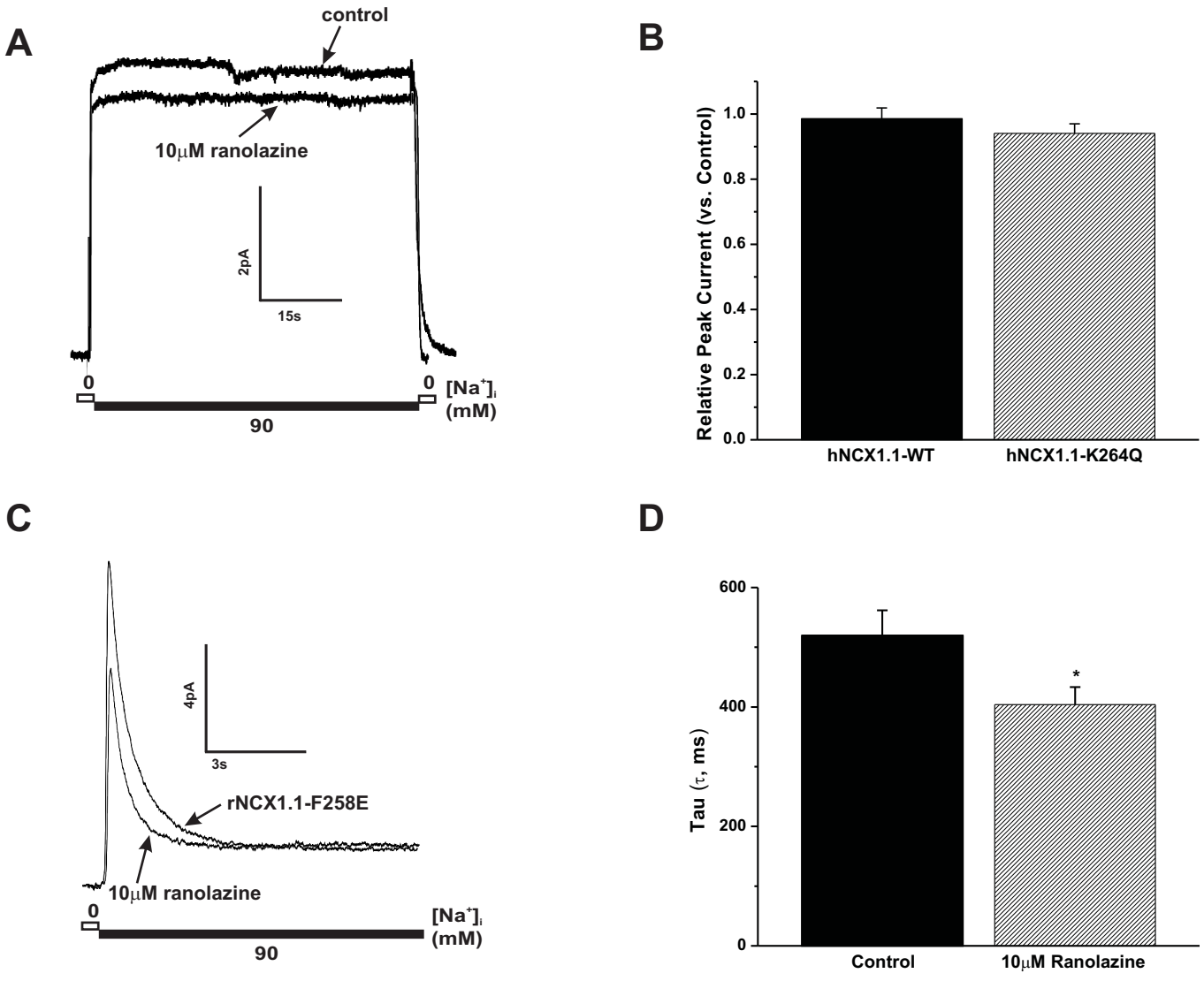
A
control
10μM ranolazine
2pA
15s
0
0
[Na+]i
(mM)
90
B
Relative Peak Current (vs. Control)
1.0
0.8
0.6
0.4
0.2
0.0
hNCX1.1-WT
hNCX1.1-K264Q
C
4pA
3s
rNCX1.1-F258E
10μM ranolazine
0
[Na+]i
(mM)
90
D
Tau (τ, ms)
600
400
200
0
*
Control
10μM Ranolazine

References

1. Barry WH. Mechanisms of myocardial cell injury during ischemia and reperfusion. J.Card.Surg. 1987 Sep;2(3):375-383.

2. Piper HM, Meuter K, Schafer C. Cellular mechanisms of ischemia-reperfusion injury. Ann.Thorac.Surg. 2003 Feb;75(2):S644-8.

3. Silverman HS, Stern MD. Ionic basis of ischaemic cardiac injury: insights from cellular studies. Cardiovasc.Res. 1994 May;28(5):581-597.

4. Tani M. Mechanisms of Ca2+ overload in reperfused ischemic myocardium. Annu.Rev.Physiol. 1990;52:543-559.

5. Ferrari R, Ceconi C, Curello S, Alfieri O, Visioli O. Myocardial damage during ischaemia and reperfusion. Eur.Heart J. 1993 Nov;14 Suppl G:25-30.

6. Eigel BN, Hadley RW. Contribution of the Na(+) channel and Na(+)/H(+) exchanger to the anoxic rise of [Na(+)] in ventricular myocytes. Am.J.Physiol. 1999 Nov;277(5 Pt 2):H1817-22.

7. Fliegel L. Regulation of the Na(+)/H(+) exchanger in the healthy and diseased myocardium. Expert Opin.Ther.Targets 2009 Jan;13(1):55-68.

8. Noble D, Noble PJ. Late sodium current in the pathophysiology of cardiovascular disease: consequences of sodium-calcium overload. Heart 2006 Jul;92 Suppl 4:iv1-iv5.

9. Ju YK, Saint DA, Gage PW. Hypoxia increases persistent sodium current in rat ventricular myocytes. J.Physiol. 1996 Dec 1;497 (Pt 2)(Pt 2):337-347.

10. Saint DA. The cardiac persistent sodium current: an appealing therapeutic target? Br.J.Pharmacol. 2008 Mar;153(6):1133-1142.

11. Lee C, Dhalla NS, Hryshko LV. Therapeutic potential of novel Na+-Ca2+ exchange inhibitors in attenuating ischemia-reperfusion injury. Can.J.Cardiol. 2005 May 1;21(6):509-516.

12. Karmazyn M, Sostaric JV, Gan XT. The myocardial Na+/H+ exchanger: a potential therapeutic target for the prevention of myocardial ischaemic and reperfusion injury and attenuation of postinfarction heart failure. Drugs 2001;61(3):375-389.

13. Antzelevitch C, Belardinelli L, Zygmunt AC, Burashnikov A, Di Diego JM, Fish JM, et al. Electrophysiological effects of ranolazine, a novel antianginal agent with antiarrhythmic properties. Circulation 2004 Aug 24;110(8):904-910.

14. Antzelevitch C, Belardinelli L, Wu L, Fraser H, Zygmunt AC, Burashnikov A, et al. Electrophysiologic properties and antiarrhythmic actions of a novel antianginal agent. J.Cardiovasc.Pharmacol.Ther. 2004 Sep;9 Suppl 1:S65-83.

15. Sossalla S, Wagner S, Rasenack EC, Ruff H, Weber SL, Schondube FA, et al. Ranolazine improves diastolic dysfunction in isolated myocardium from failing human hearts--role of late sodium current and intracellular ion accumulation. J.Mol.Cell.Cardiol. 2008 Jul;45(1):32-43.

16. Wasserstrom JA, Sharma R, O'Toole MJ, Zheng J, Kelly JE, Shryock J, et al. Ranolazine antagonizes the effects of increased late sodium current on intracellular calcium cycling in rat isolated intact heart. J.Pharmacol.Exp.Ther. 2009 Nov;331(2):382-391.

17. Fraser H, Belardinelli L, Wang L, Light PE, McVeigh JJ, Clanachan AS. Ranolazine decreases diastolic calcium accumulation caused by ATX-II or ischemia in rat hearts. J.Mol.Cell.Cardiol. 2006 Dec;41(6):1031-1038.

18. Wang L, Lopaschuk GD, Clanachan AS. H(2)O(2)-induced left ventricular dysfunction in isolated working rat hearts is independent of calcium accumulation. J.Mol.Cell.Cardiol. 2008 Dec;45(6):787-795.

19. Neely JR, Liebermeister H, Morgan HE. Effect of pressure development on membrane transport of glucose in isolated rat heart. Am.J.Physiol. 1967 Apr;212(4):815-822.

20. Wang L, Cherednichenko G, Hernandez L, Halow J, Camacho SA, Figueredo V, et al. Preconditioning limits mitochondrial Ca(2+) during ischemia in rat hearts: role of K(ATP) channels. Am.J.Physiol.Heart Circ.Physiol. 2001 May;280(5):H2321-8.

21. Wallace CH, Baczko I, Jones L, Fercho M, Light PE. Inhibition of cardiac voltage-gated sodium channels by grape polyphenols. Br.J.Pharmacol. 2006 Nov;149(6):657-665.

22. Kovacic S, Soltys CL, Barr AJ, Shiojima I, Walsh K, Dyck JR. Akt activity negatively regulates phosphorylation of AMP-activated protein kinase in the heart. J.Biol.Chem. 2003 Oct 10;278(41):39422-39427.

23. Eigel BN, Hadley RW. Antisense inhibition of Na+/Ca2+ exchange during anoxia/reoxygenation in ventricular myocytes. Am.J.Physiol.Heart Circ.Physiol. 2001 Nov;281(5):H2184-90.

24. Soliman D, Hamming KS, Matemisz LC, Light PE. Reactive oxygen species directly modify sodium-calcium exchanger activity in a splice variant-dependent manner. J.Mol.Cell.Cardiol. 2009 Nov;47(5):595-602.

25. Hurtado C, Ander BP, Maddaford TG, Lukas A, Hryshko LV, Pierce GN. Adenovirally delivered shRNA strongly inhibits Na+-Ca2+ exchanger expression but does not prevent contraction of neonatal cardiomyocytes. J.Mol.Cell.Cardiol. 2005 Apr;38(4):647-654.

26. Hamming KS, Riedel MJ, Soliman D, Matemisz LC, Webster NJ, Searle GJ, et al. Splice variant-dependent regulation of beta-cell sodium-calcium exchange by acyl-coenzyme As. Mol.Endocrinol. 2008 Oct;22(10):2293-2306.

27. Riedel MJ, Baczko I, Searle GJ, Webster N, Fercho M, Jones L, et al. Metabolic regulation of sodium-calcium exchange by intracellular acyl CoAs. EMBO J. 2006 Oct 4;25(19):4605-4614.

28. Maier LS. A novel mechanism for the treatment of angina, arrhythmias, and diastolic dysfunction: inhibition of late I(Na) using ranolazine. J.Cardiovasc.Pharmacol. 2009 Oct;54(4):279-286.

29. Shryock JC, Belardinelli L. Inhibition of late sodium current to reduce electrical and mechanical dysfunction of ischaemic myocardium. Br.J.Pharmacol. 2008 Mar;153(6):1128-1132.

30. Stone PH. Ranolazine: new paradigm for management of myocardial ischemia, myocardial dysfunction, and arrhythmias. Cardiol.Clin. 2008 Nov;26(4):603-614.

31. Butwell NB, Ramasamy R, Lazar I, Sherry AD, Malloy CR. Effect of lidocaine on contracture, intracellular sodium, and pH in ischemic rat hearts. Am.J.Physiol. 1993 Jun;264(6 Pt 2):H1884-9.

32. Belardinelli L, Shryock JC, Fraser H. Inhibition of the late sodium current as a potential cardioprotective principle: effects of the late sodium current inhibitor ranolazine. Heart 2006 Jul;92 Suppl 4:iv6-iv14.

33. Catterall WA, Cestele S, Yarov-Yarovoy V, Yu FH, Konoki K, Scheuer T. Voltage-gated ion channels and gating modifier toxins. Toxicon 2007 Feb;49(2):124-141.

34. Spencer CI. Actions of ATX-II and other gating-modifiers on Na(+) currents in HEK-293 cells expressing WT and DeltaKPQ hNa(V) 1.5 Na(+) channels. Toxicon 2009 Jan;53(1):78-89.

35. Bers DM, Barry WH, Despa S. Intracellular Na+ regulation in cardiac myocytes. Cardiovasc.Res. 2003 Mar 15;57(4):897-912.

36. Despa S, Bers DM. Na/K pump current and [Na](i) in rabbit ventricular myocytes: local [Na](i) depletion and Na buffering. Biophys.J. 2003 Jun;84(6):4157-4166.

37. Schoner W, Scheiner-Bobis G. Endogenous and exogenous cardiac glycosides and their mechanisms of action. Am.J.Cardiovasc.Drugs 2007;7(3):173-189.

38. Kjeldsen K, Bundgaard H. Myocardial Na,K-ATPase and digoxin therapy in human heart failure. Ann.N.Y.Acad.Sci. 2003 Apr;986:702-707.

39. Saini HK, Dhalla NS. Sarcolemmal cation channels and exchangers modify the increase in intracellular calcium in cardiomyocytes on inhibiting Na+-K+-ATPase. Am.J.Physiol.Heart Circ.Physiol. 2007 Jul;293(1):H169-81.

40. Altamirano J, Li Y, DeSantiago J, Piacentino V,3rd, Houser SR, Bers DM. The inotropic effect of cardioactive glycosides in ventricular myocytes requires Na+-Ca2+ exchanger function. J.Physiol. 2006 Sep 15;575(Pt 3):845-854.

41. Nishio M, Ruch SW, Wasserstrom JA. Positive inotropic effects of ouabain in isolated cat ventricular myocytes in sodium-free conditions. Am.J.Physiol.Heart Circ.Physiol. 2002 Nov;283(5):H2045-53.

42. Maltsev VA, Reznikov V, Undrovinas NA, Sabbah HN, Undrovinas A. Modulation of late sodium current by Ca2+, calmodulin, and CaMKII in normal and failing dog cardiomyocytes: similarities and differences. Am.J.Physiol.Heart Circ.Physiol. 2008 Apr;294(4):H1597-608.

43. Song Y, Shryock JC, Xia S, Belardinelli L. Ouabain increases late sodium current by a Ca2+/calmodulin kinase-mediated mechanism. JACC 2009;55(10, Supplement 1):A2.E17.

44. Iwamoto T, Kita S. Development and application of Na+/Ca2+ exchange inhibitors. Mol.Cell.Biochem. 2004 Apr;259(1-2):157-161.

45. Iwamoto T. Forefront of Na+/Ca2+ exchanger studies: molecular pharmacology of Na+/Ca2+ exchange inhibitors. J.Pharmacol.Sci. 2004 Sep;96(1):27-32.

46. Bouchard R, Omelchenko A, Le HD, Choptiany P, Matsuda T, Baba A, et al. Effects of SEA0400 on mutant NCX1.1 Na+-Ca2+ exchangers with altered ionic regulation. Mol.Pharmacol. 2004 Mar;65(3):802-810.

47. Elias CL, Lukas A, Shurraw S, Scott J, Omelchenko A, Gross GJ, et al. Inhibition of Na+/Ca2+ exchange by KB-R7943: transport mode selectivity and antiarrhythmic consequences. Am.J.Physiol.Heart Circ.Physiol. 2001 Sep;281(3):H1334-45.

48. Matsuoka S, Nicoll DA, He Z, Philipson KD. Regulation of cardiac Na(+)-Ca2+ exchanger by the endogenous XIP region. J.Gen.Physiol. 1997 Feb;109(2):273-286.

49. Fedida D, Orth PM, Hesketh JC, Ezrin AM. The role of late I and antiarrhythmic drugs in EAD formation and termination in Purkinje fibers. J.Cardiovasc.Electrophysiol. 2006 May;17 Suppl 1:S71-S78.

50. Dumaine R, Kirsch GE. Mechanism of lidocaine block of late current in long Q-T mutant Na+ channels. Am.J.Physiol. 1998 Feb;274(2 Pt 2):H477-87.

51. Wang GK, Calderon J, Wang SY. State- and use-dependent block of muscle Nav1.4 and neuronal Nav1.7 voltage-gated Na+ channel isoforms by ranolazine. Mol.Pharmacol. 2008 Mar;73(3):940-948.

52. Watano T, Harada Y, Harada K, Nishimura N. Effect of Na+/Ca2+ exchange inhibitor, KB-R7943 on ouabain-induced arrhythmias in guinea-pigs. Br.J.Pharmacol. 1999 Aug;127(8):1846-1850.

53. Renaud JF. Internal pH, Na+, and Ca2+ regulation by trimetazidine during cardiac cell acidosis. Cardiovasc.Drugs Ther. 1988 Mar;1(6):677-686.

54. Eigel BN, Gursahani H, Hadley RW. ROS are required for rapid reactivation of Na+/Ca2+ exchanger in hypoxic reoxygenated guinea pig ventricular myocytes. Am.J.Physiol.Heart Circ.Physiol. 2004 Mar;286(3):H955-63.

55. Goldhaber JI. Free radicals enhance Na+/Ca2+ exchange in ventricular myocytes. Am.J.Physiol. 1996 Sep;271(3 Pt 2):H823-33.

56. Hinata M, Matsuoka I, Iwamoto T, Watanabe Y, Kimura J. Mechanism of Na+/Ca2+ exchanger activation by hydrogen peroxide in guinea-pig ventricular myocytes. J.Pharmacol.Sci. 2007 Mar;103(3):283-292.

57. Yu L, Netticadan T, Xu YJ, Panagia V, Dhalla NS. Mechanisms of lysophosphatidylcholine-induced increase in intracellular calcium in rat cardiomyocytes. J.Pharmacol.Exp.Ther. 1998 Jul;286(1):1-8.

58. Zhou H, Ma JH, Zhang PH, Luo AT. Vitamin C pretreatment attenuates hypoxia-induced disturbance of sodium currents in guinea pig ventricular myocytes. J.Membr.Biol. 2006;211(2):81-87.

59. Ahern GP, Hsu SF, Klyachko VA, Jackson MB. Induction of persistent sodium current by exogenous and endogenous nitric oxide. J.Biol.Chem. 2000 Sep 15;275(37):28810-28815.

60. Undrovinas AI, Fleidervish IA, Makielski JC. Inward sodium current at resting potentials in single cardiac myocytes induced by the ischemic metabolite lysophosphatidylcholine. Circ.Res. 1992 Nov;71(5):1231-1241.

61. Ward CA, Giles WR. Ionic mechanism of the effects of hydrogen peroxide in rat ventricular myocytes. J.Physiol. 1997 May 1;500 (Pt 3)(Pt 3):631-642.

62. Wu J, Corr PB. Palmitoyl carnitine modifies sodium currents and induces transient inward current in ventricular myocytes. Am.J.Physiol. 1994 Mar;266(3 Pt 2):H1034-46.

Chapter 4

Co-expression of the Type-2 Diabetes Susceptibility Gene Variants *KCNJ11* E23K and *ABCC8* S1369A Alter the ATP and Sulfonylurea Sensitivities of the ATP-Sensitive Potassium Channel.

A version of this chapter has been published under the following citation:

*Hamming K.S.C., *Soliman D., Matemisz L.C., Niazi O., Lang V., Gloyn G.L., Light P.E. (2009). Co-expression of the Type-2 Diabetes Susceptibility Gene Variants KCNJ11 E23K and ABCC8 S1369A Alter the ATP and Sulfonylurea Sensitivities of the ATP-Sensitive K^+ Channel. Diabetes 58, 2419-2424. (*denotes equal contributions).

Introduction

The ATP-sensitive K^+ (K_{ATP}) channel is a central player in coupling metabolism to excitability in a variety of tissues such as the heart, vasculature and the central nervous system [1,2]. Also expressed in the β-cells of the endocrine pancreas, K_{ATP} channels are required for the physiological regulation of insulin secretion [3-5]. Insulin release is primarily stimulated by glucose metabolism, which leads to increases in cytosolic ATP levels, which results in the closure of K_{ATP} channels. Reduced K^+ efflux acts to depolarize the β-cell membrane causing L-type Ca^{2+} channel activation, which increases intracellular Ca^{2+} levels, triggering insulin granule exocytosis [4]. Therefore, K_{ATP} channels serve to transduce glucose-mediated metabolic signals into changes in membrane excitability, which works to regulate insulin secretion.

Pancreatic K_{ATP} channels are composed of the pore-forming subunit $K_{IR}6.2$ and a regulatory subunit SUR1, encoded by the *KCNJ11* and *ABCC8* genes, respectively [4,5]. Monogenic mutations discovered in either *KCNJ11* or ABCC8 highlight the necessary role of K_{ATP} channel function for insulin release, as these mutations cause neonatal diabetes or hyperinsulinism of infancy. For instance, $K_{IR}6.2$ mutations Q52R and V59G cause severe developmental delay neonatal diabetes, through stabilizing the open-state of the K_{ATP} channel, indirectly reducing ATP sensitivity [6,7]. Furthermore, recently examined mutation R1380C/L in SUR1 also causes neonatal diabetes through increasing the intrinsic MgATP catalysis in SUR1, elevating MgADP formation, which acts to relieve ATP-inhibition of the K_{ATP} channel [8,9].

Unlike monogenic mutations, single nucleotide polymorphisms (SNPs) have been found to increase risk of type-2 diabetes development. One of the first reproducibly associated susceptibility signals identified was the common E23K (rs5219) variant of *KCNJ11* [10,11]. Functional studies show that E23K slightly up-regulates K_{ATP} channel activity, which effectively reduces the responsiveness of ATP, therefore slowing insulin release in patients with normal glucose regulation [12]. Furthermore, detailed mapping of the 11p15.1 chromosomal locus containing neighbouring *KCNJ11* and *ABCC8* genes revealed that SNP rs757110, a serine to alanine mis-sense mutation at position 1369 in SUR1, showed strong linkage disequilibirum with E23K [13]. This was especially evident in African-American and Asian study panels. Therefore, individuals who carried the K risk allele of the E23K SNP in all likelihood carry the A allele of the S1369A SNP, forming the E23K-S1369A haplotype. However, the genetic evidence was not sufficient to determine which allele at 1369 is the causal variant [13].

Interestingly, a recent study using cohorts of ~1300 Chinese patients found that gliclaizide, a second-generation sulfonylurea drug used in the treatment of type-2 diabetes, was more effective at lowering blood glucose levels in patients possessing the S1369A variant [14]. Taken together, these facts highlight the need to perform functional studies to ascertain the molecular mechanism for 1) increased risk of type-2 diabetes development and 2) augmented sulfonylurea efficacy of the K_{ATP} channel E23K-S1369A haplotype. As the E23K-S1369A variant increases type-2 diabetes risk and sulfonylurea efficacy, we utilized

electrophysiological techniques to study the functional properties and SU pharmacology of the E23K-S1369A haplotype K_{ATP} channel.

Materials & Methods

Molecular Biology

The human K_{ATP} channel $K_{IR}6.2$ and SUR1 subunit clones were kindly provided by J. Byran (Pacific Northwest Diabetes Research Institute, Seattle, WA) The E23K and S1369A variants were introduced into *KCNJ11* and *ABCC8* cDNAs respectively using site-directed mutatagenesis using the protocol and reagents outlined in the Quikchange Site-Directed Mutagenesis Kit (Stratagene, La Jolla, CA).

Cell Culture & Transfection

tsA201 cells, (an SV40-transformed version of the HEK293 human embryonic kidney cell line) were cultured in Dulbecco's modified Eagle's media supplemented with 25mM glucose, 2mM L-glutamine, 10% FBS, and 0.1% penicillin/streptomycin. Cells were housed in 37ºC incubator and gased with 5% CO_2. Cells when reaching 50-70% confluency on 35mm dishes tsA201 cells were transfected with the wild-type and polymorphic *KCNJ11* and *ABCC8* clones (E23-S1369 vs. K23-A1369, respectively) using the calcium phosphate technique as previously described [15]. Positively transfected cells were identified using fluorescent optics in combination with coexpression of green fluorescent protein plasmid (Life Technologies, Gaithersburg, MD). Macroscopic recordings were made from cells 48-72 hours post-transfection, while single-channel recordings were made from cells 24-48 hours after transfection.

Electrophysiology

The inside-out excised patch clamp technique was used to measure both macroscopic and single-channel K_{ATP} channel currents from transiently expressing tsA201 cells. Macroscopic recordings were performed using patch pipettes pulled from borosilicate glass (G85150T; Warner Instrument, Hamdem CT) to yield pipettes with resistances between 600-1200KΩ, when back-filled. Patch pipettes used for single-channel recordings were pulled from borosilicate glass (PG52151-4; World Precision Instruments, Sarasota, FL), using the Sutter P87 micropipette puller (Sutter Instrument Company, Novato, CA), yielding pipette resistances of 8-9MΩ, when filled with pipette solution. Pipettes were back-filled with the following solution (in mM): 134 KCl, 10 HEPES, 1.4$MgCl_2$, 1 EGTA, 6 KOH, and 10 glucose. Solution pH was adjusted to 7.4 with KOH. Once a GΩ seal was formed, the membrane patch was excised from the cell and positioned in the path of a multi-channel perfusion pipette. The intracellular side of the membrane patch was exposed to test solutions (same as pipette solution, pH 7.2 adjusted with KOH) through the perfusion pipette (time to change solution at the tip of the recording pipette was < 2s). Membranes were held at +60mV in both macroscopic and single-channel patch clamp protocols. All patch clamp experiments were conducted at room temperature (22 ± 1ºC). An Axopatch 200B patch-clamp amplifier and pClamp 10.0 software (Molecular Devices, Silicon Valley, CA) were used for data acquisition and analysis, respectively. Macroscopic recordings were sampled at 2kHz and low-pass filtered at 100Hz.

Single-channel recordings were sampled at 5kHz and filtered at 2kHz as previously described [16].

Experimental Compounds

MgATP and MgADP (Sigma, Oakville, ON) were prepared as 10mM stocks in ddH_2O immediately prior to use. Glibenclamide, gliclazide and repaglinide (Sigma, Oakville, ON) were prepared as 10mM stocks in DMSO and stored at -20ºC until use. DMSO concentration did not exceed 0.1% v/v in all experimental solutions.

Data Analysis & Statistics

Recombinant macroscopic K_{ATP} currents were normalized and expressed as changes in current relative to control (i.e. normalized K_{ATP} channel current = $I_{test}/I_{control}$). Single-channel open probability (P_o) analysis was conducted using Clampfit v10.0 Event Detection features. Unitary current conductance (I_{UCA}) was computed using the non-stationary fluctuation analysis function in Clampfit v10.0. Statistical significance was assessed using the unpaired Student's t-test or one-way ANOVA with a Bonnferoni post hoc test, where appropriate. $P<0.05$ was considered statistically significant. Data is expressed as mean ± s.e.

Results

A1369 confers reduced MgATP sensitivity in recombinant human K_{ATP} channels.

In order to understand the nucleotide regulation of K23-A1369 variant K_{ATP} channel activity, the MgATP and MgADP sensitivities of recombinant human K_{ATP} channel containing either the K23-A1369 or the E23-S1369 variant

were investigated. We found that the K23-A1369 variant had a significantly reduced MgATP sensitivity of the K_{ATP} channel, as determined by the half-maximal inhibitory concentration (IC_{50}) derived from a concentration-inhibition curve, when compared to E23-S1369 (IC_{50} = 8.0 ± 0.8μM vs. 2.5 ± 0.2μM; K23-A1369 vs. E23-S1369; $P<0.05$, Figure 4-1A,B). As it is also reported that K23 alone can bestow a reduction in MgATP sensitivity [12,17], it was necessary to determine whether K23 or A1369 variants accounted for the reduced MgATP sensitivity. Quasi-heterologous K_{ATP} expressing either E23-A1369 or K23-S1369 were examined in order to ascertain whether A1369 or K23 bestow the changes in MgATP sensitivity. These results indicate that the *ABCC8* A1369 variant, not *KCNJ11* K23 variant, confers the diminished MgATP sensitivity to the K_{ATP} channel complex, as the E23-A1369 combination possesses an IC_{50} of 8.2 ± 1.6μM, versus the K23-S1369 combination, having an IC_{50} of 3.2 ± 0.3μM ($P<0.05$, Figure 4-1C,D).

K23-A1369 K_{ATP} channels are more active at physiological MgATP levels.

Extrapolation of the MgATP concentration-inhibition curve (Figure 4-1B, inset) to physiological millimolar intracellular MgATP levels (1-5mM) predicted that the shift in K23-A1369 MgATP IC_{50} may be due to remaining slightly more active when compared to E23-S1369. To investigate this prediction, single-channel patch clamping of recombinant human K_{ATP} channels was employed to determine the difference in K_{ATP} channel activity between E23-S1369 and K23-A1369 (Figure 4-2). We observed that there were no differences in open probability (P_o) of E23-S1369 and K23-A1369 K_{ATP} channels in the absence of

MgATP (0mM) (P_o = 0.12 ± 0.02, E23-S1369; 0.15 ± 0.03, K23-A1369; P>0.05, Figure 4-2C). However, significant differences in P_o were apparent in the K_{ATP} variants in the presence of 1mM MgATP (P_o = 0.00057 ± 0.00021, E23-S1369; 0.0028 ± 0.0008, K23-A1369; P<0.05, Figure 4-2D). Furthermore, unitary current amplitude of the K_{ATP} channel variants was also not different, signifying that the variant K23-A1369 does not affect K^+ conductance intrinsically (2.96 ± 0.18 pA vs. 3.27 ± 0.12 pA, n=3-6 recordings, P>0.05, Figure 4-2E). These results suggest that the K23-A1369 variant K_{ATP} is more active at resting MgATP levels, which slows depolarization of the β-cell membrane, impairing insulin secretion.

MgADP sensitivity is unaltered between K_{ATP} channel variants E23-S1369 and K23-A1369.

The intracellular ATP-to-ADP ratio is a major determinant of K_{ATP} channel activity because MgADP antagonizes the inhibitory effects of ATP and rare monogenic mutations in *ABCC8* that reduce MgADP antagonism are found to decrease channel activity and cause hyperinsulinism [18]. Accordingly, the stimulatory effects of varying concentrations of MgADP were tested in the presence of 0.1mM MgATP (Figure 4-3A,B,C). No significant differences were determined between the E23-S1369 and K23-A1369 K_{ATP} channel variants when a concentration-inhibition curves were constructed and IC_{50}s compared (IC_{50} = 14.3 ± 0.1 μM, E23-S1369; 13.8 ± 0.2μM, K23-A1369, Figure 4-3B).

The effects of sulfonylureas on the K_{ATP} channel: sites of action.

Sulfonylureas such as tolbutamide, gliclazide and glibenclamide, and benzamido derivatives (glinides) such as meglitinide and repaglinide, inhibit K_{ATP}

channel current by binding to high affinity sites located at the SUR1 subunit of the K_{ATP} channel complex [19-23]. Moreover, sulfonylureas and glinides can be grouped according to their binding at the A, B, or AB sites in the K_{ATP} channel complex (Figure 4-4A) [24-27]. The A-site is located close to SUR1 transmembrane segments 14-16, and the S1237Y mutation in this region (Figure 4-4) abolishes A-site drug inhibition [28]. Two regions of the K_{ATP} channel contribute to the B-site: the intracellular loop between SUR1 transmembrane segments 5 and 6 and the NH_2-terminus of $K_{IR}6.2$ (Figure 4-4A) [24]. Figure 4-4B depicts the structures of the glinide repaglinide (B-site) and the sulfonylureas glibenclamide (AB-site) and gliclazide (A-site). The SUR1 residue S1369 is in close proximity to the A-site (Figure 4-4A).

Gliclazide potently inhibits the K23-A1369 variant of the K_{ATP} channel versus glibenclamide and repaglinide.

The K_{ATP} channel is the molecular target for sulfonylurea and glinide drugs that are commonly used to stimulate insulin secretion in type-2 diabetes. Interestingly, recent clinical data suggests that diabetic patients who are homozygous for the A1369 risk allele (A/A) are more responsive to gliclazide therapy [14]. However, it is unknown whether this is due to a direct effect on the K_{ATP} channel because the inhibitory profile of gliclazide and other drugs on the K23-A1369 variant K_{ATP} channel has not been determined. As noted above, A1369 lies near the A-site, therefore A1369 variant may contribute to altered K_{ATP} channel sensitivity to A-site drugs such as gliclazide. Construction of concentration-inhibition curves revealed that the K23-A1369 variant was ~3.5-

fold more sensitive to gliclazide inhibition than the E23-S1369 variant (IC_{50} 52.7 ± 11.1nM vs. 188.7 ± 32.6nM, respectively; Figure 4-5E). Because the K23-A1369 K_{ATP} channel variant may also alter the potency of other sulfonylurea subgroups, the effects of glibenclamide (AB-site) and repaglinide (B-site) were examined. In direct contrast to the observed effects of gliclazide, no significant differences in either glibenclamide (3nM; % Inhibition = 64.6 ± 4.6% E23-S1369; 54.1 ± 5.5% K23-A1369; P>0.05) or repaglinide (10nM; % Inhibition = 59.9 ± 6.4% E23-S1369; 48.3 ± 4.9% K23-A1369; P>0.05) were found between the K23-A1369 and E23-S1369 variant K_{ATP} channels (Figure 4-5D). Furthermore, it is possible that gliclazide inhibition may be affected by intracellular MgADP. In the presence of 0.1mM MgATP and 0.1mM MgADP, gliclazide still elicited a substantially greater inhibition of the K23-A1369 variant than the E23-S1369 variant (Figure 4-6C).

Gliclazide sensitivity is conferred by residue A1369 in SUR1.

The data presented indicate that the K23-A1369 variant K_{ATP} channel is more sensitive to inhibition by gliclazide but not glibenclamide or repaglinide. However, the relative individual contributions of the *ABCC8* A1369 or *KCNJ11* K23 variants to gliclazide sensitivity have not been determined. Therefore, gliclazide inhibition was measured in quasi-heterologous K_{ATP} channels containing either the E23-A1369 or K23-S1369 variant combinations. E23-A1369 K_{ATP} channels displayed a significantly greater gliclazide (300nM) inhibition than K23-S1369 K_{ATP} channels ($I_{test}/I_{control}$ = 0.313 ± 0.038, E23-**A**1369 vs. 0.473 ± 0.039, K23-**S**1369, P<0.05) and was similar in magnitude to that observed in the

increased diabetes risk for the K23-A1369 variant K_{ATP} channel ($I_{test}/I_{control}$ = 0.307 ± 0.043, K23-A1369; Figure 4-6D,E,F). Results from these experiments indicate that the enhanced gliclazide sensitivity in the K23-A1369 K_{ATP} channel haplotype is conferred by the *ABCC8* A1369 variant and not the *KCNJ11* K23 variant.

Discussion

Previous studies have investigated the properties of the *KCNJ11* K23 variant of the K_{ATP} channel [17,29,30], although more than 95% of people homozygous for K23 are also homozygous for A1369 [13]. Therefore, this study is the first to document the properties and pharmacology of K_{ATP} channels containing both the K23 and A1369 risk alleles. This study also reveals novel differences in the MgATP and sulfonylurea sensitivity of the variant K_{ATP} channel.

With respect to MgATP sensitivity, the moderate rightward shift in IC_{50} for MgATP inhibition seen in the K23-A1369 variant results in an increased basal K_{ATP} channel activity at physiological MgATP levels. In direct contrast to the rare monogenic K_{ATP} channel mutations that cause neonatal diabetes by drastically decreasing ATP inhibition at the level of $K_{IR}6.2$, a modest up-regulation in K23-A1369 variant K_{ATP} channel activity may predispose to type-2 diabetes. This is in fact the case when considering the *KCNJ11* variant K23 alone. It is hypothesized that, given the high levels of K_{ATP} expression in pancreatic β-cells, less than 1% in K_{ATP} channel activity could significantly affect insulin secretion, making the subtle effects of the E23K substitution physiologically relevant, especially in

concert with other factors [12]. Indeed, we have previously shown that the K23 variant increases the sensitivity of the K_{ATP} channel to activation by intracellular acyl CoAs [15,30]. Moreover, we find in this study, that although the K23-S1369 possessed a slight shift in MgATP (3.2 ± 0.3μM vs. 2.5 ± 0.2μM for E23-S1369, $P<0.05$), corroborating previous reports [12,17], the A1369 variant of *ABCC8* further reduces MgATP sensitivity when expressed with either E23 or K23 variants of *KCNJ11* (Figure 4-1D). Therefore, the mechanism by which the A1369 variant confers decreased MgATP sensitivity independently of variant K23 is of importance. Free ATP inhibits K_{ATP} channel activity via binding to the $K_{IR}6.2$ subunit, in which K23 is shown to decrease ATP-sensitivity by stabilizing the open state of the K_{ATP} channel [12,17]. Paradoxically, MgATP can activate the K_{ATP} channel via intrinsic MgATPase activity of the nucleotide-binding folds in SUR1, resulting in production of MgADP that stimulates channel activity [31-34]. In direct contrast to a previous study on the *KCNJ11* K23 variant [35], our results indicate that the stimulatory effects of MgADP are unaltered in the K23-A1369 variant K_{ATP} channel, suggesting that the molecular mechanism for decreased ATP inhibition may not involve altered MgADP sensitivity. Our results also show that the observed decrease in ATP inhibition in the K23-A1369 variant K_{ATP} channel results from a direct effect of the *ABCC8* A1369 risk allele reducing ATP inhibition, perhaps via mild changes in the intrinsic K_{ATP} channel MgATPase activity. Studies investigating the molecular basis of SUR1 MgATP hydrolysis suggest that MgATP in the pre-hydrolytic state of MgATPase catalysis inhibits K_{ATP} channel current in addition to free ATP action on $K_{IR}6.2$, whereas

MgADP in the post-hydrolytic state relieves ATP inhibition of the K_{ATP} channel [32,33]. Therefore, the rate and affinity to MgATP of the intrinsic SUR1 MgATPase are critical to the regulation of the K_{ATP} channel. Indeed, several rare heterozygous mutations in *ABCC8* that cause neonatal diabetes (R1380L and R1380C) act by increasing MgATPase activity [8], thereby elevating MgADP-binding, as a result of reducing the time in the pre-hydrolytic MgATP binding state, increasing time spent in the unoccupied state, of which both instances work to increase K_{ATP} channel activity. Interestingly, the location of the *ABCC8* S1369 residue is in close proximity to the MgATPase catalytic site and residue R1380 in the SUR1 nucleotide-binding fold 2 [36]. Therefore, it is plausible that the reduction in MgATP sensitivity of the *KCNJ11* A1369 variant could be the result of an increase in the rate of MgATP hydrolysis by SUR1.

Not only are K_{ATP} channels encoded by the *KCNJ11* and *ABCC8* genes expressed in the β-cells of the pancreas, they are also expressed in pancreatic α-cells and hypothalamic neurons that centrally regulate glucose and energy homeostasis [5,37]. An individual expressing the K23-A1369 variant may in fact not only have alterations in β-cell function, but also possess changes in CNS-mediated energy homeostasis. Studies of blood glucose levels in $K_{IR}6.2$ knockout mice exhibit that not only is recovery from insulin-induced systemic hypoglycaemia significantly impaired, glucagon secretion is also dysregulated upstream of pancreatic α-cells. Based on these findings, a blood glucose homeostasis model has been put forward [38]. As blood glucose levels increase post-prandially, closure of β-cell K_{ATP} channels signals insulin secretion. As

blood glucose levels decrease from peripheral tissue glucose-uptake, hypothalamic K_{ATP} channels are activated, elevating autonomic input to pancreatic α-cells which results in glucagon secretion and restoration of euglycemia. Therefore, it is inferable that subtle increases in the activity of K23-A1369 variant K_{ATP} channels may alter centrally mediated glucose homeostasis, which can contribute to type-2 diabetes development.

Sulfonylurea and glinide drugs that inhibit K_{ATP} channels are in extensive clinical use to stimulate insulin secretion in patients with type-2 diabetes [27]. Glibenclamide is an AB-site ligand and is the most widely used sulfonylurea, whereas gliclazide is an A-site ligand selectively inhibiting K_{ATP} channels containing the SUR1 isoform, potentially mitigating any cardiotoxicity that has been associated with glibenclamide monotherapy, as glibenclamide has been shown to also inhibit cardiac K_{ATP} channels, containing SUR2A and $K_{IR}6.2$ subunits [20,39,40]. Furthermore, B-site drugs such as repaglinide also have been shown to possess higher potencies on SUR1 containing K_{ATP} channels, in light of the cardiotoxic glibenclamide effects [22,25]. Investigating the sensitivity of these particular sulfonylurea and glinide agents on the E23-S1369 and K23-A1369 K_{ATP} channel variants in this study, our results indicate that the K23-A1369 variant K_{ATP} channel is ~3.5-fold more sensitive to gliclazide. Furthermore, we also ascertained that the A1369 variant of SUR1 conferred the increase in gliclazide potency, independently of the E23K $K_{IR}6.2$ variant. This finding provides insight into the molecular mechanism of improved gliclazide potency and the intrinsic SUR1-MgATPase in K_{ATP} channels possessing the SUR1 A1369

variant. It is stated that gliclazide block of K_{ATP} channels is potentiated by the presence of Mg-nucleotides, particularly in the presence of MgADP [20,21,40]. Although there was no difference in gliclazide inhibition of E23-S1369 and K23-S1369 in the presence of 0.1mM MgADP, there was a significant increase in gliclazide inhibition reconstituted human K_{ATP} channels containing the A1369 SUR1 variant. Understanding that SUR1 residue 1369 being in proximity to the nucleotide-binding domain 2 of SUR1 which mediates intrinsic MgATPase activity and that neighbouring residue 1237 is involved in gliclazide activity, inferences can be made as to the mechanism of increased gliclazide potency in the A1369 variant SUR1 protein. As Mg-nucleotides are necessary for gliclazide action and as MgADP potentiates gliclazide inhibition, gliclazide exerts its efficacy through either stabilizing the pre-hydrolytic state of MgATPase activity, in which MgATP is bound, in a manner similar to beryllium fluoride (BeF_4^-) or by reducing the rate in which MgATP catalyzed to MgADP [32]. Detailed kinetic studies of the intrinsic SUR1-MgATPase are required to determine with certainty both the nature of the reduced MgATP sensitivity and increased gliclazide potency of the *ABCC8* A1369 variant.

Furthermore, it is also important to note that the AB-site drug glibenclamide as well as the B-site drug repaglinide exhibited no significant selectivity for either the E23-S1369 or K23-A1369 K_{ATP} channel variants, although a trend towards a decrease in potency in the K23-A1369 variant is observed for both agents. As residue 23 in $K_{IR}6.2$ is proximal to the B-site, when considering that studies have found that deletion of the first 33 amino acids in the

N-terminus of $K_{IR}6.2$ removes glibenclamide photo-affinity labelling [24], it may be possible that the glutamate to lysine switch can account for the slight change in AB or B-site drug potency. However, as glibenclamide simultaneously occupies A and B-sites to exert its inhibitory effect [24], and observing that there was no trend of an increase in potency towards A1369-containing K_{ATP} channels of both AB-site and B-site drugs examined in this study, further highlights intrinsic SUR1-MgATPase function at the A-site as a direct mediator of K_{ATP} channel gating and activity.

In conclusion, this study provides the first evidence that the *ABCC8* S1369A variant alters MgATP inhibition of the K_{ATP} channel that may contribute to the increased risk for type-2 diabetes associated with the K23-A1369 risk haplotype. These findings are the first to directly demonstrate altered sulfonylurea sensitivities of the K23-A1369 variant K_{ATP} channel and also identify the *ABCC8* A1369 risk allele as conferring this effect upon the K_{ATP} channel. Our results also provide a molecular basis for the increase in clinical efficacy of gliclazide in subjects with type-2 diabetes who are homozygous for the K23-A1369 variant [14]. The molecular and clinical efficacy of gliclazide together encourages the study of sulfonylurea pharmacogenomics in larger patient cohorts and also highlights the need for the development of screening technologies to determine favourability of sulfonylurea treatment. Moreover, further study of currently available A-site targeting sulfonylurea therapies such as natelingide, mitiglinide and others, can stratify type-2 diabetes treatment options in patients possessing the K23-A1369 K_{ATP} variant, thereby supporting rationale for tailoring

pharmacotherapy in the 20% of type 2 diabetic patients who are homozygous for these risk alleles.

Figure 4-1

The K23-A1369 variant K_{ATP} channel exhibits decreased sensitivity to MgATP. **(A)** Representative macroscopic current recordings of recombinant human K_{ATP} channel activity at 0.003mM MgATP. **(B)** MgATP inhibition response curves illustrating that the K23-A1369 variant is less sensitive to MgATP inhibition than the E23/S1369 variant. n = 3–11 patches per concentration. Extrapolation of the curves to millimolar physiological MgATP levels (inset). **(C)** Sample traces of the quasi-heterologous human K_{ATP} channel currents K23-S1369 and E23-A1369. **(D)** MgATP inhibition curves from K_{ATP} channels containing either the K23-S1369 or E23-A1369 variant combinations (n = 3–8 patches per MgATP concentration in each group). Dashed line, MgATP inhibition curve for the wild-type E23-S1369 variant replotted from panel B. *P < 0.05.

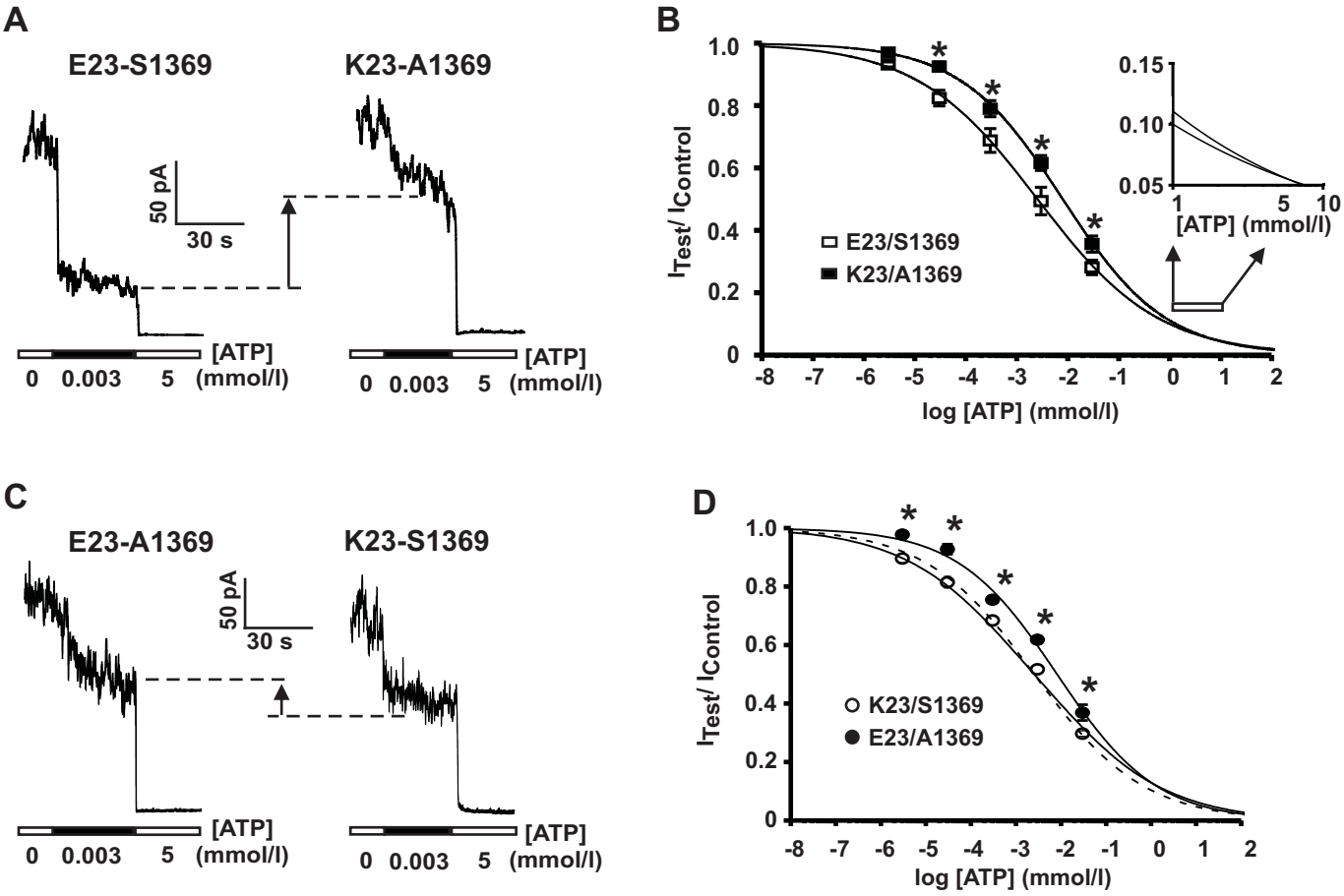
A
E23-S1369
K23-A1369
50 pA
30 s
[ATP]
0 0.003 5 (mmol/l)
[ATP]
0 0.003 5 (mmol/l)
B
1.0
0.8
0.6
0.4
0.2
0
I Test/ I Control
E23/S1369
K23/A1369
-8 -7 -6 -5 -4 -3 -2 -1 0 1 2
log [ATP] (mmol/l)
0.15
0.10
0.05
1 5 10
[ATP] (mmol/l)
C
E23-A1369
K23-S1369
50 pA
30 s
[ATP]
0 0.003 5 (mmol/l)
[ATP]
0 0.003 5 (mmol/l)
D
1.0
0.8
0.6
0.4
0.2
0
I Test/ I Control
K23/S1369
E23/A1369
-8 -7 -6 -5 -4 -3 -2 -1 0 1 2
log [ATP] (mmol/l)

Figure 4-2

The K23-A1369 variant K_{ATP} confers reduced single channel activity at physiological MgATP levels. (A & B) Representative single-channel recordings of E23-S1369 and K23-A1369 variant ATP channels at 0 and 1 mM MgATP (o, open state; c, closed state). **(C &D)** Grouped open probability (P_o) data from 3–6 patches (containing 1–4 KATP channels per patch) showing no difference in open probability at 0 mM MgATP but a significantly increased open probability in the K23-A1369 variant KATP channels at 1 mM MgATP. **(E)** Analyzed data of single-channel unitary current amplitude was not different between the variants. *$P < 0.05$.

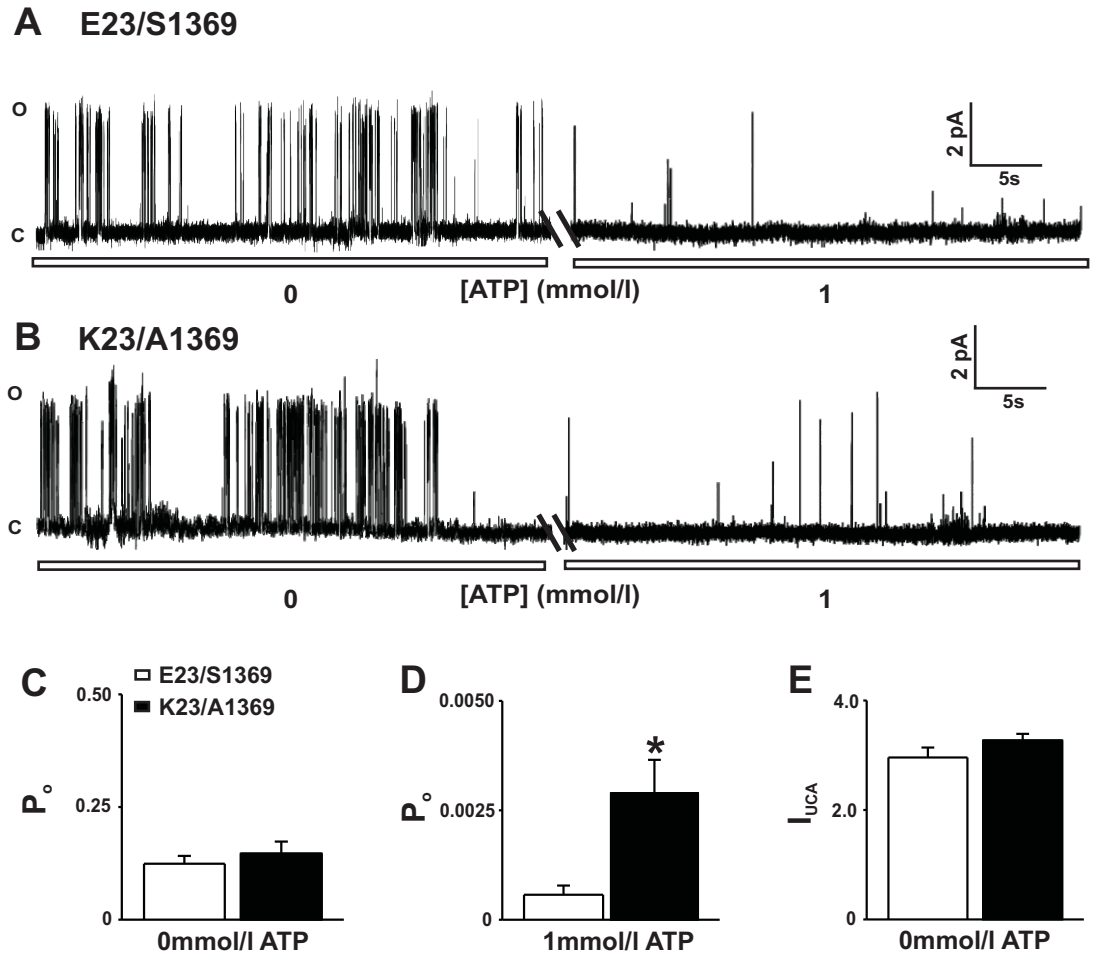
A
E23/S1369
O
C
2 pA
5s
0
[ATP] (mmol/l)
1
B
K23/A1369
O
C
2 pA
5s
0
[ATP] (mmol/l)
1
C
E23/S1369
K23/A1369
P°
0.50
0.25
0
0mmol/l ATP
D
P°
0.0050
0.0025
0
*
1mmol/l ATP
E
I_UCA
4.0
2.0
0
0mmol/l ATP

Figure 4-3

The effect of MgADP on the variant K_{ATP} channels. (A) Representative macroscopic current recordings of the MgADP stimulatory effects of 0.1 mM MgADP in the presence of 0.1 mM MgATP. **(B)** Concentration response curves for the stimulatory effects of increasing MgADP concentrations in the presence of 0.1 mM MgATP. Results show no significant differences in MgADP stimulation between the E23-S1369 and K23-A1369 haplotypes across a range of MgADP concentrations ($P > 0.05$). n = 3–10 patches per group.

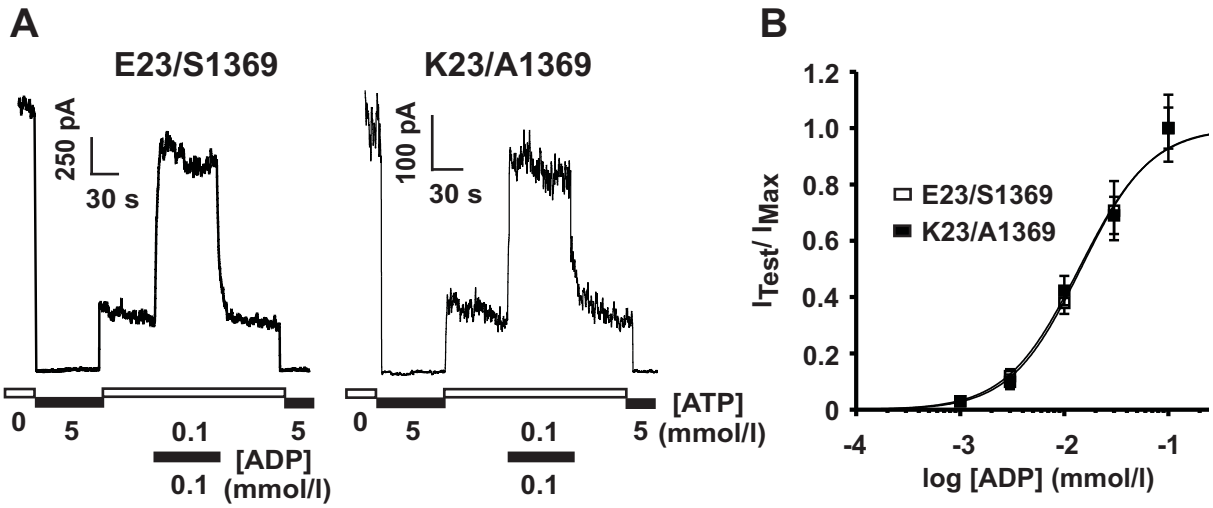
A
E23/S1369
K23/A1369
250 pA
30 s
100 pA
30 s
0
5
0.1
5
[ADP]
0.1
(mmol/l)
0
5
0.1
5
[ATP]
(mmol/l)
0.1
B
1.2
1.0
0.8
0.6
0.4
0.2
0
E23/S1369
K23/A1369
I Test/ I Max
-4
-3
-2
-1
log [ADP] (mmol/l)

Figure 4-4

Sulfonylurea drug binding sites on SUR1 and drug structures. (A) Schematic representation of the SUR1 and $K_{IR}6.2$ protein transmembrane topologies. Amino acids discussed in the text are labeled. The nucleotide-binding folds (NBF1 and 2) and the A and B ligand binding sites are indicated. **(B)** The structure and binding-site classification of sulfonylureas and glinides used in this study: repaglinide (B site), glibenclamide (AB site), and gliclazide (A site).

A

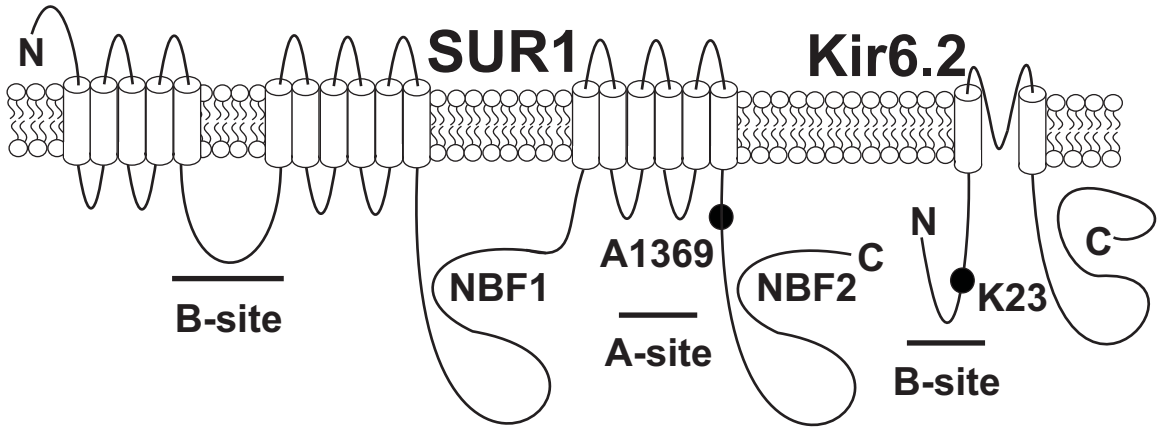
N
SUR1
Kir6.2
A1369
C
N
C
NBF1
NBF2
K23
B-site
A-site
B-site

B

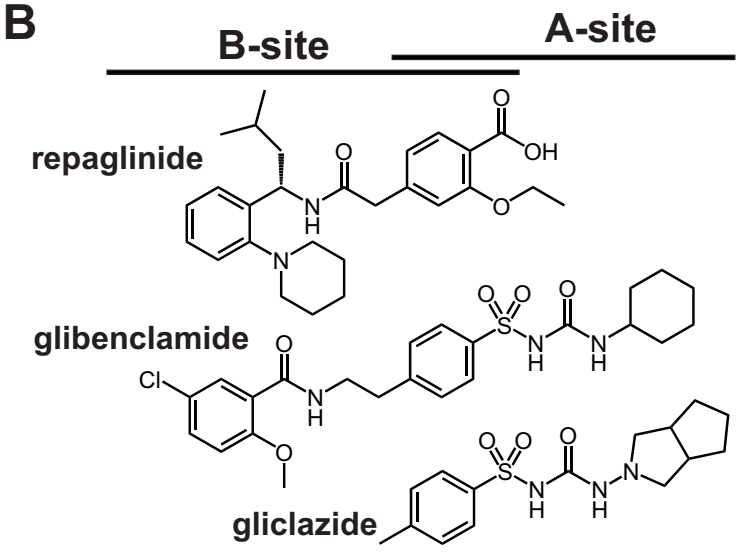
B-site
A-site
repaglinide
glibenclamide
gliclazide

Figure 4-5

Gliclazide potently inhibits the K23-A1369 variant of the K_{ATP} channel. (A, B & C) Representative macroscopic current recordings showing the effect of the A-site sulfonylurea, gliclazide (300 nM), glibenclamide (3 nM) and repaglinide (10 nM) on the E23-S1369 and K23-A1369 variant K_{ATP} channels, respectively. **(D)** Grouped data demonstrating that the K23-A1369 variant is significantly more sensitive to inhibition by gliclazide but not glibenclamide (means ± SE; 0.47 ± 0.07 vs. 0.42 ± 0.05 for E23-S1369 vs. K23-A1369, respectively; $P > 0.05$, n = 11 patches) or repaglinide (0.40 ± 0.06 vs. 0.52 ± 0.05 for E23-S1369 vs. K23-A1369, respectively; $P>0.05$, n = 11 patches). **(E)** Concentration response curves illustrating that the K23-A1369 variant K_{ATP} channel is significantly more sensitive to gliclazide inhibition (IC_{50} = 52.7 ± 11.1 vs. 188.7 ± 32.6 nM for K23-A1369 vs. E23-S1369, respectively). n = 3–12 patches per gliclazide concentration. *$P<0.05$. Glic, gliclazide; Glib, glibenclamide; Rep, repaglinide.

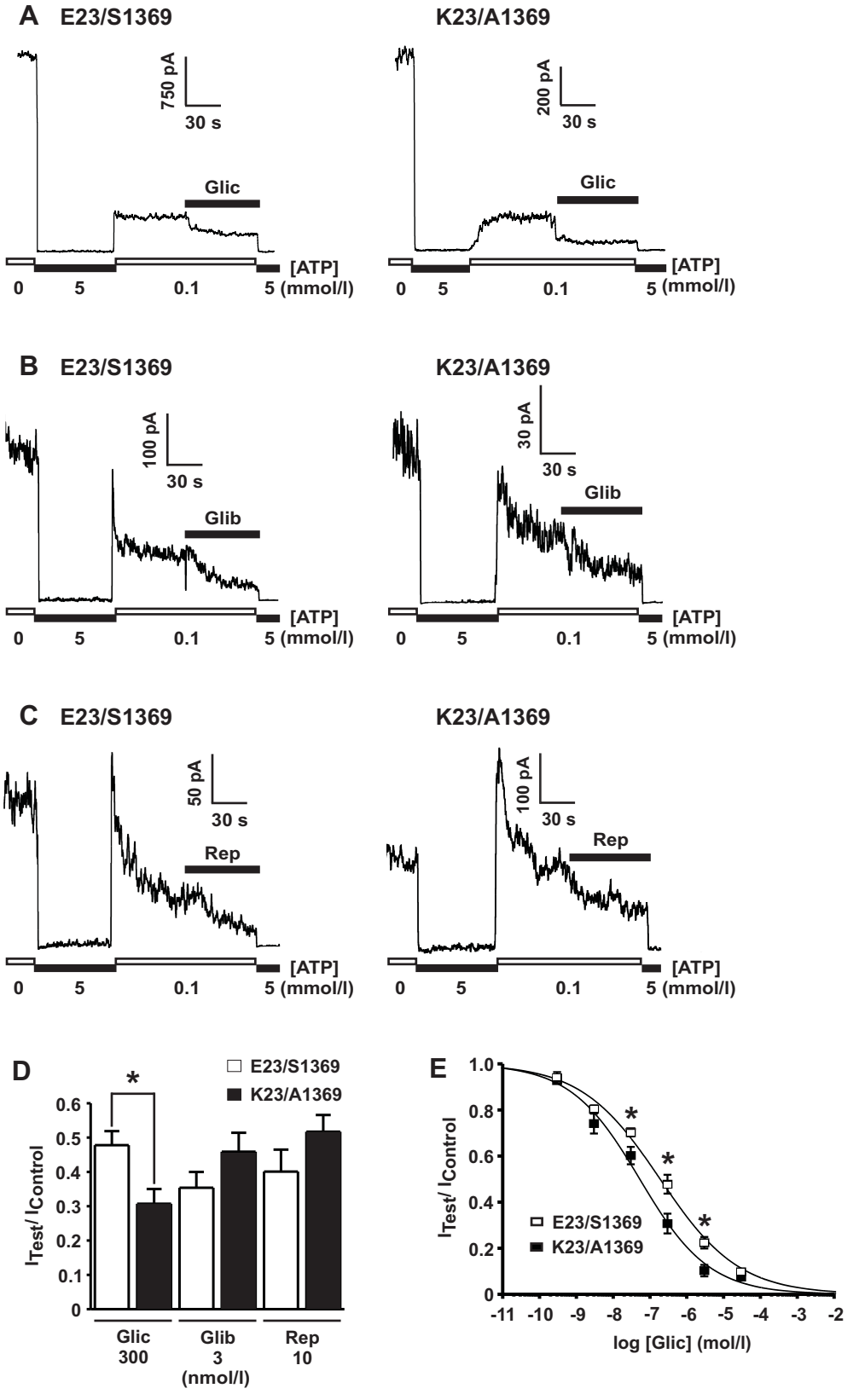
A
E23/S1369
750 pA
30 s
Glic
[ATP]
0
5
0.1
5 (mmol/l)
K23/A1369
200 pA
30 s
Glic
[ATP]
0
5
0.1
5 (mmol/l)
B
E23/S1369
100 pA
30 s
Glib
[ATP]
0
5
0.1
5 (mmol/l)
K23/A1369
30 pA
30 s
Glib
[ATP]
0
5
0.1
5 (mmol/l)
C
E23/S1369
50 pA
30 s
Rep
[ATP]
0
5
0.1
5 (mmol/l)
K23/A1369
100 pA
30 s
Rep
[ATP]
0
5
0.1
5 (mmol/l)
D
E23/S1369
K23/A1369
*
$I_{Test}/I_{Control}$
0.6
0.5
0.4
0.3
0.2
0.1
0
Glic
300
Glib
3
(nmol/l)
Rep
10
E
1.0
0.8
0.6
0.4
0.2
0
$I_{Test}/I_{Control}$
E23/S1369
K23/A1369
*
*
*
-11
-10
-9
-8
-7
-6
-5
-4
-3
-2
log [Glic] (mol/l)

Figure 4-6

The increased gliclazide sensitivity of K23-A1369 variant K_{ATP} channels is maintained in the presence of MgADP and is conferred upon the K_{ATP} channel complex by the *ABCC8* A1369 risk allele. (A & B) Representative macroscopic current recordings showing the inhibitory effect of gliclazide (300 nM) on the two variants in the presence of MgADP. **(C)** Grouped data demonstrating that the K23-A1369 variant K_{ATP} channels are significantly more sensitive to gliclazide in the presence of MgADP than the E23-S1369 variant K_{ATP} channels. n = 10–12 patches per group. **(D-F)** Representative current recordings and grouped data showing the increased gliclazide inhibitory effect is dependent on the presence of the *ABCC8* A1369 variant and not the *KCNJ11* K23 variant. n = 15 patches per group. *P < 0.05. Glic, gliclazide.

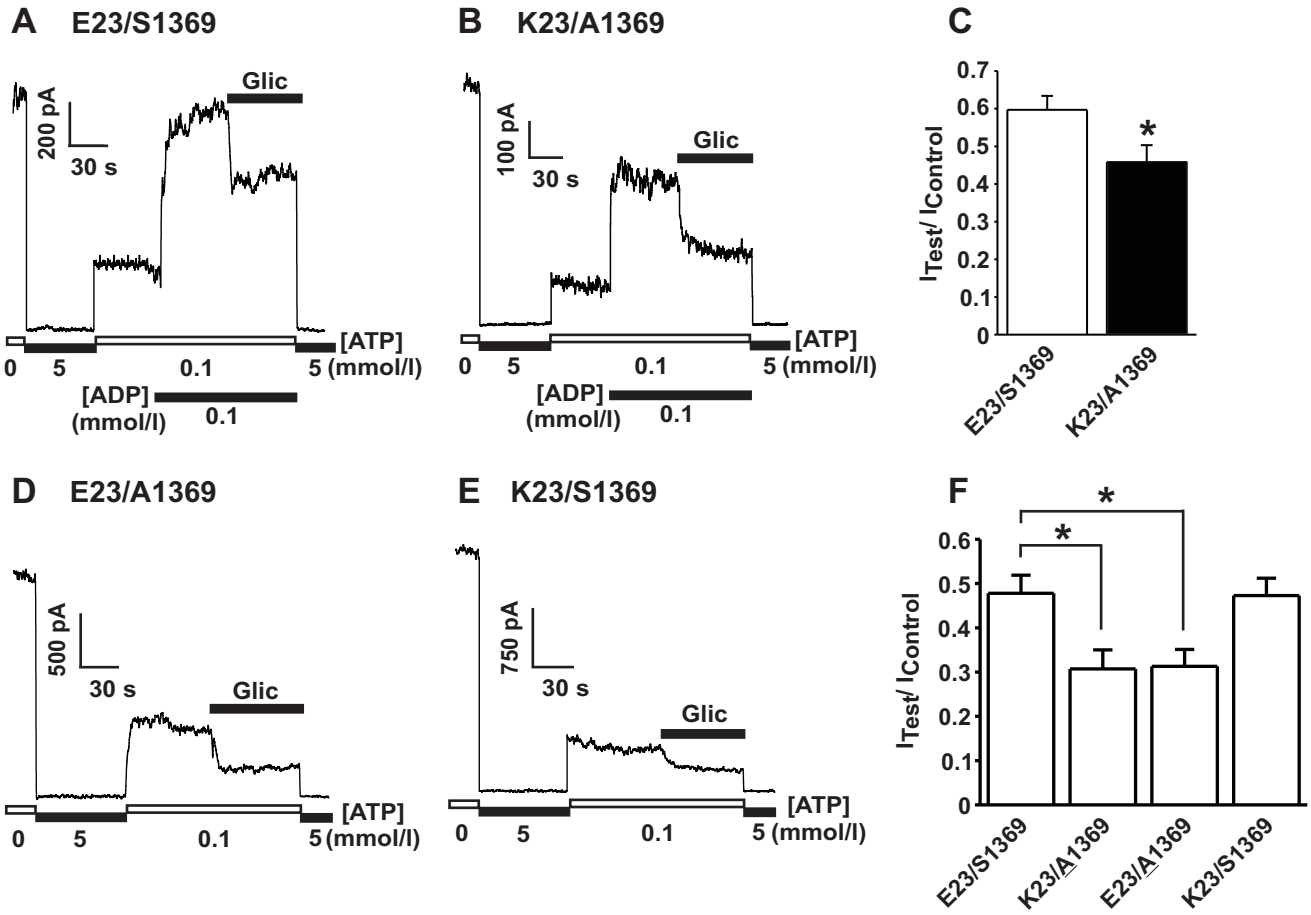
A
E23/S1369
200 pA
30 s
Glic
[ATP]
0
5
0.1
5 (mmol/l)
[ADP]
(mmol/l)
0.1
B
K23/A1369
100 pA
30 s
Glic
[ATP]
0
5
0.1
5 (mmol/l)
[ADP]
(mmol/l)
0.1
C
I Test/ I Control
0.7
0.6
0.5
0.4
0.3
0.2
0.1
0
*
E23/S1369
K23/A1369
D
E23/A1369
500 pA
30 s
Glic
[ATP]
0
5
0.1
5 (mmol/l)
E
K23/S1369
750 pA
30 s
Glic
[ATP]
0
5
0.1
5 (mmol/l)
F
I Test/ I Control
0.6
0.5
0.4
0.3
0.2
0.1
0
*
*
E23/S1369
K23/A1369
E23/A1369
K23/S1369

References

1. Shi NQ, Ye B, Makielski JC. Function and distribution of the SUR isoforms and splice variants. J.Mol.Cell.Cardiol. 2005 Jul;39(1):51-60.

2. Ashcroft SJ, Ashcroft FM. Properties and functions of ATP-sensitive K-channels. Cell.Signal. 1990;2(3):197-214.

3. Ashcroft FM, Rorsman P. Electrophysiology of the pancreatic beta-cell. Prog.Biophys.Mol.Biol. 1989;54(2):87-143.

4. Aguilar-Bryan L, Bryan J. Molecular biology of adenosine triphosphate-sensitive potassium channels. Endocr.Rev. 1999 Apr;20(2):101-135.

5. Seino S, Miki T. Physiological and pathophysiological roles of ATP-sensitive K+ channels. Prog.Biophys.Mol.Biol. 2003 Feb;81(2):133-176.

6. Gloyn AL, Pearson ER, Antcliff JF, Proks P, Bruining GJ, Slingerland AS, et al. Activating mutations in the gene encoding the ATP-sensitive potassium-channel subunit Kir6.2 and permanent neonatal diabetes. N.Engl.J.Med. 2004 Apr 29;350(18):1838-1849.

7. Tammaro P, Girard C, Molnes J, Njolstad PR, Ashcroft FM. Kir6.2 mutations causing neonatal diabetes provide new insights into Kir6.2-SUR1 interactions. EMBO J. 2005 Jul 6;24(13):2318-2330.

8. de Wet H, Rees MG, Shimomura K, Aittoniemi J, Patch AM, Flanagan SE, et al. Increased ATPase activity produced by mutations at arginine-1380 in nucleotide-binding domain 2 of ABCC8 causes neonatal diabetes. Proc.Natl.Acad.Sci.U.S.A. 2007 Nov 27;104(48):18988-18992.

9. Babenko AP, Polak M, Cave H, Busiah K, Czernichow P, Scharfmann R, et al. Activating mutations in the ABCC8 gene in neonatal diabetes mellitus. N.Engl.J.Med. 2006 Aug 3;355(5):456-466.

10. Gloyn AL, Hashim Y, Ashcroft SJ, Ashfield R, Wiltshire S, Turner RC, et al. Association studies of variants in promoter and coding regions of beta-cell ATP-sensitive K-channel genes SUR1 and Kir6.2 with Type 2 diabetes mellitus (UKPDS 53). Diabet.Med. 2001 Mar;18(3):206-212.

11. Gloyn AL, Weedon MN, Owen KR, Turner MJ, Knight BA, Hitman G, et al. Large-scale association studies of variants in genes encoding the pancreatic beta-cell KATP channel subunits Kir6.2 (KCNJ11) and SUR1 (ABCC8) confirm that the KCNJ11 E23K variant is associated with type 2 diabetes. Diabetes 2003 Feb;52(2):568-572.

12. Villareal DT, Koster JC, Robertson H, Akrouh A, Miyake K, Bell GI, et al. Kir6.2 variant E23K increases ATP-sensitive K+ channel activity and is associated with impaired insulin release and enhanced insulin sensitivity in adults with normal glucose tolerance. Diabetes 2009 Aug;58(8):1869-1878.

13. Florez JC, Burtt N, de Bakker PI, Almgren P, Tuomi T, Holmkvist J, et al. Haplotype structure and genotype-phenotype correlations of the sulfonylurea receptor and the islet ATP-sensitive potassium channel gene region. Diabetes 2004 May;53(5):1360-1368.

14. Feng Y, Mao G, Ren X, Xing H, Tang G, Li Q, et al. Ser1369Ala variant in sulfonylurea receptor gene ABCC8 is associated with antidiabetic efficacy of gliclazide in Chinese type 2 diabetic patients. Diabetes Care 2008 Oct;31(10):1939-1944.

15. Riedel MJ, Light PE. Saturated and cis/trans unsaturated acyl CoA esters differentially regulate wild-type and polymorphic beta-cell ATP-sensitive K+ channels. Diabetes 2005 Jul;54(7):2070-2079.

16. Webster NJ, Searle GJ, Lam PP, Huang YC, Riedel MJ, Harb G, et al. Elevation in intracellular long-chain acyl-coenzyme A esters lead to reduced beta-cell excitability via activation of adenosine 5'-triphosphate-sensitive potassium channels. Endocrinology 2008 Jul;149(7):3679-3687.

17. Schwanstecher C, Meyer U, Schwanstecher M. K(IR)6.2 polymorphism predisposes to type 2 diabetes by inducing overactivity of pancreatic beta-cell ATP-sensitive K(+) channels. Diabetes 2002 Mar;51(3):875-879.

18. Nichols CG, Shyng SL, Nestorowicz A, Glaser B, Clement JP,4th, Gonzalez G, et al. Adenosine diphosphate as an intracellular regulator of insulin secretion. Science 1996 Jun 21;272(5269):1785-1787.

19. Gribble FM, Tucker SJ, Ashcroft FM. The interaction of nucleotides with the tolbutamide block of cloned ATP-sensitive K+ channel currents expressed in Xenopus oocytes: a reinterpretation. J.Physiol. 1997 Oct 1;504 (Pt 1)(Pt 1):35-45.

20. Gribble FM, Tucker SJ, Seino S, Ashcroft FM. Tissue specificity of sulfonylureas: studies on cloned cardiac and beta-cell K(ATP) channels. Diabetes 1998 Sep;47(9):1412-1418.

21. Gribble FM, Ashcroft FM. Differential sensitivity of beta-cell and extrapancreatic K(ATP) channels to gliclazide. Diabetologia 1999 Jul;42(7):845-848.

22. Dabrowski M, Wahl P, Holmes WE, Ashcroft FM. Effect of repaglinide on cloned beta cell, cardiac and smooth muscle types of ATP-sensitive potassium channels. Diabetologia 2001 Jun;44(6):747-756.

23. Proks P, Reimann F, Green N, Gribble F, Ashcroft F. Sulfonylurea stimulation of insulin secretion. Diabetes 2002 Dec;51 Suppl 3:S368-76.

24. Vila-Carriles WH, Zhao G, Bryan J. Defining a binding pocket for sulfonylureas in ATP-sensitive potassium channels. FASEB J. 2007 Jan;21(1):18-25.

25. Stephan D, Winkler M, Kuhner P, Russ U, Quast U. Selectivity of repaglinide and glibenclamide for the pancreatic over the cardiovascular K(ATP) channels. Diabetologia 2006 Sep;49(9):2039-2048.

26. Winkler M, Stephan D, Bieger S, Kuhner P, Wolff F, Quast U. Testing the bipartite model of the sulfonylurea receptor binding site: binding of A-, B-, and A + B-site ligands. J.Pharmacol.Exp.Ther. 2007 Aug;322(2):701-708.

27. Bryan J, Crane A, Vila-Carriles WH, Babenko AP, Aguilar-Bryan L. Insulin secretagogues, sulfonylurea receptors and K(ATP) channels. Curr.Pharm.Des. 2005;11(21):2699-2716.

28. Ashfield R, Gribble FM, Ashcroft SJ, Ashcroft FM. Identification of the high-affinity tolbutamide site on the SUR1 subunit of the K(ATP) channel. Diabetes 1999 Jun;48(6):1341-1347.

29. Sakura H, Wat N, Horton V, Millns H, Turner RC, Ashcroft FM. Sequence variations in the human Kir6.2 gene, a subunit of the beta-cell ATP-sensitive K-channel: no association with NIDDM in while Caucasian subjects or evidence of abnormal function when expressed in vitro. Diabetologia 1996 Oct;39(10):1233-1236.

30. Riedel MJ, Boora P, Steckley D, de Vries G, Light PE. Kir6.2 polymorphisms sensitize beta-cell ATP-sensitive potassium channels to activation by acyl CoAs: a possible cellular mechanism for increased susceptibility to type 2 diabetes? Diabetes 2003 Oct;52(10):2630-2635.

31. Bryan J, Munoz A, Zhang X, Dufer M, Drews G, Krippeit-Drews P, et al. ABCC8 and ABCC9: ABC transporters that regulate K+ channels. Pflugers Arch. 2007 Feb;453(5):703-718.

32. Zingman LV, Alekseev AE, Bienengraeber M, Hodgson D, Karger AB, Dzeja PP, et al. Signaling in channel/enzyme multimers: ATPase transitions in SUR module gate ATP-sensitive K+ conductance. Neuron 2001 Aug 2;31(2):233-245.

33. Gribble FM, Tucker SJ, Ashcroft FM. The essential role of the Walker A motifs of SUR1 in K-ATP channel activation by Mg-ADP and diazoxide. EMBO J. 1997 Mar 17;16(6):1145-1152.

34. de Wet H, Mikhailov MV, Fotinou C, Dreger M, Craig TJ, Venien-Bryan C, et al. Studies of the ATPase activity of the ABC protein SUR1. FEBS J. 2007 Jul;274(14):3532-3544.

35. Schwanstecher C, Neugebauer B, Schulz M, Schwanstecher M. The common single nucleotide polymorphism E23K in K(IR)6.2 sensitizes pancreatic beta-cell ATP-sensitive potassium channels toward activation through nucleoside diphosphates. Diabetes 2002 Dec;51 Suppl 3:S363-7.

36. Masia R, Nichols CG. Functional clustering of mutations in the dimer interface of the nucleotide binding folds of the sulfonylurea receptor. J.Biol.Chem. 2008 Oct 31;283(44):30322-30329.

37. Minami K, Miki T, Kadowaki T, Seino S. Roles of ATP-sensitive K+ channels as metabolic sensors: studies of Kir6.x null mice. Diabetes 2004 Dec;53 Suppl 3:S176-80.

38. Miki T, Liss B, Minami K, Shiuchi T, Saraya A, Kashima Y, et al. ATP-sensitive K+ channels in the hypothalamus are essential for the maintenance of glucose homeostasis. Nat.Neurosci. 2001 May;4(5):507-512.

39. Evans JM, Ogston SA, Emslie-Smith A, Morris AD. Risk of mortality and adverse cardiovascular outcomes in type 2 diabetes: a comparison of patients treated with sulfonylureas and metformin. Diabetologia 2006 May;49(5):930-936.

40. Lawrence CL, Proks P, Rodrigo GC, Jones P, Hayabuchi Y, Standen NB, et al. Gliclazide produces high-affinity block of KATP channels in mouse isolated pancreatic beta cells but not rat heart or arterial smooth muscle cells. Diabetologia 2001 Aug;44(8):1019-1025.

Chapter 5

General Discussion

The Na^+-Ca^{2+} exchanger and the ATP-sensitive K^+ channel are both important to the physiological function of the myocardium and the insulin-secreting β-cells of the endocrine pancreas. Because of its crucial role in regulating intracellular Ca^{2+}, NCX1 is a focal point in the pathophysiology of cardiac IR. As NCX1 is also expressed in the CNS and vasculature, the findings that NCX1 splice variants are differentially modified by ROS can be related to other conditions such as stroke, Alzheimer's disease, multiple sclerosis, and hypertension. With NCX1 being involved in many unrelated disease states, the impetus to develop a clinical pharmacological agent to modulate NCX1 activity is warranted. Not only is NCX1 modulation important in cardiovascular and neuronal diseases, it can also be exploited to increase insulin secretion from pancreatic β-cells to treat type-2 diabetes.

Furthermore, K_{ATP} activity aids in governing the membrane potential, targeting K_{ATP} channels in type-2 diabetes has been shown to be advantageous. However, the similar sensitivity of SUs at SUR1 and SUR2A in addition to SNPs altering K_{ATP} channel function provides challenges to SU therapy. Therefore, understanding the molecular mechanisms by which SNPs affect K_{ATP} channel activity and K_{ATP} pharmacology would be insightful in developing pharmacogenomic strategies for type-2 diabetes and may be applicable in cardiac syndromes such as IR and atrial fibrillation.

It is the aim of this general discussion to provide insight on the results presented in this thesis in an effort to relate the data obtained to previous findings.

Furthermore, this discussion will act to direct future experiments with the goal of the advancing research of IHD and type-2 diabetes.

NCX1 Modification by ROS

Molecular Aspects

The earliest assertion that ROS production during cardiac IR causes a subsequent increase in intracellular Ca^{2+} levels was made by Hearse et al. [1] Thereafter, redox agents such as Fe-DTT and xanithine oxidase were shown to stimulate NCX1.1 mediated $^{45}Ca^{2+}$-uptake in bovine cardiac sarcolemmal vesicles postulating that the reduction of cysteine residues in NCX1.1 protein activated NCX1.1 activity [2,3]. Furthermore, up-regulated RM-NCX1.1 activity by H_2O_2 suspected in augmenting cardiac myocyte contractility and increased action potential duration [4]. Goldhaber also found that NCX1.1 activity was enhanced while studying the effects of ROS on guinea-pig cardiac myocytes, inferring that ROS directly modulated NCX1.1 activity [5]. Supporting this notion was the finding that removal of cysteine residues continued to exhibit increased NCX1.1 activity with the application of iron-dithiothreitol (Fe-DTT) [6]. Moreover, it was determined that over-expression of NCX1.1 predisposed cardiac myocytes to ROS-mediated injury and that NCX1.1 was reactivated during simulated cardiac IR, contributing to the intracellular Ca^{2+} overload that precipitates myocardial injury [7,8]. However, the mechanism by which ROS promotes NCX1.1 activity remained undetermined.

In my examination of NCX1 function, I determined that the stable ROS intermediate H_2O_2 increased NCX1.1 current in rat and human NCX1 isoforms, in

a time-dependent, voltage-independent and I_1-inactivation-dependent manner. Proceeding to also determine the effect of H_2O_2 on NCX1 splice variants, NCX1.3, NCX1.4 and NCX1.11, I found that NCX1.1 and NCX1.4 possessing exon A exhibited a significant increase in RM-NCX1.1 current. Conversely, possessing exon B, NCX1.3 and NCX1.11, displayed a decrease in RM-NCX1.1 current. From this result we inferred that the site of ROS modification involves the ASR which houses CBD2, as the only difference between the splice-variants tested was the exon complement. Using recently elucidated molecular models of CBD2 [9], we postulated that H_2O_2 may stabilize Ca^{2+} binding in exon A containing variants, while destabilizing Ca^{2+} binding in exon B variants. The increase in RM-NCX1.1 by ROS stabilizing Ca^{2+} binding is plausible as NCX1.1 has a higher affinity for Ca^{2+}-transport versus NCX1.3, due to the Ca^{2+}-dependent I_2-activation governed by exon A [10]. Furthermore, as the effects of ROS were only visible during I_1-inactivation of NCX1 currents highlight the functional interaction of CBD2 and the XIP region [11]. This observation adds credence to the notion that the ASR is the site of ROS-mediated alterations in NCX1 function. Finding that NCX1 splice-variants exhibit differential modification by ROS, it is important to discuss the relevant physiological and pathophysiological impositions these results may have on other tissues.

Tissue-Specific Physiological and Pathophysiological Implications of NCX1 & ROS

The study of NCX1.1 modification by ROS was initiated in cardiac IR, as the increase in ROS directly correlated to intracellular Ca^{2+} accumulation.

Knowing that NCX1 is not solely expressed in the myocardium, and is ubiquitously present in mammalian tissues, it is evident that ROS-mediated effects on NCX1 can be have implications in other tissues which also possess a propensity for ROS production.

Although much of the scientific literature focuses on the pathophysiological effects of ROS on NCX1 exchanger function, it is possible that modulating spacial and temporal elements of intracellular Ca^{2+} through ROS-mediated alteration of NCX1 may provide a physiological benefit. Pi et al. describe a mechanism by which H_2O_2 elevates insulin secretion from pancreatic β-cells [12]. As H_2O_2 is produced as a consequence of glucose metabolism and is apparently involved after stimulation of Ca^{2+}-influx, it may be possible that H_2O_2 modulates FM-NCX1.3 activity. This modulation would reduce Ca^{2+} efflux, transiently elevating intracellular Ca^{2+} levels and increasing insulin release. In fact, it has been recently shown that partial pharmacological FM-NCX1.3 inhibition stimulates insulin secretion from pancreatic β-cells [13]. However, whether the increase in insulin secretion regulated by H_2O_2 is due to a direct effect on NCX1.3 in the β-cell remains to be investigated.

In the vasculature, NCX1 also plays an important role in intracellular Ca^{2+} handling, directly modulating vascular contractility and blood pressure. Peripheral vascular resistance is dynamically mediated by vasoconstriction and vasodilation of small resistance arteries [14]. Myogenic tone is a phenomenon in which increases in intraluminal pressure of resistance arteries causes vasoconstriction, is regulated by Ca^{2+}-influx through L-type VGCCs [15,16]. In regulating myogenic

tone, NCX1 in the vasculature provides approximately 30-40% of the total intracellular Ca^{2+} clearance, while SERCA and PMCA contribute 60-70% of total cytoplasmic Ca^{2+} removal [17]. Vascular NCX1 splice variants, that possess a higher-capacity Ca $^{2+}$ transport mechanism than SERCA or PMCA, may be more relevant for sudden temporal changes in intracellular Ca^{2+} levels, such as upon neuro-hormonal activation by angiotensin II or sympathetic stimulation [18]. Furthermore, SERCA and PMCA may be responsible for on-going intracellular Ca^{2+} maintenance, such as the case in myogenic tone [17]. Despite NCX1 only contributing to 30-40% of the vascular smooth muscle's intracellular Ca^{2+}-clearing mechanisms, NCX1 is in fact a major regulator of myogenic tone and blood pressure. Studies exhibit that knockout or pharmacological inhibition of NCX1 using SEA0400 in vascular smooth muscle impairs myogenic reactivity to vasoconstrictors and alters myogenic tone in mice *in vivo* and in rat small arteries [18,19]. In fact, when vascular smooth muscle cells are operating under steady-state conditions, in which resting membrane potential is relatively constant, NCX1 functions close to its reversal potential. As NCX1 activity is electrogenic, it is sensitive to membrane potential and thus FM or RM operation is dependent on membrane potential in a Nernstian fashion, i.e. $E_{NCX1} = 3E_{Na} - E_{Ca}$ [20]. Functioning near its reversal potential may allow NCX1 to operate in RM, causing Ca^{2+}-influx, participating in vasoconstriction of resistance arteries, such as the case in tonically constricted arteries [18]. Moreover, not only does vascular RM-NCX1 contribute to the steady state conditions for myogenic tone, it is implicated in the development of salt-sensitive hypertension (SSH) [21]. Elevated

salt (NaCl) intake has been shown extensively to cause the release of endogenous ouabain by the adrenal cortex [22]. Ouabain, an inhibitor of NKA, acts to increase intracellular Na^+ levels, altering the electrochemical balance of Na^+ and Ca^{2+} favoring RM-NCX1 operation. RM-NCX1 function would work to constrict resistance arteries increasing systemic blood pressure [23,24].

In addition to the major involvement of NCX1 in blood pressure regulation and in development of SSH, ROS have also been implicated in SSH in various animal models such as in the Dahl salt-sensitive rats and the spontaneously hypertensive rats [25]. In these models, animals display increased microvascular and renal superoxide production which can react with nitric oxide (NO) to form peroxynitrite ($ONOO^-$) reducing NO-mediated vasorelaxation [26,27]. In particular, changes in the renal circulation may alone have an important contributory role. For instance, in Unlap et al., they found that a reduction in FM-NCX1.3 and FM-NCX1.7 (exons BDF) activity that was caused by H_2O_2 and $ONOO^-$, which would reduce intracellular Ca^{2+} clearance in the renal mesangium causing renal vasoconstriction. Renal vasoconstriction would reduce renal function, thereby increasing plasma volume and Na^+ reabsoption hastening the development of SSH [27]. Therefore, ROS-induced alterations in NCX1 activity may not have a direct functional consequence in the vasculature *per se*, but may have direct implications in the pathogenesis of SSH, where renal function is concerned.

In a manner more similar to the endocrine pancreas, NCX1 is directly involved in Ca^{2+} homeostasis in CNS neurons (see review [28]). At the level of

the synapse, specifically during an action potential, N-, P- and Q-type VGCCs are activated, resulting in an influx of Ca^{2+} [29]. This manner of Ca^{2+}-influx triggers the fusion of synaptic vesicles with the neuronal plasma membrane, initiating neurotransmitter exocytosis and the propagation of neuronal transmission to adjacent post-synaptic neurons. As the pre-synaptic membrane repolarizes through the action of outward K^+ currents, residual intracellular Ca^{2+} is rapidly extruded by PMCA and NCX1. NCX1, having a high transport capacity, becomes very crucial in removing intracellular Ca^{2+} as action potential trains reach nerve terminals, while PMCA works to regulate intracellular Ca^{2+} levels at rest [30].

As NCX1 is a major mechanism by which intracellular Ca^{2+} levels are controlled, it is no surprise that NCX1 is involved in Ca^{2+}-overload induced neuronal excitotoxicity in cerebral IR. Cerebral IR or stroke can be caused by an occlusion of cerebral arteries by an aneurysm or a thrombus can occur in a similar manner to coronary arteries [31]. Many studies implicate NCX1 as the cause Ca^{2+}-mishandling leading to excitotoxicity and subsequent neuronal death in cerebral IR. For example, studies have shown that knockout of NCX1 and pharmacological inhibition of NCX1 using SEA0400 are protective in models of cerebral IR [32,33]. However, not all experimental models are protected by knockdown or inhibition of NCX1, due to the differential effects of ROS on NCX1 splice variants.

Unlike cardiac IR, the contribution of ROS to neuronal Ca^{2+}-accumulation is unclear [28], as NCX isoform and NCX1 splice-variant profile in the CNS is complex. In fact, ROS alterations in neuronal NCX1 activity is determined by the

splice variant expressed in accordance with data presented in this thesis. As astrocytes and the commonly used C6 glioma cell line express NCX1 splice variants, NCX1.3 (exons BD), NCX1.7 (exons BDF) and NCX1.10 (exons BDEF), it is of no coincidence that Ca^{2+} influx is reduced as exon B containing NCX1 variants exhibit decreased activity upon ROS application. This reduction in Ca^{2+} influx may be a protective mechanism in these cell types [34,35]. Conversely, in hippocampal CA1 neurons, ROS-mediated increases in NCX1 activity is detrimental considering the expression of exon A containing splice variants NCX1.4 (exons AD) and NCX1.5 (exons ADF) [36]. Furthermore, NCX1-mediated Ca^{2+}-influx is the dominant factor in NMDA-induced Ca^{2+}-entry and excitotoxicity such as in Alzheimer's disease and the death of depolarized and glucose-starved neurons [28,37,38].

In summary, the splice-variant dependent ROS-induced alterations of NCX1 activity have significant repercussions in the development of cardiac IR, salt-sensitive hypertension, as well as cerebral IR. Not only have the observations of ROS-mediated changes to NCX1 activity substantiated the findings of other studies, they also further highlight that NCX1 inhibition can be therapeutically targeted to ameliorate cardiac IR injury and salt-sensitive hypertension. In this effort, we have examined the pharmacological effects of ranolazine, a pharmacological agent which has been shown to be protective in cardiac IR. Although much evidence suggests its mechanism of action to be inhibition of late I_{Na}, I present data which demonstrate ranolazine to be a potent inhibitor of

NCX1.1, which would aid in reducing cardiac IR injury caused by NCX1.1-mediated intracellular Ca^{2+}-overload.

Inhibition of Late I_{Na} & NCX1.1 by Ranolazine

Implications for Heart Failure

Ranolazine has been shown to be a cardioprotective agent in angina and in models of IR [39-41]. Through the inhibitory actions of ranolazine on late I_{Na} and now NCX1.1, intracellular Na^+ and Ca^{2+} homeostasis can be improved, reducing cellular dysfunction that may also be relevant in heart failure. In chronic heart failure (HF), left ventricular end diastolic pressure is elevated, as a result of impaired diastolic intracellular Ca^{2+} handling and increased preload via the venous circulation. The impairment of diastolic Ca^{2+} handing is the result of changes to the activity and expression levels of the major Ca^{2+}-handling proteins in the myocardium. SERCA2A expression and activity is commonly observed to be down-regulated in models of heart failure, possibly due to a decrease in phospholamban phosphorylation, which regulates SERCA2A function [42-44]. Meanwhile, NCX1.1 mRNA and protein expression is up-regulated [45,46]. It is plausible that the decrease in SERCA2A expression and activity is compensated by the increase in NCX1.1 expression, however, RM-NCX1.1 and SERCA2A play opposing roles in the spacial and temporal dynamics of intracellular Ca^{2+} handling [47,48]. Therefore, increased NCX1.1 expression may not be sufficient in compensating for the loss of SERCA2A contribution to intracellular Ca^{2+}.

However, impaired intracellular Na^+ levels occur upstream of intracellular Ca^{2+}-mishandling. Late I_{Na} also plays a role in heart failure recently being

implicated in the pathogenesis of cardiac IR injury by contributing to NCX1.1-mediated Ca^{2+} overload, [49]. In addition to late I_{Na}, other Na^+-handling mechanisms can contribute to unbalanced Na^+ influx and efflux during HF, leading to the accumulation of intracellular Na^+. Increased Na^+ levels can originate from up-regulated NHE1 and Na^+-HCO_3^- co-transporter (NBC) activity, augmenting Na^+-influx, while down-regulated NKA activity and expression reduces Na^+-efflux, causing a net gain of intracellular Na^+ [50,51].

Yet, changes to intracellular Na^+ regulation alone do not cause the diastolic injury or arrhythmogenesis observed in HF, as increased intracellular Na^+ alone is not expected to directly alter myocardial contractility [52]. For instance, the alterations to SERCA2A expression and function have been documented, attenuating intracellular Ca^{2+} uptake into the SR, which is a necessary process for intracellular Ca^{2+} clearance for diastole [53]. Furthermore, Na^+ and Ca^{2+} regulation are tightly coupled through NCX1.1 exchange. Having a net gain in intracellular Na^+ shifts the reversal potential of NCX1 more negatively, favouring increased RM-NCX1.1 function during systole [52]. Furthermore, the cardiac action potential duration is prolonged, due to re-modulating action potential dynamics. Late I_{Na} increases AP duration in a manner analogous to LQT3 syndromes, in which Na^+ channels possess monogenic mutations that decrease time to inactivation [54]. Therefore, as more time is spent in a depolarized state, RM-NCX1.1 functions longer, further increasing intracellular Ca^{2+} levels. Conversely, as the action potential duration prolongs, time spent in the refractory period or in diastole decreases, reducing the duration of time for

intracellular Ca^{2+} to be removed from the cytosol. Therefore, considering that SERCA2A expression is decreased and that FM-NCX1 activity is also reduced, intracellular Na^{+} levels increase amounting to the chronic elevation of diastolic Ca^{2+} causing diastolic dysfunction [52,53].

As late I_{Na} and NCX1.1 are intricately involved in the pathogenesis of diastolic dysfunction in heart failure, it is likely that ranolazine, as an inhibitor of RM-NCX1.1 and late I_{Na} may be valuable in reducing diastolic Ca^{2+} levels. Thought only to inhibit late I_{Na}, studies using ranolazine have shown improvements in diastolic Ca^{2+} handling in failing human myocardium, as well as ameliorating the susceptibility of rat cardiac myocytes to develop Ca^{2+} alternans in a model of ATX-II induced late I_{Na} [55,56]. Now considering that ranolazine also has potent inhibitory action on RM-NCX1.1, ranolazine possesses an additional target by which to prevent intracellular Na^{+} and Ca^{2+} mishandling in HF. Furthermore, ROS formation also occurs during HF [57]. Metabolic uncoupling also occurs during HF as glucose oxidation is downregulated, increasing glycolytic flux in order to maintain levels of ATP. However, up-regulated glycolysis would cause intracellular acidosis, consequently increasing Na^{+} influx via NHE1 [58]. Nevertheless, NCX1.1 becomes a more substantial target to correct diastolic intracellular Ca^{2+} handling during HF with the knowledge that RM-NCX1.1 function is augmented by ROS.

Implications for Atrial Fibrillation

Atrial fibrillation (AF) is a common cardiac arrhythmia that is associated with an underlying cardiac condition such as HF [59] or following cardiac surgery

[60]. Type-2 diabetes, hypertension, obesity and left ventricular hypertrophy and diastolic dysfunction all can predispose cardiac patients to AF [61]. The specific cause of AF in the post-operative period is in fact a direct consequence of intra-operative factors such as atrial ischemia or surgical atrial injury. In conjunction with oxidative stress and inflammatory processes, this can lead to atrial myocyte dysfunction and structural remodelling, causing electrophysiological alterations in AP conduction [61]. Dispersion of refractoriness, a critical AP conduction anomaly precipitates as damage to atrial myocytes can result in adjacent myocytes not sharing the same propensity for refractoriness. Therefore, a new AP propagation would not only face repolarized myocytes, but also depolarized myocytes as well. This increases the risk of the AP wavefront to incessantly cycle through the atrial tissue as a re-entrant AP causing premature and non-uniform contractions of the atrial myocytes [60,62,63].

Interestingly, late I_{Na} can precipitate AF after cardiac surgery. To this end, ranolazine has been shown to reduce AF duration in experimental models by reducing AP duration. Decreasing AP duration has the effect of increasing the effective refractory period and also decreases the incidence of β-agonist-induced pre-mature atrial contractions (Figure 5-3) [64,65]. With respect to Na^+ channel expression, AF induces a decrease in $Na_v1.5$ expression and increases $Na_v1.1$ expression [65]. A reduction in overall peak I_{Na} was also documented [66]. Although other Na^+ channels have displayed an ability to induce late I_{Na}, it is unknown whether ranolazine has a similar inhibitory profile at $Na_v1.1$. Nevertheless, ranolazine's anti-fibrillatory action may be the result of its targeting

of RM-NCX1.1 exchange. NCX1.1 expression is up-regulated in human AF, while RM-NCX1.1 inhibition prevented electrical re-modelling upon short-term rapid atrial pacing in a canine model of AF. These findings suggest that Ca^{2+} influx via RM-NCX1.1 contributes to early electrical remodelling in AF [67-70]. Therefore, it is quite possible that the observations reported in previous investigations may in fact be due to ranolazine action at NCX1.1, considering that we have shown ranolazine to be a potent RM-NCX1.1 blocker.

Extra-Cardiac Implications

Not only has late I_{Na} and RM-NCX1.1 exchange have been greatly implicated in cardiac syndromes, Na^+ and Ca^{2+} homeostasis is also important in other disease states in which ranolazine may provide a therapeutic benefit. It has recently been displayed that NCX1.3 inhibition or knockout in vascular smooth muscle lowers systemic blood pressure [18]. As described above, NCX1.3 plays an important role in myogenic tone, especially considering the pathophysiology of SSH. Specifically, endogenous ouabain inhibition of vascular NKA elevates intracellular Na^+ levels, causing the reversal of NCX1.3 and 1.7. Therefore, ranolazine may be an anti-hypertensive agent in SSH. However, clinical trials studying ranolazine state that ranolazine does not alter hemodynamic parameters such as blood pressure and heart rate [71]. However, the effect of ranolazine in a hypertensive cohort has yet to be determined.

Moreover, late I_{Na} and RM-NCX1 activity have also been implicated in axonal damage in the neurodegenerative disease multiple sclerosis [72]. Na^+ channel expression, disruption and function are aberrantly affected in multiple

sclerosis. In combination with a failure in NKA function, intracellular Na^+ levels rise, leading to NCX1 reversal. Furthermore, in healthy myelinated neurons, Na^+ channels are clustered at the nodes of Ranvier while in post-mortem spinal cord examinations, $Na_v1.6$ and $Na_v1.2$ are not limited to the nodes of Ranvier and are expressed throughout demyelinated axons. Furthermore, $Na_v1.6$ elicits a persistent I_{Na}, while $Na_v1.2$ expression along demyelinated axons may be a compensatory mechanism for the conduction failure. Again as NCX1 reversal and late I_{Na} are culprits in precipitating axonal injury, ranolazine can possibly mitigate Na^+ and Ca^{2+} dysfunction in multiple sclerosis [72-75].

Lastly, pharmacological NCX1 inhibition has been shown to increase insulin secretion from pancreatic β-cells. FM-NCX1.3 and NCX1.7 are important in regulating intracellular Ca^{2+} levels for Ca^{2+}-dependent insulin granule exocytosis. Partial inhibition of NCX1-mediated Ca^{2+} extrusion with KB-R7943 has been shown to increase insulin secretion in a glucose-dependent manner [13]. It is interesting to remark that analysis of HbA1c levels from ranolazine subjects in the MERLIN-TIMI-36 clinical trial has shown a significant improvement versus patients on placebo [76]. Though many of the ranolazine patients were concurrently on sulfonylurea therapy, the addition of ranolazine further decreased HbA1c levels. It is plausible that ranolazine may have an anti-diabetic effect via partial FM-NCX1 inhibition, although this remains to be determined conclusively.

K_{ATP} Channel Studies

Pharmacogenomic Implications for Type-2 Diabetes

SUs elicit their insulinotropic effects via inhibition of the K_{ATP} channel by binding to the SUR1 subunit. This subunit plays a critical role in regulating K_{ATP} channel activity, as demonstrated by the observation that gain-of-function mutations in SUR1 can result in ND while loss-of-function mutations precipitate HI [77-80]. Depending on the severity of either HI or ND, a pharmacological approach is can be employed to treat these conditions, with the use of either KCOs or SUs, respectively. Furthermore, it may be possible that specific SUs or KCOs may be more effective at regulating K_{ATP} channel activity, understanding how particular mutations affect SUR1 function. This notion has been alluded to in the treatment of ND and HI [81,82]. However, the examination of differential K_{ATP} pharmacology in ND and HI has yet to exhibit whether specific SUs or KCOs are more effective than others for specific SUR1 mutations.

Although rare monogenic mutations of the K_{ATP} channel result in ND or HI, SNPs, such as the discovered E23K in the $K_{IR}6.2$ subunit of the K_{ATP} channel, may alter K_{ATP} function in manner predisposing to type-2 diabetes. Further highlighting the K_{ATP} channel as a focal point in type-2 diabetes was the discovery that the S1369A SNP in SUR1 co-segregates with E23K with a ~95% frequency. This discovery created a K_{ATP} channel haplotype which 20% of the type-2 diabetic population already possesses [83]. Furthermore, another study detailed that the SU gliclazide was more effective in reducing blood glucose levels in patients expressing the E23K-S1369A K_{ATP} channel variant [84]. These

findings provided clinical evidence that the S1369A-SUR1 variant may also contribute to type-2 diabetes risk and that S1369A may have a direct impact on SU pharmacology. Indeed, our functional studies concluded that gliclazide, an A-site SU, more potently inhibited the haplotype K23-A1369 K_{ATP} channel versus the wild-type E23-S1369. This is a noteworthy observation as the SU A-site is located proximally to NBF2, in which the intrinsic MgATPase activity of SUR1 is located. Moreover, the haplotype K_{ATP} channel possessed a significant decrease in MgATP sensitivity. Together, these findings implicated the intrinsic MgATPase function of SUR1 which in some manner increased K_{ATP} channel activity, yet also increased gliclazide potency.

Molecular Mechanism for Increased Gliclazide Sensitivity in A1369-SUR1 containing K_{ATP} Channels.

The SUR1-MgATPase activity has recent been characterized [87]. The intrinsic MgATPase of SUR1 is housed within the NBF1 and NBF2 intracellular domains of SUR1, forming a functional dimer, which catalyzes the hydrolysis of MgATP to MgADP [85,86]. Although as separate constructs, NBF1 and NBF2 can independently catalyze MgATP at a lower rate than SUR1. Therefore, it is possible that the higher ATPase activity of full length SUR1 as part of the K_{ATP} channel complex is the result of physical-functional interactions and cooperation between proximal SUR1 subunits. These interactions may aid in conformational changes in the NBF dimer which can influence MgATP binding and hydrolysis [87]. Supporting this assertion is the finding that that a R1380L mutation in SUR1 is immediately upstream of the Walker A motif of NBF2. This particular

mutation, which causes ND, has been shown to up-regulate MgATP hydrolysis, increasing the rate of MgADP formation and its dwell time in the post-hydrolytic state [88]. Therefore, it is possible that subtle alterations to the MgATPase function of SUR1 can increase the susceptibility to develop type-2 diabetes.

As mutations in the NBD2 domain that contain the intrinsic MgATPase activity of SUR1 can cause overt ND, we investigated whether the S1369A-SUR1 mutation exhibited changes in MgATP hydrolysis. We hypothesized that S1369A would increase MgATPase function in a manner similar to what was documented in the characterization of R1380L-SUR1 [88]. To test this hypothesis, a novel flurometric assay of SUR1 was developed in our laboratory in order to measure MgATPase activity of NBF1 and NBF2 protein constructs [89]. In this assay, SUR1-MgATPase function is coupled to the generation of the fluorescent product resorufin (Figure 5-1A). Preliminary results obtained with assay exhibit that the NBF1-A1369-NBF2 has higher MgATPase activity than NBF1-S1369-NBF2 (Figure 5-1B) [90]. Not only has this been investigated using enzymatic activity measures, the difference in enzymatic activity can also be separated using GTP in inside-out patch clamp studies. GTP is unable to inhibit the K_{ATP} channel via $K_{IR}6.2$, yet it retains its ability to be hydrolyzed by the SUR1-MgATPase leading to K_{ATP} channel stimulation [91]. Therefore, a larger stimulation of K_{ATP} channel current is observed upon application of MgGTP in patches containing the haplotype channel versus the wild type channel (Figure 5-2) [92]. Together, these observations are consistent in proving the inference that S1369A- SUR1 does in fact increase intrinsic MgATPase activity. By doing so the haplotype increases the

time in which MgADP occupies the post-hydrolytic state stimulating K_{ATP} channel activity.

Furthermore, these data may also contribute to the heightened sensitivity of the haplotype K_{ATP} channel for the A-site ligand gliclazide. The mutation of serine at 1237 for tyrosine, in the intracellular loop between transmembrane helices 15 and 16, removes gliclazide inhibition of K_{ATP} channels [93]. Coincidently, residue 1237 lies within the vicinity of NBF2. Therefore it is possible that the A-site selectivity of gliclazide in the haplotype is due to a change in conformational structure relationship between the intracellular loop between transmembrane segments 15 and 16 and the NBF2 domain. Furthermore, the AB-site ligand glibenclamide did not possess any additional sensitivity for the A-site. In fact, A1369 containing K_{ATP} channels were less sensitive to glibenclamide as well as the B-site agent repaglinide. Therefore, it may be possible that the A1369 mutation reduced AB-site and B-site drug affinity as well, although this notion would require further investigation. Furthermore, it is possible that other A-site ligands such as nateglinide and mitiglinide may also have similar outcomes as gliclazide.

Therefore, functional characterization of the S1369A variant of SUR1 in conjunction with E23K in $K_{IR}6.2$ has revealed a novel molecular mechanism for the development of type-2 diabetes. Furthermore, the finding that gliclazide has a potent inhibitory effect on the haplotype K_{ATP} channel is evidence that K_{ATP} can be a pharmacogenomic target to tailor type-2 diabetes therapy. Moreover, not

only do these findings directly impact type-2 diabetes treatment, these findings can also influence myocardial function.

Extra-Pancreatic Effects of SUs: Implications on Cardiac Rhythm.

As K_{ATP} channels are also expressed in the myocardium, SUs may also affect the heart. The cardiac K_{ATP} channel, composed of $K_{IR}6.2$ and SUR2A, serves to regulate action potential duration during conditions of metabolic stress [94]. For instance, during sinus tachycardia, K_{ATP} channels are activated shortening the refractory period appropriately in order allow an elevated heart rate while maintaining a diastolic period. However during IR, the ATP:ADP ratio decreases, thereby excessively activating cardiac K_{ATP} channels. K_{ATP} activation would hyperpolarize the membrane potential, reducing intracellular Ca^{2+} influx, protecting the myocardium from ischemic damage in the way of stunning and infarct formation [95]. Therefore, opening K_{ATP} channels pharmacologically, using KCOs such as diazoxide or pinacidil have been shown to improve cardiac function after IR. Conversely, SUs would be detrimental during IR, through closing K_{ATP} channels [96]. Moreover, SUs possessing similar affinities for SUR1 and SUR2A, such as glibenclamide and meglitinide, have been implicated in producing cardiotoxicity, especially in IR [97]. However, gliclazide has a high specificity for SUR1 (IC_{50} = 184 ± 30 nM β-cell; 19.5 ± 5.4 μM, [98]) and would be better suited in for type-2 diabetes treatment, especially considering that 20% of the type-2 diabetic population possesses the K23-A1369 K_{ATP} channel haplotype [83].

However, cardiac K_{ATP} physiology has an added level of complexity. It is known that SUR1 is expressed in the atria while SUR2A is expressed in the ventricles [99]. This presents an interesting challenge in predicting the behaviour of action potential propagation and duration through the atria versus the ventricles, especially during metabolic stress. SUR2A exhibits less affinity for ATP than its SUR1 counterpart at both NBF1 and more importantly at NBF2, which possesses the intrinsic MgATPase activity of SURs [100]. In regards to MgATPase activity, SUR2A has a reported MgATP hydrolysis rate (in nM P_i/min/mg protein) of 8.6 and 10.7 for NBF1 and NBF2, respectively, while SUR1 possesses MgATPase rates of 10.2 at NBF1 and 20.4 at NBF2, respectively [101]. Therefore, K_{ATP} channels containing SUR1 would tend to be open at rest as SUR1 has a higher rate of MgATP hydrolysis and a higher affinity for MgADP [100]. Therefore, it is possible K_{ATP} channels act in the physiological maintenance of the action potential repolarization and the refractory period in the atria. However, this notion would require further investigation.

However, during AF or IR, the differential cardiac expression of SUR1 and SUR2A becomes further complex. Knockout studies exhibit that KO of either SUR2A or SUR1 is cardioprotective during IR [102,103]. Therefore, if atria solely express SUR1 and ventricles SUR2A, it is then possible that a compensatory mechanism in the models studied is acting to effect cardioprotection. Nevertheless, the differential expression of K_{ATP} in the myocardium can be exploited for the treatment of atrial arrhythmias. Lengthening the action potential is one strategy to correct atrial fibrillation [104]. Inhibitors of

the atrial specific $K_v1.5$ channel, such as AVE0118, have been developed to inhibit ultra-rapid repolarization by $K_v1.5$ [105,106]. Therefore, SUs can also be employed to treat AF, specifically those which have higher SUR1 selectivity such as gliclazide (Figure 5-3).

However, the consequence of possessing the K23-A1369 K_{ATP} channel haplotype has yet to be explored in AF, which may substantiate evidence for an independent risk association between type-2 diabetes and AF [107]. When comparing SUR2A MgATPase activity to SUR1, SUR1 has a higher rate of MgATP hydrolysis than SUR2A increasing K_{ATP} channel activity. The haplotype K_{ATP} channel has a further increased MgATPase activity, which would effectively increase the rate of MgADP binding, up-regulating K_{ATP} channel activity. It is possible that the increased rate of MgADP production and binding at A1369-SUR1, in combination with the decreased sensitivity of K23-$K_{IR}6.2$ to ATP, can be proarrhythmic as increased K_{ATP} channel opening can possibly shorten the action potential duration. Furthermore, as the A1369-SUR1, K23-$K_{IR}6.2$ K_{ATP} channel can be expressed in the atria, the selectivity of the A-site ligand gliclazide for potency at the haplotype channel can be exploited in the treatment of AF. Considering that type-2 diabetes predisposes individuals to AF, especially now in the cohort of type-2 diabetes patients possessing the haplotype K_{ATP} channel, gliclazide would in fact be the more favourable approach in treating type-2 diabetes. This approach would have the added benefit of protecting against AF while avoiding the cardiotoxicity of SUs which have similarities affinities to SUR2A such as glibenclamide or meglitinide (Figure 5-4).

Summary and Conclusions

The interaction of NCX1 and K_{ATP} in cardiac IR and type-2 diabetes is highlighted by their dependence on the membrane potential and cellular energy status. In regards to NCX1 in cardiac IR, I have shown that ROS augments RM-NCX1.1 activity, increasing intracellular Ca^{2+} which contributes to cardiac IR injury. I also delineated that the ASR region is the putative site of direct ROS-modification of NCX1 proteins, which may mediate the physiological and pathophysiological functions in the pancreas, the brain and the vasculature. As NCX1 has become a target for therapeutic modulation, I also show that the recently-approved late I_{Na} inhibitor ranolazine to be a novel NCX1 inhibitor. This finding has positive implications in cardiac IR injury, as well as AF, hypertension, and possibly type-2 diabetes. Although NCX1 inhibition in type-2 diabetes is a strong candidate for pharmacological development, SUs have been the mainstay treatment option in type-2 diabetes for years. The discovery of the haplotype K_{ATP} channel having a higher potency for the SUR1 specific agent gliclazide brings about the importance of a pharmacogenomic approach to SU therapy in type-2 diabetes. This also gives insight into the current paradigms for AF treatment, as gliclazide's potency for SUR1-K_{ATP} channels can be exploited for prophylaxis of AF, considering the co-morbidity of AF and type-2 diabetes, and 10% of the general population carrying the K23-A1369 K_{ATP} genotype.

In conclusion, the presentation of the data outlined in this thesis further supports a key role for NCX1 as the locus of myocardial injury during IR, and has advanced our understanding of the functional aspects of NCX1 and its splice

variants. Furthermore, the study of the haplotype K_{ATP} channel indicates that the intrinsic MgATPase activity is crucial to its function. As outlined above, the work contained in this thesis has direct implications on cardiac IR therapy, which can be applied directly to heart failure, arrhythmogenesis, hypertension, and type-2 diabetes treatment. Finally, an ultimate strategy would be to pharmacologically target proteins involved in both type-2 diabetes and cardiac syndromes, simultaneously improving the outcomes of these co-morbid conditions.

Figure 5-1

A Novel Enyzmatic Assay for the Detection of Liberated P_i from SUR1-MgATPase Activity. (A) The reaction scheme of a flurometric assay, which couples P_i generation from SUR1-MgATPase to the fluorescence of resorufin. **(B)** Preliminary results depicting an increase in MgATPase activity of NBF1-NBF2 protein constructs from SUR1 containing the A1369 variant. K_m(S1369) = 0.54 ± 0.03mM, K_m(A1369) = 0.37 ± 0.04mM, n=6-9 assays; V_{max}(S1369) = 2.81 ± 0.07, V_{max}(A1369) = 3.99 ± 0.12, n=3 assays. *P<0.05 [90].

A.

1. $MgATP \xrightarrow{SUR1\text{-}ATPase} MgADP + P_i$
2. $P_i + pyruvate + O_2 \xrightarrow{pyruvate\ oxidase} acetyl\text{-}PO_4 + CO_2 + H_2O_2$
3. $Amplex\ Red + H_2O_2 \xrightarrow{horseradish\ peroxidase} H_2O + resorufin^*$

B.

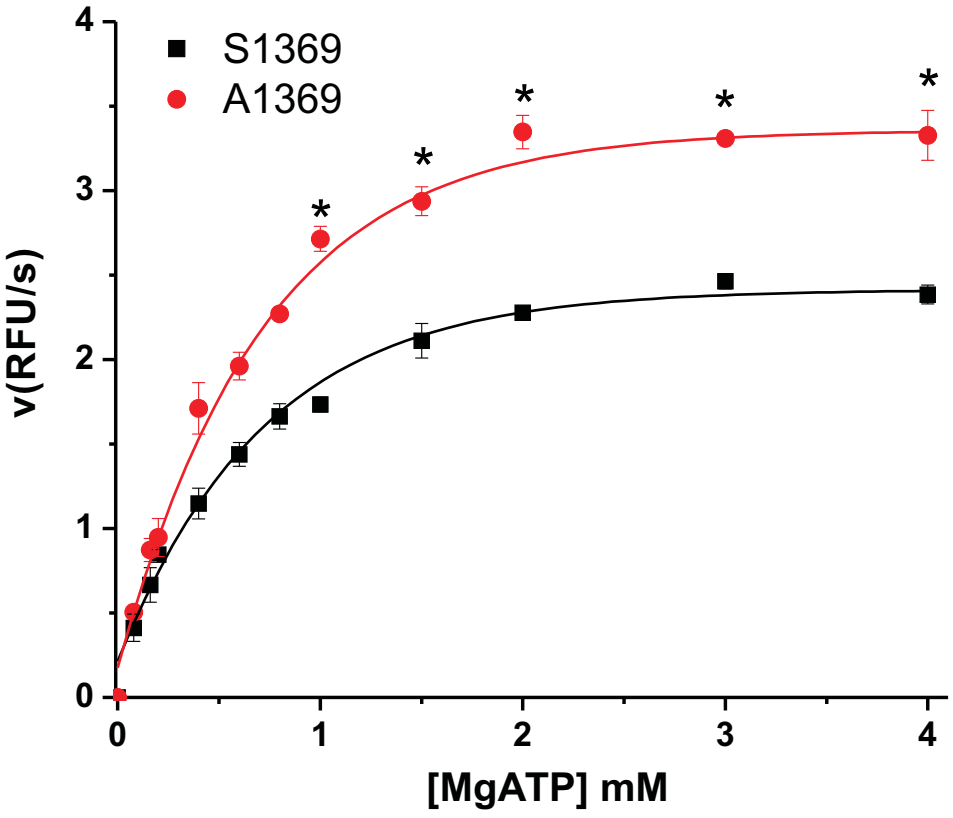

Figure 5-2

GTP Stimulation is Elevated in K_{ATP} channels containing the A1369-SUR1 Variant. (A-C) Representative recordings of the E23-S1369, K23-A1369 and E23-A1369 K_{ATP} channel variants exhibiting increases in current upon application of 1mM GTP. (D) Grouped data displaying that the A1369-expressing K_{ATP} channels have augmented GTP-mediated activation. All values are expressed as $I_{GTP+ATP}/I_{ATP}$. E23-S1369 = 1.82 ± 0.05, K23-A136 = 3.24 ± 0.14, E23-A1369 = 2.99 ± 0.14, n=17-19 patches per group, *P<0.0001. [92].

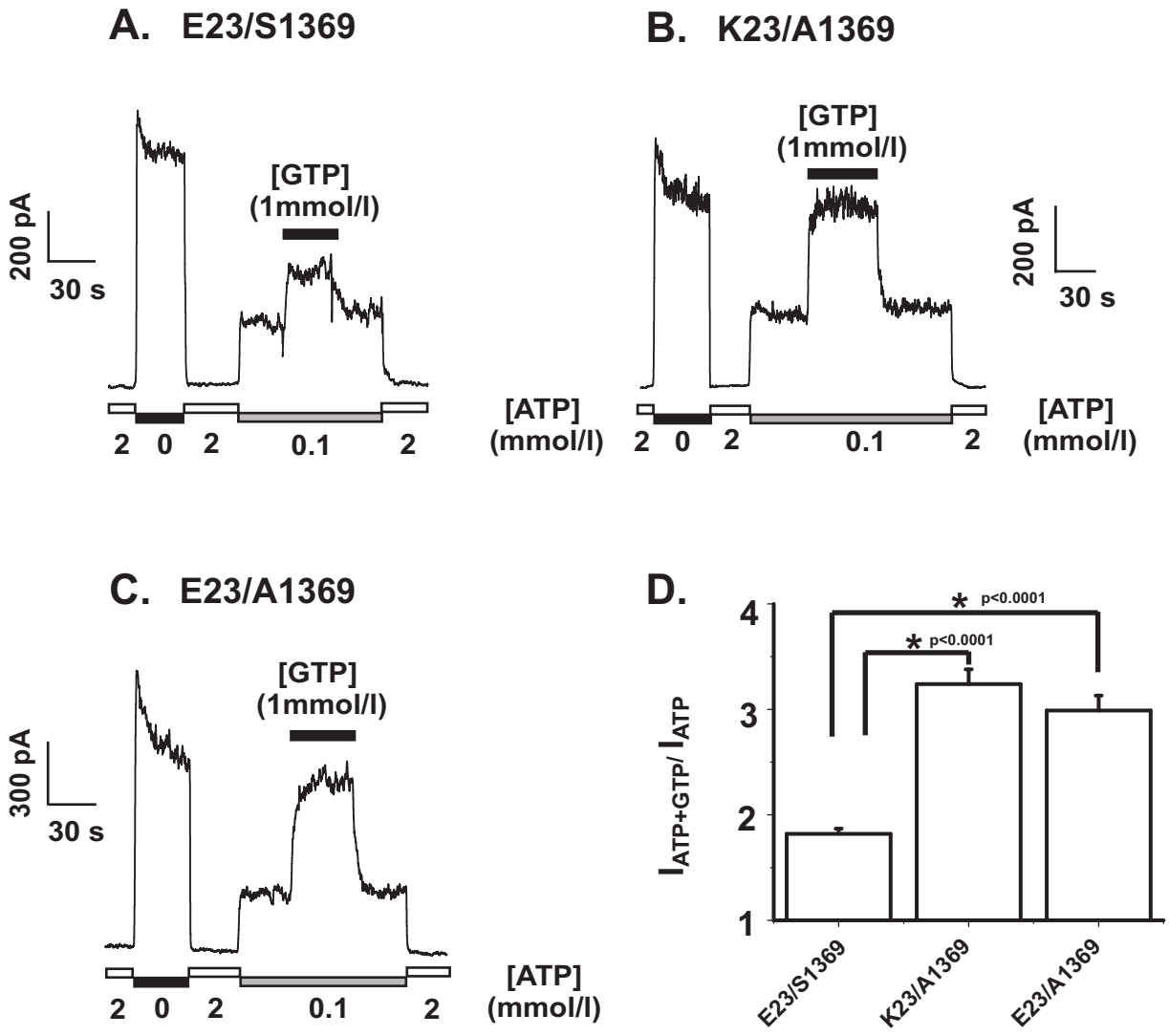
A. E23/S1369
B. K23/A1369
[GTP]
(1mmol/l)
200 pA
30 s
[ATP]
(mmol/l)
2 0 2 0.1 2
C. E23/A1369
300 pA
D.
* p<0.0001
* p<0.0001
I ATP+GTP/ I ATP
4
3
2
1
E23/S1369
K23/A1369
E23/A1369

Figure 5-3

Approaches to Normalization of the Action Potential in Atrial Fibrillation. **(A)** In AF, precipitated by a shortened action potential due to IR, as SUR1 is expressed in atria, SUR1 specific SUs such as gliclazide can act to inhibit K_{ATP} channel current, working to slow repolarization time, lengthening the action potential. **(B)** In heart failure, a lengthening of the action potential, with the susceptibility of EAD and DAD formation, leading to AF. Ranolazine inhibition of RM-NCX1.1 and also late I_{Na} would act to shorten the action potential, reducing EAD and DAD development, normalizing the action potential.

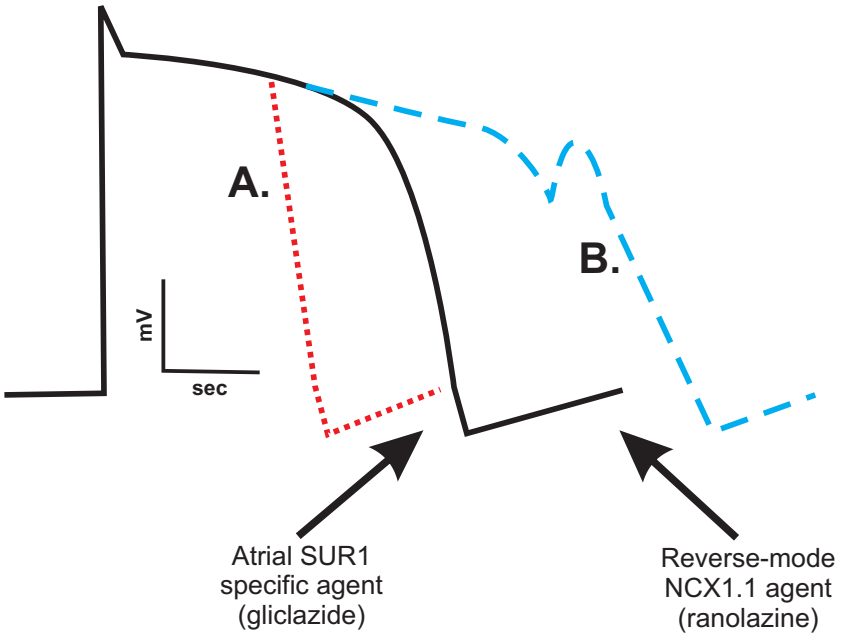
A.
B.
mV
sec
Atrial SUR1
specific agent
(gliclazide)
Reverse-mode
NCX1.1 agent
(ranolazine)

Figure 5-4

The Selectivity of Sulfonylureas and Glinides at Cardiac and Pancreatic K_{ATP} Channels. Sulfonylureas and glinide agents used in the treatment of type-2 diabetes were examined as to their reported selectivity for SUR1 receptors in the pancreas and atrial versus SUR2a in the ventricles, and the SUR1:SUR2a IC_{50} ratio calculated (see right). Also, approximate values for the steady-state plasma concentrations were plotted. [108]

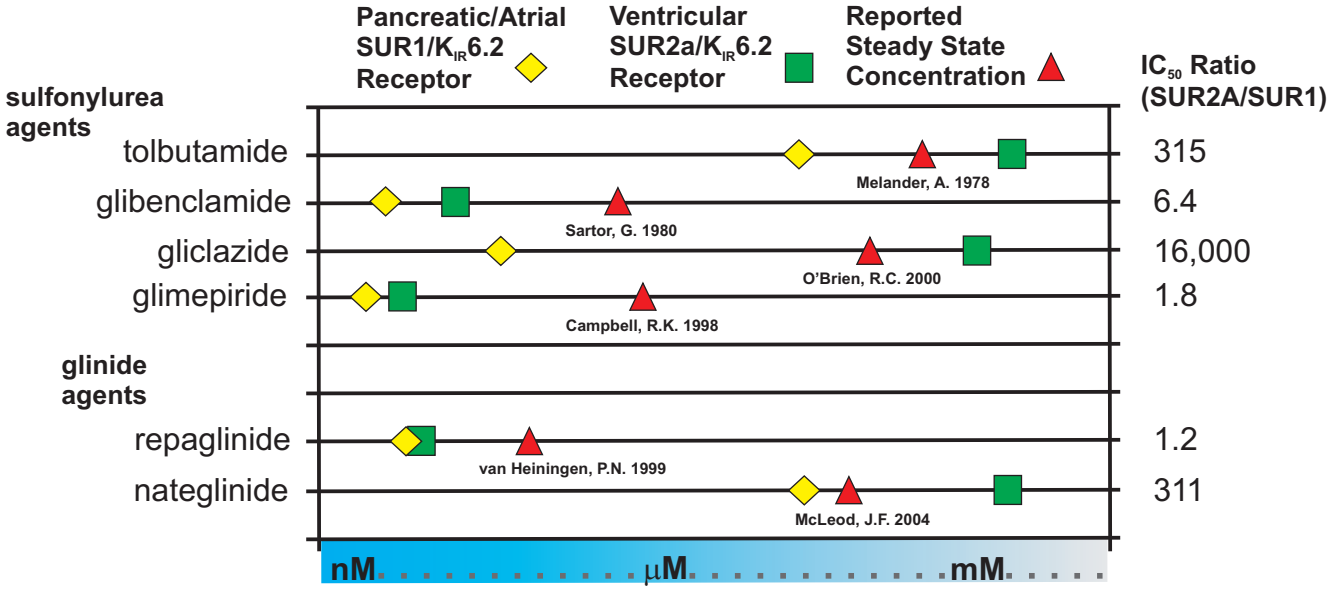
Pancreatic/Atrial
SUR1/K$_{IR}$6.2
Receptor
Ventricular
SUR2a/K$_{IR}$6.2
Receptor
Reported
Steady State
Concentration
IC$_{50}$ Ratio
(SUR2A/SUR1)
sulfonylurea
agents
tolbutamide
glibenclamide
gliclazide
glimepiride
glinide
agents
repaglinide
nateglinide
Melander, A. 1978
Sartor, G. 1980
O'Brien, R.C. 2000
Campbell, R.K. 1998
van Heiningen, P.N. 1999
McLeod, J.F. 2004
315
6.4
16,000
1.8
1.2
311
nM
μM
mM

References

1. Hearse DJ, Humphrey SM, Bullock GR. The oxygen paradox and the calcium paradox: two facets of the same problem? J.Mol.Cell.Cardiol. 1978 Jul;10(7):641-668.

2. Reeves JP, Bailey CA, Hale CC. Redox modification of sodium-calcium exchange activity in cardiac sarcolemmal vesicles. J.Biol.Chem. 1986 Apr 15;261(11):4948-4955.

3. Shi ZQ, Davison AJ, Tibbits GF. Effects of active oxygen generated by DTT/Fe2+ on cardiac Na+/Ca2+ exchange and membrane permeability to Ca2+. J.Mol.Cell.Cardiol. 1989 Oct;21(10):1009-1016.

4. Beresewicz A, Horackova M. Alterations in electrical and contractile behavior of isolated cardiomyocytes by hydrogen peroxide: possible ionic mechanisms. J.Mol.Cell.Cardiol. 1991 Aug;23(8):899-918.

5. Goldhaber JI. Free radicals enhance Na+/Ca2+ exchange in ventricular myocytes. Am.J.Physiol. 1996 Sep;271(3 Pt 2):H823-33.

6. Santacruz-Toloza L, Ottolia M, Nicoll DA, Philipson KD. Functional analysis of a disulfide bond in the cardiac Na(+)-Ca(2+) exchanger. J.Biol.Chem. 2000 Jan 7;275(1):182-188.

7. Eigel BN, Gursahani H, Hadley RW. ROS are required for rapid reactivation of Na+/Ca2+ exchanger in hypoxic reoxygenated guinea pig ventricular myocytes. Am.J.Physiol.Heart Circ.Physiol. 2004 Mar;286(3):H955-63.

8. Wagner S, Seidler T, Picht E, Maier LS, Kazanski V, Teucher N, et al. Na(+)-Ca(2+) exchanger overexpression predisposes to reactive oxygen species-induced injury. Cardiovasc.Res. 2003 Nov 1;60(2):404-412.

9. Hilge M, Aelen J, Vuister GW. Ca2+ regulation in the Na+/Ca2+ exchanger involves two markedly different Ca2+ sensors. Mol.Cell 2006 Apr 7;22(1):15-25.

10. Dunn J, Elias CL, Le HD, Omelchenko A, Hryshko LV, Lytton J. The molecular determinants of ionic regulatory differences between brain and kidney Na+/Ca2+ exchanger (NCX1) isoforms. J.Biol.Chem. 2002 Sep 13;277(37):33957-33962.

11. Maack C, Ganesan A, Sidor A, O'Rourke B. Cardiac sodium-calcium exchanger is regulated by allosteric calcium and exchanger inhibitory peptide at distinct sites. Circ.Res. 2005 Jan 7;96(1):91-99.

12. Pi J, Bai Y, Zhang Q, Wong V, Floering LM, Daniel K, et al. Reactive oxygen species as a signal in glucose-stimulated insulin secretion. Diabetes 2007 Jul;56(7):1783-1791.

13. Hamming KS, Soliman D, Webster NJ, Searle GJ, Matemisz LC, Liknes DA, et al. Inhibition of {beta}-cell sodium-calcium exchange enhances glucose-dependent elevations in cytoplasmic calcium and insulin secretion. Diabetes 2010 Apr 22.

14. Cowley AW,Jr. Long-term control of arterial blood pressure. Physiol.Rev. 1992 Jan;72(1):231-300.

15. Davis MJ, Hill MA. Signaling mechanisms underlying the vascular myogenic response. Physiol.Rev. 1999 Apr;79(2):387-423.

16. Moosmang S, Schulla V, Welling A, Feil R, Feil S, Wegener JW, et al. Dominant role of smooth muscle L-type calcium channel Cav1.2 for blood pressure regulation. EMBO J. 2003 Nov 17;22(22):6027-6034.

17. Pritchard TJ, Bowman PS, Jefferson A, Tosun M, Lynch RM, Paul RJ. Na+-K+ ATPase and Ca2+ Clearance Proteins in Smooth Muscle: A Functional Unit. Am.J.Physiol.Heart Circ.Physiol. 2010 Jun 11.

18. Zhang J, Ren C, Chen L, Navedo MF, Antos LK, Kinsey SP, et al. Knockout of Na+/Ca2+ exchanger in smooth muscle attenuates vasoconstriction and L-type Ca2+ channel current and lowers blood pressure. Am.J.Physiol.Heart Circ.Physiol. 2010 May;298(5):H1472-83.

19. Raina H, Ella SR, Hill MA. Decreased activity of the smooth muscle Na+/Ca2+ exchanger impairs arteriolar myogenic reactivity. J.Physiol. 2008 Mar 15;586(6):1669-1681.

20. Blaustein MP, Lederer WJ. Sodium/calcium exchange: its physiological implications. Physiol.Rev. 1999 Jul;79(3):763-854.

21. Iwamoto T, Kita S, Zhang J, Blaustein MP, Arai Y, Yoshida S, et al. Salt-sensitive hypertension is triggered by Ca2+ entry via Na+/Ca2+ exchanger type-1 in vascular smooth muscle. Nat.Med. 2004 Nov;10(11):1193-1199.

22. Blaustein MP, Zhang J, Chen L, Song H, Raina H, Kinsey SP, et al. The pump, the exchanger, and endogenous ouabain: signaling mechanisms that link salt retention to hypertension. Hypertension 2009 Feb;53(2):291-298.

23. Iwamoto T, Kita S, Katsuragi T. Salt-sensitive hypertension, Na+/Ca2+ exchanger, and vascular smooth muscle. Trends Cardiovasc.Med. 2005 Nov;15(8):273-277.

24. Blaustein MP, Zhang J, Chen L, Hamilton BP. How does salt retention raise blood pressure? Am.J.Physiol.Regul.Integr.Comp.Physiol. 2006 Mar;290(3):R514-23.

25. Manning RD,Jr, Meng S, Tian N. Renal and vascular oxidative stress and salt-sensitivity of arterial pressure. Acta Physiol.Scand. 2003 Nov;179(3):243-250.

26. Ma XL, Gao F, Nelson AH, Lopez BL, Christopher TA, Yue TL, et al. Oxidative inactivation of nitric oxide and endothelial dysfunction in stroke-prone spontaneous hypertensive rats. J.Pharmacol.Exp.Ther. 2001 Sep;298(3):879-885.

27. Unlap MT, Bates E, Williams C, Komlosi P, Williams I, Kovacs G, et al. Na+/Ca2+ exchanger: target for oxidative stress in salt-sensitive hypertension. Hypertension 2003 Sep;42(3):363-368.

28. Annunziato L, Pignataro G, Di Renzo GF. Pharmacology of brain Na+/Ca2+ exchanger: from molecular biology to therapeutic perspectives. Pharmacol.Rev. 2004 Dec;56(4):633-654.

29. Evans RM, Zamponi GW. Presynaptic Ca2+ channels--integration centers for neuronal signaling pathways. Trends Neurosci. 2006 Nov;29(11):617-624.

30. Blaustein MP, Juhaszova M, Golovina VA, Church PJ, Stanley EF. Na/Ca exchanger and PMCA localization in neurons and astrocytes: functional implications. Ann.N.Y.Acad.Sci. 2002 Nov;976:356-366.

31. Zemke D, Smith JL, Reeves MJ, Majid A. Ischemia and ischemic tolerance in the brain: an overview. Neurotoxicology 2004 Dec;25(6):895-904.

32. Matsuda T, Arakawa N, Takuma K, Kishida Y, Kawasaki Y, Sakaue M, et al. SEA0400, a novel and selective inhibitor of the Na+-Ca2+ exchanger, attenuates reperfusion injury in the in vitro and in vivo cerebral ischemic models. J.Pharmacol.Exp.Ther. 2001 Jul;298(1):249-256.

33. Luo J, Wang Y, Chen X, Chen H, Kintner DB, Shull GE, et al. Increased tolerance to ischemic neuronal damage by knockdown of Na+-Ca2+ exchanger isoform 1. Ann.N.Y.Acad.Sci. 2007 Mar;1099:292-305.

34. Amoroso S, Tortiglione A, Secondo A, Catalano A, Montagnani S, Di Renzo G, et al. Sodium nitroprusside prevents chemical hypoxia-induced cell death through iron ions stimulating the activity of the Na+-Ca2+ exchanger in C6 glioma cells. J.Neurochem. 2000 Apr;74(4):1505-1513.

35. He S, Ruknudin A, Bambrick LL, Lederer WJ, Schulze DH. Isoform-specific regulation of the Na+/Ca2+ exchanger in rat astrocytes and neurons by PKA. J.Neurosci. 1998 Jul 1;18(13):4833-4841.

36. Schroder UH, Breder J, Sabelhaus CF, Reymann KG. The novel Na+/Ca2+ exchange inhibitor KB-R7943 protects CA1 neurons in rat hippocampal slices against hypoxic/hypoglycemic injury. Neuropharmacology 1999 Feb;38(2):319-321.

37. Kiedrowski L. N-methyl-D-aspartate excitotoxicity: relationships among plasma membrane potential, Na(+)/Ca(2+) exchange, mitochondrial Ca(2+) overload, and cytoplasmic concentrations of Ca(2+), H(+), and K(+). Mol.Pharmacol. 1999 Sep;56(3):619-632.

38. Czyz A, Kiedrowski L. In depolarized and glucose-deprived neurons, Na+ influx reverses plasmalemmal K+-dependent and K+-independent Na+/Ca2+ exchangers and contributes to NMDA excitotoxicity. J.Neurochem. 2002 Dec;83(6):1321-1328.

39. Hasenfuss G, Maier LS. Mechanism of action of the new anti-ischemia drug ranolazine. Clin.Res.Cardiol. 2008 Apr;97(4):222-226.

40. Stone PH. Ranolazine: new paradigm for management of myocardial ischemia, myocardial dysfunction, and arrhythmias. Cardiol.Clin. 2008 Nov;26(4):603-614.

41. Maier LS. A novel mechanism for the treatment of angina, arrhythmias, and diastolic dysfunction: inhibition of late I(Na) using ranolazine. J.Cardiovasc.Pharmacol. 2009 Oct;54(4):279-286.

42. Vandecaetsbeek I, Raeymaekers L, Wuytack F, Vangheluwe P. Factors controlling the activity of the SERCA2a pump in the normal and failing heart. Biofactors 2009 Nov-Dec;35(6):484-499.

43. Hu ST, Shen YF, Liu GS, Lei CH, Tang Y, Wang JF, et al. Altered intracellular Ca2+ regulation in chronic rat heart failure. J.Physiol.Sci. 2010 Mar;60(2):85-94.

44. Armoundas AA, Rose J, Aggarwal R, Stuyvers BD, O'rourke B, Kass DA, et al. Cellular and molecular determinants of altered Ca2+ handling in the failing rabbit heart: primary defects in SR Ca2+ uptake and release mechanisms. Am.J.Physiol.Heart Circ.Physiol. 2007 Mar;292(3):H1607-18.

45. Hobai IA, O'Rourke B. Enhanced Ca(2+)-activated Na(+)-Ca(2+) exchange activity in canine pacing-induced heart failure. Circ.Res. 2000 Oct 13;87(8):690-698.

46. Pogwizd SM, Schlotthauer K, Li L, Yuan W, Bers DM. Arrhythmogenesis and contractile dysfunction in heart failure: Roles of sodium-calcium exchange,

inward rectifier potassium current, and residual beta-adrenergic responsiveness. Circ.Res. 2001 Jun 8;88(11):1159-1167.

47. Bers DM. Regulation of cellular calcium in cardiac myocytes. In: Page E, Fozzard HA, Solaro RJ, editors. New York, New York, USA: Oxford University Press; 2002. p. 335.

48. Bers DM, Despa S. Cardiac myocytes Ca2+ and Na+ regulation in normal and failing hearts. J.Pharmacol.Sci. 2006;100(5):315-322.

49. Undrovinas NA, Maltsev VA, Belardinelli L, Sabbah HN, Undrovinas A. Late sodium current contributes to diastolic cell Ca2+ accumulation in chronic heart failure. J.Physiol.Sci. 2010 Jul;60(4):245-257.

50. Baartscheer A, van Borren MM. Sodium ion transporters as new therapeutic targets in heart failure. Cardiovasc.Hematol.Agents Med.Chem. 2008 Oct;6(4):229-236.

51. Swift F, Birkeland JA, Tovsrud N, Enger UH, Aronsen JM, Louch WE, et al. Altered Na+/Ca2+-exchanger activity due to downregulation of Na+/K+-ATPase alpha2-isoform in heart failure. Cardiovasc.Res. 2008 Apr 1;78(1):71-78.

52. Toth A, Kiss L, Varro A, Nanasi PP. Potential therapeutic effects of Na+/Ca2+ exchanger inhibition in cardiac diseases. Curr.Med.Chem. 2009;16(25):3294-3321.

53. Bers DM. Altered cardiac myocyte Ca regulation in heart failure. Physiology (Bethesda) 2006 Dec;21:380-387.

54. Moss AJ, Zareba W, Schwarz KQ, Rosero S, McNitt S, Robinson JL. Ranolazine shortens repolarization in patients with sustained inward sodium current due to type-3 long-QT syndrome. J.Cardiovasc.Electrophysiol. 2008 Dec;19(12):1289-1293.

55. Sossalla S, Wagner S, Rasenack EC, Ruff H, Weber SL, Schondube FA, et al. Ranolazine improves diastolic dysfunction in isolated myocardium from failing human hearts--role of late sodium current and intracellular ion accumulation. J.Mol.Cell.Cardiol. 2008 Jul;45(1):32-43.

56. Wasserstrom JA, Sharma R, O'Toole MJ, Zheng J, Kelly JE, Shryock J, et al. Ranolazine antagonizes the effects of increased late sodium current on intracellular calcium cycling in rat isolated intact heart. J.Pharmacol.Exp.Ther. 2009 Nov;331(2):382-391.

57. Ferrari R, Guardigli G, Mele D, Percoco GF, Ceconi C, Curello S. Oxidative stress during myocardial ischaemia and heart failure. Curr.Pharm.Des. 2004;10(14):1699-1711.

58. Stanley WC, Recchia FA, Lopaschuk GD. Myocardial substrate metabolism in the normal and failing heart. Physiol.Rev. 2005 Jul;85(3):1093-1129.

59. Deedwania PC, Lardizabal JA. Atrial fibrillation in heart failure: a comprehensive review. Am.J.Med. 2010 Mar;123(3):198-204.

60. Hogue CW,Jr, Hyder ML. Atrial fibrillation after cardiac operation: risks, mechanisms, and treatment. Ann.Thorac.Surg. 2000 Jan;69(1):300-306.

61. Echahidi N, Pibarot P, O'Hara G, Mathieu P. Mechanisms, prevention, and treatment of atrial fibrillation after cardiac surgery. J.Am.Coll.Cardiol. 2008 Feb 26;51(8):793-801.

62. Cox JL, Canavan TE, Schuessler RB, Cain ME, Lindsay BD, Stone C, et al. The surgical treatment of atrial fibrillation. II. Intraoperative electrophysiologic mapping and description of the electrophysiologic basis of atrial flutter and atrial fibrillation. J.Thorac.Cardiovasc.Surg. 1991 Mar;101(3):406-426.

63. Konings KT, Kirchhof CJ, Smeets JR, Wellens HJ, Penn OC, Allessie MA. High-density mapping of electrically induced atrial fibrillation in humans. Circulation 1994 Apr;89(4):1665-1680.

64. Kumar K, Nearing BD, Carvas M, Nascimento BC, Acar M, Belardinelli L, et al. Ranolazine exerts potent effects on atrial electrical properties and abbreviates atrial fibrillation duration in the intact porcine heart. J.Cardiovasc.Electrophysiol. 2009 Jul;20(7):796-802.

65. Sossalla S, Kallmeyer B, Wagner S, Mazur M, Maurer U, Toischer K, et al. Altered Na(+) currents in atrial fibrillation effects of ranolazine on arrhythmias and contractility in human atrial myocardium. J.Am.Coll.Cardiol. 2010 May 25;55(21):2330-2342.

66. Yue L, Melnyk P, Gaspo R, Wang Z, Nattel S. Molecular mechanisms underlying ionic remodeling in a dog model of atrial fibrillation. Circ.Res. 1999;84:776-784.

67. Schotten U, Greiser M, Benke D, Buerkel K, Ehrenteidt B, Stellbrink C, et al. Atrial fibrillation-induced atrial contractile dysfunction: a tachycardiomyopathy of a different sort. Cardiovasc.Res. 2002 Jan;53(1):192-201.

68. El-Armouche A, Boknik P, Eschenhagen T, Carrier L, Knaut M, Ravens U, et al. Molecular determinants of altered Ca2+ handling in human chronic atrial fibrillation. Circulation 2006 Aug 15;114(7):670-680.

69. Miyata A, Zipes DP, Hall S, Rubart M. Kb-R7943 prevents acute, atrial fibrillation-induced shortening of atrial refractoriness in anesthetized dogs. Circulation 2002 Sep 10;106(11):1410-1419.

70. Schotten U, Verheule S, Kerfant BG, Greiser M. Enhanced late na(+) currents in atrial fibrillation new drug target or just an epiphenomenon? J.Am.Coll.Cardiol. 2010 May 25;55(21):2343-2345.

71. Antzelevitch C, Belardinelli L, Zygmunt AC, Burashnikov A, Di Diego JM, Fish JM, et al. Electrophysiological effects of ranolazine, a novel antianginal agent with antiarrhythmic properties. Circulation 2004 Aug 24;110(8):904-910.

72. Kurnellas MP, Donahue KC, Elkabes S. Mechanisms of neuronal damage in multiple sclerosis and its animal models: role of calcium pumps and exchangers. Biochem.Soc.Trans. 2007 Nov;35(Pt 5):923-926.

73. Craner MJ, Lo AC, Black JA, Waxman SG. Abnormal sodium channel distribution in optic nerve axons in a model of inflammatory demyelination. Brain 2003 Jul;126(Pt 7):1552-1561.

74. Craner MJ, Newcombe J, Black JA, Hartle C, Cuzner ML, Waxman SG. Molecular changes in neurons in multiple sclerosis: altered axonal expression of Nav1.2 and Nav1.6 sodium channels and Na+/Ca2+ exchanger. Proc.Natl.Acad.Sci.U.S.A. 2004 May 25;101(21):8168-8173.

75. Craner MJ, Hains BC, Lo AC, Black JA, Waxman SG. Co-localization of sodium channel Nav1.6 and the sodium-calcium exchanger at sites of axonal injury in the spinal cord in EAE. Brain 2004 Feb;127(Pt 2):294-303.

76. Chisholm JW, Goldfine AB, Dhalla AK, Braunwald E, Morrow DA, Karwatowska-Prokopczuk E, et al. Effect of ranolazine on A1C and glucose levels in hyperglycemic patients with non-ST elevation acute coronary syndrome. Diabetes Care 2010 Jun;33(6):1163-1168.

77. Gloyn AL, Pearson ER, Antcliff JF, Proks P, Bruining GJ, Slingerland AS, et al. Activating mutations in the gene encoding the ATP-sensitive potassium-channel subunit Kir6.2 and permanent neonatal diabetes. N.Engl.J.Med. 2004 Apr 29;350(18):1838-1849.

78. Shyng SL, Ferrigni T, Shepard JB, Nestorowicz A, Glaser B, Permutt MA, et al. Functional analyses of novel mutations in the sulfonylurea receptor 1

associated with persistent hyperinsulinemic hypoglycemia of infancy. Diabetes 1998 Jul;47(7):1145-1151.

79. Ashcroft FM. ATP-sensitive potassium channelopathies: focus on insulin secretion. J.Clin.Invest. 2005 Aug;115(8):2047-2058.

80. Babenko AP, Polak M, Cave H, Busiah K, Czernichow P, Scharfmann R, et al. Activating mutations in the ABCC8 gene in neonatal diabetes mellitus. N.Engl.J.Med. 2006 Aug 3;355(5):456-466.

81. Sattiraju S, Reyes S, Kane GC, Terzic A. K(ATP) channel pharmacogenomics: from bench to bedside. Clin.Pharmacol.Ther. 2008 Feb;83(2):354-357.

82. Koster JC, Remedi MS, Dao C, Nichols CG. ATP and sulfonylurea sensitivity of mutant ATP-sensitive K+ channels in neonatal diabetes: implications for pharmacogenomic therapy. Diabetes 2005 Sep;54(9):2645-2654.

83. Florez JC, Burtt N, de Bakker PI, Almgren P, Tuomi T, Holmkvist J, et al. Haplotype structure and genotype-phenotype correlations of the sulfonylurea receptor and the islet ATP-sensitive potassium channel gene region. Diabetes 2004 May;53(5):1360-1368.

84. Feng Y, Mao G, Ren X, Xing H, Tang G, Li Q, et al. Ser1369Ala variant in sulfonylurea receptor gene ABCC8 is associated with antidiabetic efficacy of gliclazide in Chinese type 2 diabetic patients. Diabetes Care 2008 Oct;31(10):1939-1944.

85. Nichols CG. KATP channels as molecular sensors of cellular metabolism. Nature 2006 Mar 23;440(7083):470-476.

86. Masia R, Nichols CG. Functional clustering of mutations in the dimer interface of the nucleotide binding folds of the sulfonylurea receptor. J.Biol.Chem. 2008 Oct 31;283(44):30322-30329.

87. de Wet H, Mikhailov MV, Fotinou C, Dreger M, Craig TJ, Venien-Bryan C, et al. Studies of the ATPase activity of the ABC protein SUR1. FEBS J. 2007 Jul;274(14):3532-3544.

88. de Wet H, Rees MG, Shimomura K, Aittoniemi J, Patch AM, Flanagan SE, et al. Increased ATPase activity produced by mutations at arginine-1380 in nucleotide-binding domain 2 of ABCC8 causes neonatal diabetes. Proc.Natl.Acad.Sci.U.S.A. 2007 Nov 27;104(48):18988-18992.

89. Holt A. Unpublished observations. 2010.

90. Raja M. Unpublished observations. 2010.

91. Trapp S, Tucker SJ, Ashcroft FM. Activation and inhibition of K-ATP currents by guanine nucleotides is mediated by different channel subunits. Proc.Natl.Acad.Sci.U.S.A. 1997 Aug 5;94(16):8872-8877.

92. Fatehi M. Unpublished observations. 2010.

93. Winkler M, Stephan D, Bieger S, Kuhner P, Wolff F, Quast U. Testing the bipartite model of the sulfonylurea receptor binding site: binding of A-, B-, and A + B-site ligands. J.Pharmacol.Exp.Ther. 2007 Aug;322(2):701-708.

94. Zingman LV, Alekseev AE, Hodgson-Zingman DM, Terzic A. ATP-sensitive potassium channels: metabolic sensing and cardioprotection. J.Appl.Physiol. 2007 Nov;103(5):1888-1893.

95. Baczko I, Giles WR, Light PE. Resting membrane potential regulates Na(+)-Ca2+ exchange-mediated Ca2+ overload during hypoxia-reoxygenation in rat ventricular myocytes. J.Physiol. 2003 Aug 1;550(Pt 3):889-898.

96. Baczko I, Jones L, McGuigan CF, Manning Fox JE, Gandhi M, Giles WR, et al. Plasma membrane KATP channel-mediated cardioprotection involves posthypoxic reductions in calcium overload and contractile dysfunction: mechanistic insights into cardioplegia. FASEB J. 2005 Jun;19(8):980-982.

97. Negroni JA, Lascano EC, del Valle HF. Glibenclamide action on myocardial function and arrhythmia incidence in the healthy and diabetic heart. Cardiovasc.Hematol.Agents Med.Chem. 2007 Jan;5(1):43-53.

98. Lawrence CL, Proks P, Rodrigo GC, Jones P, Hayabuchi Y, Standen NB, et al. Gliclazide produces high-affinity block of KATP channels in mouse isolated pancreatic beta cells but not rat heart or arterial smooth muscle cells. Diabetologia 2001 Aug;44(8):1019-1025.

99. Flagg TP, Kurata HT, Masia R, Caputa G, Magnuson MA, Lefer DJ, et al. Differential structure of atrial and ventricular KATP: atrial KATP channels require SUR1. Circ.Res. 2008 Dec 5;103(12):1458-1465.

100. Burke MA, Mutharasan RK, Ardehali H. The sulfonylurea receptor, an atypical ATP-binding cassette protein, and its regulation of the KATP channel. Circ.Res. 2008 Feb 1;102(2):164-176.

101. Masia R, Enkvetchakul D, Nichols CG. Differential nucleotide regulation of KATP channels by SUR1 and SUR2A. J.Mol.Cell.Cardiol. 2005 Sep;39(3):491-501.

102. Elrod JW, Harrell M, Flagg TP, Gundewar S, Magnuson MA, Nichols CG, et al. Role of sulfonylurea receptor type 1 subunits of ATP-sensitive potassium channels in myocardial ischemia/reperfusion injury. Circulation 2008 Mar 18;117(11):1405-1413.

103. Stoller D, Kakkar R, Smelley M, Chalupsky K, Earley JU, Shi NQ, et al. Mice lacking sulfonylurea receptor 2 (SUR2) ATP-sensitive potassium channels are resistant to acute cardiovascular stress. J.Mol.Cell.Cardiol. 2007 Oct;43(4):445-454.

104. Ehrlich JR. Inward rectifier potassium currents as a target for atrial fibrillation therapy. J.Cardiovasc.Pharmacol. 2008 Aug;52(2):129-135.

105. Gogelein H, Brendel J, Steinmeyer K, Strubing C, Picard N, Rampe D, et al. Effects of the atrial antiarrhythmic drug AVE0118 on cardiac ion channels. Naunyn Schmiedebergs Arch.Pharmacol. 2004 Sep;370(3):183-192.

106. Wirth KJ, Paehler T, Rosenstein B, Knobloch K, Maier T, Frenzel J, et al. Atrial effects of the novel K(+)-channel-blocker AVE0118 in anesthetized pigs. Cardiovasc.Res. 2003 Nov 1;60(2):298-306.

107. Movahed MR, Hashemzadeh M, Jamal MM. Diabetes mellitus is a strong, independent risk for atrial fibrillation and flutter in addition to other cardiovascular disease. Int.J.Cardiol. 2005 Dec 7;105(3):315-318.

108. Simpson S. Unpublished observations .2010.

109. Melander A, Sartor G, Wahlin E, Schersten B, Bitzen PO. Serum tolbutamide and chlorpropamide concentrations in patients with diabetes mellitus. Br.Med.J. 1978 Jan 21;1(6106):142-144.

110. Sartor G, Melander A, Schersten B, Wahlin-Boll E. Serum glibenclamide in diabetic patients, and influence of food on the kinetics and effects of glibenclamide. Diabetologia 1980 Jan;18(1):17-22.

111. O'Brien RC, Luo M, Balazs N, Mercuri J. In vitro and in vivo antioxidant properties of gliclazide. J.Diabetes Complications. 2000 Jul-Aug;14(4):201-206.

112. Campbell RK. Glimepiride: role of a new sulfonylurea in the treatment of type 2 diabetes mellitus. Ann.Pharmacother. 1998 Oct;32(10):1044-1052.

113. van Heiningen PN, Hatorp V, Kramer Nielsen K, Hansen KT, van Lier JJ, De Merbel NC, et al. Absorption, metabolism and excretion of a single oral dose of (14)C-repaglinide during repaglinide multiple dosing. Eur.J.Clin.Pharmacol. 1999 Sep;55(7):521-525.

114. McLeod JF. Clinical pharmacokinetics of nateglinide: a rapidly-absorbed, short-acting insulinotropic agent. Clin.Pharmacokinet. 2004;43(2):97-120.